

**OPTICAL DATING OF BARRIER ISLANDS
IN THE GULF OF MEXICO**

**THE LATE QUATERNARY EVOLUTION OF THE APALACHICOLA
BARRIER ISLAND COMPLEX, NORTH-EAST GULF OF MEXICO, AS
DETERMINED FROM OPTICAL DATING**

by

GLORIA INÉS LÓPEZ-CADAVID, Geologist, M.Sc.

A Thesis

Submitted to the School of Graduate Studies

in Partial Fulfilment of the Requirements

for the Degree

Doctor of Philosophy

McMaster University

© Copyright by Gloria Inés López-Cadavid, September 2007

DOCTOR OF PHILOSOPHY (2007)
(Geography and Earth Sciences)

McMaster University
Hamilton, Ontario, Canada

TITLE: The Late Quaternary Evolution of the Apalachicola Barrier Island Complex, North-East Gulf of Mexico, as determined from Optical Dating.

AUTHOR: Gloria I. López C.

Geologist
(Universidad EAFIT, Medellín,
Antioquia, Colombia, 1993)

M.Sc.
(University of Victoria, Victoria, British
Columbia, Canada, 2002)

SUPERVISOR: Professor W. Jack Rink

NUMBER OF PAGES: xx, 264 pp.

ABSTRACT

Optical stimulated luminescence (OSL) studies of clastic-rich coastal environments have been increasingly the focus of attention, mostly over the past five years, due to the improvement of protocols used to obtain reliable and accurate optical ages on minerals such as quartz. Using 55 quartz-separate samples extracted from at least two different depth intervals on sediment cores (long vertical and short horizontal) retrieved from multiple beach / dune ridges that decorate four Holocene coastal barriers and a Pleistocene lower mainland, the supra-tidal evolution of the western portion of the Apalachicola Barrier Island Complex, on the NE region of the Gulf of Mexico, has been re-evaluated. This study not only provides new reliable OSL ages for the region but also addresses the feasibility of a) quantifying rates of coastal aggradation and progradation; b) interpreting the temporal chronology of the coastal geomorphology; and c) constraining the results with other geochronometric data available at a more precise level (e.g. inter-correlations with accurate [x,y,z] parameters).

OSL results show equivalent doses (D_E) ranging between 0.01 ± 0.00 and 52.28 ± 1.26 Gy, associated to samples linked to both wind- and water-lain processes, depicting the two principal components of these ridges: a most probable swash-built ridge base and an aeolian cap. The optical ages obtained range from 22 ± 4 to $154,200 \pm 10,400$ years ago (based on 2004 to 2006 datum), representing *terminus ante quem* ages of formation of the ridges and the ages of the aeolian component at that particular depth. Modern analogues were also optically analyzed to determine the degree of exposure of these types of sediments to sunlight. The results show zero D_E , implying zero ages. The sedimentary deposits hosting the cores collected show minimal contents of Uranium and Thorium ($\ll 4$ ppm with an average of 0.5 ppm). The Potassium content seems to be more linked to temporal variations (i.e. different stages of evolution of the barrier islands) than to geographical position relative to the Apalachicola River mouth.

D_E distribution analyses show that frequency histograms coupled with cumulative frequency (%) curves and radial plots should be used together to better evaluate the overall behaviour of the distribution. For most of the samples OSL-dated for this research, one or two outliers (i.e. aliquots outside $\pm 2\sigma$) were present upon analysis of the D_E distribution, but excluded from the final D_E calculation used to compute the optical age of each sample. Skewness coefficient ranges were determined and skewness values were calculated to quantify the degree of symmetry of the D_E distribution for each sample. This parameter was used to assess the final total error (i.e. $\pm 1\sigma$ or 1 standard error) to be associated with each final D_E value, as well as the heterogeneity or homogeneity of the dose within each sample and see any indications of possible incomplete zeroing or

biogeoturbation. Moreover, and associated with the latter, the use of smaller aliquots (e.g. 3 and 1 mm mask sizes) was also implemented to detect if the samples had undergone any significant post- or pre-depositional disturbance. None was found; rather, analyses show that with decreasing mask size, an increasing resolution in the D_E distribution was obtained where the values obtained for the larger aliquots (i.e. 8 and 5 mm mask size) were encompassed within those obtained for the smaller aliquots (i.e. 3 and 1 mm mask size).

This dissertation presents the first assessment of supra-tidal coastal evolution using optical ages to determine both the vertical accretion and lateral progradation rates throughout different segments of the coastline. The multi-directionality, patterns and truncations shown by the hundreds of beach and dune ridges and ridge sets demonstrate the morpho- and hydro-dynamic complexity of these coastal barrier systems, located on the apex of the Floridian Panhandle. Assessments of such morphological characteristics as well as detailed analyses of air-photographs, satellite imagery, ancient nautical and topographic charts/maps, and previous studies were also incorporated in this research to better constraint the proposed Late Holocene spatial-temporal history of this ~ 60 km-long coastal complex perched on the NE corner of the Gulf of Mexico. Six major time intervals were differentiated with the chronological evolution of these barrier islands since the last ~ 4,000 years. Furthermore, based on the oldest ages obtained during this research, it is hypothesized that sea level may have stabilized ~ 3,000 years ago in this region, enabling the emergence and continuous progradation of these coastal barrier systems until present times.

ACKNOWLEDGMENTS

After almost five years at McMaster, running in between my Ph.D. work, the Teaching and Field Assistantships I held, my own side research in the high Andes of Colombia, the dating of underwater samples off Caesarea Maritima (Israel), my involvement in dating other graduate students' samples, going on contracted field seasons in the U.S.A. and Portugal, and all the commercial dating I was in charge of for the past year, I have to, first and foremost, sincerely thank my Ph.D. supervisor, William Jack Rink, for his everlasting patience, good humour, understanding, support, enthusiasm, generosity and supervision during all my endeavours and time here. Thank you for your trust in me and allowing me to "be in charge" of the AGE Laboratory, the several assistants we had, my research, and my fieldwork. I owe a debt of gratitude to you for encouraging me to start writing papers since the first set of results came ashore. It really made my life easier along the Ph.D. road, even though challenging at times of publication submission and revision. Thank you for meticulously reading all the original drafts and final versions of all the manuscripts, and for the insightful discussions, comments and editorial advice during the revisions and throughout this research.

I would also like to thank my thesis committee, Joe I. Boyce and Eduard G. Reinhardt, for all their support, advice, comments and chats. Thank you for being more than just committee members. Thank you Joe for sharing your knowledge with me, your time during one of my field seasons and getting me actively involved with GPR. We still have to write that White Sands manuscript! Thank you Ed for introducing me to Caesarea (and the challenges of dating underwater sediments!) and getting me actively involved in your labs, research, as well as your students' work. I will always appreciate the token of confidence both of you have had towards me.

This Ph.D. research would not have been possible without the unquestionable support of several Federal and State Agencies and individuals who look after and protect the beautiful lands and beaches I was lucky enough to study.

To the T.H. Stone Memorial St. Joseph Peninsula State Park (Florida Department of Environmental Protection) – thank you for letting me core and walk over those magnificent dunes, ridges and backcountry. I do not have enough words to thank you for your financial and logistic support for and during this research, such as lending us trucks, four/six wheelers, radios, tools and paying for the gas we used during every single field season! Thank you for all your "rescues" and help in the field when needed, your enthusiasm, laughs, questions and patience. Thank you "Park People" for accepting me and letting me be part

of your world, specially: Anne Harvey (Park Manager at the time), Cynthia Emrich (Assistant Park Manager at the time), Ronnie Bailey, Joe Mitchell, James Skinner, Michael Nash, Everett Horton, Allan Ritchie, George Royal, and Diane Gillespie.

To the Apalachicola National Estuarine Research Reserve (Florida Department of Environmental Protection) – immense thanks for giving us financial and logistic support for and during this research, such as free lodging at the St. Joseph Bay Buffer Preserve Centre during several field seasons, driving us by boat to Little St. George Island and allowing us into all the Preserve's areas. My most sincere thanks to Roy Ogles (Resource Management Coordinator), Tammy Mae Summers (Aquatic Preserve Manager at the time), Jimmy Moses III, Captain Patrick Millender, George Watkins, Ricky Hathcock II, Mary Wittington, Marie Steele, and Jason Isbell. Thank you for all your help in the field, for taking care of us at the Centre, and for all the laughs and good times.

To the U.S. Fish and Wildlife Service for granting us permission to core on the St. Vincent National Wildlife Refuge island. Special thanks to Terry Peacock (Refuge Manager) and Monica Harris as well as all other members that ferried us onto the island and provided us with trucks during our research there.

Many thanks to Billy C. Quinn Jr., Resident Park Manager of the Wm. J. Rish Recreation Park for letting us dig a trench, take a core and do many beach profiles.

I am extremely thankful to the Eglin Air Force Base (U.S. Air Force) for allowing us to enter into their premises and do research, mostly because we were foreigners, “Colombian” and “Canadians”, which, during those first field seasons, was indeed a little “suspicious” to deal with. Special thanks to Robert D. Whitfield, Judith Watts, and Mark Collier for making coring possible.

I could not forget the memorable Indian Pass Raw Bar and its undeniable exquisite cuisine and characters! There were many crab legs, shrimp and a ceiling fan “devoured” at that place!

Last but not least, to Jimmy and Penny Meadows my most sincere thanks for opening your house and hearts to us every time we drove down to Apalachicola. You truly showed me the “Southern Hospitality” way.

Sometimes one forgets to acknowledge the people that make the instruments your “life” depends on to function. In my case, the “everlasting” RISØ Reader in the AGE darkroom lab. For about 12 months (on and off) it suffered from all sorts of “disorders”, both mechanical and electronic, that resulted in the horrifying unwanted “*DATA ERROR*” screen. Trying to fix it proved to be interestingly challenging: a lot of patience, weeks of trial-and-error, a dreadful time difference (Canada/Denmark) and countless emails to and from the staff at RISØ (especially

Henrik C. Christiansen, Jorgen Jakobsen and Kristina Thomsen) were needed every time. Among all the chaos, two other people came “to play”, Kendrick Chin (Physics) and Jeroen Thompson (my office/lab mate): thank you for your time, knowledge in electronics and input when deciphering the reader in and out. In the end, and after writing an entire “problem log book”, the machine only needed “a little love”!

Acknowledging and thanking everybody that has supported, encouraged, understood, and helped me literally and figuratively during my time here at the School and McMaster in general would be a task for the fabulous *Don Quijote de la Mancha*... almost impossible in prose but achievable in dreams and prayers. Without naming you individually, I thank you **ALL** for your friendship, love, respect, and advice. You know who you are so names need not to be listed here. Thank you for been on my side when I needed it; for sharing questions and discussions; trips and labs; laughs and tears; thoughts, files and books; music, patios and beers. I cannot express the gratitude I have towards you for making me feel welcomed and accepted since my very first day, in this now “not so foreign” wild country.

I could not forget all the other good friends I left behind after coming here, new and old, far and away, around the World... who gave me so much love, time and positive energy through letters, e-mails and phone calls. You will always be a big part of my life, now, then and hereafter.

But above all, and from the deepest of my soul and heart, I must thank my entire family for their constant love, involvement, understanding, spiritual and economical support, and cheers. We have always been and will always be together, geographical distances aside. Thank you for everything you have given me through these calm and rough waters. Thank you for being there every time I needed you... no matter the hour of the day. Thank you for making me part of the big moments of our great family’s life, even though I missed most of your engagements, weddings, first births, graduations, and funerals. Thank you for sharing it all. To my two sisters, thank you for all the times we shared everything through waves and lines. To my parents, there are no words that could describe the admiration, love and respect I have for you.

Mil Gracias – Merci Bien – Muito Obrigado

Face à des problèmes poly-disciplinaires,
multidimensionnels, transnationaux, globaux et
planétaires, il faut une tête bien faite qui sache
traiter les ensembles complexes, les interactions et
rétroactions complexes entre parties et tout ...

L'éducation pour une tête bien faite devrait répondre
aux défis de la globalité et de la complexité dans la
vie sociale, politique, nationale et mondiale.

Hommage à Edgar Morin: L'Humaniste Planétaire
G. López Ospina & N. Vallejo Gómez
UNESCO, 2001



This Ph.D. Dissertation is dedicated to my amazing parents

Gustavo López Ospina & Amparo Cadavid de López

Thank you for teaching me...

... the love for nature and adventure

... the value of education, knowledge and books

... that happiness is in what one loves and best if done with passion

*... "to learn, first, by using one's hands, and, only afterwards, by pressing
buttons"*

Thank you for letting me be, go and pursue my dreams

I owe it all to you

Infinitas gracias por todo y más aún por creer en mi

Los adoro



TABLE OF CONTENTS

ABSTRACT	iii
ACKNOWLEDGMENT	v
TABLE OF CONTENTS	ix
LIST OF FIGURES	xiii
LIST OF TABLES	xviii
PREFACE	xix
Chapter 1	1
INTRODUCTION	1
1.1. Research Justification and Context	3
1.2. Research Objectives	4
1.3. Dissertation Structure	6
References	9
Chapter 2	11
NEW QUARTZ OPTICAL STIMULATED LUMINESCENCE AGES FOR BEACH RIDGES ON THE ST. VINCENT ISLAND HOLOCENE STRANDPLAIN, FLORIDA, UNITED STATES	11
Abstract	13
2.1. Introduction	13
2.1.1. Study Area	14
2.1.2. Previous Geological, Geochronological and Archaeological Work	15
2.2. Samples and Methodology	18
2.3. Results	20
2.4. Discussion	23
2.5. Conclusions	29
Acknowledgements	30
References	30
Chapter 2 – Figures	34
Chapter 2 – Tables	40
Chapter 3	44
CHARACTERISTICS OF THE BURIAL ENVIRONMENT RELATED TO QUARTZ SAR-OSL DATING AT ST. VINCENT ISLAND, NW FLORIDA, U.S.A.	44
Abstract	46
3.1. Introduction	46
3.2. Methods	47
3.2.1. Sampling Strategy	47
3.2.2. Sample Preparation and Dose-Rate Measurements	48

3.2.3. OSL Measurements	48
3.3. Results and Discussion	49
3.4. Conclusions	52
Acknowledgements	52
References	52
Chapter 3 – Figures	55
Chapter 3 – Appendix A. Supplementary materials	59
Chapter 4	65
OPTICALLY STIMULATED LUMINESCENCE AGE OF THE OLD CEDAR MIDDEN, ST. JOSEPH PENINSULA STATE PARK, FLORIDA	65
Abstract	67
4.1. Introduction	67
4.2. Method	68
4.3. Results and Discussion	70
4.4. Conclusion	72
Acknowledgments	72
References	73
Chapter 4 – Figures	75
Chapter 4 – Tables	79
Chapter 4 – Appendix A. Supplementary Data	83
Chapter 5	84
OPTICAL DATING OF AN ANCIENT COASTAL OCCUPATION SITE AND UNDERLYING LAND ON THE NORTHWEST GULF COAST OF FLORIDA, NEAR APALACHICOLA, U.S.A.	84
Abstract	85
5.1. Introduction	85
5.2. Geological and Archaeological Background	87
5.2.1. Prehistoric Cultural Chronology of the Region	89
5.2.1.1. The Richardson’s Hammock Site	89
5.3. Field And Laboratory Procedures And Age Calculations	90
5.4. Results And Discussion	93
5.5. Conclusions	97
Acknowledgements	97
References	98
Chapter 5 – Figures	101
Chapter 5 – Tables	113
Chapter 6	116
PENINSULAR EVOLUTION AND OPTICAL DATING OF YOUNG COASTAL RIDGES ALONG THE GULF OF MEXICO	116
Abstract	117

6.1. Introduction	117
6.2. Study Area and Sampling Sites	118
6.3. OSL Dating	120
6.4. Results	124
6.4.1. OSL Characteristics of the Samples	124
6.4.2. OSL Dating Results	125
6.4.2.1. SAR-OSL Ages of St. Joseph Peninsula Precursor Nuclei	127
6.4.2.2. SAR-OSL Ages of Interior Ridges	128
6.4.2.3. SAR-OSL Ages along the Peninsula's Western Margin and Spit Terminus	128
6.5. Discussion	130
6.5.1. Assessing the Relationship between OSL and the Depositional Environment	131
6.5.2. Peninsular Evolution of St. Joseph	132
6.6. Conclusions	136
Acknowledgements	137
References	138
Chapter 6 – Figures	141
Chapter 6 – Tables	153
Chapter 7	161
EVOLUTION AND OPTICAL LUMINESCENCE DATING OF A PLEISTOCENE AND HOLOCENE COASTAL BARRIER COMPLEX, NE GULF COAST, FLORIDA, U.S.A.	161
Abstract	162
7.1. Introduction	162
7.1.1. Previous Studies	165
7.2. Study Area and Methodologies	168
7.2.1. Apalachicola Barrier Island Complex	168
7.2.2. Sample Locations	169
7.2.3. Dating Methodology	170
7.3. Results	172
7.3.1. OSL Characteristics and Data	172
7.3.2. OSL Age Results in the Context of Barrier Geochronology and Development Phases	173
7.3.2.1. Richardson's Hammock OSL Ages	175
7.3.2.2. St. Vincent Island (SVI) OSL Ages	175
7.3.2.3. St. Joseph Peninsula (SJP) OSL Ages	176
7.3.2.4. Little St. George Island (LSGI) OSL Ages	177
7.3.2.5. Cape San Blas (CSB) OSL Ages	177
7.4. Discussion	178
7.5. Conclusions	183
7.6. Acknowledgements	184

7.7. References	184
Chapter 7 – Figures	188
Chapter 7 – Tables	206
Chapter 8	213
GENERAL CONCLUSIONS AND FUTURE RESEARCH	213
8.1. Geological and Geochronological	215
8.2. Archaeological	218
8.3. Methodological	218
Appendix I	222
List of all the Cores taken for this Ph.D. Research	222
Appendix II	228
Programs Used for OSL Measurements / Analyses and Age Calculations	228
Appendix III	230
Guidelines for OSL Sample Collection and Laboratory Preparation	230
Appendix IV	235
General Single-Aliquot Regenerative-Dose (SAR) Protocol	235
Appendix V	238
Parameters for Aliquot Analysis and Guidelines for DE Determination	238
Appendix VI	247
Parameters for Skewness	247
Appendix VII	249
Parameters for OSL Age Calculations	249
Appendix VIII	250
Age Calculation: Two Possible Models – Linear or Instant Accumulation	250
Appendix IX	252
Age Calculation: Accounting for Geometry	252
Appendix X	254
SAR-OSL Dated Samples: Specifics, Ages and Results	254

LIST OF FIGURES

All figures are located in consecutive manner at the end of each Chapter, as per the general style required for submission of manuscripts to peer-reviewed journals.

CHAPTER 2

Figure 2.1. Site location map of St. Vincent Island, NW Florida, U.S.A.

Figure 2.2. St. Vincent Island beach ridge sets.

Figure 2.3. Schematic cross-sections of two transects across beach ridges: A) Along Road 4 (Transect Road 4 – general strike N45°E to N50°E) on the southwestern area of St. Vincent Island fronting the Gulf of Mexico. B) Along Road 5 (Transect Road 5 – general strike NS) on the north-eastern area.

Figure 2.4. Average sediment accumulation rate (ASAR) as a function of distance from Gulf of Mexico shoreline.

Figure 2.5. Frequency distribution of 24 aliquots from sample SVI #3 OSL1 obtained using 8 mm mask.

Figure 2.6. Examples of vegetation cover atop the crest of an inland ridge on St. Vincent.

CHAPTER 3

Figure 3.1. Site location map of St. Vincent Island, NW Florida, U.S.A.

Figure 3.2. Photo-mosaics of two split cores (exposed halves).

Figure 3.3. Examples of a) decay and b) response curves obtained for sample SVI #5 OSL1.

Figure 3.4. Examples of D_E frequency distributions for two samples from St. Vincent Island.

Figure 3.S1. Examples of D_E pre-heat plateau plots for samples from cores a) SVI #0 and b) SVI #5.

Figure 3.S2. Examples of the dose-recovery test done on samples a) SVI #0 OSL1 and b) SVI #5 OSL2.

Figure 3.S3. Thermal transfer test plots obtained for two samples from St. Vincent Island.

Figure 3.S4. Example of the radial plot for sample SVI #5 OSL1.

CHAPTER 4

Figure 4.1. Map of Florida, USA. Area within the box is shown in the inset of Fig. 2.

Figure 4.2. Study area (FDEP, 1999). Inset: St. Joseph Peninsula. Aerial photographs courtesy USGS.

Figure 4.3. Histograms of measured D_E 's for OC1 (midden) with varying mask sizes.

Figure 4.4. Histograms of measured D_E 's for OCg1 (beach ridge) with varying mask sizes.

Figure 4.S1. Mean D_E versus pre-heat temperature for OC1 (midden) and OCg1 (beach ridge).

CHAPTER 5

Figure 5.1. Site location map of St. Joseph Peninsula.

Figure 5.2. Site location map of Richardson's Hammock.

Figure 5.3. Schematic drawing showing position of dated samples.

Figure 5.4. Test Unit E, Floor 3 (30 cm depth below the surface), showing distribution of artifacts and far fewer large shells, characteristic of the Middle Woodland component at the site.

Figure 5.5. Stratigraphic profiles showing the OSL samples taken within Test Unit E in July 2003.

Figure 5.6. Photographs of Test Unit E.

Figure 5.7. Photograph of the beach ridge on the bay-shore where sample RH-GEO-1 was taken.

Figure 5.8. D_E distributions of sample RH-TUE-1 at different mask sizes.

Figure 5.9. D_E distributions of sample RH-TUE-2 at different mask sizes.

Figure 5.10. D_E distributions of sample RH-GEO-1 at different mask sizes.

Figure 5.11. D_E distributions of sample RH-A (bottom of long vertical core) at different mask sizes.

Figure 5.12. D_E distributions of sample RH-B (top of long vertical core) at different mask sizes.

CHAPTER 6

Figure 6.1. General location of St. Joseph Peninsula within the Apalachicola Barrier Island Complex, north-eastern Gulf of Mexico, U.S.A.

Figure 6.2. Geomorphological map of St. Joseph Peninsula.

Figure 6.3. St. Joseph Peninsula ridge sets and previous historical shorelines.

Figure 6.4. Example of D_E frequency histograms for both large and small sized aliquots.

Figure 6.5. Transversal section and associated photo-mosaic of the Deer Ridge area.

Figure 6.6. Transversal section and associated photographs of the SJ002 area.

Figure 6.7. Average sediment accumulation rate (ASAR) plot of all cores corresponding to Table 4.

Figure 6.8. Previous chronologies reported for St. Joseph Peninsula.

Figure 6.9. Proposed multiple-nuclei positioning and evolution for St. Joseph Peninsula based on this study.

CHAPTER 7

Figure 7.1. General location of the Apalachicola Barrier Island Complex on the Florida Panhandle, U.S.A.

Figure 7.2. Coring the Apalachicola Barrier Islands.

Figure 7.3. Little St. George Island preserve.

Figure 7.4. Richardson's Hammock, Cape San Blas and western lower mainland area.

Figure 7.5. St. Joseph Peninsula.

Figure 7.6. Site location map of St. Vincent Island (U.S. National Wildlife Refuge).

Figure 7.7. Chronological evolution of the central-eastern barriers pertaining to the Apalachicola Complex based on optical ages obtained by López (2007).

Figure 7.8. Optical ages of 28 individual quartz fractions retrieved from the ridges decorating the central-western Apalachicola Barrier Island Complex.

Figure 7.9. Lower Average Sediment Accumulation Rate (ASAR) vs. distance from the Gulf shorelines, calculated from the two consecutive samples within each core or site (i.e. between A and B and OSL1 and OSL2).

Figure 7.10. Optical ages versus Longitude positioning (Geographical NAD 83) for all five barrier systems studied.

Figure 7.11. General interpretation of the supra-tidal evolution of the western portion of the Apalachicola Barrier Island Complex as suggested by Stapor (1973, 1975).

Figure 7.12. General interpretation of the supra-tidal evolution of the western portion of the Apalachicola Barrier Island Complex as suggested by Otvos (2005a).

LIST OF TABLES

All tables are located in consecutive manner at the end of each Chapter following the corresponding figures, as per the general style required for submission of manuscripts to peer-reviewed journals.

CHAPTER 2

Table 2.1. Location of cores taken on St. Vincent Island and depths of samples OSL-dated.

Table 2.2. SAR - OSL ages and data for samples taken from beach ridges on St. Vincent Island.

Table 2.3. Average sediment accumulation rates (ASAR) between OSL samples at different intervals within each sediment core.

Table 2.4. Average ridge accretion and coastal progradation rates estimates.

CHAPTER 3

Table 3.S1. Values for temperatures, durations of stimulation, and regeneration doses employed in the SAR protocol assigned to each sample dated in this study.

Table 3.S2. SAR-OSL ages and data for samples taken from beach ridges on St. Vincent Island.

CHAPTER 4

Table 4.1. Periods, cultures, and accepted dates for the northwest Florida cultural sequence (after Benchley and Bense, 2001).

Table 4.2. Our single aliquot regeneration protocol.

Table 4.3. Variation in mean equivalent dose with mask size.

Table 4.4. Dose rates and OSL burial ages for each sample.

CHAPTER 5

Table 5.I. Generalized Prehistoric cultural chronology for the Apalachicola area.

Table 5.II. Results of Tests done on all Richardson Hammock samples prior to the final D_E estimation.

Table 5.III. SAR - OSL ages and data for quartz sand samples taken at Richardson Hammock.

CHAPTER 6

Table 6.1. Location of cores taken on St. Joseph Peninsula (NW Florida, U.S.A.) and details regarding samples OSL-dated.

Table 6.2. SAR - OSL Equivalent Dose data for quartz sand samples taken from St. Joseph Peninsula, Florida, U.S.A.

Table 6.3. SAR - OSL ages and data for quartz sand samples taken from St. Joseph Peninsula, Florida, U.S.A.

Table 6.4. Average sediment accumulation rates (ASAR) between OSL samples at different depth intervals within individual core or sites.

Table 6.5. Proposed time intervals for the formation and evolution of St. Joseph Peninsula.

CHAPTER 7

Table 7.1. Geographical coordinates (NAD 83) and SAR-OSL equivalent dose (D_E) data for quartz fractions recovered during this study from the lower mainland, Cape San Blas and Little St. George Island, Florida, U.S.A.

Table 7.2. SAR-OSL ages and data obtained for quartz fractions (150-212 μ m) from the long vertical sediment cores recovered from the lower mainland, Cape San Blas and Little St. George Island, Florida, U.S.A.

Table 7.3. Compilation of SAR-OSL ages obtained for the remainder barriers of the Apalachicola Complex, Florida, U.S.A. Geographical coordinates (NAD 83) are also given.

Table 7.4. Compilation of Average Sediment Accumulation Rate (ASAR) for cores and archaeological sites having been sampled at two different depth intervals. Distances of cores to the modern shoreline are also given as well as whether or not the samples' ages are statistically distinguishable from each other.

PREFACE

This dissertation compiles a collection of research papers that were either published at different stages of this Ph.D., are presently in press (i.e. proof corrected), or are under review or in the process of being submitted. The objectives and relationship among the various papers are described in the introductory chapter. The final Chapter Eight, Conclusions, summarizes the major contributions obtained during this research. The different research papers presented herein are the following:

Chapter Two:

LÓPEZ, G.I., and RINK, W.J., 2007. New quartz optical stimulated luminescence ages for beach ridges on the St. Vincent Island Holocene strandplain, Florida, United States. *Journal of Coastal Research*, 23(0), 000-000 (*in press; proof corrected*).

Chapter Three:

LÓPEZ, G.I., and RINK, W.J., 2007. Characteristics of the Burial Environment related to Quartz SAR-OSL Dating at St. Vincent Island, NW Florida, U.S.A. *Quaternary Geochronology*, 2, 65-70.

Chapter Four:

THOMPSON, J., RINK, W.J., and LÓPEZ, G.I., 2007. Optically Stimulated Luminescence age of the Old Cedar Midden, St. Joseph Peninsula State Park, Florida. *Quaternary Geochronology*, 2, 350-355.

Chapter Five:

LÓPEZ, G.I., RINK, W.J., AND WHITE, N.M. Optical Dating Of An Ancient Coastal Occupation Site And Underlying Land On The Northwest Gulf Coast Of Florida, Near Apalachicola, U.S.A. *Geoarchaeology*, (*submitted December 2006; under review*).

Chapter Six:

LÓPEZ, G.I., and RINK, W.J. Peninsular Evolution and Optical Dating of Young Coastal Ridges along the Gulf of Mexico.
(*prepared for Quaternary Geochronology; ready for submission July 2007*)

Chapter Seven:

LÓPEZ, G.I., and RINK, W.J. Evolution and Optical Luminescence Dating of a Pleistocene and Holocene Coastal Barrier Complex, NE Gulf Coast, Florida, U.S.A.
(*prepared for Earth Science Reviews; ready for submission July 2007*)

Even though all of the research papers were co-authored, the first author (i.e. the doctoral candidate) conducted all the research surrounding the objectives of this investigation, literature review, selection of core sites and sampling strategies, core collection, laboratory sample treatments and analyses, luminescence measurements and analyses, and manuscripts writing. Dr. Rink provided guidance on the direction of this research, discussion of the results at the different stages of achievement, critique of papers and invaluable editorial advice. Different levels of collaboration exist on the multi-authored publications. For the paper reproduced in Chapter Four, the doctoral candidate taught J. Thompson (first author on that particular manuscript) how to optically date the samples collected at the Old Cedar archaeological site (including all field and laboratory procedures), guided him throughout the luminescence analyses and helped with some of the literature review as well as some sections of manuscript writing. In Chapter Five, Dr. Nancy Marie White, one of the leading experts in north-western Floridian archaeology, contributed by guiding the doctoral candidate through the archaeological background of the studied area, and in interpreting the importance of the candidate's dating results from an archaeological perspective, as well as editorial advice. All co-authors have reviewed and approved the final manuscripts before submission.

The chapters in this dissertation, being a "sandwich" type, show different formatting styles as each individual research paper follows the style required by the journals to which they were submitted. Moreover, and also due to its structure, the reader may encounter minor repetition between papers, especially during some of the descriptions regarding the study area, the geological setting, field and laboratory methodologies, and in some aspects of the various literature reviews and discussions. In compliance to McMaster University copyright regulations, the appropriate permissions were requested for those research papers already published and/or in press. Copies of the reproduction permissions are given at the beginning of the chapters requiring it.

CHAPTER 1

INTRODUCTION

*To see a world in a grain of sand,
And a heaven in a wild flower,
Hold infinity in the palm of your hand,
And eternity in an hour ...*

– William Blake (ca. 1800-03)

If only an eternal luminescence signal could be captured in a single grain of sand, optical dating could encompass the entire Earth's history. Even though such idealistic view is only a dream, optical dating is quite a reality.

Quaternary deposits may be dated by a variety of methods that require a variety of suitable materials. Radiocarbon dating has been the most widely used geochronometric technique for dating Quaternary sediments associated with a diverse range of depositional environments. However, dating sediments lacking the delicate and decomposable carbonaceous materials needed for this geochronometric technique has always been a problem. Moreover, the time range of radiocarbon is also a limitation: a) young (< 1,000 years old) fossil organic matter is impossible to date accurately due to large fluctuations of ^{14}C in the atmosphere, resulting in problematic calibration and large age uncertainties; b) relatively old (> 40,000 years old) organic materials cannot be ^{14}C -dated (Stuiver, 1978). On the other hand, other absolute dating techniques that may exceed the age range of ^{14}C dating (e.g. K-Ar, Ar-Ar, fission track, amino acid racemization) require special materials that may not always be present in all Quaternary deposits.

In general, the specific time of emplacement of a sedimentary deposit was a challenge to obtain until the emergence of optical dating. Optical dating was first introduced as a technique for dating unconsolidated inorganic deposits (e.g. quartz and feldspar) that were difficult or impossible to date by other geochronometric methods. Huntley *et al.* (1985) pioneered optical stimulated luminescence (OSL) dating while looking for a method to determine when sediments were last exposed to sunlight based on the physics behind the luminescence properties of certain minerals. Optical dating of geological materials is based on several fundamental assumptions: a) the OSL signal may be zeroed by exposure to sunlight during transport and/or prior to deposition; b) the natural OSL signal of the sample (i.e. accumulated during burial and resulting from exposure to natural radiation) can be measured in the laboratory; c) it is possible to reliably regenerate and measure the OSL signal produced artificially in the laboratory; d) the environmental dose rate is measurable, constant in time, and uniform within the sample; e) the cosmic-ray dose rate can be realistically

calculated; f) sedimentologically complex units should be avoided; g) the depositional environment has been relatively stable through time; h) there is no disequilibrium in the uranium decay chain.

Over the past 20 years, improvements in the accuracy and precision of OSL methodologies have made optical dating a reliable geochronometric technique. The principles of optical dating can be found in Aitken (1985, 1998) and Bøtter-Jensen *et al.* (2003). Although optical dating was first successfully tested on quartz extracted from well independently-dated beach dunes in south-east South Australia (Huntley *et al.*, 1985), much of the consequent studies used feldspars due to the costs involving laser and blue emitting diode stimulation sources, much needed for the study of quartz (Bøtter-Jensen *et al.*, 2003). Some of the early work done on sedimentary coastal environments was achieved by Ollerhead *et al.* (1994, 1995) on a sequence of dunes on Buctouche Spit (north-east coast of New Brunswick, Canada). They reported some of the first OSL ages obtained on feldspar grains recovered from young sediments (< 800 years old) using infrared stimulation and an additive dose protocol. The ages were in agreement with geomorphological and historical evidence as well as the ^{14}C ages obtained in the study, leading to the calculation of accretion rates for the spit. In a subsequent study, van Heteren *et al.* (2000) presented the first study to use optical dating of K-feldspars to determine relative sea level changes on a coastal barrier system on the southern edge of Cape Cod Bay (Massachusetts, U.S.A.). Even though the ages obtained were slightly younger than the estimated ^{14}C ages, this study demonstrates the feasibility of using optical dating of well preserved inorganic sea level markers, provided an accurate interpretation of the sedimentary facies.

After the development of relatively inexpensive stimulation sources and the Single-Aliquot Regenerative-dose (SAR) protocol (Murray & Wintle, 2000, 2003; Wintle & Murray, 2006), interest in the study of quartz rapidly augmented, leading to an increase in the range of ages obtained for clastic coastal environments and the reliability of such ages. Bailey *et al.* (2001) successfully applied the SAR protocol on quartz grains obtained from a young dune field in North Wales. The OSL chronologies obtained were in excellent agreement with both historical evidence and the stratigraphical record obtained using ground penetrating radar. Berger *et al.* (2003) obtained quartz OSL ages on back-barrier coastal dunes in North Carolina (U.S.A.) using the SAR protocol. Their chronologies were consistent with the general stratigraphy and ^{14}C ages available for the region. Moreover, Banerjee *et al.* (2003) corroborated the precision and accuracy of the SAR-OSL procedure on quartz by comparing their resulting ages with the existing well-known thermoluminescence (TL) chronologies previously obtained by Huntley *et al.* (1993, 1994), as well as other independent dating methods, on a well-studied sequence of stranded coastal barriers in south-east South Australia. The ages obtained for the beach dunes ranged from 0 to 250,000

years, proving the applicability of the method as a good chronological tool for the study of sea-level variations and coastal systems over millennia.

The potential of quartz SAR-OSL dating for high-resolution reconstruction of clastic-rich coastal sedimentary environments was explored by Ballarini *et al.* (2003). Their resulting chronologies (< 10 to a few hundred years) allowed them to evaluate the evolution of a barrier island off the coast of the northern Netherlands, which in turn, was in excellent agreement with well-known historical evidence. Quantification of coastal progradation rates on barrier islands and dune systems has only been attempted by a few authors (i.e. Ballarini *et al.*, 2003; Murray-Wallace, *et al.*, 2002). Lately, most of the research involving SAR-OSL in coastal environments has been focused towards understanding the influences of pedogenesis and post-depositional disturbances on sedimentary deposits and climate change assessments (e.g. Argyilan, *et al.*, 2005; Bateman *et al.*, 2007a). The short- and long-range limits of optical dating are still under investigation, as well as its full range of applications.

1.1. RESEARCH JUSTIFICATION AND CONTEXT

Due to the relatively young age of optical dating and the rapid improvement of methodological laboratory approaches, any further contribution to this dating method is important. Previous successful studies on OSL accuracy and precision continue to encourage the scientific community to pursue further investigations on the applications of optical dating not only as a chronometric tool but also as a proxy to understand sedimentary deposits, evaluate their evolution at a high-resolution scale as well as past environmental conditions. Such understanding of the sedimentary environment and the processes involved (i.e. transport and deposition) may be also applied to improve or develop land management tools and strategies.

An integrated understanding of the overall evolution of any given coastal system is critical due to the dynamic nature of these marginal environments. Time is of particular interest in this equation. “When” did a system start to form and “for how long” did it generate and/or maintain itself are fundamental questions related to the evolution of any coastal environment. Such questions may be answered in a relative or absolute form, depending on the availability and type of data relevant to the system.

In the early days, when exploration was lead by qualitative observation, most of the hypotheses dealing with the evolution of a coastal area were based on the information available at the surface, i.e. any observable geomorphological, geometrical, and geographical characteristics. For instance, morphological details such as truncation, width, height, directionality and curvature of ridges, help elucidate relative ages and the general direction of progradation/accretion of a ridge plain or barrier island. Detailed field observation and mapping of such

geomorphological features are still important to understand relative spatial chronologies. However, the most reliable form of portraying the history of any given environment should be by quantitative analysis of depositional environments using sedimentologic techniques and absolute dating methods. The spatial variations of depositional environments and processes can be better appraised when ages are available to constrain these events.

Reliable ages are fundamental pieces in the evolution puzzle. They provide the necessary time-frame to understand not only the changes of any coastal landscape, but also the sequence of geological, biological or anthropogenic processes leading to those changes. Both relative and absolute ages are significant, but most important is to know how to appraise them. Sometimes relative ages are either easier to obtain and/or the only temporal chronology available. Such is the case when working for example with dates associated to archaeological sites. In other instances, and sadly common, absolute ages (e.g. ^{14}C , ^{210}Pb , ^{137}Cs , optical dating, etc.) exist for certain locations throughout the area of study, but their significance is diminished when vital details such as geographic coordinates and burial depth are omitted in the literature. In this case, they must be treated as mere “relative” ages because it would be difficult to put them assertively in the spatial-temporal sequence of events relevant to the study area. This is of particular importance when, for example, the sedimentary depositional history of a site is under study. Hence, it is fundamental to associate locational information, including latitude, longitude and elevation, to all dating values in order to be able to systematically apply dates within their proper spatial context. When properly georeferenced, geochronometric data provide the means to understand the lateral and vertical evolution of any given coastal system. Whenever possible, comparison of ages obtained for the same deposit by multiple dating methods should be encouraged. Hence, correct optical ages from litho-stratigraphic units of known age should lend more credibility to OSL. However, it is somewhat uncommon to see literature that compares known ages obtained by other geochronometric methods to optical ones. Such scarcity of constraints can also be related to the low abundance/availability of suitable materials used in the different dating techniques.

1.2. RESEARCH OBJECTIVES

The purpose of this dissertation is to assess the supra-tidal evolution of a group of four coastal barriers based on the spatial-temporal analysis of their chronologies. The Apalachicola Barrier Island Complex is situated in the NE margin of the Gulf of Mexico, in a region called the Florida Panhandle (U.S.A.). It is composed of a series of barrier islands which from East to West are: Dog Island, St. George Island, Little St. George Island, St. Vincent Island, and St. Joseph Peninsula. Each of the barrier islands is decorated by a series of parallel to

sub-parallel beach and dune ridges and swales that, may or not, be truncated in some areas. Dog Island, a renowned pirate location in the 1800's, is the smallest of all. St. Vincent Island is one of the best examples of strandplain development in the Gulf of Mexico. The St. George islands are narrower barriers, depicting fewer successions of ridges. St. Joseph Peninsula is a classic example of a barrier spit with active ridge and inter-tidal flat progradation at the spit-end.

These previously poorly-dated systems are magnificent examples of ridge-forming strandplains, cusped forelands and barrier islands believed to have evolved since the Last Glacial Maximum. The major problem encountered in the Apalachicola Barrier Island Complex is the low number of available ages (geological and archaeological). The consideration of obtaining new absolute ages for this area would not only improve the age constraints on the coastal evolution of the Apalachicola Complex, but would also provide a valuable tool for the evaluation of previously published coastal progradation models. Moreover, the quartz OSL ages obtained from this research would help elucidate the timing of ridge formation between and within each of the barriers studied within the complex. In this regard, the optical ages may contribute to the understanding of the evolutionary history of this barrier complex.

In particular, this dissertation examines the application of OSL as the most accurate dating method to be used in this type of coastal setting. The validity of the OSL ages presented in this dissertation relies on the fact that this dating method captures the last depositional moment of any given grain of quartz, i.e. the burial date of the deposit. The analytical strategies pursued to obtain the most reliable equivalent doses, which in turn are used to obtain the OSL ages, are a critical element of this research. This dissertation was built on the understanding of the depositional environment of the sand grains analyzed, the geomorphological processes affecting deposition, and the significance of each sample's equivalent dose (OSL) data. Also, any syn- or post-depositional effect that could potentially lead to disturbances in the environmental dosimetry and the sample's equivalent dose distribution were also assessed. The findings of this research put into context past geomorphological evolution hypotheses with new temporal vertical-lateral chronologies from an absolute point of view.

Two specific objectives were established for this dissertation:

- To determine the OSL ages of a sequence of beach/dune ridges present on St. Joseph Peninsula, Cape San Blas, St. Vincent Island and Little St. George Island.
- To re-evaluate the supra-tidal evolutionary history of the barrier islands within the Apalachicola Barrier Island Complex based on new optical ages.

Four goals have guided this research. They are:

- To determine the feasibility of obtaining reliable quartz-OSL ages from long-vertical sediment vibra-cores, from diverse beach/dune ridges, at least at two different depth intervals within each sediment core.
- To quantify rates of coastal progradation of the barrier islands when possible.
- To compare and verify resulting OSL ages against reported ^{14}C -dates and any other geochronometric data obtained from archaeological and geological materials.
- To reconstruct the temporal chronology of the coastal geomorphology over the last several thousand years.

1.3. DISSERTATION STRUCTURE

Due to the extent of the study area, the number of samples dated and the objectives proposed for this investigation, it was possible to brake down this dissertation into various research papers, which lead to individual chapters. This dissertation starts with a general introductory chapter and ends with general conclusions presenting a synthesis of the major results obtained during this research, related to geology, archaeology and optical luminescence methodology, and recommendations for future research. The appendices encompass and frame all relevant information and methodologies used to obtain the resulting OSL ages presented throughout this dissertation in what has been intended to be a very comprehensible approach. Moreover, all the generalities concerning the environment where all the samples were collected as well as the entire compilation of resulting data are presented in the appendices.

While the brief discussion above provides a general overview of the concepts involved and intentions of this research, specific background knowledge, detailed objectives and fuller discussions are covered in the following individual chapters, which comprise the main body of the dissertation. The work presented in each chapter is based on six individual manuscripts: two short contributions and four long papers. Two of these papers have already been published in *Quaternary Geochronology*, one is currently in press (i.e. proof corrected) in *Journal of Coastal Research*, another has already been submitted and is currently under peer review (submitted in December 2006 to *Geoarchaeology*), while the last two are ready for submission to *Quaternary Geochronology* and *Earth Science Reviews*. The reader may find some unavoidable overlap of information throughout the different chapters in terms of study area, general theoretical background, some literature reviews as well as methodological aspects.

Chapter 2

“New quartz optical stimulated luminescence ages for beach ridges on the St. Vincent Island Holocene strandplain, Florida, United States.”

The first barrier island for which OSL results first came afloat was St. Vincent Island, the sole focus of Chapter 2. Here, a detailed review of all previously published archaeological and geological chronologies concerning this textbook example of strandplain is presented. Besides providing the reader with a new set of 14 OSL ages for the island, this paper also presents a comprehensive explanation of the significance of the age values related to depth within the sedimentary package. A regression analysis is also attempted to determine horizontal progradation and vertical sediment accumulation rates for the strandplain. The paper notes the absence of a standardized method for reporting OSL age results in terms of “years before date of measurement”, i.e. *datum*. It also identifies and reports, for the first time, the lack of [X,Y,Z] parameters associated to previously published (but while the paper was in review) OSL ages by other authors.

Chapter 3

“Characteristics of the Burial Environment related to Quartz SAR-OSL Dating at St. Vincent Island, NW Florida, U.S.A.”

Chapter 3 describes in detail the characteristics of the OSL data obtained from the samples retrieved from St. Vincent Island, which evolution is assessed in Chapter 2. It specifically focuses on the behaviour of the equivalent dose distributions in order to determine any possible relations to potential pedogenesis and/or post-depositional disturbances within each depositional environment. This short paper was presented at the LED 2005 Conference (Cologne, Germany), the most important luminescence and ESR conference in the World, from which proceedings were recently published in the newly (as of December 2006) individually established *Quaternary Geochronology* journal (formerly edited as special issues within *Quaternary Science Reviews*).

Chapter 4

“Optically Stimulated Luminescence age of the Old Cedar Midden, St. Joseph Peninsula State Park, Florida.”

Chapter 4 is the first of two geoarchaeology research papers presented in this dissertation. It conveys the results obtained from a single ridge on the bay-side of central St. Joseph Peninsula, from both a shell-rich midden surficial deposit and its underlying beach ridge. The importance of the site is related to the scarcity of well-preserved seasonal coastal settlements in the Apalachicola region. It is the first time an absolute dating chronology is obtained for this site.

Chapter 5

“Optical Dating Of An Ancient Coastal Occupation Site And Underlying Land On The Northwest Gulf Coast Of Florida, Near Apalachicola, U.S.A.”

The multi-authored paper reproduced in Chapter 5 associates the spatial-temporal OSL chronologies obtained from Richardson’s Hammock with the archaeological evidence found on the easternmost edge of this study area. Richardson’s Hammock was analyzed as a separate system due to its individual geological and archaeological significance. The importance of the hammock’s emergence in terms of development of coastal occupational sites in the region by early Floridian Peoples is assessed. The relationship between these atypical Richardson’s Hammock shell- and artifact-rich middens and those found along the other Apalachicola complex barrier islands is discussed.

Chapter 6

“Peninsular Evolution and Optical Dating of Young Coastal Ridges along the Gulf of Mexico.”

Chapter 6 describes the OSL findings for St. Joseph Peninsula and makes an attempt at unveiling the progradation of this barrier spit based on a new evolution hypothesis. It also involves the results obtained in Chapter 5, as these are essential to the primary stages of formation of the peninsula. Further to the optical ages, OSL data is also discussed in detail as new behaviour of equivalent dose distributions is evidenced, contrary to previous theoretical beliefs. This chapter also highlights a lack of detail given to location parameters associated with previously published ages obtained by different chronometric techniques.

Chapter 7

“Evolution and Optical Luminescence Dating of a Pleistocene and Holocene Coastal Barrier Complex, NE Gulf Coast, Florida, U.S.A.”

This final analysis chapter assembles the major results drawn from each one of the studied barrier islands pertaining to the Apalachicola River complex: St. Joseph Peninsula, Cape San Blas, St. Vincent Island and Little St. George Island. It discusses the general evolution of the complex as a whole by reviewing the OSL ages revealed in the previous chapters and introduces new data obtained from samples derived from the most ancient beach ridges of the region, located on the mainland, as well as the results obtained on Little St. George Island and Cape San Blas. Earlier evolutionary assumptions, mostly lacking geochronological data, are also assessed and re-evaluated. A new hypothesis regarding the timeline of progradation of each barrier and the relationship among all four studied areas is proposed.

REFERENCES

- Aitken, M.J., 1998. *An introduction to optical dating: the dating of quaternary sediments by the use of photon-stimulated luminescence*. Oxford: Oxford University Press, 267p.
- Aitken, M.J., 1985. *Thermoluminescence dating*. London: Academic Press, 359p.
- Argyilan, E. P., Forman, S. L., Johnston, J. W., & Wilcox, D. A. (2005). Optically stimulated luminescence dating of Late Holocene raised strandplain sequences adjacent to Lakes Michigan and Superior, Upper Peninsula, Michigan, U.S.A. *Quaternary Research*, 63(2), 122-135.
- Bailey, S.D., Wintle, A.G., Duller, G.A.T., & Bristow, C.S. (2001). Sand deposition during the last millennium at Aberffraw, Anglesey, North Wales as determined by OSL dating of quartz. *Quaternary Science Reviews*, 20, 710-704.
- Ballarini, M., Wallinga, J., Murray, A. S., van Heteren, S., Oost, A. P., & Bos, A. J. J. (2003). Optical dating of young coastal dunes on a decadal time scale. *Quaternary Science Reviews*, 22(10-13), 1011-1017.
- Banerjee, D., Hildebrand, A. N., Murray-Wallace, C. V., Bourman, R. P., Brooke, B. P., & Blair, M. (2003). New quartz SAR-OSL ages from the stranded beach dune sequence in south-east South Australia. *Quaternary Science Reviews*, 22(10-13), 1019-1025.
- Bateman, M. D., Boulter, C. H., Carr, A. S., Frederick, C. D., Peter, D., & Wilder, M. (2007a). Detecting post-depositional sediment disturbance in sandy deposits using optical luminescence. *Quaternary Geochronology*, 2, 57-64.
- Berger, G.W., Murray, A.S., & Havholm, K.G. (2003). Photonic dating of Holocene back-barrier coastal dunes, northern North Carolina, U.S.A. *Quaternary Science Reviews*, 22, 1043-1050.
- Bøtter-Jensen, L., McKeever, S.W.S. & Wintle, A.G., 2003. *Optically Stimulated Luminescence Dosimetry*. Elsevier, Amsterdam, 355 pp.
- Huntley, D. J., Godfrey-Smith, D. I., & Thewalt, M. L. W. (1985). Optical dating of sediments. *Nature*, 313, 105-107.
- Huntley, D.J., Hutton, J.T., & Prescott, J.R. (1993). The stranded beach dune sequence of south-east South Australia: a test of thermoluminescence dating. *Quaternary Science Reviews*, 12, 1-20.
- Huntley, D.J., Hutton, J.T., & Prescott, J.R. (1994). Further thermoluminescence dates from the dune sequence in the south-east of South Australia. *Quaternary Science Reviews*, 13, 201-207.

- Murray, A. S., & Wintle, A. G. (2000). Luminescence dating of quartz using an improved single-aliquot regenerative-dose procedure. *Radiation Measurements*, 32, 57-73.
- Murray, A.S., & Wintle, A.G. (2003). The single aliquot regenerative dose protocol: potential for improvements in reliability. *Radiation Measurements*, 37, 377-381.
- Murray-Wallace, C. V., Banerjee, D., Bourman, R. P., Olley, J. M., & Brooke, B. P. (2002). Optically stimulated luminescence dating of Holocene relict foredunes, Guichen Bay, South Australia. *Quaternary Science Reviews*, 21(8-9), 1077-1086.
- Ollerhead, J., Huntley, D.J., & Berger, G.W. (1994). Luminescence dating of sediments from Buctouche Spit, New Brunswick. *Canadian Journal of Earth Sciences*, 31, 523-531.
- Ollerhead, J., & Davidson-Arnott R.G.D. (1995). The evolution of Buctouche Spit, New Brunswick, Canada. *Marine Geology*, 124, 215-236.
- Stuiver, M. (1978). Radiocarbon timescale tested against magnetic and other dating methods. *Nature*, 273, 271-274.
- Van Heteren, S., Huntley, D.J., van de Plassche, O., & Lubberts, R.K. (2000). Optical dating of dune sand for the study of sea-level change. *Geology*, 28, 411-414.
- Wintle, A.G., & Murray, A.S. (2006). A review of quartz optically stimulated luminescence characteristics and their relevance in single-aliquot regeneration dating protocols. *Radiation Measurements*, 41, 369-391.

CHAPTER 2

NEW QUARTZ OPTICAL STIMULATED LUMINESCENCE AGES FOR BEACH RIDGES ON THE ST. VINCENT ISLAND HOLOCENE STRANDPLAIN, FLORIDA, UNITED STATES

Gloria I. López *

W. Jack Rink

McMaster University, School of Geography and Geology, AGE Laboratory
1280 Main Street West, Hamilton, Ontario, Canada, L8S 1M5

* Corresponding author: lopezgi@mcmaster.ca

Citation:

LÓPEZ, G.I., and RINK, W.J., 2007. New quartz optical stimulated luminescence ages for beach ridges on the St. Vincent Island Holocene strandplain, Florida, United States. *Journal of Coastal Research*, 23(0), 000-000.

Journal of Coastal Research: Coastal Education and Research Foundation (CERF), U.S.A., ISSN 0749-0208.

Status: accepted 2 December 2005, proof corrected September 2006, in press.

Copyright © (2007) Coastal Education & Research Foundation.

From Journal of Coastal Research, by Gloria I. López.

Reprinted by permission of Alliance Communications Group, a division of Allen Press, Inc.



810 East 10th Street
Lawrence, KS 66044 USA
Phone: 785-843-1235, 800-627-0932
Fax: 785-843-1853
E-Mail: acg@acgpublishing.com

To: Gloria I. Lopez C.
McMaster University
School of Geography and Earth Sciences
1280 Main Street West
Hamilton, Ontario, Canada L8S 4K1

From: Crystal Macmillan
Phone: 785-843-1235, ext. 256
Fax: 785-843-1853

Dear Gloria Lopez,,

On behalf of the Alliance Communications Group, I am pleased to grant permission to you reproduce the following article,

“New Quartz-OSL dating of Beach Ridges on the St. Vincent Island Holocene Strandplain, Florida, USA” in press for the *Journal of Coastal Research*.

... to appear in your Ph.D. thesis (McMaster University).

This permission is a one-time, non-exclusive, non-electronic worldwide grant for English language use as described in this letter, and is subject to the following conditions:

1. Payment of \$0.00 will be required.
2. Each copy containing our material that you reproduce or distribute must bear the appropriate copyright information, crediting the author, journal, and publisher:

Copyright © (year) Coastal Education & Research Foundation
From *Journal of Coastal Research*, by (author(s) name)
Reprinted by permission of Alliance Communications Group, a division of Allen Press, Inc.

3. The original author’s permission must also be independently obtained before permission is granted.

To ensure that any further permissions requests are processed in a timely manner, PLEASE EMAIL Crystal Macmillan at cmacmillan@acgpublishing.com.

If these terms are acceptable, please sign and date, and fax back to my attention at 785-843-1853. This permission will be effective upon our receipt of the signed contract. When sending payment, please make clear reference to our title and author. Materials should be addressed to *Journal of Coastal Research*, ACG, P.O. Box 7052, Lawrence, KS 66044.

Sincerely,

Crystal Macmillan
Publishing Manager
ACG, A Division of Allen Press, Inc.

AGREED: _____

DATE: Oct 17, 2006

_____ We have elected not to use this material.

ABSTRACT

St. Vincent Island, located on the northwest Gulf of Mexico coast of Florida, U.S.A., preserves a well-developed beach ridge plain that is generally believed to have begun to form in Mid-Holocene time. This study evaluates the potential of optical stimulated luminescence (OSL) to appraise the proposed evolution and progradation of this strandplain. OSL was used to obtain the ages of the quartz samples extracted from 7 vibra-cores at two depth intervals. The SAR-OSL ages increase from the shores on the Gulf of Mexico to St. Vincent Sound. The younger ridge set yielded ages of 370 ± 49 to $1,890 \pm 292$ years (A.D. 2004 datum) conferring an inter-ridge accretion time range of 78 to 148 years assuming uniform sediment accumulation. The oldest ridge set yielded ages of $2,733 \pm 404$ to $2,859 \pm 340$ years, consistent with the estimated age based on archaeological materials of 3,000-4,000 years ago. For the south-western beach ridge set, the ages provide insights on the aeolian accumulation and re-working processes effective throughout the ridges despite their vegetation cover. Our results highlight the potential of OSL as an application to use not only for dating but also for coastal dynamics assessments. The SAR-OSL ages presented herein provide new reliable absolute ages on the beach ridge sequence of St. Vincent Island and improve the age control on formation of barrier island sequences in the Florida Panhandle region.

2.1. INTRODUCTION

This study attempts to examine the proposed evolutionary history of the St. Vincent Island strandplain with absolute ages obtained with Optical Stimulated Luminescence (OSL) and compare them with other age estimates found in previously published studies for the area. At the time of review of this paper, new valuable data was published regarding the age assigned to some of St. Vincent Island's beach ridges (cf. OTVOS, 2005). However, the dates presented here appear to be the first group of quartz derived OSL ages to have realistic values and therefore follow a consecutive order for the island. Moreover, this is the first study reporting OSL samples obtained from long vertical sediment cores (> 2 m of sediment) recovered from Holocene coastal deposits.

OSL is considered a young absolute geochronological method, which has been improved considerably over the last few years (i.e. measurement apparatus, estimation technique and analysis of resulting data). The principle of optical dating is based on the ability of naturally occurring minerals (such as feldspar and quartz) to record the amount of natural ionizing radiation (in the form of α , β , γ and cosmic rays) present in the environment (HUNTLEY *et al.*, 1985; AITKEN, 1998). The liberation of such energy (charge trapped in the mineral) gives rise to an OSL signal, which can be measured. Hence, the method depends on the capacity of the mineral to absorb (i.e. exposure) and conceal (i.e. burial) sunlight

from the point of their most recent deposition. By measuring the natural luminescence signal and subsequent signals artificially produced by controlled laboratory doses on the same sample, an estimate of the radiation intensity to which the sample was originally exposed to during its burial time can be obtained (i.e. equivalent burial dose). Thus, OSL is particularly interesting for active sedimentary systems such as coastal environments as their sediments in many cases have been well exposed to sunlight just prior to burial. Results from studies developed for quartz-rich coastal deposits around the world have consistently shown the value of OSL in these environments, which may sometimes lack suitable materials to be dated by other means. Intricate barrier spit parabolic dune complexes, young coastal dunes, relict foredune sequences, and stranded beach dune sequences have been assessed for accuracy and precision of quartz-OSL dating and the ages obtained have been in accordance with both the proposed evolution of those areas and the ages acquired by other independent dating methods (e.g. MURRAY-WALLACE *et al.*, 2002; BALLARINI *et al.*, 2003; BANERJEE *et al.*, 2003).

2.1.1. STUDY AREA

The study area is a barrier island located in the north-eastern area of the Gulf of Mexico about 10 km south-west of the city of Apalachicola in Franklin County, Florida, U.S.A. (**Figure 2.1**). The island is triangular in shape, extends 14 km east-west and about 6-7 km at its maximum north-south width and is situated 2-3 km offshore to the south of the Florida Panhandle mainland. It comprises most of the St. Vincent Island National Wildlife Refuge, with an area of 12,358 acres. St. Vincent Island is part of the Apalachicola river delta barrier island complex and is geomorphologically characterized as a strandplain dominated by east-west trending, elongate, curvilinear beach ridges separated by lowlands, which are flooded during periods of high rainfall. The south-eastern area of the island is characterized by seasonal ponds, which occur within the beach ridge sequences at their south-eastern terminations. Located further north on the east side of the island are intermittent streams, which drain the lowlands to the coast or into ponds.

The island can be divided into two main areas with respect to general beach ridge elevations. Elevations of the beach ridges are generally higher, most often slightly higher than 2 m but occasionally up to 4 m in the south-western beach ridges to the south of Big Bayou, while to its north, the ridge elevations are much lower, not exceeding 1 m. All the beach ridges seen on the strandplain can be categorized as established ridges due to the high vegetation and soil development. Only the modern foredune ridges located just above maximum high tide level landward of the foreshore on the southern shorelines of the island can be categorized as incipient ridges with ephemeral grass-type vegetation.

The vegetation (MILLER *et al.*, 1981) on the southern part of the island is dominated by ridge crests mainly occupied by mature stunted oaks and shrubs that form a scrub oak dune environment, while the beach ridges adjacent to the northerly St. Vincent Sound are characterized by hardwood hammock with magnolia, juniper and oak trees. The lowlands on the Gulf side are occupied by a slash pine - cabbage palm hammock, while the northernmost lowlands occur in a tide marsh environment north of the hardwood hammocks.

2.1.2. PREVIOUS GEOLOGICAL, GEOCHRONOLOGICAL AND ARCHAEOLOGICAL WORK

Even though determining what parameters induced the construction of the St. Vincent beach ridges and strandplain is not the primary goal of this paper, it is important to review some of the factors responsible for the formation of beach ridges. To date, there is no widely accepted beach ridge building model as many authors continue to debate this matter (e.g. TANNER, 1995; TAYLOR and STONE, 1996; OTVOS, 2000). What is apparent, in general, is that sandy beach ridges are formed by the interaction of a multitude of factors throughout their time of development. As OTVOS (2000) states, a beach ridge is a relict coastal ridge that may consist of a combination of water- and later wind-deposited material. A detailed study of the different lithosomes composing the ridge (i.e. sedimentary structures, grain size), its geometry and size (i.e. elevation) may elucidate which process has been more relevant during formation (OTVOS, 2000) but they may not be specific for every existing landform. For example, steep broad beach ridges showing cross-strata and fine to medium coarse sand are associated with a foredune origin, i.e., a wind-built ridge at the landward edge of the backshore, just above the high tide limit (SHERMAN and HOTTA, 1990; OTVOS, 2000). On the other hand, beach ridges with distinct parallel laminations and/or relatively low-angle cross strata and fine to coarse sand characterize water-laid berm-associated ridges. The dimensions of these relict berm ridges, once situated at the limit between the foreshore and backshore, are variable as they depend directly on oceanographic conditions at the time of development (i.e. wave, current, tides and water-level conditions) (OTVOS, 2000).

Previous geological and sedimentological studies on St. Vincent Island and surrounding areas have been ongoing since about the early 1960's. STAPOR (1973, 1975) studied in detail the sedimentology and geomorphology of the St. Vincent Island ridges arguing that they were primarily swash-built with little to no aeolian decoration developed atop. According to STAPOR (1975), the beach ridge plain was reported to record a complex history of interrupted deposition as seen by the different ridge shapes and elongations, primarily due to variations in the volume and direction of delivery of sand supplied. Moreover and related to these variations, STAPOR (1975), TANNER (1988, 1995) and TANNER *et al.* (1989) argue that these water-laid semi-parallel to parallel landforms with

elevations up to 4 m above mean sea level were controlled by a succession of sea level fluctuations during the last 6,500 years. This is subject of much conjecture as the elevation of the ridges may not be suitable to establish past sea level positions (OTVOS, 2000) but rather intense aeolian influence and built-up.

The beach ridges from this strandplain were first divided into “pattern sets” by STAPOR (1973, 1975) and later into “Ridge Sets” defined based on geomorphological (e.g. orientation), sedimentological and elevation characteristics (**Figure 2.2.**) (STAPOR and TANNER, 1977; TANNER *et al.*, 1989; TANNER, 1992). The earliest sequence of ridges (Ridge Sets A, B, C) is located north of Big Bayou, followed to the south and west of it by Ridge Sets D, E, F, G, and to the southeast corner of the island with the later formed Ridge Sets labelled H, I, and J. The ridges on the south-western and south Gulf shores were labelled K and L and are considered to be the very youngest sets. An interpretation of the Holocene history of the sequence of beach ridge formation of St. Vincent Island and St. Joseph Peninsula to the west was reported by STAPOR (1973). In this interpretation, the earliest formed, northerly beach ridge sets above Big Bayou (Tanner’s Ridge Sets A, B, C) were formed between 6,500 and 4,000 years ago. The parts of the sequence corresponding to Tanner’s D, E, F and G Ridge Sets were reported to have been formed between 3,000 and 1,000 years ago, and all of the remaining ridge sets were formed after that time.

Previous dating studies on St. Vincent Island have yielded a number of age estimates based on geological and found archaeological materials. A report by MILLER *et al.* (1981) provided much sought details on the initial investigations of archaeological sites on the oldest beach ridges on the north side of the island. Details regarding location and original site numbers from first excavations on St. Vincent Island (now in the current Florida Master Site File – FMSF- number for archaeological and historical data) are better specified in older maps and location figures (e.g. MILLER *et al.*, 1981; STAPOR, 1975) than in some newer publications. Up to 16 pre-historic shell midden locations have been reported on the island as well as few other historical sites since the preliminary archaeological survey in 1970 by David S. Phelps (MILLER *et al.*, 1981). On the Pickalene Shoreline along the northwest side of the island (see **Figure 2.1.**), the earliest sites that have been reported are associated with Late Archaic period settlements containing fiber-tempered ceramics (MILLER *et al.*, 1981; WHITE, 2003). Examples of these early peoples’ sites are locations 8Fr360, 8Fr361, 8Fr71 (FMSF numbers) where the ceramics were found within shell-rich clay layers or in shell middens overlaying the respective beach ridges (STAPOR, 1975 and CAMPBELL, 1984). The generally accepted age range for these primary types of northwest Floridian pottery sherds is 5,000 to 3,000 years ago (i.e. 3,000 to 1,000 B.C.) (MILANICH, 1994; WHITE, 2003). DONOGHUE and WHITE (1995) reported that “the oldest ridges (on St. Vincent Island) are approximately 3,000 to 4,000 years old, based on the presence of Late Archaic artefacts and a

few radiocarbon dates”, citing STAPOR (1973) and STAPOR (1975) with regard to the radiocarbon dates.

Either associated with the previously mentioned Late Archaic fiber-tempered pottery sites (e.g. site 8Fr361) or located individually (e.g. site 8Fr364), post-Archaic materials have also been found along the Pickalene Shoreline (MILLER *et al.*, 1981; CAMPBELL, 1984). These ceramics pertaining to the Deptford Culture (Early Woodland period) provide a younger time range for the existence of this northern area of the island, extending from as early as 3,000 to 1,800 years ago (i.e. 1,000 B.C. to ~ 200 A.D.) (MILLER *et al.*, 1981; MILANICH, 1994; DONOGHUE and WHITE, 1995). Hence, the presence of the Late Archaic ceramics on St. Vincent Island can be used as a good tool to suggest the minimum age for the formation of the northern shoreline ridges to > 3,000-4,000 years ago. In other words, the beach ridge(s) that contain Late Archaic middens could not have been formed after ~ 3,000 years ago if the oldest ceramic elements truly date to ~3,000 years ago.

Unfortunately, very few radiocarbon ages done on geological materials have been reported and/or published for the island. At site 8Fr71 on Paradise Point (see **Figure 2.1.**), a clay layer containing charcoal lenses has been inferred to be 1,710 years B.P. (MILLER *et al.*, 1981; BRALEY, 1982; CAMPBELL, 1984) on the basis of its “archaeological content”, and a radiocarbon age of $2,110 \pm 130$ years B.P. was attributed using *Mulinia* sp. shells (STAPOR, 1975; CAMPBELL, 1984) from a marine shell bed in a location named “Site B” about 3 km south of St. Vincent Point on the east side of the island.

More recently and while this paper was in review, new but quite anomalous luminescence ages obtained from this strandplain complex were published (i.e. OTVOS, 2005). Eight ridges throughout St. Vincent Island were sampled by OTVOS (2005) to obtain a total of 15 OSL ages (including duplicates of the same sample) and two thermoluminescence (TL) ages. Interestingly enough, the sites selected by OTVOS (2005) follow almost the same geographical pattern that we chose for our samples and nearly all are located in the same “Tanner’s Ridge Sets” that we selected (c.f. OTVOS, 2005, Figure 16). For comparison purposes, only the OSL ages would be taken into account knowing that the OSL age protocol he used was the same that the one we used to obtain our OSL ages. For the northern side of the island, he reports ages that range between $6,930 \pm 790$ and $3,950 \pm 530$ years ago as for the ridge closest to the Gulf shoreline, an age range of 10 ± 3 to 602 ± 71 years ago was obtained (c.f. OTVOS, 2005, Table 2a). Furthermore, the ages that he reports for the central area of the island range from -6 ± 3 to 564 ± 69 years which is completely unrealistic. Even though in general OTVOS (2005) OSL ages are decreasing from North to South, the values do not portray realistically the time between ridge formations. A possible explanation to these strange OSL values is given in the

discussion section of this paper accounting for the depth of sampling that OTVOS (2005) used (i.e. 30 cm below ground surface).

2.2. SAMPLES AND METHODOLOGY

Seven sediment cores were recovered from St. Vincent Island in July 2003. Sample locations are shown on **Figure 2.1.** and listed in **Table 2.1.** Their locations were determined with a hand-held Garmin global positioning system unit using the NAD 83 map coordinate system, U.S. Geological Survey 1:24,000 topographic and bathymetric maps for the area (USGS, 1982) and the 1999 Digital Orthographic Quarter-Quad (DOQQ) photographic maps for the island (FDEP, 1999). Our southern group of core sites is located on ridges crossed by Road 4 towards the south-central part of the St. Vincent and the other two core locations were accessed through the northern portion of Road 5 at the North end of the island (**Figure 2.2.**). Five of the seven core sites were located on crests of ridges with the exceptions of core SVI #2b which was recovered from the landward slope of the ridge where core SVI #2 was taken, and SVI #5 which was recovered from a vegetated tidal flat among isolated patches of cabbage palm present on the high grounds of the northernmost beach ridge. The sampling strategy in these two cases allowed potentially deeper penetration into the ridge structure. The cores were collected using soft aluminium irrigation pipes (diameter 7 cm; length 3 to 6 m) to avoid exposure of sediments to sunlight. The inside of each pipe was carefully cleaned and ends temporarily capped prior to coring to minimize the risk of external contamination. Up to 3 cm of sediment from the surface of each coring site was removed immediately before the initiation of coring to minimize any contamination with surface grains exposed to daylight. Coring was done using a portable gas-operated vibracore and a 1.2 m-long truck jack was used to retrieve the sediment cores. The maximum core length obtained was 2.20 m of compacted unconsolidated sediment (core SVI #3) and the minimum core length was 2.12 m (core SVI #1). Sediment cores were cut into manageable lengths and transported to the AGE Laboratory (McMaster University) where they were split open under low-level orange illumination.

All laboratory procedures and treatments involving samples for OSL determination were conducted under low intensity orange lighting conditions. Samples from cores were selected based on visual observations of homogeneity of the sediment within 30 cm of its location along one split half of each core in order to insure uniform γ irradiation (i.e. samples near lithologies containing significant concentrations of heavy minerals were avoided). Sufficient material for OSL analyses could be obtained from one of the two split halves of clastic-rich unconsolidated sediment cores. The removed samples were 5 cm-long slabs of sediment. Material from the outermost area of the sample closest to the edges of the pipe was excluded to minimize contamination from material dragged along the core during collection. The upper sample from each core (sub-sample OSL2)

met the criterion that its original burial depth was at least 50 cm below the surface. This criterion was established to avoid the effects of soft cosmic rays (which are essentially electrons) which get absorbed within the first half metre below ground surface (AITKEN, 1985, 1998). Original sample depths relative to the ground surface were calculated by taking into account the degree of compaction and are reported in **Table 2.1**.

Sand-sized quartz separates from 14 core samples were used for the age estimations. Water content determination was derived directly by oven-drying each OSL sample at 55° C. Sub-samples (~5 g) extracted from each dried whole sample were sent to the Centre for Neutron Activation Analysis at the McMaster University Nuclear Reactor facility (Hamilton, Ontario, Canada) for ²³⁸U, ²³²Th and ⁴⁰K content determination (**Table 2.1**). The remainder samples were initially treated with 10% HCl, 30% H₂O₂ and then oven-dried. The samples were then dry-sieved (20 minutes standard per sediment load in sieves) to obtain the 150-212 µm fraction of sediment. The quartz grains were obtained and separated from any heavy minerals and potassium feldspars by heavy-liquid separation using Li-polytungstate (2.62 – 2.70 g/cm³). A 40-minute immersion in 40% HF (to etch the outer 10 µm of each quartz grain thereby eliminating the dose contributions from external α-particles and to dissolve plagioclase feldspar) and another 40-minute treatment with 10% HCl finalized the procedure. Each quartz sample separate was checked under petrographic microscope to determine its purity.

An automated RISØ TL-DA-15 reader was used for all the single aliquot OSL measurements. Blue light-emitting diodes (470 ± 30 nm) were used for stimulation at 90% of their power and at 125° C for 100s. The resulting OSL signal was measured through a single 6 mm-thick Hoya U-340 filter (280 to 370 nm detection window). Laboratory irradiations were done using a calibrated ⁹⁰Sr beta source attached to the reader.

The 150-212 µm quartz separates from each sample were mounted on individual aluminium discs (10 mm in diameter) using an 8 mm silicon spray mask (which glues ~ 1,000 grains onto the aliquot). An initial check for feldspar contamination was done using infrared stimulation (830 nm detection window). Prior to the equivalent-dose (D_E) determination, pre-heat plateau tests were performed on 12 aliquots of each sample at 4 different temperatures (160°, 200°, 240° and 280° C) to assess the effect of pre-heating on the grains. A flat plateau across the temperature range from 160° to 280° C was observed in all cases. A 10 s pre-heat at 160° C was selected for use on all samples. D_E was determined using the single-aliquot regenerative-dose (SAR) protocol (MURRAY and WINTLE, 2000) on 24 aliquots of each sample. Laboratory regeneration doses were estimated based on initial D_E assessments performed on 3 aliquots of each sample prior to the application of the SAR protocol. Distributions of D_E values among

aliquots of the same sample were examined as frequency distributions with a spacing of 0.01 Gy.

D_E data obtained after each measurement was analyzed with the RISØ Luminescence Analyst program (version 2.22) using linear fitting of the regenerated luminescence. The luminescence signal intensity was determined using the first 0.4 s of emission. Only recycling ratios between 0.90 and 1.10 were used for the age determinations. Age estimates, age errors and cosmic-ray dose rates were determined using the Anatol program (version 0.72B) provided by N. Mercier. The cosmic-ray dose rate was calculated using a 2 g/cm^3 of overburden density. Internal concentrations of 0.06650 ± 0.02194 ppm of ^{238}U and 0.11350 ± 0.04248 ppm of ^{232}Th were used based on RINK and ODOM (1991) calculations for granitic quartz. External γ and β dose rates were calculated assuming secular equilibrium in the ^{238}U and ^{232}Th decay chains. A standard F-value of 0.8 ± 0.2 (AITKEN, 1985) was used (i.e. deals with the saturation level -porosity- existent at the moment of burial) and a global systematic error of 20% was also added to the equation (i.e. conservative value that deals with any other potential error external to laboratory procedures including that of the unknown actual moisture content during burial).

2.3. RESULTS

Sediments recovered in cores were mainly medium to fine sands, and some significant occurrences of peaty sandy clays in the cores SVI #5 and SVI #6. Grain sizes ranged from <90 to $>250 \mu\text{m}$. Scarce fine particles of organic matter also occur throughout the cores. Roots generally occurred toward the top of the cores, except for SVI #5 and SVI #6, where they also occurred deeper, at depths of 90 to 100 cm below the surface. Orange to brown staining of sand grains generally occurred below 100 cm depth, but in SVI #0 and SVI #1 this staining was evident at shallower depths. Extracted portions of the core used for dating analysis were composed of 1-5 wt.% potassium-rich feldspar, 1-5 wt.% organic matter plus carbonates, 5-20 wt.% heavy minerals, and up to 93% quartz plus plagioclase feldspar. The lower sample from each core (sub-sample OSL1) had sedimentological characteristics of foreshore facies (sub-horizontal to horizontal laminae) with heavy minerals either dispersed or showing thin laminae ($< 1 \text{ mm}$). The upper sample from each core (sub-sample OSL2) was sedimentologically concordant with dune facies characterizing an aeolian lithosome towards the top of each core. Based on the lithological and sedimentological analyses, St. Vincent Island beach ridges seem to have been initiated as berm ridges which later were initially buried by aeolian material forming the relatively steep shoreline beach ridges we see nowadays.

All samples showed Late Holocene depositional ages. The SAR-OSL ages are referred to the date of the measurement, in this case November-

December 2004 (i.e. A.D. 2004 datum). This is important to account for when comparing with ^{14}C -derived ages due to the offset of years between the ^{14}C and OSL values, and the reference datum used for the ^{14}C age (i.e. A.D. 1950 or A.D. 2000 datum). If the time elapsed between different measurements is large enough, the offset between different published OSL ages for the same area should also be taken into account (given a datum is provided). The results are shown in **Table 2.2.** along with the results of the U, Th and K concentrations obtained on sub-samples of each OSL sample as a whole (i.e. these sub-samples did not undergo chemical treatment prior to NAA). We note the very large contribution of the cosmic-ray dose rate that ranged from 47 to 75% of the total dose rate. The ages were calculated assuming a constant sedimentation rate (thus we used a value of $\frac{1}{2}$ of the present day burial depth for calculation of the cosmic-ray dose rate). In other words, we assumed that these beach ridges were progressively formed throughout time rather than “instantaneously”, giving time for wind-laid sand to build up the ridges atop initial water-laid landforms which constituted the base for each ridge. This is justified by the very large difference in D_E at different sample depths in the same core, which excludes the possibility of very rapid burial. Samples showed increasing age with depth in five of the cores (SVI #0, SVI #1, SVI #2, SVI #2b, SVI #3). In the other two cores (SVI #5, SVI #6) ages from samples at different depths were statistically indistinguishable from one another.

Figure 2.3. shows the ages plotted as a function of depth within each of the cored ridge sites and distance from the nearest shoreline. The more southerly group of beach ridges (SVI #0, SVI #1, SVI #2, SVI #2b, SVI #3, hereafter referred to as the south-western group) yielded ages ranging from 370 ± 49 to $1,890 \pm 292$ years ago. The remaining two ridges (SVI #5, SVI #6, hereafter referred to the north-eastern group) yielded ages ranging from $2,733 \pm 404$ to $2,859 \pm 340$ years ago. Since we have no clear indication that we reached the base of the ridges in the cores (i.e. the relict berm-ridge or the base of the relict and superimposed foredune), the ages represent minimum ages of formation of each ridge. In order to avoid any confusion regarding “minimum” and “maximum” ages, we opted to use the terms terminus ante quem (i.e. formed prior to the given age) and terminus post quem (i.e. formed after the given age) when referring to the age of formation of the ridges based on our OSL ages. Hence, the ages obtained from the deeper intervals of the cores (i.e. sub-sample OSL1) mark a terminus ante quem for the formation of the beach ridges.

Two of the cores (SVI #2 and #2b) were taken on the same ridge, with the former on the ridge crest and the latter at a slightly lower elevation and about 10 m landward of the SVI #2. The uppermost samples from these two cores showed statistically indistinguishable ages of 782 ± 97 and 842 ± 100 years ago, showing good agreement between cores only 10 m apart. The deeper samples showed different ages, with SVI #2b showing a younger age of $1,102 \pm 126$ years ago at a sample depth of ~ 160 cm, while the deeper sample coming from SVI #2 (at 217

cm depth) showed a much older age of $1,641 \pm 208$ years ago. This result allows us to see age differences that probably correspond to lateral homogeneity during the time of deposition across this distance (i.e. if we had had samples from equivalent depths in the deeper levels of both cores, we probably would have obtained the same age). The upper ages in the cores (i.e. sub-sample OSL2) then may represent individual times of formation of the aeolian lithosome of the ridges. The explanation for the large gap in time between these values and the lower ones is further discussed later and we believe it has implications for beach ridge evolution.

From the dating results we were able to calculate an average sediment accumulation rate (ASAR) over two depth intervals in each core (**Table 2.3.**). **Figure 2.4.** shows the results for the south-western set of beach ridges. Given that the deeper samples are *terminus ante quem* for the initiation of the ridges and that the upper samples correspond to ages associated with aeolian activity on the island post-dating the formation of the relict berm ridges, these accumulation rates are just an estimate of the amount of material deposited vertically through time to form the current shapes of the inland St. Vincent Island beach ridges. Hence, our ASAR values may be considered as apparent sedimentation rates for the south-western set of beach ridges as they grew in time. It is known that for an incipient foredune to grow both vertically and laterally the existence of some plant species has to occur and the vegetation growth has to keep up with the ridge's build-up process (HESP, 2002). In ridge-type environments, foredune ridge accretion rates are relatively high as the incipient foredune progresses into an established dune (with higher vegetation) as the system accretes seaward and the ridge grows vertically (HESP, 2002).

It is seen that the ASAR in the upper 1 m of all the south-western cores ranges from 0.11 to 0.28 cm/yr (data set B) while in deeper intervals of the same cores the ASAR ranges from 0.14 to 2.08 cm/yr (data set A). It is clear that the upper interval in all cores shows a slower ASAR than in the lower interval, consistent with expectation that with increasing distance from shore through time (due to the accretion of new ridges shoreward through time), the sand accumulation rate should decrease landward. In addition, ASAR in both the of the landward-most ridges is effectively the same in both intervals of each core, showing that recent accumulation in the upper parts occurred slowly and at a similarly very slow rate in the deeper interval. Both of these cores come from ridges that are about 1,200 and 1,600 m from the present day Gulf shoreline. Similar calculations of ASAR in the older ridges of the north-eastern group of samples yielded values of only 0.04 and 0.03 cm/yr for the upper 1 m of sediment, values that are roughly 1/3 of observed values for the slowest accumulation rates in the south-western group.

Distributions of equivalent doses were examined for all samples. Remarkably, all 24 aliquots in every sample fell within the accepted recycling ratio range between 0.90 and 1.10 (for the 8 mm diameter sample size, which was used for the ages in this study). For most samples, a simple nearly normal distribution of D_E was observed, with no significant change when mask size was reduced to 3 mm for each set of 24 aliquots. We interpret this as a negative evidence for incomplete zeroing at burial. Most samples did show a single aliquot (of 24) with a value greater than $+2\sigma$ of the mean in the D_E distribution, in which case the single value was excluded from recalculation of the mean. A typical frequency histogram of D_E values seen in this study is shown in **Figure 2.5**. Anomalously high values of D_E are probably due to the proximity of some of the grains in the aliquot to highly radioactive grains *in situ*. Detailed analyses of D_E distributions and sedimentological characteristics of the sediment sequence are presented elsewhere (LÓPEZ and RINK, 2005).

2.4. DISCUSSION

The oldest age estimate found in this study is $2,859 \pm 340$ years ago for the northernmost ridge location on St. Vincent Sound (core SVI #5). This yields a maximum *terminus ante quem* date of 3,199 years ago (i.e. age plus error) for the deposition of this ridge in Tanner's Ridge Set A. Since we are not sure how close this sample is to the base of the ridge, we must assume that the ridge started to form (i.e. the relict berm ridge) before the deposition of the sand dated, thus $\sim 3,200$ years ago is the *terminus ante quem* estimated for the beginning of this ridge's formation. Furthermore, we interpret SVI #5 to be located on the oldest beach ridge on the island. The position of this ridge corresponds with a series of nearby archaeological sites on the eroding Pickalene Shoreline further west which contained Late Archaic fibre-tempered pottery that overlie the beach ridge at sites 8Fr360, 8Fr361 and 8Fr364 (WHITE, 2003). The accepted time range for this pottery style is $> 3,000$ -4,000 years ago. From the original base maps used in that study, these sites lie on the edge of the Pickalene Shoreline on eroding beach ridges that may either belong in Tanner's Ridge Set A or B according to the orientation and shape of the ridges (see **Figure 2.2**). Thus our OSL age estimate of up to 3,200 years ago agrees with the younger portion of the accepted ages for Late Archaic pottery occurring on ridges that correlate with ridge A or the next ridge inland, and is consistent with occupation of this land by makers of the earliest style of north-western Floridian fibre-tempered pottery. Stratigraphically, our maximum *terminus ante quem* age of 3,200 years ago is almost certainly at lower elevation than the position of the Late Archaic archaeological sites, nonetheless they are consistent with the younger part of the age range of the Pickalene Shoreline (i.e. 3 to 4 ka). We believe that if it is later shown by high resolution elevation determinations that are samples are lower, it may be a result of the subsidence of the ridge sequence on the north-eastern corner of the island.

In any case, the north-eastern sequence does not extend westward into the Pickalene area and we acknowledge that a direct correlation of these ridge sequences is tentative at best.

The ages for core SVI #6, associated with Tanner's Ridge Set B are statistically indistinguishable from those for core SVI #5, in Ridge Set A indicating sedimentation within ridges within an interval corresponding to the range of the maximum and minimum ages determined by OSL (i.e. age minus its error and age plus its error). This corresponds to times between 2,439 and 3,199 years ago. Furthermore, a very rapid sediment accumulation may be implied for this area based on the closeness of OSL ages between these two ridges (within the limits of the ages' uncertainties). Hence, this northernmost area of St. Vincent Island may have experienced a high sediment supply ~3 ka ago for at least the 700 m closest to the St. Vincent Sound shoreline which comprise Tanner's Ridge Sets A and B.

OTVOS published OSL ages (2005) for the north-western, north-eastern and south-western parts of St. Vincent Island. Otvos' sample 7 from near the North end of Road 5 (c.f. OTVOS, 2005, Figure 16) yields considerably older results than our sample SVI #6 from the same vicinity (**Figures 2.1.** and **2.2.**). Despite a considerable time difference, our terminus ante quem age of $2,777 \pm 338$ years ago is concordant with his age for this ridge of $6,001 \pm 660$ and $6,930 \pm 790$ years ago (i.e. OSL values obtained for Otvos' sample 7). At the north-western segment of the island, Otvos' samples 1 and 2 come from the northernmost part of the ridge sequence on Road 3 that sampled to the southeast on Road 4 (see **Figure 2.2.**). From North to South his samples 1 and 2 yielded ages of $3,950 \pm 530$ (with a duplicate sample giving $5,220 \pm 606$ years) and $3,080 \pm 260$ years ago, which are older than and thus concordant with our dated sequence whose oldest ridge (our sample SVI #3) yielded a terminus ante quem age of $1,890 \pm 292$ years ago.

However, in this same area Otvos' sequence of ages for samples on Road 3 in equivalent ridges to our sequence on Road 4 (see **Figure 2.2.**), are only consistent with our ages that come from the upper intervals of our cores. For example, our sample SVI #2 at a depth of 1 m yielded an age of 782 ± 97 years and his sample 5 yielded an age of 244 ± 27 years at a depth of only 30 cm. A detailed discussion of the ages and formation episodes of the sediment in the upper intervals of our cores in this south-western sequence are discussed later, which we believe explain in part why both OTVOS (2005) ages and our upper interval ages significantly postdate the time of ridge formation.

The older beach ridges that host the north-eastern group of OSL ages on the north side of the island are much lower in elevation than those of the south-western group. Unfortunately, no high precision GPS surveying has yet been done on these ridges to determine their accurate elevation above present sea level.

However, it is clear from the topographic maps (i.e. USGS, 1982) that these ridges do not surpass 1 m in elevation, being the lowest throughout the island. Moreover, the presence of vast active vegetated and un-vegetated inter-tidal marsh flats on the northern edge of the island (i.e. mostly encompassing the area of Tanner's Ridge Set A) confirms the low elevation state of this part of the island (i.e. as seen in the field by the authors). These low elevations have been used by others to infer low sea level stands in Holocene time (STAPOR, 1975; TANNER *et al.*, 1989; STAPOR *et al.*, 1991; DONOGHUE and TANNER, 1992; TANNER, 1992). However, given their type, it is not appropriate to assign sea level conditions based on the elevations of the crests of these ridges as there has been a long history of aeolian activity present throughout their formation. We note that the low-lying ridges north and east of Big Bayou and the round to semi-round ponds (and lagoonal areas) within Ridge Sets D and C (see **Figures 2.1.** and **2.2.**) seem to reflect the possibility that significant amounts of subsidence have occurred on this north – north-eastern part of the island. OTVOS (1985) attributed the formation of the lagoonal areas to subsidence of ridge plain swales due to compaction of mud-rich units present below the Holocene strandplain sequences forming the surficial topography of the island. This same process may also have been responsible for lowering the island's northern ridges as also noted by OTVOS (1995).

We further note that similar to St. Vincent Island but on the Atlantic coast of Florida, analogous landforms also occur on the north-western side of Merritt Island, which lies just west of Cape Canaveral. Merritt Island was also an ancient barrier island which formed before the deposition of Cape Canaveral. The low lying landforms lay on the landward side of this ancient barrier island. These have been suggested to reflect karst development there (BROOKS, 1972), a process that has also been suggested as a possibility for the Floridian mainland just north of St. Vincent Island (OTVOS, 1995; 1999). Further deep-coring will be needed to establish if the land surface is sinking on St. Vincent Island and hence help us understand whether the low lying ridges on the northern part of St. Vincent might really reflect Holocene sea level low stands.

The only radiocarbon date from St. Vincent Island of $2,110 \pm 130$ years B.P. comes from shells recovered from a core extending from mean high water to about 8 m below that level (STAPOR, 1975; CAMPBELL, 1984). The precise location of the dated sample in the core is not shown in the publications we have reviewed, but comes from a marine shell bed above a clay layer in the area of Tanner's Ridge Set D. In any case we cannot relate the stratigraphic position of this ^{14}C -dated sample to the beach ridges we have studied. However, in general it falls in between the time period elapsed since the deposition of the deeper sand dated from core SVI #3 and that of core SVI #6.

Moving to the south-western part of the study area, four ridges were dated and an analysis of the accretion rates, based on a constant accretion rate model was conducted for this south-western group of samples. For the deepest samples in each core (i.e. the ones giving us the *terminus ante quem* for the formation of their respective ridges) there is a steady progression of increasingly younger ages from northeast to southwest, with the oldest age being $1,890 \pm 292$ years (SVI #3) and the youngest being 408 ± 58 years (SVI #0). These cored ridges are ~1,360 m apart along Road 4, a transect perpendicular to shore that crosses ridges consistently parallel to each other and the modern Gulf side foredune (see **Figures 2.3.** and **2.4.**). Ten ridges with elevations higher than 2 m exist along this transect based on the topographic map (USGS, 1982). On the other hand, a total of 18 ridges of different elevations can be seen to lay between and include our sample SVI #0 and the ridge attributed to core SVI #3 inclusive based on the DOQQ images (FDEP, 1999) (see **Figures 2.1.** and **2.2.**). Based on the lower interval ages (sub-samples OSL1 taken at depths >1.5 m), this whole south-western group sequence formed in a time period of about 1,482 years (**Table 2.4.**). If we assume that this time range corresponds to the actual accretion interval (i.e. considering that each lower sample age is the *terminus ante quem* for ridge formation) we can estimate an average ridge accretion rate. Therefore, over the past ~2 ka, one ridge with an elevation equal or higher to 2 m has formed about every 148.2 years (**Table 2.4.**) in this south-western region of St. Vincent Island. Alternatively, if we count all 18 ridges, we estimate an average ridge formation rate of 82.3 years per ridge, indifferent of ridge crest elevation (**Table 2.4.**). Moreover, we can estimate an average coastal progradation rate of 91.77 m every 100 years for this southern part of the island (i.e. given that we only have four ridges to determine linear progradation), reflecting a relatively low influx of sediment during this late Holocene period for this area. This land accretion rate is slower than at Cape Canaveral, another well developed strandplain on the Florida Atlantic Coast, where the average was 135 ± 12 m / 100 years (RINK and FORREST, 2005). However, the Cape Canaveral OSL ages were determined at depths of only 1 m, so this may not truly correspond to deeper intervals in the same ridges that may better record the true land accumulation rates.

If we consider only the OSL samples recovered from 1 m depth (i.e. sub-samples OSL2), the story is very different for this south-western group of ridges. The three oldest ridges have ages at this depth that are statistically indistinguishable from one another (SVI #1, SVI #2 and SVI #3), with an average age of 803 ± 107 years, while the youngest ridge (SVI #0) has an age at the same depth of 370 ± 49 years. Thus samples taken from relatively shallow depths are clearly not indicative of the moment of initiation of the ridges themselves. These upper ages rather give us information regarding the history of accumulation of wind-deposited (and re-worked) sand material within the upper part of the presently established and mature relict ridges. As stated by OTVOS (2000), it is

possible for incipient small embryonic foredunes to start forming atop relict berm-type water-laid ridges. As these foredunes grow in size and vegetation, they gradually merge together and develop an established shore-parallel foredune ridge as progradation of the strandplain continues seaward (OTVOS, 2000; HESP, 2002). What is important to realize is that as this ridge grows further in width, its late stage, landward-stranded aeolian constituent is the primary force behind its present shape. As the ridge expands in size and recombines with sand coming from the slopes of the ridge, the sandy material gets re-worked and the ridge gets re-broadened. A similar model is portrayed by OTVOS (2000) during the merging process of incipient embryonic foredunes with either pre-existing landward dunes or terraces (c.f. OTVOS, 2000, Figure 7). We agree that St. Vincent Island is a strandplain with a ridge-swale type of sequence and not a ridge-terrace type of sequence. However, we believe that the aeolian process continuing on the upper sections of the St. Vincent Island ridges (since the formation of the early aeolian lithosome) is responsible for the similar values obtained among our upper OSL ages (**Figure 2.3., Table 2.2.**). This “in-place crestal lateral particle re-distribution” model we propose is similar to the formation of a sand-sheet constrained to the upper sections of the ridges: the material at the crest of the ridge gets re-distributed perpendicular to the ridge-length orientation and eventually is re-worked with sand from the stoss and lee slopes of the ridge. Studies regarding wind flows and effects over various types of vegetated foredunes and dunes have revealed that it is possible to have some kind of aeolian transport being effective across the dune field (SHERMAN and HOTTA, 1990; HESP, 2002). Certainly, the effects are more vigorous the closer the foredune is to the seaward side and wind velocities are greater up the stoss slopes and ridge crests (HESP, 2002). Sediment fluxes pulsed by wind flows may exist at a micro scale over the St. Vincent Island ridges. Directions of sand movement may fluctuate between the lee and stoss slopes of each ridge continuously giving rise to a continuous re-working of the ridges’ wind-deposited sediment. We further acknowledge that very high wind velocities at points well inland would occur at times of hurricane impact, offering short, episodic intervals for re-working of sands even in the vegetated inland areas.

Such process affects the luminescence signal of the upper section of the ridges as re-working may imply re-exposure of the sand to direct sunlight but at the same time up-bringing of deeper “older” sand grains from the ridge’s interior core. As the vegetation grows, this sand-sheet like process may eventually diminish but it was indeed more active during the early stages of formation of the aeolian lithosome within each beach ridge. It is worth mentioning that despite the heavy vegetation St. Vincent Island holds (see **Figure 2.1.**), most of the tall trees are concentrated in the swales and low lying areas of the island. Sparse bushes with mature oaks among considerable bare sandy areas decorate the crests of the

ridges (**Figure 2.6.**). These sandy areas confirm the modern aeolian character of this environment favouring ridge crest aeolian transport and re-working.

The interesting aspect of this proposed model is that it may happen at the same time throughout several ridges. This implies that similar OSL ages may be found along ridges in a relatively close distance. We see this happening for the upper interval samples of cores SVI #1, SVI #2, SVI #2b and SVI #3 (within respective age errors) taken at relatively similar depths from the ridges ground surface (**Figures 2.3.** and **2.4.**). Over a distance of 1 km we can see that these ages remain relatively close to each other possibly implying that all ridge crests at that moment were experiencing continuous aeolian re-working and re-distribution. This result has obvious implications for both sedimentology and wind-type ridge evolution as this type of process has never been evidenced via another method besides sedimentary structures and wind-flow studies on dunes. The OSL dating approach used here provides a method to establish an unambiguous distance from shore where the coastal environment is still being affected by wind transport and re-working despite some cover given by the sparse vegetation that populates the crest of the ridges.

Interestingly, unexpected young ages in the upper intervals of our cores do not occur in the north-eastern part of the study area (i.e. our samples SVI #5 and SVI #6), nor in the 30 cm depth samples collected by OTVOS (2005) on the north-western (i.e. his samples 1 and 2) or in the north-eastern (i.e. his sample 7) parts of the ridge sequences. Thus, these older ridges show no evidence of late stage aeolian processes.

Figure 2.2. shows that Tanner's Ridge Set H truncates the eastern end of Ridge Set G and therefore some part of H must be younger than some of the ridges within G. However, since we are not sure of the eastward extent of G before truncation, it is not certain if the ridge containing SVI #1 or that containing SVI #2 and SVI #2b is the time marker that can be used to set the terminus post quem age of Ridge Set H. Assuming that Ridge Set G was fully developed laterally (i.e. eastern part of ridges existed) before truncation occurred, the terminus post quem age for Ridge Set H corresponds to the youngest ridge in G (i.e. ridge containing SVI #1). Since the youngest deeper interval age among SVI #1, SVI #2 and SVI #2b is 812 ± 97 years ago, it corresponds to a terminus post quem age for Ridge Set H.

Ridge Set I (see **Figure 2.2.**) truncates Ridge Set H but Ridge Set K truncates Ridge Set I. Hence, Ridge Set I must be intermediate in age to H and K, yielding a time range of 812 ± 97 to 408 ± 58 years ago. Ridge Set L hosts a historic archaeological site (Fort Mallory; see **Figure 2.1.**) which is known to pre-date 1862 A.D. (MILLER *et al.*, 1981) but the set also truncates Ridge Set H. Therefore, this Ridge Set L must have formed sometime between 812 ± 97 and 142 years ago but certainly not earlier than first European contact in this area (i.e.

1528 A.D. with the arrival of Spaniards Panfilio de Narváez and Alvaro Nuñez Cabeza de Vaca to the Florida Gulf shores).

Interestingly, OTVOS (2005) newly published OSL results from St. Vincent Island were also collected along one of the islands' roads perpendicular to the Gulf shoreline (c.f. Road 3 – OTVOS, 2005, Figure 16). Road 3 reaches the Pickalene Shoreline but is located on the central-west portion of the island. Our transect, along Road 4, is located in the centre of the island but gets interrupted ~300 m before Big Bayou (see **Figure 2.1.**). OTVOS (2005) samples are located along Tanner's Ridge Sets K through C and southern group of samples span along Sets K and G. Even though the positioning of the samples may yield a good basis for comparison, OTVOS (2005) OSL ages along Road 3 are discordant with our southern group of ages from Road 4. According to OTVOS (2005) values, Tanner's Ridge Sets K, G, and F have ridges with OSL ages of 10 ± 3 years (602 ± 71 years for the duplicate), 244 ± 27 to 336 ± 39 , and 564 ± 69 years respectively. Due to the fact that all his samples were collected at a depth of only 30 cm from the ground surface, we believe that OTVOS (2005) OSL ages are a representation of late stage, landward-stranded aeolian re-working processes showing active re-setting of the luminescence signal on the uppermost sections of the beach ridges he sampled. We believe that is why his results in the south-western sequence are unexpectedly young and generally support our "in-place crestal lateral particle re-distribution" model for late stage, landward-stranded ridge re-working by aeolian processes.

2.5. CONCLUSIONS

OSL ages on sediments from cores provided a *terminus ante quem* age of ridge formation and an average sediment accumulation rate at four core-hole locations on the south-western part of St. Vincent Island. Our ages offer a new reliable absolute age constraint to the beach ridge grouping (i.e. Ridge Set sequences) made by Tanner in the late 1970's which was based on topographical, geomorphological and sedimentological analyses to elucidate the evolution of the strandplain. Even though archaeological remains provided early general time estimates on the formation of the strandplain, the new OSL ages are clearly superior. The OSL age estimates for the ridges are all in sequential order and conform to expectations based on the geomorphology of the island (younging to the southwest): the north-eastern-most ridge studied is older than $2,859 \pm 340$ years ago and the south-western-most ridge yielded a minimum age estimate of 408 ± 48 years ago (A.D. 2004 *datum*), which makes it the youngest ridge in the sequence studied. Emergent land on St. Vincent Island has thus been deposited over a period that is somewhat >3,000 years, but to determine the actual time of initiation of beach ridge formation, deeper cores would be needed on the northernmost ridge and along the Pickalene Shoreline, where OTVOS' (2005) ages suggest there may be an older episode of accretion >5,000 years ago.

For the past ~2,000 years, the southern- and younger-most section of the island has been experiencing a mean progradation of ~92 m every 100 years, yielding the formation of one beach ridge every ~82 years (though these could be underestimates since our ages remain *terminus ante quem* estimates). Constraints upon the ages of younger ridge sets on the south-eastern area of the island are also provided by considering the OSL ages of the ridges that are truncated. With OTVOS' (2005) own admission of the problematic nature of his OSL age estimates and the lack of alternative absolute ages for St. Vincent Island, the OSL ages presented here provide the first internally consistent chronology available for the island, supporting both our field and laboratory methodologies. In general, we find concordance with some of OTVOS' (2005) results and believe we have shed light on the ages he felt were unexpectedly young in the south-western portion of the island.

Average sediment accumulation rates were also calculated at each location. The deeper portions of each core showed more rapid sediment accumulation rates than those between approximately 1 m-depth and the surface, showing that deep cores are required to establish good estimates of sediment accumulation soon after the ridges form. The upper intervals in each core showed that the environment is still being affected by wind transport and re-working of ridge sands despite some sparse vegetation cover atop the crest of the ridges.

ACKNOWLEDGEMENTS

This research was possible thanks to the St. Vincent National Wildlife Refuge (U.S. Fish and Wildlife Service) permit and co-operative project “St. Vincent NR03 SU Permit 03-41650-1”. Special thanks to Terry Peacock (Refuge manager), and other members of the refuge staff, especially Monica Harris. Field assistance by K. Moretton and J. Pilarczyk are greatly appreciated. We thank the Natural Sciences and Engineering Research Council of Canada (NSERC) and the Apalachicola National Estuarine Research Reserve (ANERR – Florida Department of Environmental Protection) for all financial and logistic support received for and during this research.

Dr. E.G. Otvos and two other anonymous reviewers peer revised this manuscript.

REFERENCES

- AITKEN, M.J., 1998. *An Introduction to Optical Dating: The dating of Quaternary Sediments by the use of photon-stimulated luminescence*. Oxford: Oxford University Press, 267p.

- AITKEN, M.J., 1985. *Thermoluminescence Dating*. London: Academic Press, 359p.
- BALLARINI, M.; WALLINGA, J.; MURRAY, A.S.; VAN HETEREN, S.; OOST, A.P.; BOS, A.J.J., and VAN EIJK, C.W.E., 2003. Optical dating of young coastal dunes on a decadal time scale. *Quaternary Science Reviews*, 22(10-13), 1011-1017.
- BANERJEE, D.; HILDEBRAND, A.N.; MURRAY-WALLACE, C.V.; BOURMAN, R.P.; BROOKE, B.P., and BLAIR, M., 2003. New quartz SAR-OSL ages from the stranded beach dune sequence in south-east South Australia. *Quaternary Science Reviews*, 22(10-13), 1019-1025.
- BRALEY, C.O., 1982. Archeological testing and evaluation of the Paradise Point Site (8Fr71), St. Vincent National Wildlife Refuge, Franklin County, Florida. Athens, Georgia: Southeastern Wildlife Services Inc., *Report*, 102p.
- BROOKS, H.K., 1972. Geology of Cape Canaveral. Tallahassee, Florida: *Space Age Geology, 16th Field Conference Southeastern Geology Society*, 35-44.
- CAMPBELL, K.M., 1984. St. Vincent Island (St. Vincent Island National Wildlife Refuge). Tallahassee, Florida: Florida Geological Survey, *Open File Report No. 8*, 15p.
- DONOGHUE, J.F. and TANNER, W.F., 1992. Quaternary terraces and shorelines of the Panhandle Florida region. *Quaternary Coasts of the United States: Marine and Lacustrine Systems, SEPM Special Publication No. 48*, pp. 233-241.
- DONOGHUE, J.F. and WHITE, N.M., 1995. Late Holocene sea level change and delta migration, Apalachicola River region, northwest Florida, U.S.A. *Journal of Coastal Research*, 11(3), 651-663.
- FDEP, 1999. *Digital Orthographic Quarter-Quads Q4642 and Q4641*. Indian Pass –West Pass, Florida: Florida Department of Environmental Protection ortho-photographs 1 m resolution, UTM projection, NAD 83 datum, 8 quarter-quads. <http://data.labins.org/2003/MappingData/DOQQ/doqq.cfm>
- HESP, P., 2002. Foredunes and blowouts: initiation, geomorphology and dynamics. *Geomorphology*, 48, 245-268.
- HUNTLEY, D. J.; GODFREY-Smith; D. I., and THEWALT, M. L. W., 1985. Optical dating of sediments. *Nature*, 313, 105-107.
- LÓPEZ, G.I. and RINK, W.J., *in review*. Characteristics of the burial environment related to Quartz SAR-OSL dating at St. Vincent Island, NW Florida, U.S.A. *Quaternary Science Reviews (Quaternary Geochronology)*.
- MILANICH, J.T., 1994. *Archaeology of Precolumbian Florida*. Gainesville: University Press of Florida, 476p.
- MILLER, J.J.; GRIFFIN, J.W.; FRYMAN, M.L., and STAPOR, F.W., 1981. *Archeological and Historical survey of St. Vincent National Wildlife Refuge, Florida*. Tallahassee, Florida: U.S. Fish and Wildlife Service, Contract A-5831(79), 101p.

- MURRAY, A.S. and WINTLE A. G., 2000. Luminescence dating of quartz using an improved single-aliquot regenerative-dose procedure. *Radiation Measurements*, 32, 57-73.
- MURRAY-WALLACE, C.V.; BANERJEE, D.; BOURMAN, R.P; OLLEY, J.M., and BROOKE, B.P., 2002. Optically stimulated luminescence dating of Holocene relict foredunes, Guichen Bay, South Australia. *Quaternary Science Reviews*, 21(8-9), 1077-1086.
- OTVOS, E.G., 1985. Barrier Islands Genesis – Questions of alternatives for the Apalachicola coast, north east Gulf of Mexico. *Journal of Coastal Research*, 1(3), 267-278.
- OTVOS, E.G., 1995. Multiple Pliocene-Quaternary marine highstands, northeast Gulf coastal plain – fallacies and facts. *Journal of Coastal Research*, 11(4): 984-1002.
- OTVOS, E.G., 1999. Sediment and Geomorphic Criteria for Reconstructing Sea-Level Positions. Multiple Pliocene-Quaternary marine highstands on the northeastern Gulf of Mexico coastal plain? Reply to a discussion, *Journal of Coastal Research*, 14(2), 669-674 (1998). *Journal of Coastal Research*, 15(4), 1181-1187.
- OTVOS, E.G., 2000. Beach ridges - definitions and significance. *Geomorphology*, 32, 83-108.
- OTVOS, E.G., 2005. Coastal barriers, Gulf of Mexico: Holocene Evolution and Chronology. *Journal of Coastal Research*, Special Issue No. 42, 141-163.
- RINK, W.J. and FORREST, B., 2005. Dating evidence for the accretion history of beach ridges on Cape Canaveral and Merritt Island, Florida, U.S.A. *Journal of Coastal Research*, 21(5), 1000-1008.
- RINK, W.J. and ODOM, A.L., 1991. Natural alpha recoil particle radiation and ionizing radiation sensitivities in quartz detected with EPR: Implications for geochronometry. *Nuclear Tracks and Radiation Measurements D*, 18(1-2), 163-173.
- SHERMAN, D.J. and HOTTA, S., 1990. Aeolian sediment transport: theory and measurement. In: NORDSTROM, K.F., PSUTY, N., and CARTER, B. (Eds.) *Coastal Dunes: Form and Process*. Chichester, England: John Wiley & Sons, Ltd., pp. 17-38.
- STAPOR, F.W., 1973. Coastal Sand Budgets and Holocene Beach Ridge Plain Development, Northwest Florida. Tallahassee, Florida: Florida State University, Ph.D. Thesis, 221 p.
- STAPOR, F.W., 1975. Holocene beach ridge plain development, northwest Florida. *Zeitschrift für Geomorphologie*, 22, 116-144.
- STAPOR, F.W. and TANNER, W.F., 1977. Late Holocene mean sea level data from St. Vincent Island and the shape of the Late Holocene mean sea level curve. In: TANNER, W.F. (ed.) *Coastal Sedimentology*. Tallahassee, Florida: Florida State University, pp. 35-68.

- STAPOR, F.; MATHEWS, T., and LINDFORS-KEARNS, F., 1991. Barrier-island progradation and Holocene sea-level history in southwest Florida. *Journal of Coastal Research*, 7(3), 815-838.
- TANNER, W.F., 1988. Beach Ridge Data and Sea Level History from the Americas. *Journal of Coastal Research*, 4(1), 81-91.
- TANNER, W.F., 1992. Three thousand years of sea level change. *Bulletin American Meteorological Society*, 73(3), 297-303.
- Tanner, W.F., 1995. Origin of beach ridges and swales. *Marine Geology*, 129: 149-161.
- TANNER, W.F.; DEMIRPOLAT, S.; STAPOR, F.W., and ALVAREZ, L., 1989. The Gulf of Mexico Late Holocene sea level curve. *Transactions Gulf Coast Association of Geological Societies*, 39, 553-562.
- TAYLOR, M., and STONE, G.W., 1996. Beach-Ridges: A Review. *Journal of Coastal Research*, 12(3), 612-621.
- USGS, 1982. *Indian Pass, Fla. 29085-F2-TB-024 7.5 minute series Orthophotomap*. Indian Pass, Florida: 1:24,000, 1 sheet.
- WHITE, N.M., 2003. Late Archaic in the Apalachicola / Lower Chattahoochee Valley, North-West Florida, Southwest Georgia, and Southeast Alabama. *The Florida Anthropologist*, 56(2), 69-90.

CHAPTER 2 – FIGURES

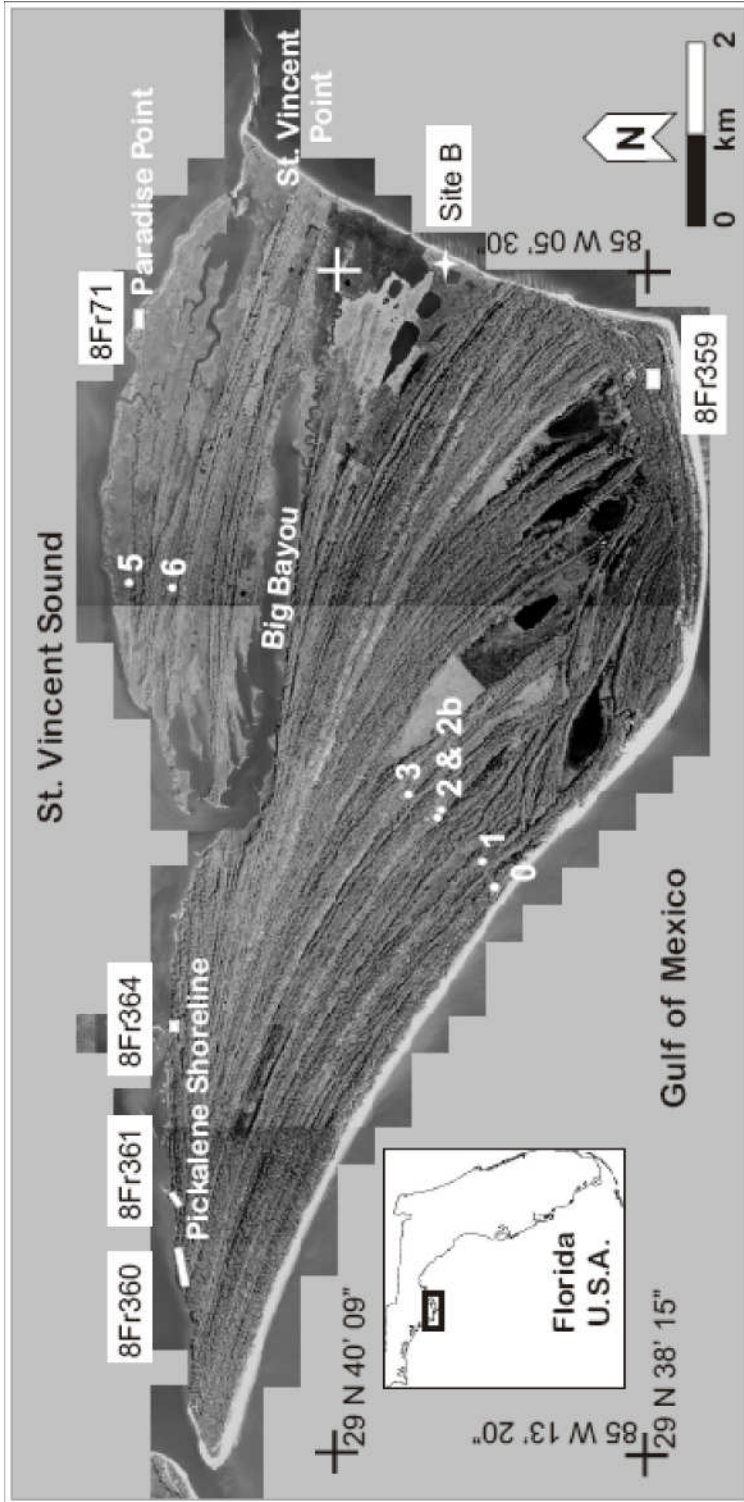


Figure 2.1. Site location map of St. Vincent Island, NW Florida, U.S.A. Location of sediment cores recovered from coring sites are marked by white circles with corresponding SVI numbers. Archaeological sites are shown as white rectangles with corresponding labels in white rectangles are site numbers. Image source: Digital Ortho-Quadrangle images by U.S. Geological Survey (January 10th, 1999), <http://terraserver-usa.com/default.aspx>.

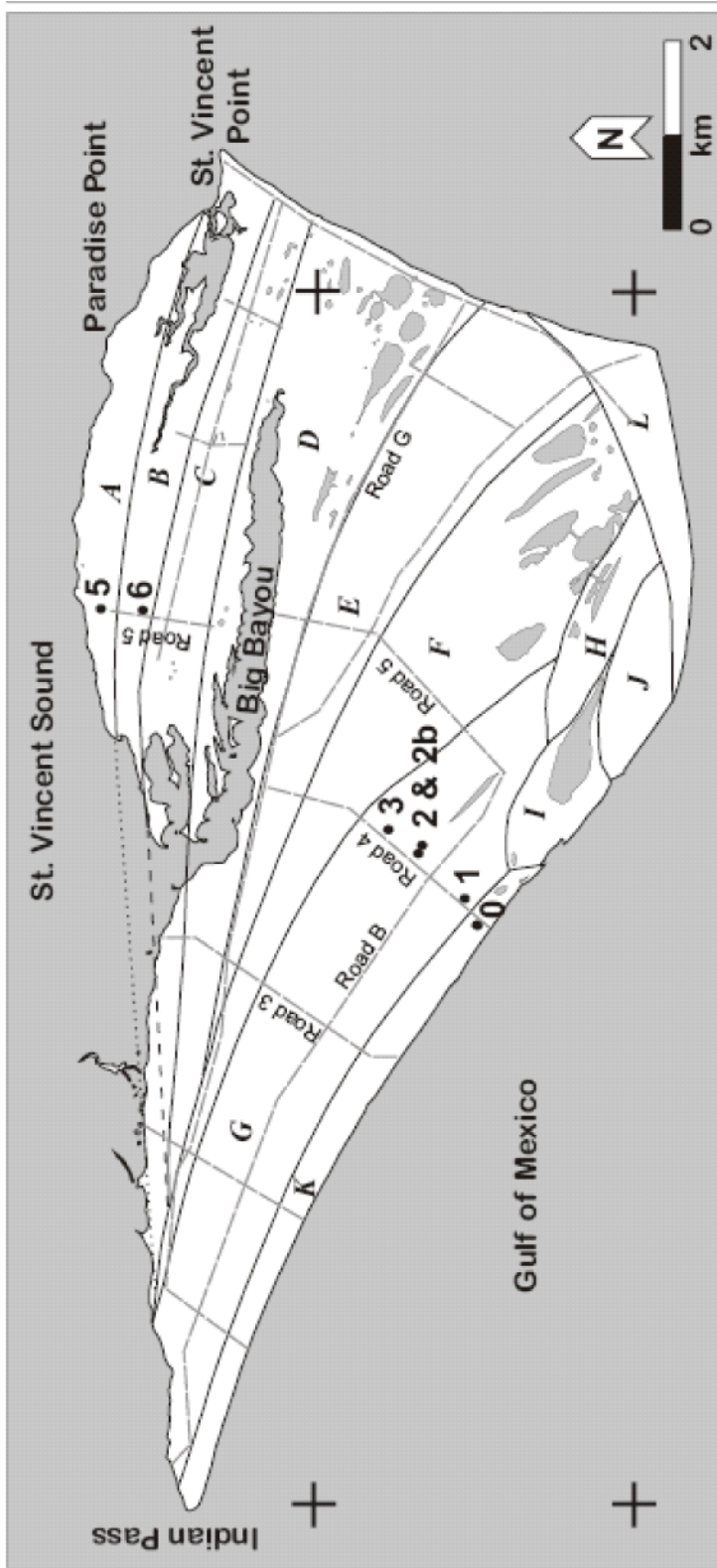
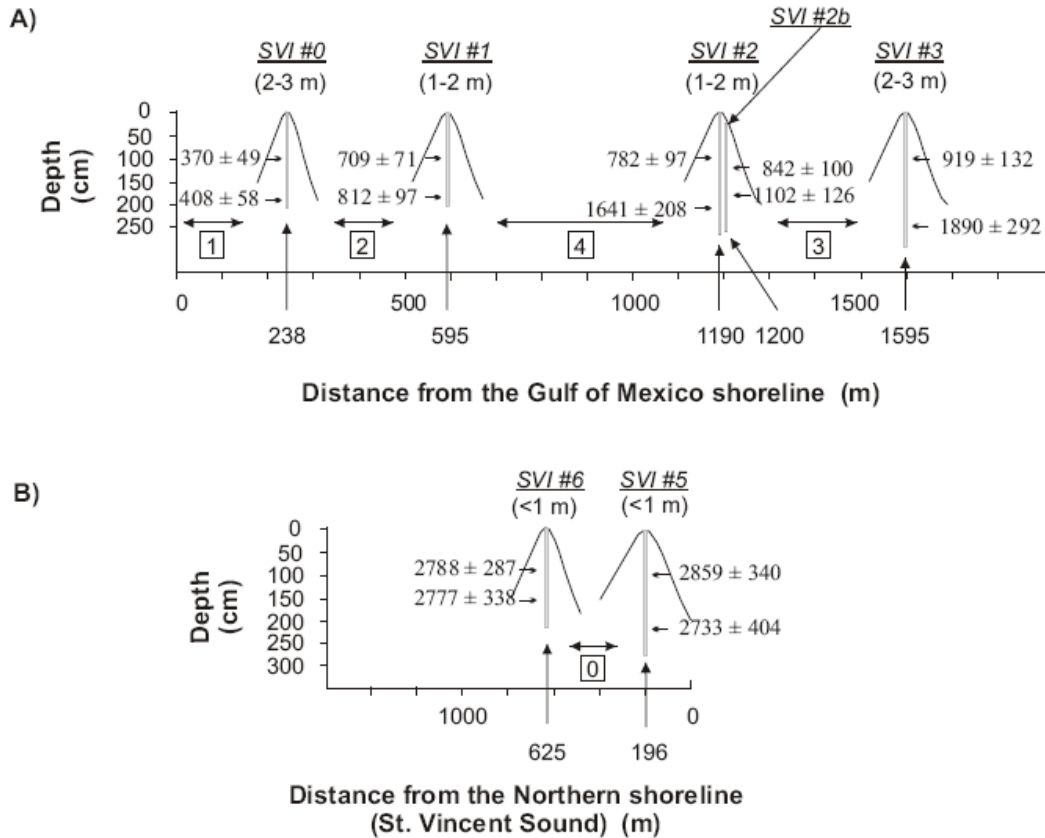


Figure 2.2. St. Vincent Island beach ridge sets. Capital letters from A (oldest) to L (youngest) indicate chronological sequence of Ridge Sets (modified from TANNER *et al.*, 1989 and TANNER, 1992). Dotted and short-dashed lines along northern shorelines are attempted correlation of ridges between east and west portions of the coastline as inferred from air-photographs. Location of coring sites along Roads 4 and 5 are shown by black circles with corresponding core numbers. Some of the island's bush/fire off-roads are indicated by long-dashed lines. Island has been digitized from Digital Ortho-Quadrangles for the area (U.S. Geological Survey, January 10th, 1999).

**Figure 2.3.**

Schematic cross-sections of two transects across beach ridges: A) Along Road 4 (Transect Road 4 – general strike N45°E to N50°E) on the south-western area of St. Vincent Island fronting the Gulf of Mexico. B) Along Road 5 (Transect Road 5 – general strike NS) on the north-eastern area. Depth to dated samples and maximum penetration of core are plotted against distance from closest shoreline. Ridge crest surfaces represent the modern day land surface shown here. Elevation on topographic map (USGS, 1982) of ridge crest at core location given in parentheses below core name. OSL ages in years are also given at actual depth obtained. Numbers in boxes provide the number of beach ridges with elevations greater than 2 m above mean sea level in between dated ridge (based on USGS topographic map data, 1982).

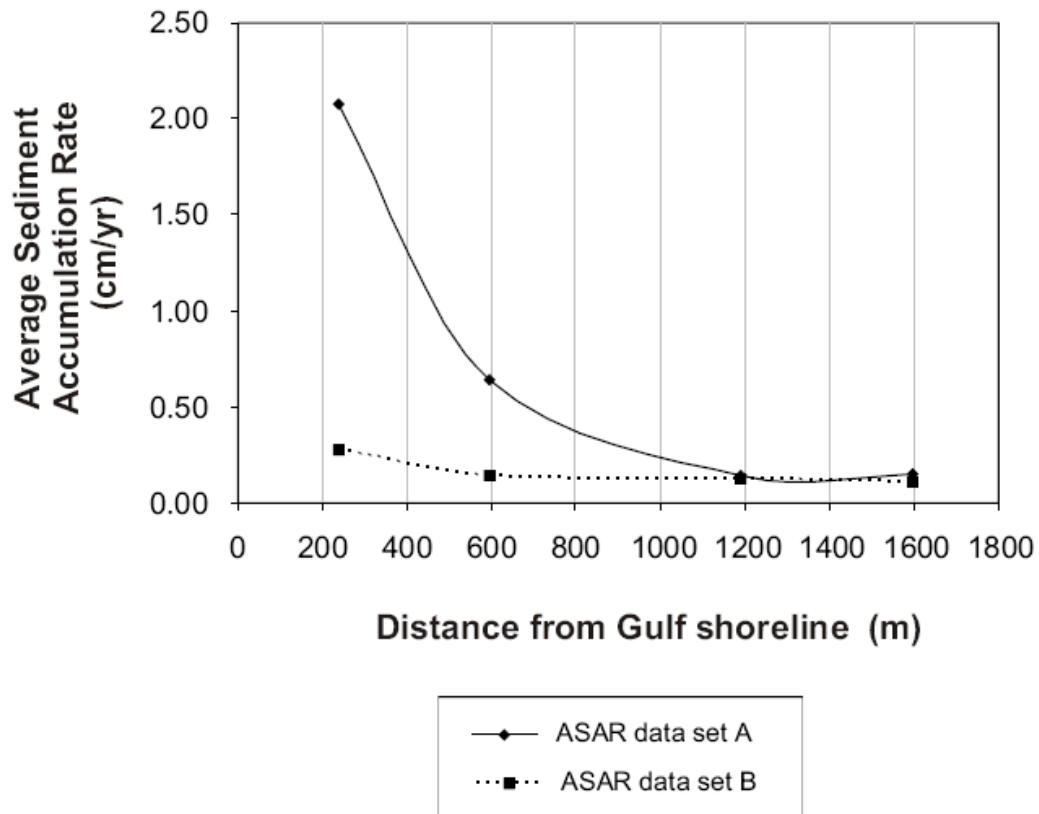


Figure 2.4.

Average sediment accumulation rate (ASAR) as a function of distance from Gulf of Mexico shoreline. ASAR data set A is calculated from the age difference and depth difference between the deepest core sample and the uppermost core sample. ASAR data set B is calculated from the age difference and depth difference of the uppermost sample and an assumed zero age at the modern ground surface.

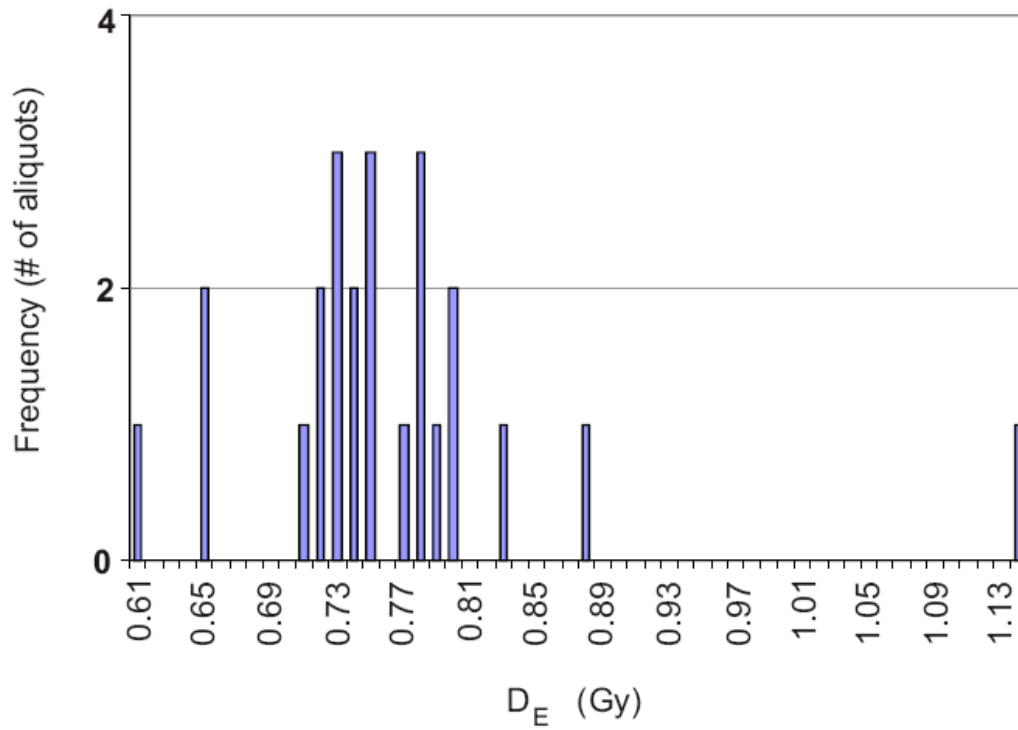


Figure 2.5.

Frequency distribution of 24 aliquots from sample SVI #3 OSL1 obtained using 8 mm mask. This example is representative of the type of distribution seen among most of the samples. Note single outlier at D_E of 1.14 Gy.

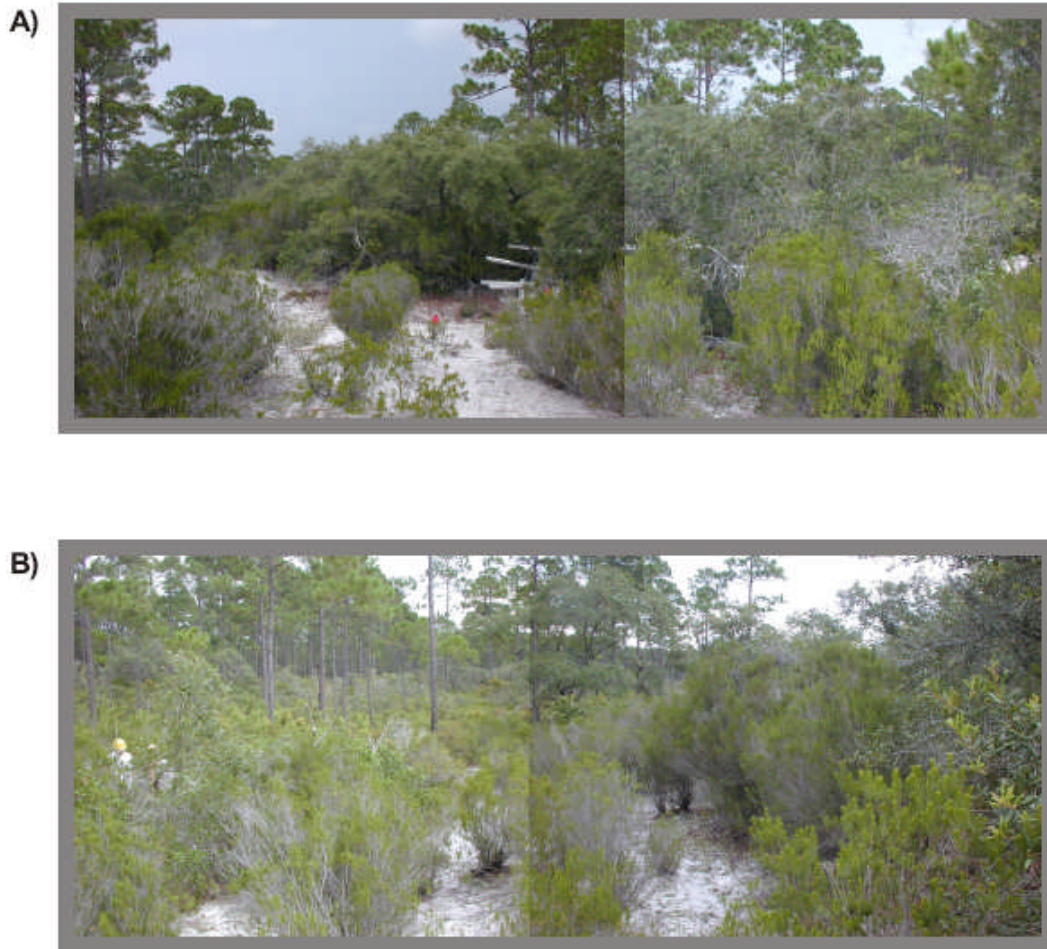


Figure 2.6.

Examples of vegetation cover atop the crest of an inland ridge on St. Vincent Island. This greyscale photo-mosaic was taken at core site SVI #2: note the sparse bushes and sandy areas along the ridge crest while tall trees are concentrated in the swales. A) View to the West (towards Road 4); and B) View to the East (note location of SVI #2b on the left bottom corner by people with hard hats). All photographs taken by G.I. López July 22, 2003.

CHAPTER 2 – TABLES

Table 2.1.
Location of cores taken on St. Vincent Island and depths of samples OSL-dated.

Core No.	Tanner's ridge set [a]	Latitude N {Northing} [b]	Longitude W {Easting} [b]	Environment	Total length of core {uncompacted length} (cm) [c]	Core sample	Burial depth (cm) [d]
SVI #0	K	n/a	n/a	Crest of vegetated beach ridge on "scrub oak dune" environment	165 {219}	SVI #0 OSL2 SVI #0 OSL1	102.4 180.9
SVI #1	G	29° 39.113' {3281633}	85° 09.384' {678444}	Crest of vegetated beach ridge on "scrub oak dune" environment	137 {212}	SVI #1 OSL2 SVI #1 OSL1	100.8 167.4
SVI #2	G	29° 39.383' {3282139}	85° 09.101' {678893}	Crest of vegetated beach ridge on "scrub oak dune" environment	156 {269}	SVI #2 OSL2 SVI #2 OSL1	99.9 217.1
SVI #2b	G	29° 39.389' {3282150}	85° 09.093' {678906}	Landward slope of vegetated beach ridge on "scrub oak dune" environment	122 {239}	SVI #2b OSL2 SVI #2b OSL1	98.5 159.6
SVI #3	G	29° 39.543' {3282438}	85° 08.955' {679124}	Crest of vegetated beach ridge on "scrub oak dune" environment	220 {288}	SVI #3 OSL2 SVI #3 OSL1	103.8 246.4
SVI #5	A	29° 41.138' {3285421}	85° 07.566' {681317}	Vegetated tidal flat within cabbage palm vegetated beach ridge	184 {281}	SVI #5 OSL2 SVI #5 OSL1	103.6 222.6
SVI #6	B	29° 40.889' {3284960}	85° 07.581' {681300}	Slash pine - cabbage palm hammock vegetated beach ridge	200 {217}	SVI #6 OSL2 SVI #6 OSL1	88.9 156.1

[a] Tanner's beach ridge set nomenclature (TANNER *et al.*, 1989; TANNER, 1992).

[b] GPS latitude longitude (NAD 83) and converted UTM Zone 16 coordinates. GPS error = ± 2.5 m.

[c] Total length of core = total retrieved sediment, uncompacted length = actual depth of sample.

[d] Actual burial depth of center of the sample considering compaction during coring.

Table 2.2.
SAR - OSL ages and data for samples taken from beach ridges on St. Vincent Island.

Core sample	Laboratory No.	De (Gy)	238-U (ppm) [b]	232-Th (ppm) [b]	K (%) [b]	Water Content (%) [c]	Cosmic		SAR-OSL age (a) [f]*
							Dose Rate ($\mu\text{Gy/a}$) [d]*	Annual Dose ($\mu\text{Gy/a}$) [e]*	
SVI #0 OSL2	GL04026	0.11 ± 0.01	0.18 ± 0.1	0.42 ± 0.04	0.018 ± 0.002	19.05	198.86	285.8 ± 14.6	370 ± 49
SVI #0 OSL1	GL04025	0.12 ± 0.01	0.15 ± 0.1	0.48 ± 0.04	0.022 ± 0.002	2.75	185.43	284.0 ± 16.8	408 ± 58
SVI #1 OSL2	GL04027	0.21 ± 0.01	0.16 ± 0.1	0.43 ± 0.04	0.032 ± 0.002	23.27	199.47	297.3 ± 14.1	709 ± 71
SVI #1 OSL1	GL04027	0.28 ± 0.02	0.35 ± 0.1	0.85 ± 0.06	0.024 ± 0.002	14.41	186.96	343.2 ± 15.3	812 ± 97
SVI #2 OSL2	GL04019	0.23 ± 0.02	0.20 ± 0.1	0.52 ± 0.04	0.019 ± 0.001	13.82	199.47	300.4 ± 15.2	782 ± 97
SVI #2 OSL1	GL04019	0.45 ± 0.04	0.13 ± 0.1	0.55 ± 0.04	0.013 ± 0.001	2.40	180.70	271.6 ± 16.8	1641 ± 208
SVI #2b OSL2	GL04020	0.25 ± 0.02	0.19 ± 0.1	0.57 ± 0.06	0.017 ± 0.001	15.86	200.12	299.0 ± 15.1	842 ± 100
SVI #2b OSL1	GL04020	0.30 ± 0.02	0.15 ± 0.1	0.36 ± 0.04	0.015 ± 0.001	2.94	187.98	272.1 ± 16.7	1102 ± 126
SVI #3 OSL2	GL04022	0.67 ± 0.06	0.97 ± 0.1	4.18 ± 0.28	0.027 ± 0.002	6.70	198.27	725.0 ± 21.2	919 ± 132
SVI #3 OSL1	GL04022	0.76 ± 0.10	0.53 ± 0.1	1.11 ± 0.08	0.019 ± 0.001	3.17	177.31	404.1 ± 17.1	1890 ± 292
SVI #5 OSL2	GL04030	0.82 ± 0.08	0.19 ± 0.1	0.31 ± 0.04	0.025 ± 0.005	18.79	198.27	286.4 ± 14.9	2859 ± 340
SVI #5 OSL1	GL04030	1.04 ± 0.13	0.53 ± 0.1	0.84 ± 0.07	0.033 ± 0.005	14.24	180.21	381.8 ± 15.7	2733 ± 404
SVI #6 OSL2	GL04031	0.76 ± 0.06	0.17 ± 0.1	0.35 ± 0.04	0.007 ± 0.003	23.68	203.78	272.9 ± 14.2	2788 ± 287
SVI #6 OSL1	GL04031	0.84 ± 0.08	0.26 ± 0.1	0.55 ± 0.04	0.013 ± 0.002	8.67	188.50	303.1 ± 15.9	2777 ± 338

[a] OSL1 corresponds to sample taken towards the bottom of the core and OSL2 to the one taken towards the top of the core at depths greater than 50 cm below surface.

[b] U, Th and K values determined by NAA on sub-samples derived from the OSL samples prior to chemical treatments.

[c] Water content as a fraction of dry weight determined from laboratory measurements.

[d] Cosmic dose rate value calculated using an overburden density of 2 g/cm³.

[e] All β and γ dose rates were calculated based on U, Th and K concentrations of each sample accounting for moisture values of the sample.

[f] Datum for SAR-OSL ages is A.D. 2004.

* Ages were calculated assuming constant sediment accumulation rates.

Table 2.3.

Average sediment accumulation rates (ASAR) between OSL samples at different intervals within each sediment core.

Core sample [a]	SAR-OSL age (a)	Core No.	ASAR data set A (cm/yr) [b]	ASAR data set B (cm/yr) [c]
SVI #0 OSL2	370 ± 49	SVI #0	2.08	0.28
SVI #0 OSL1	408 ± 48			
SVI #1 OSL2	709 ± 71	SVI #1	0.64	0.14
SVI #1 OSL1	812 ± 97			
SVI #2 OSL2	782 ± 97	SVI #2	0.14	0.13
SVI #2 OSL1	1641 ± 208			
SVI #2b OSL2	842 ± 100	SVI #2b	0.24	0.12
SVI #2b OSL1	1102 ± 126			
SVI #3 OSL2	919 ± 132	SVI #3	0.15	0.11
SVI #3 OSL1	1890 ± 292			
SVI #5 OSL2	2859 ± 340	SVI #5	n/a	0.04
SVI #5 OSL1	2733 ± 404			
SVI #6 OSL2	2788 ± 287	SVI #6	n/a	0.03
SVI #6 OSL1	2777 ± 338			

Actual depths of samples are given in Table 2.1.

[a] OSL1 corresponds to sample taken towards the bottom of the core and OSL2 to the one taken towards the top of the core at depths greater than 50 cm below surface.

[b] Values corresponding to the lower part of the core: calculations for depth interval between samples OSL1 and OSL2.

[c] Values corresponding to the upper part of the core: calculations for depth interval between sample OSL2 and the ground surface.

Table 2.4.

Average ridge accretion and coastal progradation rates estimates.

Core sample	SAR-OSL age (a)	Time range between cores (a)	Ridge accretion rate (a) [a]	Ridge accretion rate (a) [b]	Progradation rate (m/100a) [c]
SVI #0 OSL1	408 ± 58	1482	148.20	82.30	91.77
SVI #3 OSL1	1890 ± 292				

Actual depths of samples are given in Table 2.1.

[a] Considering 10 ridges with elevations higher than 2 m above mean sea level.

Based on USGS (1982) topographic-bathymetric orthophotomap of St. Vincent Island (Indian Pass, Fla. Sheet).

[b] Considering 18 ridges based on FDEP (1999) DOQQ orthophotographs for St. Vincent Island (Q4642 and Q4641).

[c] Distance between SVI #0 and SVI #3 is ~1,360 m.

CHAPTER 3

CHARACTERISTICS OF THE BURIAL ENVIRONMENT RELATED TO QUARTZ SAR-OSL DATING AT ST. VINCENT ISLAND, NW FLORIDA, U.S.A.

Gloria I. López *

W. Jack Rink

AGE Laboratory, School of Geography and Earth Sciences, McMaster University.
1280 Main Street West, Hamilton, Ontario, L8S 4K1, Canada

* Corresponding author's Email address: lopezgi@mcmaster.ca

Citation:

LÓPEZ, G.I., and RINK, W.J., 2007. Characteristics of the Burial Environment related to Quartz SAR-OSL Dating at St. Vincent Island, NW Florida, U.S.A. *Quaternary Geochronology*, 2, 65-70.

Quaternary Geochronology: Elsevier Science, Oxford, ISSN 1871-1014 (Imprint: Elsevier).

Status: received 12 October 2005, accepted 17 May 2006, available online 13 July 2006, published.

“Reprinted from *Quaternary Geochronology*, (2), López, G.I. and Rink, W.J., Characteristics of the Burial Environment related to Quartz SAR-OSL Dating at St. Vincent Island, NW Florida, U.S.A., 65-70, © (2007), with permission from Elsevier”.

From: "Jones, Jennifer (ELS-OXF)" <J.Jones@elsevier.co.uk>
To: "Gloria I. López C." <lopezgi@mcmaster.ca>
Subject: RE: thesis
Date: October 20, 2006 03:05

Dear Gloria I Lopez

We hereby grant you permission to reproduce the material detailed below at no charge in your thesis subject to the following conditions:

1. If any part of the material to be used (for example, figures) has appeared in our publication with credit or acknowledgement to another source, permission must also be sought from that source. If such permission is not obtained then that material may not be included in your publication/copies.
2. Suitable acknowledgment to the source must be made, either as a footnote or in a reference list at the end of your publication, as follows:

"Reprinted from Publication title, Vol number, Author(s), Title of article, Pages No., Copyright (Year), with permission from Elsevier".
3. Reproduction of this material is confined to the purpose for which permission is hereby given.
4. This permission is granted for non-exclusive world English rights only. For other languages please reapply separately for each one required. Permission excludes use in an electronic form. Should you have a specific electronic project in mind please reapply for permission.
5. This includes permission for the Library and Archives of Canada to supply single copies, on demand, of the complete thesis. Should your thesis be published commercially, please reapply for permission.

Yours sincerely,

Jennifer Jones
Rights Assistant

ABSTRACT

St. Vincent Island, on the northwest Gulf coast of Florida, U.S.A., preserves a well-developed beach ridge plain that began to form ~4,000 years ago based on inferred ages of pottery artefact assemblages. Seven vibra-cores up to 2.88 m in length (un-compacted sediment) were retrieved from six ridges across the island. The single-aliquot regenerative-dose (SAR) procedure was used to obtain two optically stimulated luminescence (OSL) ages per core at different depths within each core.

The geographically youngest ridges gave ages of 370 ± 50 to $1,900 \pm 300$ years, yielding an inter-ridge accumulation time of ~150 years assuming uniform sediment accumulation. The oldest ridge sets yielded ages of $2,700 \pm 400$ to $2,800 \pm 300$ years. Dating results are evaluated in terms of equivalent dose (D_E) distributions and other characteristics in relation to aspects of the burial environment, including pedogenesis.

3.1. INTRODUCTION

Over the past few years, some Holocene coastal deposits have been successfully dated using Optically Stimulated Luminescence (OSL). Relict dune and beach ridge sequences have been assessed for accuracy and precision of quartz-OSL dating, confirming the reliability and usefulness of this method in young coastal deposits (e.g. Murray-Wallace *et al.*, 2002; Ballarini *et al.*, 2003; Berger *et al.*, 2003). This study is part of ongoing research that attempts to examine the proposed evolutionary history of the Apalachicola barrier island complex (Florida, U.S.A.) by OSL-dating different recent and relict beach and dune ridge sequences throughout four of the six barrier systems that form this Gulf Coast complex (López and Rink, 2006; López, in preparation). This study attempts not only to date samples from the upper aeolian facies of the cored ridges but also from the deeper foreshore facies (i.e. closer to the time of formation of each ridge). In this paper, we present the quartz-OSL dating results obtained for a series of beach ridges located on St. Vincent Island. To date, this is the first time that continuous, long, vertical sediment cores (>2 m of un-compacted sediment) have been retrieved from the St. Vincent Island National Wildlife Refuge for OSL purposes.

St. Vincent is a barrier island located on the north-eastern Gulf of Mexico at the southernmost point of the Apalachicola River Delta Barrier Island Complex (**Figure 3.1.**). More than 100 pristine beach ridges, predominantly east-west trending, decorate the island. They consist of well-vegetated, mostly linear, mature relict ridges. This highly vegetated uninhabited island is dominated on its Gulf side by a scrub oak dune environment surrounded by slash pine - cabbage palm hammock covered lowlands, while the northerly St. Vincent Sound is

characterized by hardwood hammocks and tidal marshes (Miller *et al.*, 1981). In general, each individual ridge is separated by lowlands, which are flooded seasonally. This coastal region is characterized by a mixture of entisols, spodosols and histosols, typical of the coastal land types of the Florida coast within the northern thermic temperature regime region (Brown *et al.*, 1990).

The island can be divided into 2 main areas with respect to general beach ridge elevations (**Figure 3.1.**): a) beach ridges with elevations up to 4 m above mean sea level occur to the south of Big Bayou; and b) ridges to the north of Big Bayou do not exceed 1 m. Previous geological and sedimentological studies on St. Vincent Island have been ongoing since the early 1970s, related to the origin and formation of the ridges (e.g. Stapor, 1973; Tanner *et al.*, 1989). Few ages exist for the island, most of which are relative estimates using general time ranges for found archaeological materials (e.g. Miller *et al.*, 1981; Braley, 1982; Donoghue and White, 1995). Additionally, fewer numerical ages (as well as their precise stratigraphic locations and types of material dated) exist for the Apalachicola Delta region (e.g. Stapor, 1975; Campbell, 1984). More recently, and while this paper was in review, some new, but quite anomalous, OSL ages were published for the island (Otvos, 2005). A review of these ages and comparison with those presented herein is given in López and Rink (2006).

3.2. METHODS

3.2.1. SAMPLING STRATEGY

Six relict ridges were cored throughout St. Vincent Island in July 2003. The cored sites can be divided into two major groups based on the consecutiveness of the coring strategy (**Figure 3.1.**). Cores SVI #0, SVI #1, SVI #2 and SVI #3 were retrieved almost consecutive to each other in the southern part of the island. Cores SVI #5 and SVI #6 constitute the northern set of cored ridges. With the exception of core SVI #2b, which was recovered from the landward slope of the ridge where core SVI #2 was taken, the cores were taken from the crest and center of elongated ridges (**Figure 3.1.**). Soft aluminium pipes (7 cm in diameter; 3 to 6 m-long), a portable gas-operated vibra-core and a 1.2 m-long truck jack were used to collect the sediment cores. To minimize the risk of external contamination, the inside of each aluminium pipe was kept clean prior to coring and the first centimetre of surface sediment was removed at each coring site immediately before coring.

The maximum and minimum core lengths obtained were 2.88 m (SVI #3) and 2.12 m (SVI #2b) of un-compacted sediment respectively. Compaction due to coring varied between 17 cm (SVI #6) and 113 cm (SVI #2). Sediment cores were split open under low-level orange illumination at the AGE Laboratory (McMaster University). The selection of the various OSL sample locations along each core was done on the exposed halves of the cores which underwent standard

sedimentological analyses (**Figure 3.2.**). Uniform gamma irradiation was insured by selecting locations along each core with at least 30 cm of sedimentological homogeneity on either side of the sampling location. Two OSL samples were extracted from each core meeting the following criteria: a) the burial depth of the upper sample (OSL2) was at least 50 cm below the surface (i.e. un-compacted sediment); b) the lower sample (OSL1) was taken as deep in the core as possible but close to areas of horizontal laminations (i.e. possible foreshore-related depositional environment); and c) the sample was located 20-25 cm away from any heavy mineral-rich layers or within an homogenous layer with respect to gamma dosimetry. Five cm-long slabs of sediment were extracted for each OSL sample on the light-sensitive core half, which was only handled in the darkroom laboratory (i.e. subdued orange lighting).

3.2.2. SAMPLE PREPARATION AND DOSE-RATE MEASUREMENTS

A total of 14 OSL samples were obtained and dated from the St. Vincent Island cores. Details of sample preparation are given in López and Rink (2006). A highly pure quartz separate was obtained from each core sample.

The Neutron Activation Analysis (NAA) technique (at the McMaster University Nuclear Reactor facility) was used to estimate the elemental concentrations of radioactive ^{238}U , ^{232}Th and ^{40}K in small, homogenized, untreated, sub-samples of the original dry OSL samples. Cosmic-ray dose rates were calculated using a value of $\frac{1}{2}$ of the sample's burial depth (i.e. assuming a constant sedimentation rate or linear sediment accumulation) and a 2 g/cm^3 of overburden density using calculations by Prescott and Hutton (1988) with the ANATOL program version 0.72B (provided by N. Mercier, CNRS, Paris). Internal ^{238}U and ^{232}Th dose rates ($0.067 \pm 0.022 \text{ ppm}$ and $0.114 \pm 0.043 \text{ ppm}$ respectively) were calculated from the average concentration of those radioisotopes in granitic quartz, based on the Rink and Odom (1991) values.

3.2.3. OSL MEASUREMENTS

An automated RISØ TL-DA-15 reader was used for all the single-aliquot OSL measurements, employing blue light-emitting diodes ($470 \pm 30 \text{ nm}$) at 90% of their power and a single 6 mm-thick Hoya U-340 filter (280 to 370 nm detection window). Laboratory irradiations were done using a calibrated $^{90}\text{Sr}/^{90}\text{Y}$ beta source.

Prior to the equivalent-dose (D_E) determination, the following tests were performed on 8-mm mask size aliquots of each sample:

- Initial estimates of D_E were made by attempting to bracket the natural signal size with a series of administered doses performed on 3 aliquots of each sample.

- A feldspar contamination check was done using infrared stimulation (830 nm detection window) on 3 aliquots of each sample.
- The appropriate pre-heat temperature was determined by pre-heat plateau tests at 160°, 200°, 240° and 280°C for 10 s each, performed on 12 aliquots of each sample (i.e. 3 aliquots per temperature).
- A thermal transfer test as a function of pre-heat temperature was performed on 4 aliquots of each sample (protocol as per Madsen *et al.*, 2005) to identify any problematic samples and any dependency of the D_E on pre-heat temperature (Ballarini *et al.*, 2003).
- A dose-recovery test as a function of pre-heat temperature was made on 4 aliquots of each sample (protocol as per Madsen *et al.*, 2005) to determine the ability and efficacy of the single-aliquot regenerative-dose (SAR) protocol (Murray and Wintle, 2000) used in this study.

D_E was determined using the SAR protocol (Murray and Wintle, 2000) on 24 aliquots of each sample. All samples were illuminated at 125 °C for 100 s. The luminescence signal intensity was determined using the first 0.4 s of emission and the last 4 s were subtracted as background. Only aliquots with recycling ratios between 0.90 and 1.10 were accepted for the age determinations. D_E data was analyzed with the RISØ Luminescence Analyst program (version 2.22) using linear fitting of the regenerated luminescence. Age estimates and errors were determined using the ANATOL program.

3.3. RESULTS AND DISCUSSION

A flat plateau across the temperature range from 160° to 280° C was observed in all cases (e.g., **Figure 3.S1.**). A 160° C pre-heat temperature was selected for use on all samples based on both the former and the dose recovery test (successful at the 95% confidence level) (**Table 3.S1.** and **Figure 3.S2.**). No evidence of thermal transfer was seen using the selected pre-heat temperature (e.g., **Figure 3.S3.**).

Some representative examples of OSL decay and response curves are shown in **Figure 3.3.** Examples of histograms obtained from two samples taken from the geographically youngest and oldest ridges are shown in **Figure 3.4.** Frequency distributions of D_E values were examined for all samples with a bin width of 0.01 Gy to better observe the spread in the distribution (as opposed to a smaller bin size). For most samples, a simple nearly symmetric distribution of D_E was observed, with no significant change when mask size was reduced to 1 mm (**Figure 3.4.**). This result excludes any significant extent of partial zeroing at burial. The coefficient of variation of the D_E values obtained for each OSL sample was less or equal to 10 %, being ~1 % for the geographically younger samples and 10 % for the older ones (e.g., **Figure 3.S4.**).

The D_E of each sample was obtained from calculating the average of the D_E values obtained from each aliquot measured. Most samples did contain a single-aliquot (out of 24) with a value greater than $+2\sigma$ of the mean in the D_E distribution. The D_E mean was then recalculated excluding this single value (i.e. outlier); however no statistically significant difference was seen in the mean D_E after the removal of this aliquot.

In general, sediments recovered from the cores were mainly medium to fine sands with little carbonate material (<5%). Significant occurrences of peaty sandy clays were only found in cores SVI #5 and SVI #6. However, the sediment underlying these soil-type horizons was not disturbed by pedogenesis and alterations from its original parent material were minimal (i.e. original laminations in the sand are still visible). Scarce fine particles of organic matter (<5%) occur throughout the southern set of cores (SVI #0, SVI #1, SVI #2, SVI #2b and SVI #3) and, in general, root systems may be only present in the first meter of sediment. Several distinct leaching horizons, some underlain by an organically-rich layer, were found in the first ~1.5 m of sediment. Such a profile is concordant with spodosol-type, moderate soil formation (**Figure 3.2.**).

No evidence for post-depositional burrowing was seen around the areas surrounding the OSL sample locations. Particular care was taken when sampling for OSL2 samples, as roots and bioturbation may result in mixing of younger grains and likely affect the OSL age (e.g. Bateman *et al.*, 2003). However, this did not seem to be the case with the upper samples (i.e. OSL2) of our St. Vincent Island cores.

Remarkably, the youngest sample (SVI #0 OSL2) showed the tightest D_E distribution among all the samples in the study area, and the smallest D_E coefficient of variation (1%) among individual aliquots of the sample, both at the 8 mm and 1 mm mask sizes. For the oldest samples, the coefficient of variation reached 40% (at 8 and 1 mm mask sizes). All the other samples had a coefficient of variation of 10%. The relative standard deviation of the samples' D_E values was used as a measure of the scatter of the D_E distributions, which was smallest (1%) for the youngest sample but larger (13%) for the oldest sample in the study area (**Figure 3.4.**). This higher over-dispersion on the D_E distributions in older samples (SVI #5 and SVI #6), may probably be due to a stronger pedogenesis (i.e. formation of histosol-type soil) but not necessarily due to partial bleaching (**Figure 3.4.** and **Figure 3.S4.**). These results may indicate that a) the abundant root systems present in this Floridian environment disturb the substrate only minimally; b) the formation of spodosol-type soils (as seen in these ridges) does not affect OSL ages, or spodosols have not fully developed in this younger ridge environment; and c) the aeolian reworking atop the ridges is minimal (leading us to believe that this system is in equilibrium with sediment supply).

All samples showed Late Holocene depositional ages (A.D. 2004 *datum*; **Table 3.S2.**). The OSL ages increased (within statistical error) both with depth and from south to north. The more southerly group of almost consecutive beach ridges (**Figure 3.1.** and **Table 3.S2.**) yielded ages ranging from 370 ± 50 to $1,900 \pm 300$ years ago. The northern set of ridges cored yielded ages ranging from $2,700 \pm 400$ to $2,900 \pm 300$ years. The ages for core SVI #6 are statistically indistinguishable from those for core SVI #5, indicating formation of both ridges within a relatively short time interval. This corresponds to times between 2,500 and 3,100 years ago. According to our results, this northernmost area of St. Vincent Island may have experienced a high sediment supply of about 1 cm/a around 3 ka ago (for at least the 700 m closest to the St. Vincent Sound shoreline) probably aided by its ability of forming soil. Histosols are organically-rich soils and may develop atop sands in extremely wet environments (Brown *et al.*, 1990), similar to the one encountered to the north of Big Bayou on St. Vincent Island. Our calculated accumulation rate of ~ 1 cm/a obtained for cores SVI #5 and SVI #6 is an order of magnitude higher than the modern average rate of ~ 0.08 cm/a for histosol accumulation calculated for Florida (Brown *et al.*, 1990). The ridges on this north and north-eastern side of the island have the lowest elevations and the highest number of lagoonal areas. These factors seem to reflect possible subsidence along the north end of the island.

Since we have no clear indication that we reached the base of the ridges in the cores (i.e. nearshore/foreshore formation limit), the lower set of samples (i.e. OSL1, taken at burial depths >1.5 m) represent minimum ages of formation of each ridge. These samples were collected as deep as possible within each core, in some cases showing evidence of horizontal lamination (i.e. pertaining to the foreshore facies). All of the upper samples (i.e. OSL2) were recovered around the 1 m burial depth. They are clearly not indicative of ridge formation age but of vertical dune accretion periods, as they had sedimentological characteristics of aeolian facies.

In the southern set of cores, the deepest samples (i.e. OSL1) as well as the upper samples (i.e. OSL2) show an increase of age from south (the Gulf side) to north (**Table 3.S2.**). The youngest age in this study is 370 ± 50 years (SVI #0 OSL2) and the oldest age of this southern set of cores is $1,900 \pm 300$ years (SVI #3 OSL1). These four ridges are $\sim 1,360$ m apart along a transect perpendicular to shore that crosses ridges consistently parallel to each other and the modern Gulf-side foredune. Based on the lower section ages (i.e. OSL1 samples), which are the closest to a possible foreshore environment (i.e. near or at sea level at the moment of deposition), this whole southern set formed in a time period of $\sim 1,500$ years, yielding an average accretion rate of one ridge about every 82 years. A more detailed analysis of the inter-ridge formation rates and average sediment accumulation rates is given by López and Rink (2006).

3.4. CONCLUSIONS

OSL ages on quartz grains from cores provided minimum age estimates on the time of ridge formation at each of the seven core-hole locations on St. Vincent Island. The OSL age estimates for the ridges are all in sequential order and conform to expectations based on the geomorphology of the island. Emergent land on St. Vincent has existed since ~4,000 years ago.

The scatter on the D_E distribution may be used as a proxy for soil formation in clastic-rich environments such as these Floridian beach ridges. Recently formed ridges showed tighter D_E distributions compare to those pertaining to older ridges showing buried palaeo-marsh layers. Moreover, the older the age the higher the coefficient of variation was among aliquots of the same sample. In situations showing some D_E dispersion, cleaning statistical outliers prior to the final D_E calculation, such as aliquots found outside the 2σ range, helps to obtain the best D_E for age estimation.

ACKNOWLEDGEMENTS

This research was possible thanks to the St. Vincent National Wildlife Refuge (U.S. Fish and Wildlife Service) under permit and co-operative project “St. Vincent NR03 SU Permit 03-41650-1”. Special thanks to Terry Peacock (Refuge manager) and other members of the refuge staff, especially Monica Harris. Field assistance by K. Moretton and J. Pilarczyk was greatly appreciated.

Editorial handling by: R. Roberts

APPENDIX A. SUPPLEMENTARY MATERIALS

Supplementary data associated with this article can be found in the online version at doi:10.1016/j.quageo.2006.05.035.

REFERENCES

- Ballarini, M., Wallinga, J., Murray, A.S., Van Heteren, S., Oost, A.P., Bos, A.J.J., Van Eijk, C.W.E., 2003. Optical dating of young coastal dunes on a decadal time scale. *Quaternary Science Reviews* 22, 1011-1017.
- Bateman, M.D., Frederick, C.D., Jaiswal, M.K., Singhvi, A.K., 2003. Investigations into the potential effects of pedoturbation on luminescence dating. *Quaternary Science Reviews* 22, 1169-1176.
- Berger, G.W., Murray, A.S., Havholm, K.G., 2003. Photonic dating of Holocene back-barrier coastal dunes, northern North Carolina, USA. *Quaternary Science Reviews* 22, 1043-1050.

- Braley, C.O., 1982. Archeological testing and evaluation of the Paradise Point Site (8Fr71), St. Vincent National Wildlife Refuge, Franklin County, Florida. Report. Southeastern Wildlife Services Inc. (102 pp).
- Brown, R.B., Stone, E.L., Carlisle, V.W., 1990. Soils. In: Myers, R.L., Ewel, J.J. (Eds.) Ecosystems of Florida. University of Central Florida Press, Orlando.
- Campbell, K.M., 1984. St. Vincent Island (St. Vincent Island National Wildlife Refuge). Open File Report No. 8. Florida Geological Survey (15 pp).
- Donoghue, J.F., White, N.M., 1995. Late Holocene sea level change and delta migration, Apalachicola River region, northwest Florida, U.S.A. *Journal of Coastal Research* 11, 651-663.
- FDEP, 1999. Digital Orthographic Quarter-Quads Q4642 and Q4641. Indian Pass –West Pass, Florida: Florida Department of Environmental Protection ortho-photographs 1 m resolution, UTM projection, NAD 83 datum, 8 quarter-quads. <http://data.labins.org/2003/MappingData/DOQQ/doqq.cfm>
- López, G.I., *in preparation*. Optical dating of Barrier Island sequences along the Florida Gulf Coast near Apalachicola. Ph.D. Thesis, McMaster University, Hamilton, Canada.
- López, G.I., Rink, W.J., 2007. Quartz-OSL dating of Beach Ridges on the St. Vincent Island Holocene Strandplain, Florida North-West Gulf Coast, U.S.A. *Journal of Coastal Research*, *in press*.
- Madsen, A.T., Murray, A.S., Andersen, T.J., Pejrup, M., Breuning-Madsen, H., 2005. Optically stimulated luminescence dating of young estuarine sediments: a comparison with ^{210}Pb and ^{137}Cs dating. *Marine Geology* 214, 251-268.
- Miller, J.J., Griffin, J.W., Fryman, M.L., STAPOR, F.W., 1981. Archeological and Historical survey of St. Vincent National Wildlife Refuge, Florida. Contract A-5831 (79). U.S. Fish and Wildlife Service (101 pp).
- Murray, A.S., Wintle A.G., 2000. Luminescence dating of quartz using an improved single-aliquot regenerative-dose procedure. *Radiation Measurements* 32, 57-73.
- Murray-Wallace, C.V., Banerjee, D., Bourman, R.P., Olley, J.M., Brooke, B.P., 2002. Optically stimulated luminescence dating of Holocene relict foredunes, Guichen Bay, South Australia. *Quaternary Science Reviews* 21, 1077-1086.
- Otvos, E.G., 2005. Coastal barriers, Gulf of Mexico: Holocene Evolution and Chronology. *Journal of Coastal Research*, Special Issue No. 42, 141-163.
- Prescott, J.R., Hutton, J.T., 1988. Cosmic ray and gamma ray dosimetry for TL and ESR. *Nuclear Tracks and Radiation Measurements* 14, 223–227.
- Rink, W.J., Odom, A.L., 1991. Natural alpha recoil particle radiation and ionizing radiation sensitivities in quartz detected with EPR: Implications for geochronometry. *Nuclear Tracks and Radiation Measurements* D18, 163-173.
- Stapor, F.W., 1973. Coastal Sand Budgets and Holocene Beach Ridge Plain Development, Northwest Florida. Ph.D. Thesis, Florida State University (221 pp).

- Stapor, F.W., 1975. Holocene beach ridge plain development, northwest Florida. *Zeitschrift für Geomorphologie* 22, 116-144.
- Tanner, W.F., Demirpolat, S., Stapor, F.W., Alvarez, L., 1989. The Gulf of Mexico Late Holocene sea level curve. *Transactions Gulf Coast Association of Geological Societies* 39, 553-562.

CHAPTER 3 – FIGURES

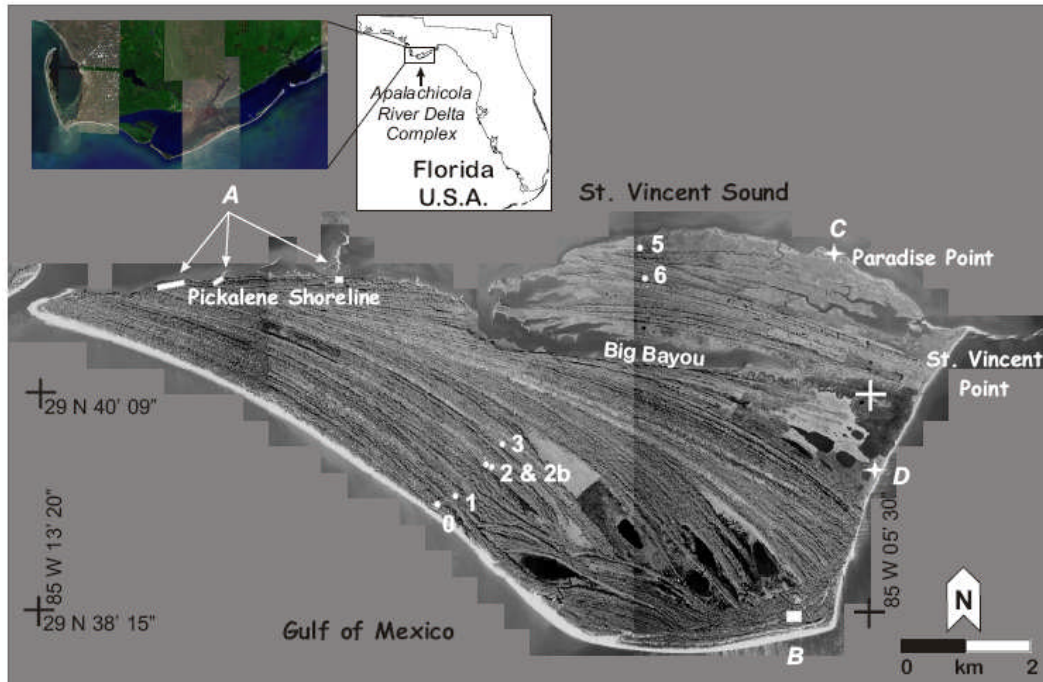


Figure 3.1.

Site location map of St. Vincent Island, NW Florida, U.S.A. Location of sediment cores recovered from coring sites are marked by white circles with corresponding SVI numbers. Archaeological sites are shown as white rectangles with ages as follows: A) 2,000 to >3,000-4,000 years ago based on pottery artefacts; B) <1862 A.D. based on remains of Fort Mallory (historical). Geological materials previously dated are shown as white stars with ages as follows: C) 1,710 years B.P. (un-calibrated ^{14}C) based on clay layer with charcoal lenses (Miller *et al.*, 1981; Campbell, 1984); D) $2,110 \pm 130$ years B.P. (un-calibrated ^{14}C) based on *Mulinia sp.* (Stapor, 1975). Image source: FDEP, 1999.

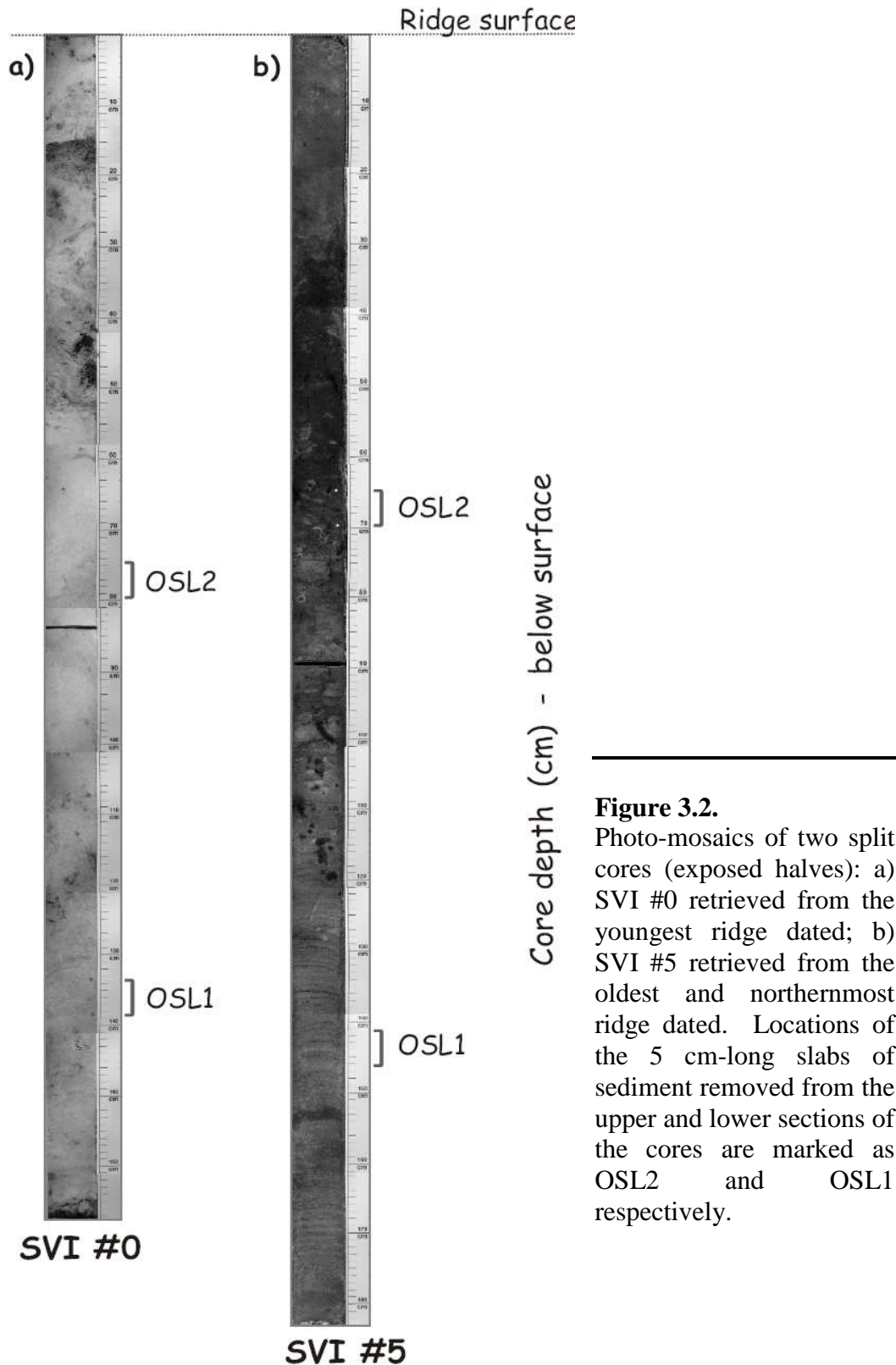


Figure 3.2. Photo-mosaics of two split cores (exposed halves): a) SVI #0 retrieved from the youngest ridge dated; b) SVI #5 retrieved from the oldest and northernmost ridge dated. Locations of the 5 cm-long slabs of sediment removed from the upper and lower sections of the cores are marked as OSL2 and OSL1 respectively.

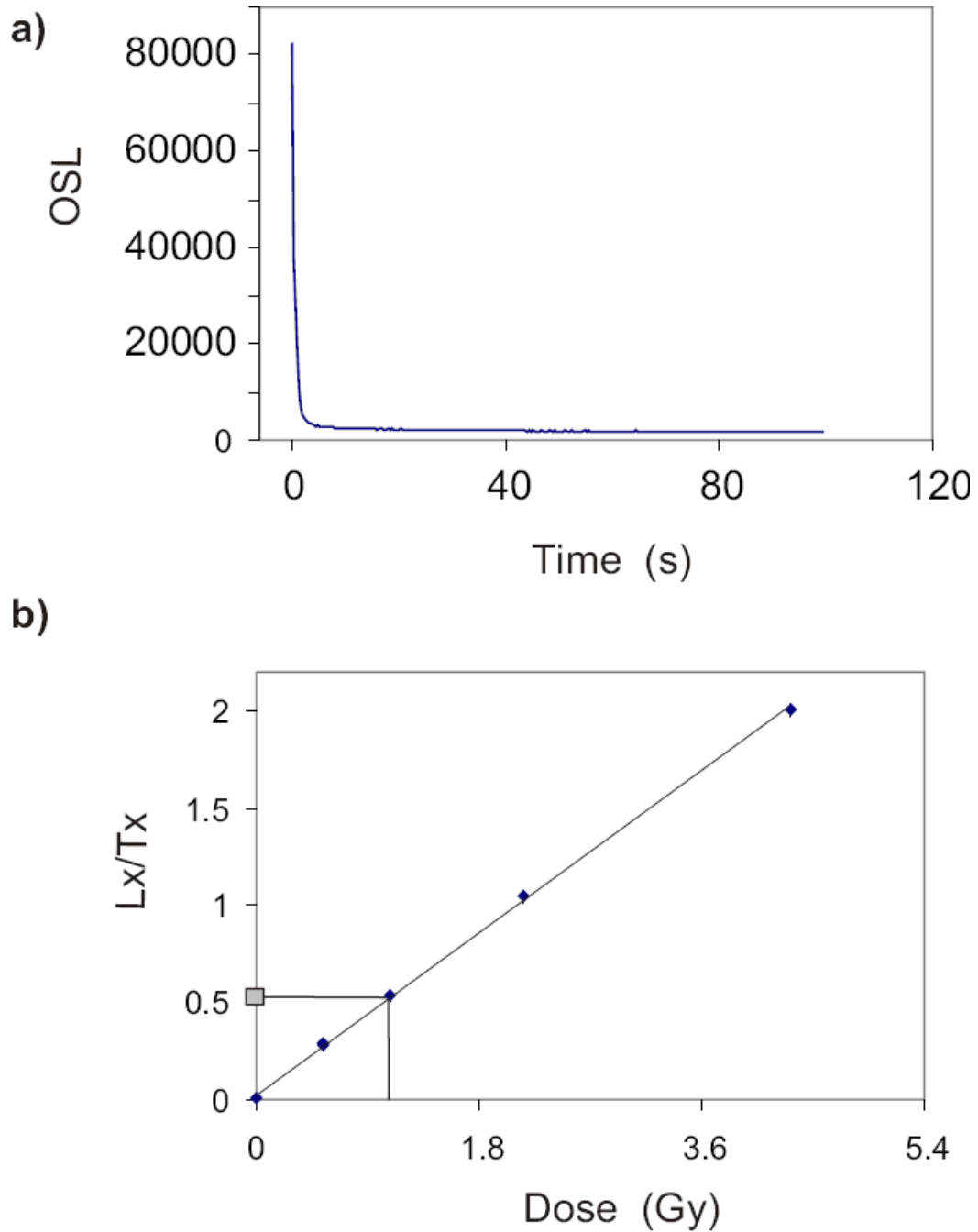
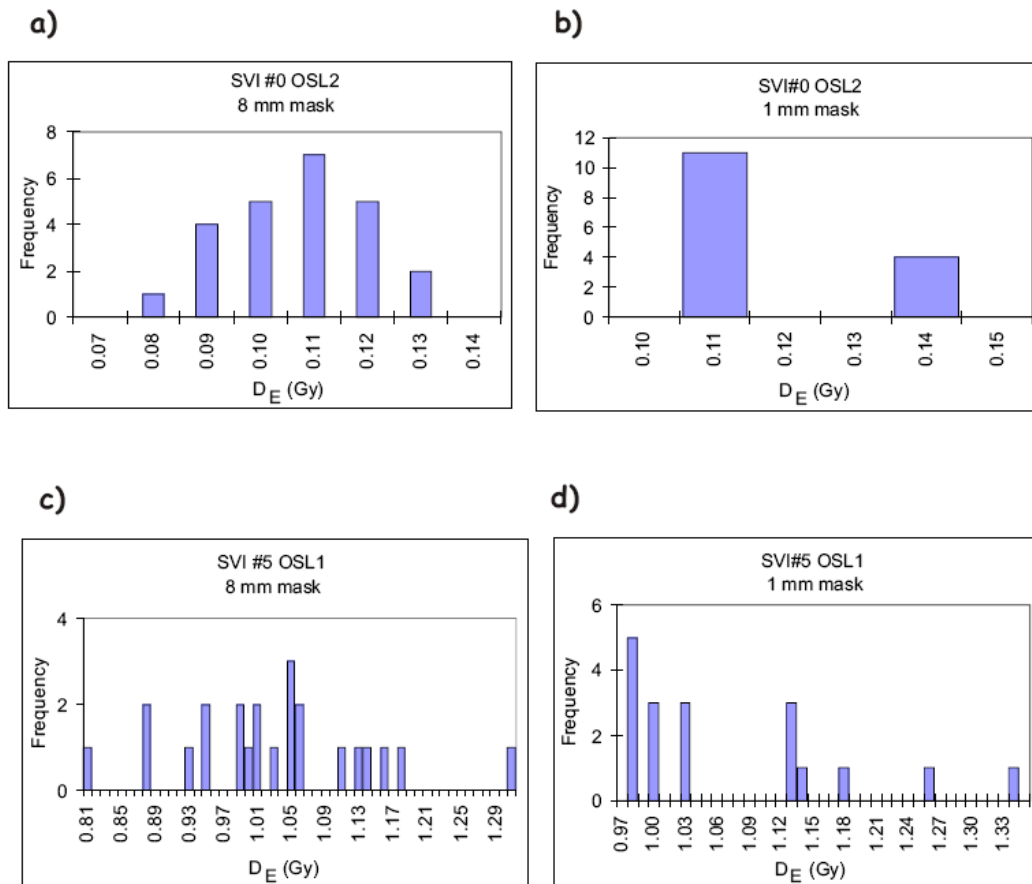
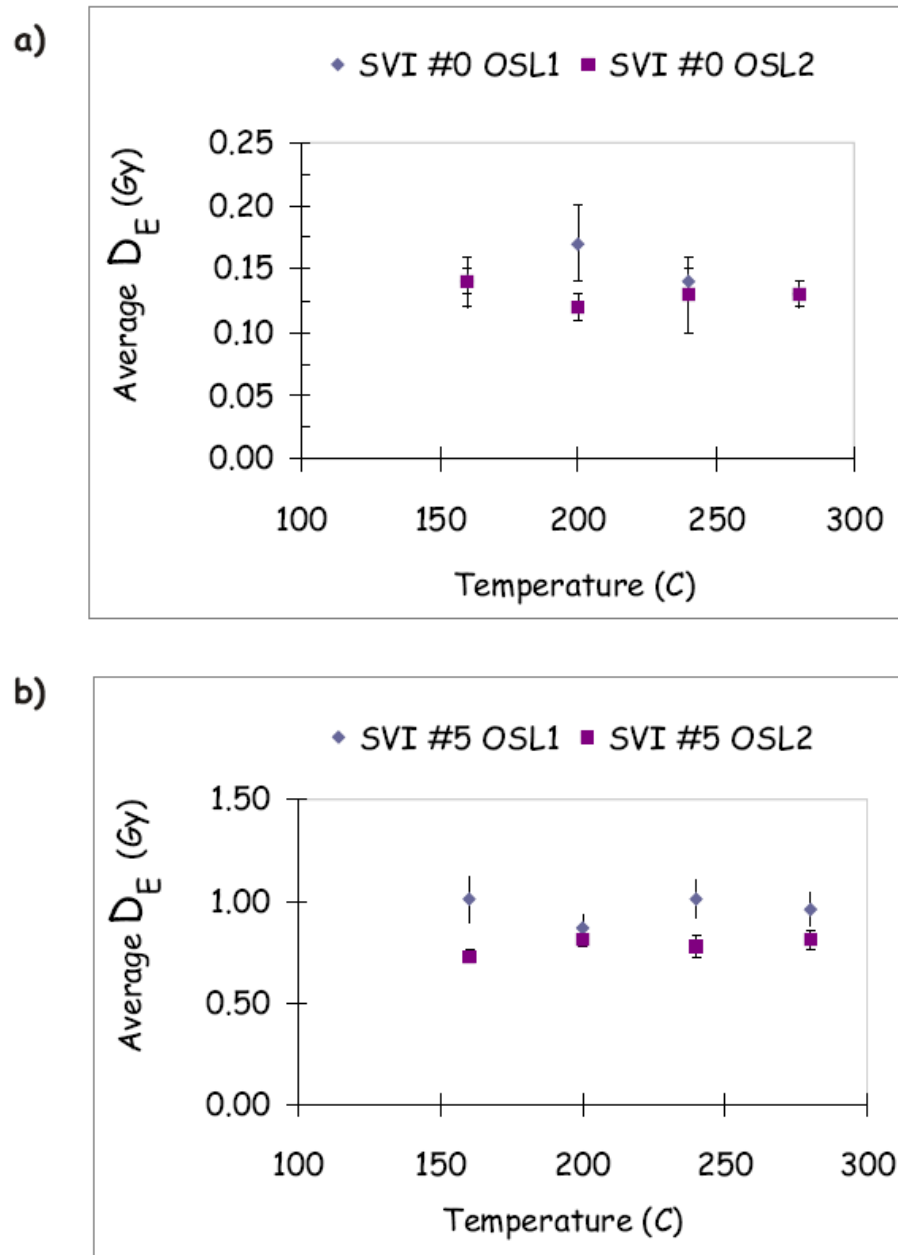


Figure 3.3. Examples of a) decay and b) response curves obtained for sample SVI #5 OSL1.

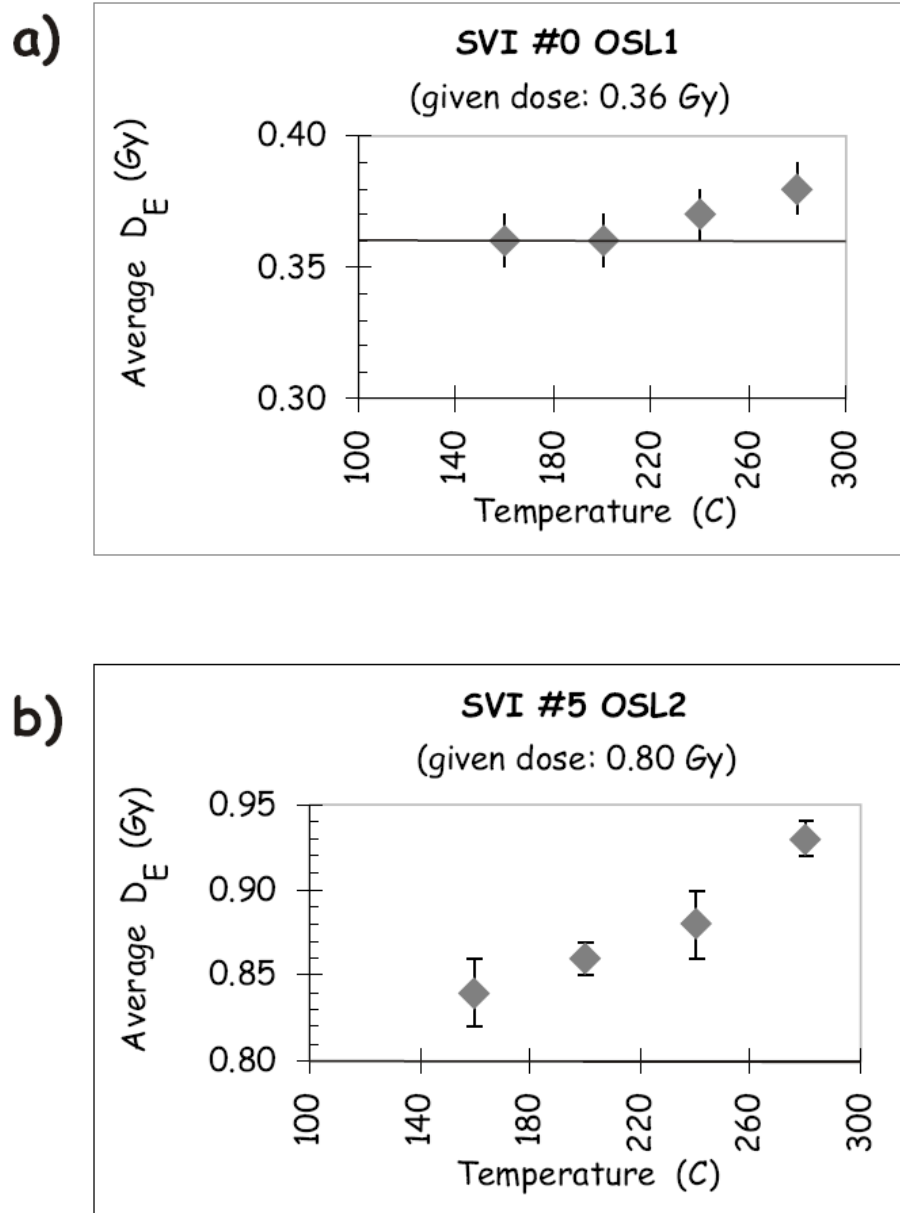
**Figure 3.4.**

Examples of D_E frequency distributions for the youngest (SVI #0 OSL2) and oldest (SVI #5 OSL1) samples dated in this study: a) and c) obtained using 8 mm masks; and b) and d) obtained using 1 mm masks.

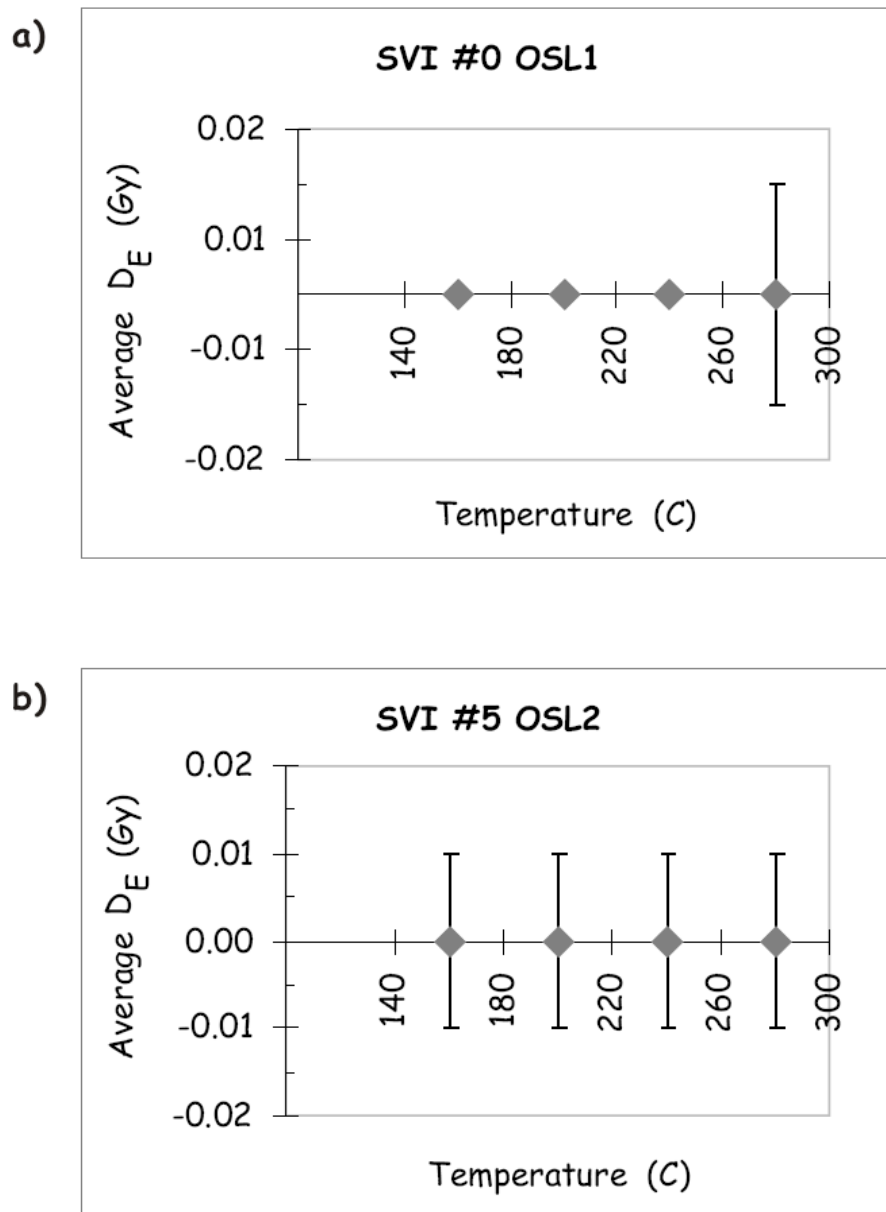
CHAPTER 3 -- APPENDIX A. SUPPLEMENTARY MATERIALS

**Figure 3.S1.**

Examples of D_E pre-heat plateau plots for samples from cores a) SVI #0 and b) SVI #5. No thermal transfer is seen on these initial tests.

**Figure 3.S2.**

Examples of the dose-recovery test done on samples a) SVI #0 OSL1 and b) SVI #5 OSL2. A pre-heat temperature of 160° C for 10 s was used in both cases and the known doses used were 0.36 Gy (a) and 0.80 Gy (b) respectively.

**Figure 3.S3.**

Thermal transfer test plots obtained for samples a) SVI #0 OSL1 (lower sample taken from youngest ridge dated in this study) and b) SVI #5 OSL2 (upper sample taken from the northernmost ridge cored in this study). The selected pre-heat temperature used to obtain the average D_E values for the OSL age determinations was 160°C for 10 s for all samples.

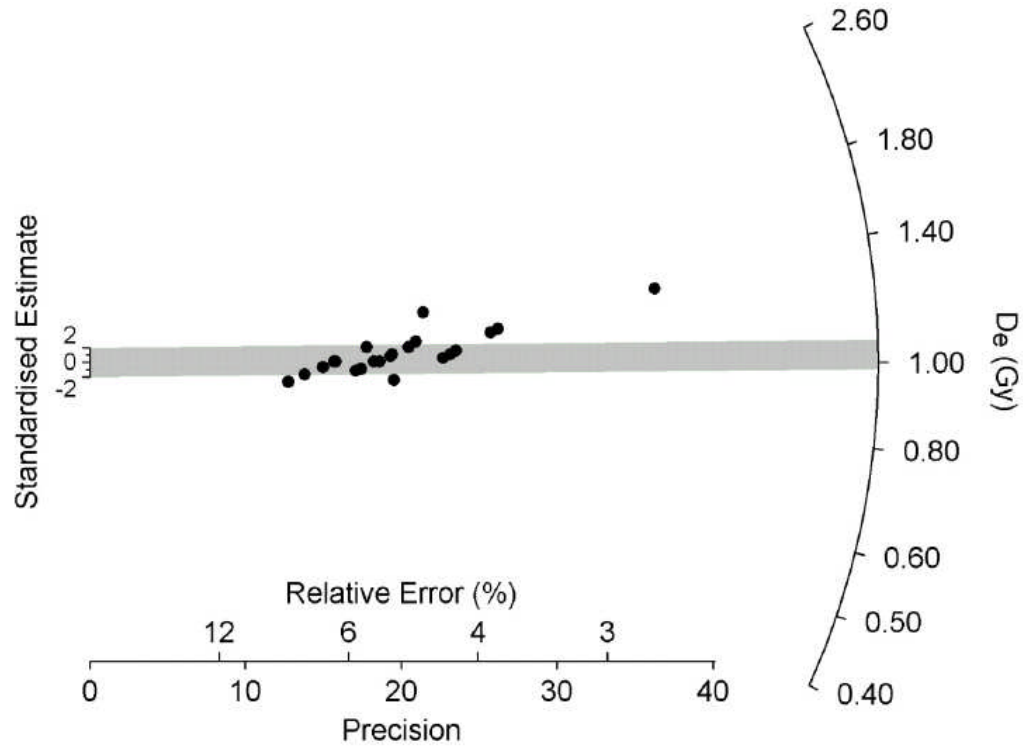


Figure 3.S4.

Example of the radial plot for sample SVI #5 OSL1. The mean observed for this sample was 1.018 Gy with 79% of the aliquots within 2σ .

Table 3.S1. Values for temperatures, durations of stimulation, and regeneration doses employed in the SAR protocol assigned to each sample dated in this study.

Core *	# Aliquots	Initial Preheat Temperature [time]	OSL Temperature of Natural [time]	Test Dose & Dose Preheat Temperatures [time] **	OSL							
					Temperature of Test Dose & Regeneration Doses [time]	Test Dose (Gy)	RD1 (Gy)	RD2 (Gy)	RD3 (Gy)	RD4 (Gy)	RD5 (Gy)	RD6 (Gy)
SVI #0 to SVI #2b	24	160°C [10 s]	125°C [100 s]	160°C [10 s]	125°C [100 s]	0.45	0.36	0.54	0.72	0.90	0	0.36
SVI #3	24	160°C [10 s]	125°C [100 s]	160°C [10 s]	125°C [100 s]	0.90	0.45	0.90	1.81	2.71	0	0.45
SVI #5 & SVI #6	24	160°C [10 s]	125°C [100 s]	160°C [10 s]	125°C [100 s]	1.98	0.54	1.08	2.16	4.33	0	0.54

* Both samples (OSL1 and OSL2) from the same core were measured using the same SAR protocol.

** Test dose preheat time was 0 s (cut-heat).

Table 3.S2.
SAR-OSL ages and data for samples taken from beach ridges on St. Vincent Island.

Core Sample [a]	D_e (Gy)	^{238}U (ppm) [b]	^{232}Th (ppm) [b]	K (%) [b]	Water Content (%) [c]^	Cosmic Ray Dose Rate ($\mu\text{Gy/a}$) [d]^*	Annual Dose ($\mu\text{Gy/a}$) [c]^*	SAR-OSL age (a) [f]^*	SAR-OSL age range (A.D.) at 1σ [f]	
SVI #0 OSL2	0.11 ± 0.01	0.18 ± 0.1	0.42 ± 0.04	0.018 ± 0.002	19	199	286 ± 15	370 ± 50	min 1584	max 1684
SVI #0 OSL1	0.12 ± 0.01	0.15 ± 0.1	0.48 ± 0.04	0.022 ± 0.002	3	185	284 ± 17	410 ± 60	1534	1654
SVI #1 OSL2	0.21 ± 0.01	0.16 ± 0.1	0.43 ± 0.04	0.032 ± 0.002	23	199	297 ± 14	710 ± 70	1224	1364
SVI #1 OSL1	0.28 ± 0.02	0.35 ± 0.1	0.85 ± 0.06	0.024 ± 0.002	14	187	343 ± 15	810 ± 100	1094	1294
SVI #2 OSL2	0.23 ± 0.02	0.20 ± 0.1	0.52 ± 0.04	0.019 ± 0.001	14	199	300 ± 15	780 ± 100	1124	1324
SVI #2 OSL1	0.45 ± 0.04	0.13 ± 0.1	0.55 ± 0.04	0.013 ± 0.001	2	181	272 ± 17	1640 ± 210	154	574
SVI #2b OSL2	0.25 ± 0.02	0.19 ± 0.1	0.57 ± 0.06	0.017 ± 0.001	16	200	299 ± 15	840 ± 100	1064	1264
SVI #2b OSL1	0.30 ± 0.02	0.15 ± 0.1	0.36 ± 0.04	0.015 ± 0.001	3	188	272 ± 17	1100 ± 130	774	1034
SVI #3 OSL2	0.67 ± 0.06	0.97 ± 0.1	4.18 ± 0.28	0.027 ± 0.002	7	198	725 ± 21	920 ± 130	954	1214
SVI #3 OSL1	0.76 ± 0.10	0.53 ± 0.1	1.11 ± 0.08	0.019 ± 0.001	3	177	404 ± 17	1900 ± 300	176 B.C.	404
SVI #5 OSL2	0.82 ± 0.08	0.19 ± 0.1	0.31 ± 0.04	0.025 ± 0.005	19	198	286 ± 15	2900 ± 300	1196 B.C.	516 B.C.
SVI #5 OSL1	1.04 ± 0.13	0.53 ± 0.1	0.84 ± 0.07	0.033 ± 0.005	14	180	382 ± 16	2700 ± 400	1126 B.C.	326 B.C.
SVI #6 OSL2	0.76 ± 0.06	0.17 ± 0.1	0.35 ± 0.04	0.007 ± 0.003	24	204	273 ± 14	2800 ± 300	1076 B.C.	496 B.C.
SVI #6 OSL1	0.84 ± 0.08	0.26 ± 0.1	0.55 ± 0.04	0.013 ± 0.002	9	189	303 ± 16	2800 ± 300	1116 B.C.	436 B.C.

[a] OSL1 corresponds to sample taken towards the bottom of the core and OSL2 to the one taken towards the top of the core at depths > 50 cm below surface.
[b] U, Th and K values determined by NAA.
[c] Water content as a fraction of dry weight determined from laboratory measurements.
[d] Cosmic ray dose rate value calculated using an overburden density of 2 g/cm³.
[e] All β and γ dose rates were calculated based on U, Th and K concentrations of each sample, accounting for moisture values of the samples.
[f] Datum for SAR-OSL ages is A.D. 2004.
^ Values rounded off to sensible numbers of precision.
* Ages were calculated assuming constant sediment accumulation rates.

CHAPTER 4

OPTICALLY STIMULATED LUMINESCENCE AGE OF THE OLD CEDAR MIDDEN, ST. JOSEPH PENINSULA STATE PARK, FLORIDA

Jeroen Thompson^{a,*}

W. Jack Rink^{a,b}

Gloria I. López^b

^a Department of Medical Physics and Applied Radiation Sciences

^b School of Geography and Earth Sciences

McMaster University

1280 Main Street West, Hamilton, Ontario, L8S 4K1, Canada

* Corresponding author's Email address: thompjw@mcmaster.ca

Citation:

THOMPSON, J., RINK, W.J., and LÓPEZ, G.I., 2007. Optically Stimulated Luminescence age of the Old Cedar Midden, St. Joseph Peninsula State Park, Florida. *Quaternary Geochronology*, 2, 350-355.

Quaternary Geochronology: Elsevier Science, Oxford, ISSN 1871-1014 (Imprint: Elsevier).

Status: received 12 October 2005, accepted 1 May 2006, available online 19 June 2006, published.

“Reprinted from *Quaternary Geochronology*, (2), Thompson, J., Rink, W.J., and López, G.I., Optically Stimulated Luminescence age of the Old Cedar Midden, St. Joseph Peninsula State Park, Florida, 350-355, © (2007), with permission from Elsevier”.

From: "Jones, Jennifer (ELS-OXF)" <J.Jones@elsevier.co.uk>
To: "Gloria I. López C." <lopezgi@mcmaster.ca>
Subject: RE: thesis
Date: October 20, 2006 03:05

Dear Gloria I Lopez

We hereby grant you permission to reproduce the material detailed below at no charge in your thesis subject to the following conditions:

1. If any part of the material to be used (for example, figures) has appeared in our publication with credit or acknowledgement to another source, permission must also be sought from that source. If such permission is not obtained then that material may not be included in your publication/copies.

2. Suitable acknowledgment to the source must be made, either as a footnote or in a reference list at the end of your publication, as follows:

"Reprinted from Publication title, Vol number, Author(s), Title of article, Pages No., Copyright (Year), with permission from Elsevier".

3. Reproduction of this material is confined to the purpose for which permission is hereby given.

4. This permission is granted for non-exclusive world English rights only. For other languages please reapply separately for each one required. Permission excludes use in an electronic form. Should you have a specific electronic project in mind please reapply for permission.

5. This includes permission for the Library and Archives of Canada to supply single copies, on demand, of the complete thesis. Should your thesis be published commercially, please reapply for permission.

Yours sincerely,

Jennifer Jones
Rights Assistant

ABSTRACT

We report optically stimulated luminescence (OSL) dating results from the Old Cedar midden in St. Joseph Peninsula State Park, located between the Gulf of Mexico and St. Joseph Bay near Port St. Joe, FL, USA. The Old Cedar site (8GU85) is located on top of a relict beach ridge which is actively eroding into St. Joseph Bay. Old Cedar is noted for its conch shell tool assemblage, otherwise rare at northwest Florida archaeological sites, and is believed to have been utilized during the Late Woodland Weeden Island and possibly the Fort Walton periods [Benchley, E.D., Bense, J.A., 2001. *Archaeology and history of St. Joseph Peninsula State Park: Phase I investigations. Report of Investigations, No. 89, University of West Florida Archaeology Institute*]. After removing surficial erosion deposits, we extracted OSL core samples from both the midden layer and the underlying beach ridge. The resulting OSL age is compared with the age of another beach ridge on St. Joseph Peninsula. We hope that this study will aid in the investigation and conservation of Old Cedar specifically and other Weeden Island sites in the St. Joseph Bay area.

4.1. INTRODUCTION

The Old Cedar site is a shell midden located on top of an eroding relict beach ridge in the St. Joseph Peninsula State Park, located between the Gulf of Mexico and St. Joseph Bay near Port St. Joe, FL, USA (see **Figures 4.1.** and **4.2.**). The site is located at a latitude of 29° 14' 54" N and longitude of 85° 23' 28" W and is designated as site 8GU85 in the Florida Master Site File. The midden is exposed at an eroding bluff along the St. Joseph Bay. Along the bay shore bluff, the midden consists of a dark brown sandy soil, approximately 30–40 cm thick, located directly above a sugary-white dune sand deposit. Shell fragments, whelk tools, and potsherds are visible in the midden layer, sand apron, and in the bay itself.

Although the midden is exposed for approximately 40 m along a gently rising bluff, the site of Old Cedar is much larger. Survey work has indicated that the midden extends for roughly 175 m along the beach ridge in an approximately NNE direction (Benchley and Bense, 2001) and is over 50 m wide at its widest point. The site is covered with dense, mature maritime hammock vegetation, which is associated with the organic soil of the midden. A popular park trail permits access to the site; pothole-style looting has been reported. In addition, the marsh past the known western boundary of the site is considered a promising location for future excavations.

Old Cedar is rich in artifacts. Diagnostic potsherds indicate Late Woodland Weeden Island period occupation with a possible subsequent occupation during the Fort Walton (**Table 4.1.**) (Benchley and Bense, 2001). An

extensive shell tool assemblage, otherwise rare in northwest Florida, is also present at Old Cedar, consisting primarily of worked shells of *Busycon contrarium* (lightning whelk).

4.2. METHOD

OSL samples (OC1 and OCg1, from the midden and relict beach ridge, respectively) were collected with the goal of minimizing disturbance to the archaeological site. The midden layer was lightly exposed at the coring location with a trowel. A small trench was dug into the sand apron (light grey) in order to ensure exposure of the relict dune (sugary white). Light-tight aluminium core tubes were hammered into the exposed surfaces. The cores were removed and sealed tightly for transport. Sediment samples were removed from the rear of the bore-hole and placed into plastic bags, which were tightly sealed for transport and subsequent moisture content analysis. Artifacts encountered in situ (whelk fragments and potsherds) were bagged and returned to St. Joseph Peninsula State Park.

Sediment was removed from the cores and dried in an oven (< 60 °C). Whole untreated sediment was taken for neutron activation analysis for measurement of the radioisotopes 232 thorium (Th), and 40 potassium (K) and delayed neutron counting for measurement of 238 uranium (U). The samples were treated with 10% HCl and 30% H₂O₂ in order to remove carbonates and organics. The sediment was sieved in order to obtain the desired 150–212 μm fraction. Heavy liquid separation was used to remove feldspars and heavy minerals. The quartz fraction was treated with 40% HF for 40 min in order to remove plagioclase as well as the outer layer (external alpha dose) of the quartz grains. A subsequent 40 min treatment with 10% HCl was used to remove precipitated fluorites.

Quartz grains were mounted onto aluminium disks with silicone spray; masks of varying sizes were used to obtain aliquots with varying numbers of quartz grains. OSL measurements were taken with a Risø TL/OSL System (Model TL-DA-15), equipped with a ^{90}Sr source (beta dose rate: 0.089 Gy/s). OSL measurements were made with blue LEDs (470 nm) and a 7 mm thick Hoya U-340 bandpass filter (270–400 nm). Feldspar contamination was tested with infrared-stimulated luminescence (IRSL) using an infrared laser diode (830 nm).

OSL measurements (Wintle, 1997) were made using a single-aliquot regenerative dose (SAR) protocol based on Murray and Wintle (2000). Each aliquot is given multiple regenerative doses, and the OSL signal measured after each dose, with a constant test dose used to correct for changes in sensitivity. Details of our SAR protocol are given in **Table 4.2**. The OSL signal intensity was taken to be the integrated luminescence intensity for the initial 0.4 s, while the background was taken to be the integrated intensity for the final 4.0 s of a 100 s measurement.

The equivalent doses (D_E 's) were estimated by an initial study, which also included a test for feldspar contamination. The D_E 's were estimated by comparing the natural OSL (preheat $T = 160$ °C) of 3 aliquots (mask size 8 mm) to the regenerated OSL given by a single dose ($R = 0.89$ Gy). A second identical regeneration dose was applied, and the IRSL was measured. A ratio of IRSL to regenerated OSL signal intensity of less than 1% was observed for all aliquots, indicating no significant feldspar contamination (Forrest et al., 2003).

The preheat temperature was determined by a preheat plateau test. Three aliquots from each sample were measured for every preheat temperature of 160, 200, 240, and 280 °C using the SAR protocol (mask size: 8 mm). The mean D_E versus preheat temperature is shown in **Figure 4.S1**. The preheat temperature of 200 °C was selected as the appropriate preheat for both OC1 and OCg1, as the error bars overlap with all other measurements for each sample.

Thermal transfer and dose recovery tests (Murray and Wintle, 2003; Madsen et al., 2005) were applied to each sample. For both tests, the aliquots were optically cleaned through illumination by the blue LEDs for 40 s, and again for another 40 s after a waiting time of 10,000 s. For the dose recovery test only, the aliquots were given a known dose (0.36Gy for OC1 and 0.45 Gy for OCg1). Both tests continued with the SAR protocol shown in **Table 4.2.**, except that the initial preheat was held constant ($T_1 = 160$ °C) while the subsequent preheat temperature varied ($T_2 = 160, 200, 240,$ and 280 °C), with three aliquots measured using each preheat temperature. Twelve aliquots of both samples (mask size: 8 mm) were prepared for each test with three aliquots using each preheat temperature (T_2).

From each sample 24 aliquots were measured with a mask size of 8 and 5 mm, respectively, and 48 aliquots from each sample were measured with a mask size of 3 mm, to determine the mean D_E for each sample. Any aliquot which had a recycling ratio outside the range 0.90–1.10 was excluded from further analysis. An initial mean was calculated for each set of measurements. Aliquots with a D_E outside of the initial mean plus or minus twice the initial standard deviation were removed from the analysis. The final mean and standard deviation were recalculated (**Table 4.3.**).

As no evidence of incomplete zeroing was found using 5 and 3 mm masks, the equivalent doses for each sample were determined using the 8mm mask size. The dose rates and ages were calculated using Anatol 0.72B (courtesy of N. Mercier, CNRS, Paris), which incorporates the energy release data of Adamiec and Aitken (1998). Beta and gamma radiation dose rates were computed from the U, Th and K concentrations of the whole sediment. In addition to the statistical errors of all parameters input into Anatol, we assume a global systematic error of 20%. The ages are reported with a total (i.e., including both statistical and systematic) error. The internal dose rates from U and Th are calculated from the

average concentrations of those two radioisotopes in granitic quartz (Rink and Odom, 1991).

We have calculated the cosmic dose rate assuming both instant accumulation and linear accumulation of overburden through time. For the linear accumulation calculation, we use the cosmic dose rate calculated at a depth equal to half the depth of the extracted core. For all calculations, we assume an infinite-planar overburden with density 2.0 g/cm^3 .

4.3. RESULTS AND DISCUSSION

The radioisotope concentrations in the bulk sediments are presented in **Table 4.4**. The measured moisture contents are 3.4% and 0.5% for OC1 and OCg1, respectively (% dry weight). The total organic and carbonate contents are 9.6% and 3.0% for OC1 and OCg1, respectively (% dry weight). We assume a constant moisture content with time. Dissolution of shell could affect the uranium-series dose rates, but we note that uranium concentration is low in these samples ($< 1 \text{ ppm}$), so that a potential disequilibrium would not greatly affect the dose rates.

The thermal transfer test is used to ensure that the preheat temperature does not affect the measured D_E . For both OC1 and OCg1, no change in the measured D_E was observed over the range of preheat temperatures, except at the highest temperature for OCg1 in which the measured D_E is too low. As an additional check, the dose recovery test was applied. Although a linear trend towards increasing D_E 's with increasing preheat temperature was observed for both samples, at the chosen preheat temperature of $200 \text{ }^\circ\text{C}$, the ratio of recovered dose to given dose is not significantly different from unity for both samples.

Varying mask sizes are used to test for incomplete zeroing. However, no evidence of incomplete zeroing has yet been found for OSL studies in the St. Joseph Bay/Apalachicola region. The histogram of D_E 's for OC1 is shown in **Figure 4.3**. The scatter in D_E 's is larger for the 3 mm mask when compared to the 5 and 8 mm masks. However, the largest D_E 's measured with a mask size of 3 mm do not represent a tail toward increasing equivalent doses. Note that the mask size of 3 mm also results in smaller equivalent doses (in fact, the mean D_E is slightly less than that for the 8 mm mask). Any possible tail towards increasing equivalent doses, which would be indicative of partial zeroing, is not present when using the 5 mm mask. We conclude that the outliers obtained with the 3 mm mask are simply natural variation due to inhomogeneities in the dose rate. Aliquots which have a measured D_E outside the range of the initial mean D_E plus or minus twice the standard deviation were removed from the calculations. The mean D_E and standard deviation were then re-calculated (see **Table 4.3**). No statistically significant difference in the mean D_E was seen among mask sizes, either before or after removal of aliquots.

The histogram of D_E 's for OCg1 is shown in **Figure 4.4**. Again there is no consistent trend with decreasing mask size. The mean D_E and standard deviation were recalculated for each mask size (**Table 4.3**), using the same procedure as outlined for OC1. There may be a slight trend towards decreasing D_E 's with decreasing mask size, but the mean D_E 's for each mask size agree within the two-sigma errors. In addition, we do not see a tail towards increasing D_E 's with either the 5 mm mask or the 3 mm mask, when compared against the data obtained with the 8 mm mask. Neither OC1 nor OCg1 shows any evidence of incomplete zeroing.

The OSL ages for the midden deposit and the underlying ridge are given in **Table 4.4**. The ages are calculated using both linear and instant accumulation models (LA and IA, respectively) for each sample. The ages are computed using the re-calculated mean D_E 's obtained with the 8 mm mask size (0.38 ± 0.03 and 0.47 ± 0.03 Gy, for OC1 and OCg1, respectively). We find that the midden has an age of 940 ± 100 years (IA) while the underlying ridge is approximately 800 years older, with an age of 1780 ± 130 years (LA). We can also calculate the ages using the mean D_E 's obtained with the 3 mm mask size (0.38 ± 0.07 and 0.43 ± 0.07 Gy, for OC1 and OCg1, respectively). In this case, we obtain ages for the midden and ridge of 940 ± 190 years (IA) and 1650 ± 250 years (LA), respectively. Clearly using the 3 mm masks has fairly little effect on the ages, except for dramatically increasing the error range. We feel the ages calculated using the 8 mm mask size are the most reliable (**Table 4.4**), as these reflect the bulk environmental dose rates.

The difference in ages between the relict beach ridge (OCg1) and the overlying midden (OC1) allows us to rule out instant accumulation as a possible model for the deposition of the whole deposit. Sample OCg1 was collected approximately 0.3 m below the ridge–midden boundary; this sizeable quantity of sediment suggests a lengthy depositional history for the beach ridge. Linear accumulation, therefore, is the best model for the beach ridge deposit.

The midden deposit extends upward to within a few cm of the surface without any anthropogenic accumulation overlying it. Thus the overburden above the dated sample largely accumulated during the archaeological occupation, and therefore formed during a time that is short compared to the time since abandonment. This makes an instantaneous accumulation model for the overburden more appropriate for the midden OSL sample. Furthermore, the geomorphic location of the dune (on the bay margin: the protected side of the peninsula) strongly suggests a stable surface has been present since abandonment. Along the St. Joseph Peninsula, the prevailing winds are from the west. Accumulation of sediment therefore decreases as the ridge forms and is stranded inland. Therefore additional supra-midden accumulation and subsequent erosion is unlikely. In the present day, the organic soil of the midden is associated with

dense vegetation, which may have helped to stabilize the midden surface post-abandonment. We therefore use instant accumulation as the best model for the midden deposit.

In any case, the difference between LA and IA ages for the beach ridge and for the midden are not large, as both models agree within error. The OSL age of the midden places occupation of the Old Cedar site into the Late Weeden Island period (**Table 4.1.**), consistent with expectation based on the artifactual assemblage.

We assume secular equilibrium in the decay chains and that the radioisotope concentrations have remained constant over time. Dissolution of shell, for example, could affect the uranium concentration in the sediment. However, for our samples, the uranium concentration is very low ($< 1 \text{ ppm } ^{238}\text{U}$). In the case of OC1 (midden), the uranium decay chain is responsible for only 23% of the annual external gamma dose rate, and an even smaller proportion of the total dose rate (10%). Changes in the uranium concentration, as well as disequilibrium in the decay chain, would not have a large impact on the dose rates.

Based on previous OSL dating on the north end of the peninsula (Forrest, 2003), ridges have accumulated northward through time. For example, Deer Ridge (López, in preparation) is located to the north of the Old Cedar beach ridge (**Figure 4.2.**) and has been dated to 1030 ± 40 years ago (LA, *datum* 2005). The age of the relict beach ridge below the Old Cedar midden (1780 ± 130 years ago, LA, *datum* 2005) is consistent with this pattern, being about 750 years older than Deer Ridge.

4.4. CONCLUSION

We have provided an age (940 ± 100 years) for the Old Cedar midden in St. Joseph Peninsula State Park, Florida, which indicates occupation during the Late Weeden Island cultural phase. The underlying relict beach ridge has also been dated (1780 ± 130 years). The Old Cedar site is a unique and valuable archaeological site, noted for its conch shell tool collection, which is rare at other northwest Florida archaeological sites. The site is greatly threatened by erosion at the bay shore and also by sporadic looting. We hope that these results will aid in conservation of the site and in any future excavations.

ACKNOWLEDGMENTS

The authors gratefully acknowledge Anne Harvey, Cynthia Emrich, and the staff of St. Joseph Peninsula State Park for their assistance in this study. Dr. E.D. Benchley kindly provided a reprint of the Phase I archaeological survey for the Park. We also thank the reviewer for helpful comments regarding this manuscript.

Editorial handling by: R. Grün

APPENDIX A. SUPPLEMENTARY DATA

Supplementary data associated with this article can be found in the online version at doi:10.1016/j.quageo.2006.05.005.

REFERENCES

- Adamiec, G., Aitken, M., 1998. Dose-rate conversion factors: update. *Ancient TL* 16, 37–50.
- Benchley, E.D., Bense, J.A., 2001. Archaeology and history of St. Joseph Peninsula State Park: Phase I investigations. University of West Florida Archaeology Institute, Report of Investigations, No. 89.
- FDEP, 1999. Digital Orthographic Quarter-Quads Q4643, Q4644, Q4743, and Q4744. Cape San Blas—St. Joseph Peninsula—Port St. Joe—St. Joseph Point, Florida. Florida Department of Environmental Protection ortho-photographs 1 m resolution, Albers projection, NAD 83 datum, 9 quarter-quads. <http://data.labins.org/2003/MappingData/DOQQ/doqq.cfm>
- Forrest, B.M., 2003. Application of luminescence techniques to coastal studies at the St. Joseph Peninsula, Gulf County, Florida. M.Sc. Thesis, McMaster University, Hamilton, Canada, unpublished.
- Forrest, B., Rink, W.J., Bicho, N., Ferring, C.R., 2003. OSL ages and possible bioturbation signals at the Upper Paleolithic site of Lagoa do Bordoal, Algarve, Portugal. *Quaternary Science Reviews* 22, 1279–1285.
- López, G.I., Optical dating of barrier island sequences along the Florida Gulf Coast near Apalachicola. Ph.D. Thesis, McMaster University, Hamilton, Canada, in preparation.
- Madsen, A.T., Murray, A.S., Anderson, T.J., Pejrup, M., Breuning-Madsen, H., 2005. Optically stimulated luminescence dating of young estuarine sediments: a comparison with ²¹⁰Pb and ¹³⁷Cs dating. *Marine Geology* 214, 251–268.
- Murray, A.S., Wintle, A.G., 2000. Luminescence dating of quartz using an improved single-aliquot regenerative-dose protocol. *Radiation Measurements* 32, 57–73.
- Murray, A.S., Wintle, A.G., 2003. The single aliquot regenerative dose protocol: potential for improvements in reliability. *Radiation Measurements* 37, 377–381.
- Rink, W.J., Odom, A.L., 1991. Natural alpha recoil particle radiation and ionizing radiation sensitivities in quartz detected with EPR: implications for geochronometry. *Nuclear Tracks and Radiation Measurements* 18, 163–173.

Wintle, A.G., 1997. Luminescence dating: laboratory procedures and protocols. *Radiation Measurements* 27, 769–817.

CHAPTER 4 – FIGURES



Figure 4.1.
Map of Florida, USA. Area within the box is shown in the inset of Figure 4.2.

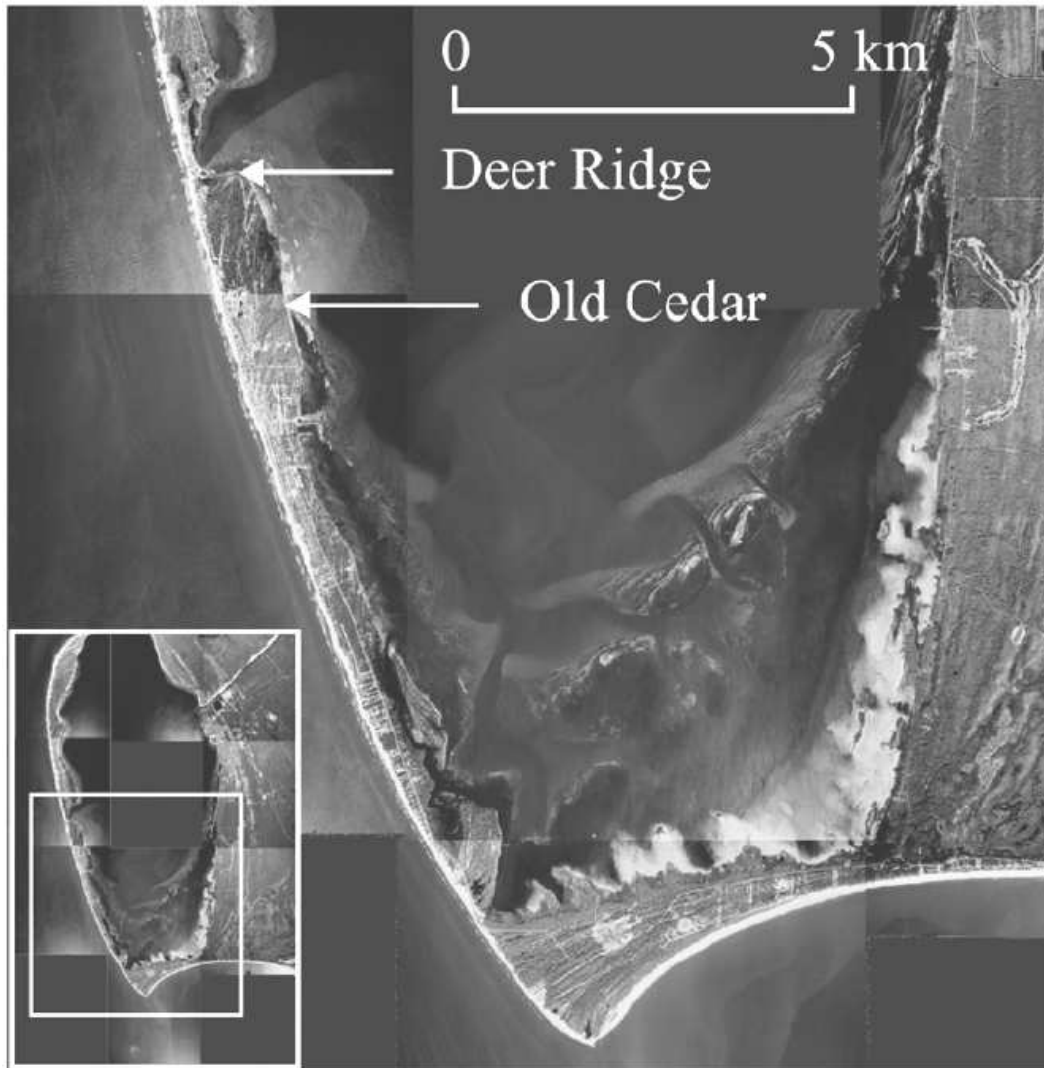


Figure 4.2. Study area (FDEP, 1999). Inset: St. Joseph Peninsula. Aerial photographs courtesy USGS.

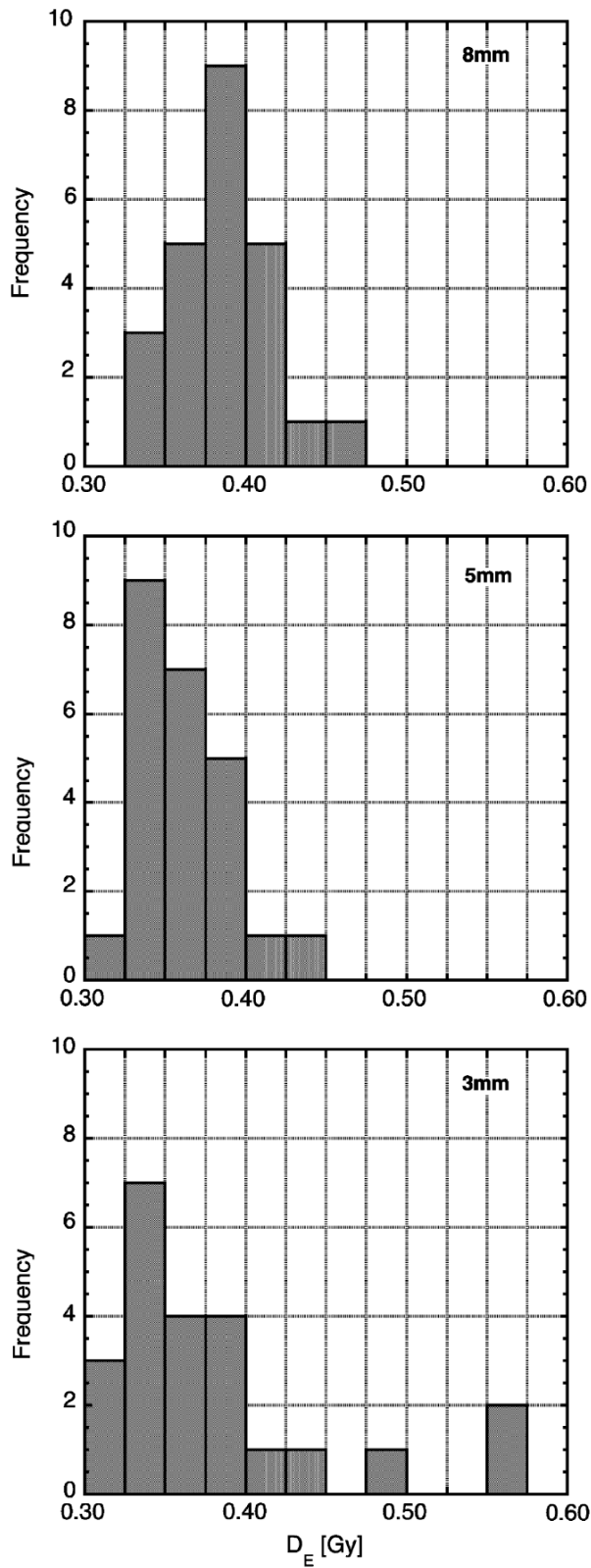


Figure 4.3. Histograms of measured D_E 's for OC1 (midden) with varying mask sizes.

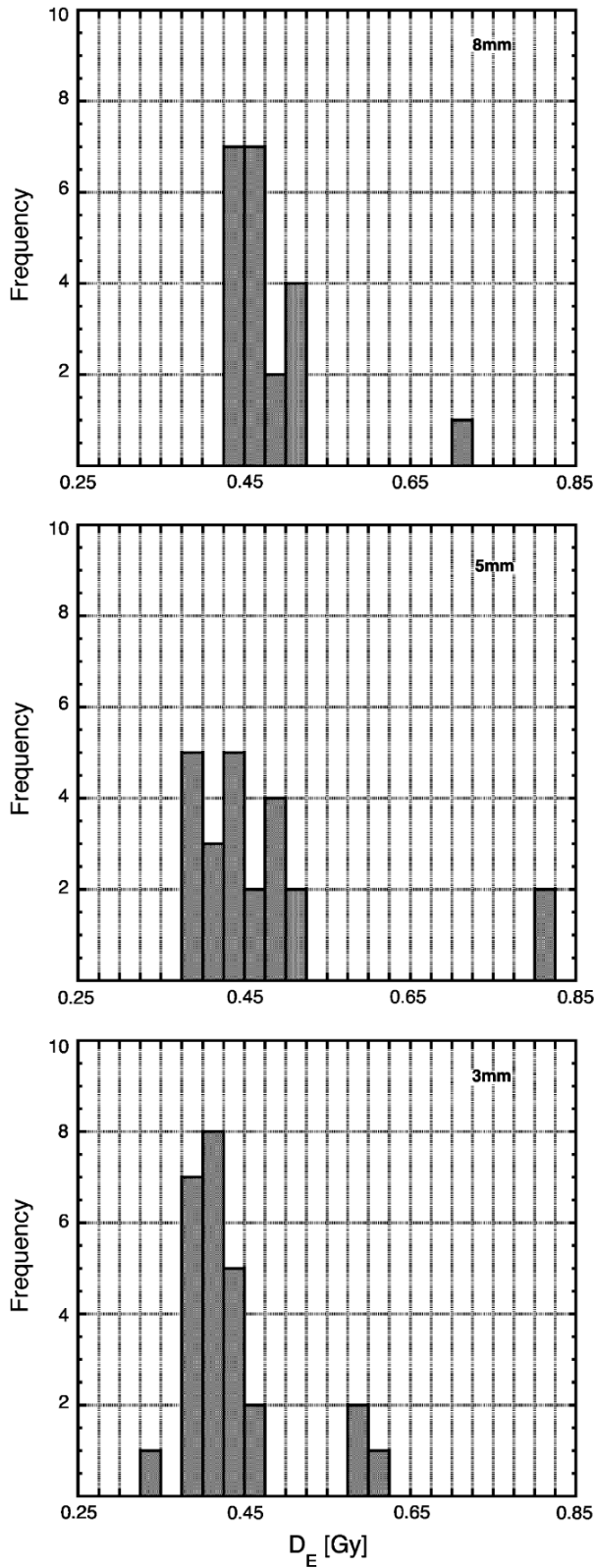


Figure 4.4.
Histograms of measured D_E 's for OCg1 (beach ridge) with varying mask sizes.

CHAPTER 4 – TABLES

Table 4.1.

Periods, cultures, and accepted dates for the northwest Florida cultural sequence (after Benchley and Bense, 2001).

Period	Culture	Ages (years ago)
Early Woodland	Deptford	3000–1800
Middle Woodland	Santa Rosa/Swift Creek	1800–1500
Late Woodland I	Early Weeden Island	1500–1200
Late Woodland II	Late Weeden Island	1200–800
Middle Mississippian	Early Fort Walton	800–500
Late Mississippian	Late Fort Walton	550–400

Table 4.2.

Our single aliquot regeneration protocol.

1.	Preheat T_1 [10 °C/s, 10 s]
2.	Measure natural OSL [125 °C, 10 °C/s, 100 s]
3.	Apply test dose [0.89 Gy]
4.	Cut-heat [160 °C, 10 °C/s, 0 s]
5.	Measure OSL [125 °C, 10 °C/s, 100 s]
6.	Apply regeneration dose $R = R_0$
7.	Preheat T_2 [10 °C/s, 10 s]
8.	Measure OSL [125 °C, 10 °C/s, 100 s]
9.	Apply test dose [0.89 Gy]
10.	Cut-heat [160 °C, 10 °C/s, 0 s]
11.	Measure OSL [125 °C, 10 °C/s, 100 s]
12.	Repeat (6)–(11) with $R = 2R_0, 3R_0, 4R_0, 0, R_0$

The preheat temperature varied for the preheat plateau test ($T_1 = T_2 = 160, 200, 240,$ and 280 °C). For the thermal transfer and dose recovery tests, T_2 varied as before ($T_1 = 160$ °C). For the final measurements, $T_1 = T_2 = 200$ °C. $R_0 = 0.36$ Gy.

Table 4.3.

Variation in mean equivalent dose with mask size.

Sample	8 mm mask	5 mm mask	3 mm mask
OC1	0.39 ± 0.03 (24)	0.36 ± 0.03 (24)	0.38 ± 0.07 (23)
	0.38 ± 0.03 (23)	0.36 ± 0.02 (23)	0.36 ± 0.04 (21)
OCg1	0.48 ± 0.06 (22)	0.47 ± 0.12 (23)	0.43 ± 0.07 (26)
	0.47 ± 0.03 (21)	0.44 ± 0.04 (21)	0.41 ± 0.03 (23)

The initial mean is followed by the re-calculated mean (see text for details). The number of accepted aliquots is shown in parentheses. The errors are one standard deviation. Units are Gy.

Table 4.4.
Dose rates and OSL burial ages for each sample.

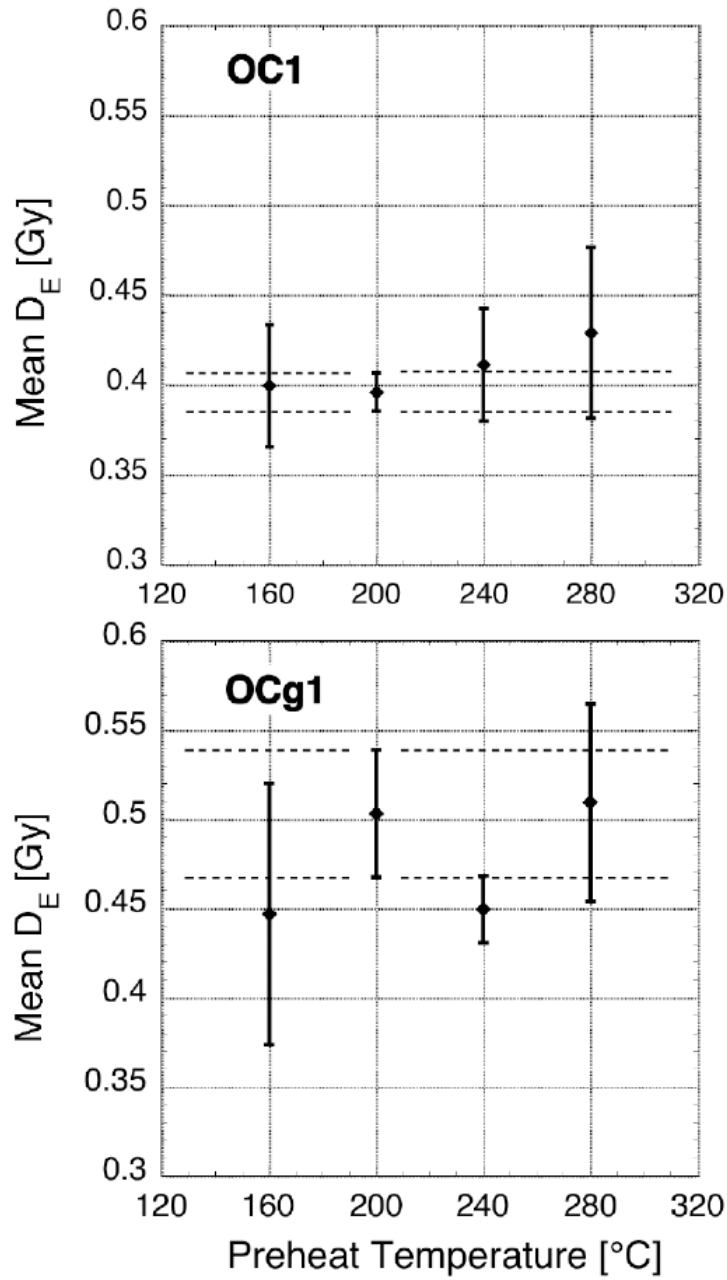
Sample	^{238}U (ppm)	^{232}Th (ppm)	^{40}K (ppm)	Alpha ($\mu\text{Gy/a}$)	Beta ($\mu\text{Gy/a}$)	Gamma ($\mu\text{Gy/a}$)	Cosmic ($\mu\text{Gy/a}$)	Total ($\mu\text{Gy/a}$)	Burial age (a)
OC1 ^a	0.36 ± 0.1	139 ± 40	2.81 ± 0.18	8.6 ± 2.2	13.7 ± 3.4	169.5 ± 8.3	243.6 (LA)	435.6 ± 9.2	880 ± 90
OCgl ^b	0.16 ± 0.1	112 ± 30	0.29 ± 0.05	8.6 ± 2.2	13.7 ± 3.4	169.5 ± 8.3	215.0 (IA)	406.9 ± 9.2	940 ± 100
				8.6 ± 2.2	13.6 ± 3.4	32.0 ± 2.3	209.3 (LA)	263.5 ± 4.7	1780 ± 130
				8.6 ± 2.2	13.6 ± 3.4	32.0 ± 2.3	189.9 (IA)	244.1 ± 4.7	1920 ± 150

The cosmic dose rate is calculated according to the linear accumulation (LA) and instant accumulation (IA) models. Datum is 2005 AD.

^aMoisture content: 3.4% (% dry weight); organic and carbonate content: 9.6% (% dry weight).

^bMoisture content: 0.5% (% dry weight); organic and carbonate content: 3.0% (% dry weight).

CHAPTER 4 -- APPENDIX A. SUPPLEMENTARY DATA

**Figure 4.S1.**

Mean D_E versus pre-heat temperature for OC1 (midden) and OCg1 (beach ridge). Horizontal lines are guides for the eye.

CHAPTER 5

OPTICAL DATING OF AN ANCIENT COASTAL OCCUPATION SITE AND UNDERLYING LAND ON THE NORTHWEST GULF COAST OF FLORIDA, NEAR APALACHICOLA, U.S.A.

Gloria I. López^{a*}

W. Jack Rink^a

Nancy Marie White^b

^a Archaeometry & Geochronology (AGE) Laboratory
School of Geography and Earth Sciences, McMaster University
1280 Main Street West, Hamilton, Ontario, Canada, L8S 1M5

^b Department of Anthropology, University of South Florida
Tampa, Florida, 33620, U.S.A.

* Corresponding author: lopezgi@mcmaster.ca
 glopez@eafit.edu.co

Citation:

LÓPEZ, G.I., RINK, W.J., and WHITE, N.M. Optical Dating of an Ancient Coastal Occupation Site and Underlying Land on the Northwest Gulf Coast of Florida, Near Apalachicola, U.S.A. *Geoarchaeology* (under review).

Geoarchaeology – An International Journal: John Wiley & Sons Inc., N.J., ISSN 0883-6353.

Status: under review, submitted December 2006.

ABSTRACT

Optical Stimulated Luminescence (OSL) of quartz grains from the southern end of St. Joseph Peninsula (north-western Florida, U.S.A.) have given new insights on the earliest time of formation of this peninsula and have constrained the end age range for the coastal chronology corresponding to Swift Creek / Early Weeden Island culture (Middle Woodland-age). A shell midden on Richardson's Hammock archaeological site (Florida 8Gu10), containing large gastropods and Middle Woodland ceramics was successfully OSL-dated to A.D. 505–705. The importance of this archaeological site may lie in the age of the ground onto which it was established rather than its geographical location when comparing to other less developed sites along St. Joseph Peninsula. The sedimentary unit that underlies the shell midden provided OSL-dates between 1595–995 B.C., a *terminus ante quem* age for the formation of the emergent north-eastern side Richardson's Hammock, and the so far oldest published age for St. Joseph Peninsula. Newer land on the hammock's south-western side emerged around 494–95 B.C. Hence, land overall Richardson's Hammock could not have formed any later than about 2800 years ago and yet the oldest signs of cultural settlements only date to about 1400 years ago. Optical Stimulated Luminescence can be used not only to date coastal shell middens but also to determine the time between newly emergent land and prehistoric human site occupation.

5.1. INTRODUCTION

Several important and sometimes poorly and/or ambiguously-dated coastal prehistoric archaeological sites are found along the valleys and shores along the Floridian Panhandle (U.S.A.), on the north-eastern region of the Gulf of Mexico. Most of these coastal and estuarine sites at the mouth of the Apalachicola River are shell middens, sometimes mounded, enriched in a variety of coastal and freshwater faunal specimens and ceramic artifacts that reflect the abundance of food resources in this coastal ecosystem, and the diversity of aboriginal groups that lived in this area through time (N. M. White, 2003; N. M. White et al., 2002). Of special interest are the shores surrounding St. Joseph Bay where the resulting shell midden sites are characterized by large gastropods and other saltwater species instead of the typical prehistoric piles of oyster or clamshell (**Figure 5.1**). Dating coastal sites like these can be often difficult due to a variety of factors: the heavy overburden and vegetation accumulated through time, the indeterminate limits or boundaries of some sites and the unfortunate on-going pillage (looting) which destroys the original context of the cultural deposit.

Sites often contain datable organic materials such as shells, charcoal, bones and plant remains, which, if younger than about 50,000 years, can be dated using radiocarbon. The reliability of the radiocarbon age in such locations depends on a) whether or not the sample specimen was recovered *in situ*; and b) how precisely the material is associated with the cultural deposit. In some cases,

cultural sediments or organic materials have been re-worked through time within the strata, hence, the radiocarbon age obtained may not represent the time of deposition of the cultural layer.

Important archaeological objects such as pottery artifacts may also help determining the age of the deposit, provided that a well-dated sequence of pottery age determinations exists for the region. However, they may only provide a rough age estimate for the site, since they can exist over significant periods in a region. Ceramic vessels, once fired, may be dated using Thermoluminescence (TL), a well established archaeometric technique (Aitken, 1985). However, as with organic materials, post-depositional vertical displacement of artifacts may also be a problem.

Since the development of Optical Stimulated Luminescence (OSL) to date natural sediments (Huntley et al., 1985), different types of archaeological materials from diverse anthropogenic settings have been successfully dated or are now possible to date, including burnt stones and heated pot sherds (Bøtter-Jensen & Duller, 1992; Feathers, 1997a; Roberts, 1997). OSL is used to determine the time since a sediment was last buried, hence its last exposure to sunlight. Once the sediment is buried, its exposure to cosmic rays and the radioactive decay of ^{238}U , ^{232}Th and ^{40}K present within the surrounding environment (Aitken, 1998), produces ionizing radiation that results in the storage of trapped charge in crystalline defects in certain minerals such as quartz, feldspar and zircon. The luminescence emission is a measure of this trapped charge. Calibration of the luminescence emission against laboratory irradiation leads to an estimate of the time elapsed since the last burial. This provides a direct date of deposition of the sediment. Hence, when determining the absolute age of un-burnt clastic-rich archaeological deposits such as mounds or middens, OSL may be the most reliable technique to use, as it targets the time of the event directly: its construction (*e.g.* Feathers, 1997b; Thompson et al., 2007). Natural bioturbation, soil formation and internal sediment re-working may also affect OSL ages. However, it is possible to examine these effects in the sample while analyzing its luminescence signal, and be able to select a reliable age estimate for the targeted deposit as evidenced by López & Rink (2007a).

The shell middens around St. Joseph Bay (**Figure 5.1.**) are poorly dated and only a few have associated radiocarbon ages. The importance of these middens is based on their geographical location, along the only non-estuarine body of water found on the eastern shores of the Florida Gulf Coast (Stewart & Gorsline, 1962), and the atypical large faunal species associated with them. An interesting example is Richardson's Hammock, located at the southern extremity of St. Joseph Peninsula (**Figures 5.1.** and **5.2.**). The hammock has one of the largest and most continuous shell middens ever discovered in the area. The question to assess is why this hammock is so heavily settled compared to other

poorly developed sites along St. Joseph Peninsula. Is it because it was an ancient ground or is it because it represented a selective resource extraction site? We present herein the OSL age determined for the Richardson's Hammock prehistoric archaeological site and four other ages associated with the geological formation and evolution of the hammock. Moreover, we assess the possibility of re-working and bioturbation in our OSL ages and demonstrate the reliability of the method at these coastal locations.

5.2. GEOLOGICAL AND ARCHAEOLOGICAL BACKGROUND

On the southern end of St. Joseph Peninsula, neighbouring Cape San Blas, lies Richardson's Hammock, a Gulf Coastal Lowland (Cooke, 1939; W. A. White, 1970) (**Figure 5.1.**). The hammock is a small sandy strandplain, about 1.5 km-long, oriented northeast-southwest projecting into the south-western waters of St. Joseph Bay. It is separated from the Gulf of Mexico by a narrow stretch of St. Joseph Peninsula, about 200 m wide (**Figure 5.2.**), which is commonly overwashed by severe storms and hurricanes that strike the area, as seen yearly since the fall of 2002.

The hammock is considered one of the oldest geological formations along St. Joseph Peninsula (Otvos, 1992; Rizk, 1991; Stapor, 1975), and it may have started as a small island prior to the full development of the peninsula, based on geomorphological observations regarding the progression of beach ridges decorating the area. The two first published uncalibrated radiocarbon ages associated with the evolution of this strandplain "island" (Stapor, 1975) come from a peat layer (near the salt marsh at the central-south end of the hammock – see **Figure 5.2.**), which was assigned a 750 year B.P. age (unknown specifics), and a 2000–3000 year-old estimate on cultural materials found on the hammock (unknown specifics). Recently, and while we were doing this research, Otvos (2005) published one OSL age for Richardson's Hammock and several for St. Joseph Peninsula. According to his results, the hammock was emergent 2900 years B.P. (Otvos, 2005; Otvos, 2006 personal communication), forming the "high ground" from which the peninsula evolved subsequently to the north (Otvos, 1992, 2005). The St. Joseph Peninsula OSL dates obtained by Otvos (2005) will not be discussed in this paper as it is only intended to analyze the history of Richardson's Hammock. Future papers by the authors, currently in preparation, will appropriately discuss the evolution of both, St. Joseph Peninsula and Cape San Blas as well as the evolution of the Apalachicola River barrier complex as a whole (López, 2007). Furthermore and in relation to the other islands pertaining to the Apalachicola barrier group, our interpretation of the chronology of the neighbouring St. Vincent Island strandplain can be found in López and Rink (2007b).

A succession of north-northeast trending beach ridges and swales heavily vegetated by assemblages of oak and palm trees decorate Richardson's Hammock. The beach ridges are grouped in four sets marking different wave direction trends existent during the formation of the strandplain (**Figure 5.2.**). Interestingly, the southern marshy area of the hammock is quite similar to the northern and oldest portion of the St. Vincent Island strandplain, where low-lying, almost submerged, beach ridges emerge from a marshy/swampy area, implying a possible submergence of this part of the strandplain (López & Rink, 2007b).

Richardson's Hammock, once private land (N. M. White et al., 2002), is now under the protection of the Apalachicola National Estuarine Research Reserve (ANERR). It is part of the St. Joseph Bay State Buffer Preserve lands, which encompass about 8000 acres of south-western Gulf County territory, around the eastern and south – south-western shores of St. Joseph Bay, an Aquatic Preserve itself.

With limited circulation from the Gulf, St. Joseph Bay has a great variety of animals and plant species, reflecting high productivity that prevailed in the bay probably since prehistoric times. Hence, it may have been an invaluable source of food and other resources for ancient peoples (N. M. White, 2005). Such features, and some of the area's relatively high elevation above mean sea level, may have been distinct determinants for ancient cultures to select occupational sites along the bay's shoreline (N. M. White, 2003, 2005), in particular Richardson's Hammock. The archaeological sites located on Richardson's Hammock, like the other prehistoric sites surrounding St. Joseph Bay, are atypical in terms of shell specimens if compared to other Apalachicola estuarine and coastal shell middens: the predominance of large gastropod shells such as lightning whelks (*Busycón sinistrum*) and horse conchs (*Pleuroploca gigantea*) with a much smaller number of the more typical smaller sized oyster and/or clam shells found in the coastal middens around Apalachicola Bay (Benchley & Bense, 2001; N. M. White et al., 2002). This type of large faunal assemblage is characteristic of salty waters receiving little fresh water input (*i.e.* St. Joseph Bay). Even though these large gastropods are abundant and most visible, other types of estuarine and freshwater shellfish and fish species, as well as a variety of ceramic artifacts are also present within these rich coastal archaeological middens.

Two large gastropod-rich prehistoric shell midden sites are found along the bay's shoreline on eastern Richardson's Hammock (**Figure 5.2.**): Richardson's Hammock (8Gu10) and the more recently discovered Firetower South (8Gu139) along the north – north-eastern and eastern shores respectively (N. M. White, 2005; N. M. White et al., 2002). Both shell-middens are found on the surface of the hammock. In general, the upper first ~50 cm of black humic-rich sand correspond to the midden, a relatively shallow stratum compared to the underlying sands that built this small "island". The entire Richardson's

Hammock site is a continuous shell midden situated atop a long curved beach ridge (N. M. White et al., 2002). It was extensively investigated between the years 2000 and 2002 by White et al. (2002) and various test units were dug at different localities within the site. In the year 2003, we were granted permission to re-open Test Unit E (**Figure 5.3.**), which sources the archaeological age in this study.

5.2.1. PREHISTORIC CULTURAL CHRONOLOGY OF THE REGION

The cultural periods in Florida were originally defined by Willey (1949). The Gulf Coastal Lowlands of the Florida Panhandle have a complex prehistoric chronology spanning over the past 12,000 years, due to the different ecosystem adaptations and material evidence types which characterize the socio-cultural evolution of the ancient peoples inhabiting these shores (see **Table 5.I.**). Cultural periods are largely defined on the basis of ceramic typology, when pottery is present (Milanich, 1994), and a few radiocarbon ages. The oldest cultural remains in the Apalachicola River valley are 12,000 years old, stone tools. While the oldest ceramics found inland are Late Archaic (*ca.* 3000–1000 B.C.), dating back to 5000 years B.P. (Donoghue & White, 1995; N. M. White, 2003), the earliest coastal sites along the shores of St. Joseph Bay seem to be from the Early Woodland period (*ca.* 1000 B.C. – A.D. 200), as evidenced by some Deptford material found at Richardson’s Hammock. Late Woodland period (*ca.* A.D. 600–1000) coastal sites have been found along the bay shores of St. Joseph Peninsula: the Old Cedar archaeological site (8Gu85), near Eagle Harbour (**Figure 5.1.**), was recently OSL dated to 940 ± 100 years ago (Thompson et al., 2007).

5.2.1.1. THE RICHARDSON’S HAMMOCK SITE

The Richardson’s Hammock archaeological site (8Gu10) extends about 350 m north-south along a very narrow (<40 m wide) beach ridge adjacent to St. Joseph Bay (**Figures 5.2.** and **5.3.**). The cultural deposits are black midden soils up to a half-meter thick, with shell, bone, artifacts, and charcoal, lying atop white dune sands (**Figures 5.4.** and **5.5.**). There is a Middle Woodland (**Figure 5.4.** and **Table 5.I.**) component at the north end, including a heavily looted burial mound, manifested by Swift Creek and early Weeden Island cultures ceramics. At the south end, the deposits contain a greater number of large conch and whelk shells and all the ceramics indicate a later Fort Walton culture occupation. Investigations by Mr. Wayne Childers, a local archaeologist, indicated possible intrusive Fort Walton burials in the Middle Woodland mound, as well. In the general central area of the site, the Fort Walton materials overlie the deeper, earlier component to an unknown extent. Fieldwork by University of South Florida archaeologists from 2000–2002 involved excavation of five test units, with a total of 14 m² of land opened in area.

The presence of two Deptford fabric-marked sherds recovered from two different test units in the north and central area suggests at least a small occupation as early as Early Woodland, with an age possibly as early as 1000 B.C. (N. M. White, 2005; N. M. White et al., 2002). However, the major components of the site are Middle Woodland (*ca.* A.D. 200–600), the time of the height of burial mound construction in this area, and Fort Walton (*ca.* A.D. 1000–1500), with an apparent increase in the age of the occupation from south to north.

The only radiocarbon age obtained from the Richardson's Hammock site (8Gu10) comes from the bottom of the Fort Walton cultural layer within Test Unit B, at the southern end of the site: 650 ± 40 years B.P. (Beta 191276; charcoal; $^{13}\text{C} = -25.0\text{‰}$) giving a calibrated age range of A.D. 1280–1400 (N. M. White, 2005). The Firetower South site (8Gu139) may have some Fort Walton culture materials. It is composed of small, discrete areas of large gastropod shell midden with plain, check-stamped, and indeterminate incised ceramic sherds; no radiocarbon date has yet been associated with this site (N. M. White, 2005).

Based on archaeological findings, it appears that the Late Woodland period (A.D. 600–1000) is missing at Richardson's Hammock but may be present farther north on St. Joseph Peninsula at the Eagle Harbor site (8Gu81). It is known to be present at the Old Cedar site (8Gu85), which lies on the shores of St. Joseph Bay, south of Eagle Harbor (**Figure 5.1**). Here, Late Weeden Island culture ceramics have been found spread along the shoreline (Benchley & Bense, 2001). Thompson et al. (2007) obtained an OSL age for the Old Cedar site midden of 940 ± 100 years ago, and an age for the underlying relict beach ridge of 1780 ± 130 years ago. The shell midden result (A.D. 965–1165), in good agreement with the expected age based on the Late Woodland ceramic assemblage from the studies made by Benchley & Bense (2001) at this location, attests to the viability of the optical luminescence technique for use in Florida coastal shell middens. It also shows that the method can be used to determine the length of time before occupation on newly emergent land, in this case, about 900 years (López, 2007; Thompson et al., 2007).

5.3. FIELD AND LABORATORY PROCEDURES AND AGE CALCULATIONS

Two 25 cm-long and 7 cm-diameter horizontal sediment cores were collected for optical dating at Richardson's Hammock archaeological site (8Gu10) in July 2003, while a third was collected east of the site by trenching into the geological unit exposed by erosion on the bay's shoreline. Earlier in July 2002, a 3.78 m-long vertical vibra-core was retrieved from a ridge located on the central-west limit of the hammock, close to the main highway into St. Joseph Peninsula (**Figure 5.1**).

The two former small horizontal cores were retrieved from two cleaned partial walls of the original Test Unit E excavated by White et al. (2002) which had already been backfilled, but was re-opened for this study (**Figure 5.3.**). The dimensions of the re-opened trench coincided in width and length with the original excavation (1 m x 2 m), however, the depth we reached was 100 cm lower than the original excavation (**Figures 5.5.** and **5.6.**), ensuring we had attained the clean white sand from the underlying beach ridge. Sample RH-TUE-1 was taken from the shell-midden stratum at a depth of 30 cm below the surface by coring horizontally (eastward) into the intact east wall of the unit, 25 cm north of the southeast corner. This depth corresponds with the bottom of archaeological Level 3 and top of Level 4, since the unit was excavated in 10 cm arbitrary levels. Materials recovered from both these levels, which would have been directly adjacent to the location of the sample, include an unidentified bone, 77 shell ecofacts (eg. *Busycon sinistrum*, *Macrocallista nimbosa*, *Fasciolaria tulipa*, and worked and unidentified shell fragments), 6 shell tools (e.g. hammers, scoop, and pointed *columella* tools), some lithic debitage, and ceramic sherds of mostly Middle Woodland types, such as Swift Creek Complicated-Stamped, check-stamped, and net-marked.

Though the black (10YR3/1) (Munsell, 1975) midden soils extended only about 50 cm deep in this unit (**Figures 5.5.** and **5.6.**), the cultural materials in it extended to a depth of 61 cm in light gray (10YR6/1) soil that faded to the culturally sterile white (10YR8/1) sand. The second small core, sample RH-TUE-2, was retrieved from the bottom of the unit, well below the archaeological materials, in the evident white beach ridge sand (**Figures 5.5.** and **5.6.**). It was a core taken horizontally southward into the south wall of TUE, 8 cm west of the southeast corner and at a depth of 190 cm.

The third small core, sample RH-GEO-1 was taken from a small trench dug into the foot of the exposed relict beach ridge closest to St. Joseph Bay located about 16 m northeast of Test Unit E (**Figures 5.3.** and **5.7.**) at a depth of about 230 cm below the ground surface (referenced to TUE's unit datum point marker). The fourth core, RH, was vibra-cored into the crest of what is believed to be the third continuous youngest ridge on Richardson's Hammock, beyond the boundaries of the archaeological site, at its central-west edge (**Figures 5.1.** and **5.2.**). Two samples were retrieved from this long vertical core: a) bottom sample RH-A, at a depth of 3.18 m below ground surface; and b) upper sample RH-B at 1.70 m depth. RH-A is believed to pertain to the swash-built, horizontally laminated basal region of the ridge, while RH-B is believed to be part of the dune-built, upper aeolian sediments capping the ridge.

Splitting of the sediment cores and subsequent laboratory treatments and analyses were done at the AGE Laboratory of McMaster University (Canada) under dim orange lighting. Samples subject to OSL dating cannot be exposed to

natural and/or bright light as this will erase the accumulated luminescence signal. Once split, only the center-most 10 cm of sediment from one split half from each sediment core were used in the analysis to avoid any external contamination from the core edges (*i.e.* small horizontal cores) or subsequent layers (*i.e.* long vertical core). Quartz grains were extracted from each sample after being oven-dried (< 60 °C) and chemically treated with 10 % HCl acid and 30 % H₂O₂, dried-sieved using various size-fractions, and the heavy mineral and potassium feldspar grains separated from the targeted quartz separate by dense liquid separation. The quartz separate from the 150-212 µm fraction was then etched in 40 % HF acid for 40 minutes to remove the alpha-dose component of the grains and a final 40-minute treatment with 10 % HCl acid finalized the procedure. A small (< 5 g) sub-sample of each whole, untreated sample was taken for Neutron Activation Analysis (NAA) to measure ²³²Th and ⁴⁰K radioisotopes, and delayed-neutron counting for the determination of ²³⁸U concentrations at the McMaster University Nuclear Reactor facility.

An automated RISØ TL-DA-15 reader was used to measure the samples' ultraviolet OSL emission signal response to blue light stimulation. The single-aliquot regenerative-dose (SAR) protocol (Murray & Wintle, 2000) was utilized to determine the equivalent dose (D_E) of each sample. A series of tests using the SAR protocol were done on each sample prior to the final D_E determination: a) feldspar contamination was tested with infrared-stimulated luminescence (IRSL); b) preheat plateau test at different temperatures (160 °C, 200 °C, 240 °C, and 280 °C) to determine the most suitable preheat temperature to use for the SAR protocol; c) thermal transfer test (Murray & Wintle, 2003) to determine any sensitivity changes with increasing temperature (160 °C, 200 °C, 240 °C, and 280 °C); and d) dose recovery test (Madsen et al., 2005) to determine which temperature (160 °C, 200 °C, 240 °C, and 280 °C) was the best when recovering a known applied dose. Twelve aliquots from each sample were used in each one of the above tests.

No feldspar contamination was observed on the samples as the IRSL/OSL ratios were less than 0.03% (see also Forrest et al. (2003)). Furthermore, no thermal transfer was observed and the most suitable preheat temperatures to use for the analyses were 280 °C for RH-TUE-1, RH-TUE-2 and RH-GEO-1, and 200 °C for RH-A and RH-B, based on the preheat plateaus and dose recovery tests (**Table 5.II**).

At least 24 aliquots were measured to determine the mean D_E from each sample using the SAR protocol at three different aliquot mask sizes (8 mm, 5 mm and 3 mm) (**Figures 5.8., 5.9., 5.10., 5.11. and 5.12.**). The different aliquot mask sizes were used to assess the degree of scatter among frequency histograms as mask size is reduced. Each aliquot was optically stimulated at 125 °C for 100s, given six regenerative doses (from which one was zero and the final one was the

repeat of the first dose given) at 280 °C for 10 s each and one test dose at 160 °C for zero seconds.

The OSL signal intensity was calculated based on first 0.4 s of illumination time and the signal integrated over the final four seconds was subtracted as background. Only aliquots with a recycling ratio value between 0.90 and 1.10 were used for the D_E analyses. The D_E of each sample was determined from the values obtained from measurements on 24 aliquots to hence, find the initial mean D_E of the frequency distribution. Any value (*i.e.* aliquot) lying outside the mean $D_E \pm 2 \sigma$ (*i.e.* twice the initial standard deviation) was excluded from the final D_E calculation (**Figures 5.8., 5.9., 5.10., 5.11. and 5.12.**), which was the palaeodose used to determine the OSL age.

The cosmic and annual dose rates and OSL ages were calculated using the Anatol 0.72B program (courtesy of N. Mercier, CNRS, Paris, France), which uses the dose rate conversion factors of Adamiec & Aitken (1998). Cosmic dose rates were calculated using a value of half of the sample's burial depth (*i.e.* assuming linear sediment accumulation) for the beach ridge samples RH-TUE-2, RH-GEO-1, RH-A and RH-B. The cosmic dose rate for the shell-midden sample RH-TUE-1 was calculated assuming an instant accumulation (*i.e.* using the value of the sample's depth). A 2 g/cm^3 overburden density was used in the cosmic dose rate calculations (Prescott & Hutton, 1988). Internal ^{238}U and ^{232}Th dose rates of 0.067 ± 0.022 ppm and 0.114 ± 0.042 ppm respectively for grains of granitic quartz (Rink & Odom, 1991) were also assumed. A global systematic error of 20 % was also used to calculate each age. It accounts for the variations in water content through time and any other unspecified error during procedures. All OSL ages are given in years prior to A.D. 2005 (*i.e.* the year in which the measurements were made) and one standard deviation for the error. Any effects associated with any disequilibrium in the uranium-series decay chain can only have been vanishingly small due to the very small concentrations of uranium found in the sediment.

5.4. RESULTS AND DISCUSSION

All three optical ages obtained from Richardson's Hammock Test Unit E and the associated geological samples are in correct stratigraphic order (**Figure 5.5.** and **Table 5.III.**) and showed Holocene depositional ages (*datum* A.D. 2005). According to our results, the shell-midden at 30 cm-depth has an OSL absolute age of $1,400 \pm 100$ years ago (RH-TUE-1), which corresponds to the A.D. 505–705 period. This age agrees well with expectation for the associated early Middle Woodland cultural deposits. The geological samples RH-TUE-2, from the bottom of Test Unit E, and RH-GEO-1 (**Figures 5.5.** and **5.6.** and **Table 5.III.**), taken from the sandy unit on the shoreline, correspond to the relict beach ridge underlying the archaeological site. The ages obtained, 3300 ± 300 and $2700 \pm$

400 years respectively, are statistically indistinguishable from each other. As for the ages obtained on the central-west side of the hammock, associated with the vertical core RH, they revealed to be 3100 ± 300 and 2300 ± 200 years for the bottom and upper samples, respectively (**Figure 5.2.** and **Table 5.III.**).

Figures 5.8. through 5.12. show the D_E distributions obtained for each sample at the different mask sizes analyzed. The interpretation of the frequency histograms obtained as mask size is reduced (*i.e.* the amount of quartz grains on each aliquot is deliberately decreased) may give insight on the behaviour of the sample during burial and its surroundings. For example, the degree of scatter within each (*i.e.* skewness) and among the different mask size distributions (*i.e.* how much the values of each distribution differ from the others) of the same sample may reveal any evidence for bio- or pedo-turbation, and possible differences in the sediment's source (López, 2007). In general for all five samples (RH-TUE-1, RH-TUE-2, RH-GEO-1, RH-A, and RH-B) the histograms show symmetrical to slightly positively skewed distributions, with no evidence of extreme values affecting the calculation of the mean. Moreover, the D_E values obtained for the smaller mask sizes (*i.e.* 5 and 3 mm) fall within the range of values obtained for the 8 mm mask size, indicative of the good behaviour of each sample, which further demonstrates that turbation is not affecting the samples in question. Interestingly, most of the samples show unimodal behaviour with the exception of RH-B (**Figure 5.12.**), the uppermost sample from the long vertical sediment core taken on the central-west side of Richardson's Hammock. The bimodal behaviour seen on RH-B's distributions may suggest two different sedimentary sources or a combination of them. Located on the vulnerable upper zone of the central-west region of the hammock, it may be possible that the sediments capping this ridge may have been influenced not only by coastal but also by bay processes due to the proximity of both environments to the locale.

RH-TUE-1 was taken at a depth of 30 cm, which coincides with the estimated stratigraphic boundary between the Fort Walton (A.D. 1000–1500) and the Swift Creek – early Weeden Island (A.D. 200–600) cultural deposits (**Figure 5.4.**). Swift Creek Complicated-Stamped sherds, as well as sand-tempered plain ceramics and others in the levels most closely associated with the sample, are typical of this Middle Woodland component. The single Fort Walton sherd, which came from Level 3, between 20 and 30 cm depth, could be interpreted as representing the earliest of the Fort Walton deposits. The single Deptford sherd, which also came from Level 3, could be either the result of mixing earlier materials by later people, or of Middle Woodland people continuing to make this type of fabric-marked pottery. The only other such fabric-marked pottery recovered at the entire site was from a small pit feature in Test Unit C, farther to the north near the mound (N. M. White, 2005). No other ceramic sherds diagnostic of Deptford, such as cross-stamped or linear check-stamped types, were recovered from this site.

The general distribution of ceramic materials in this north-central area of the site shows that Swift Creek – early Weeden Island pottery is distributed below ~30 cm while the much younger Fort Walton component is distributed above 30 cm (**Figure 5.5.**). Our OSL age at 30 cm of 1400 ± 100 years corresponds closely with the Middle Woodland-age ceramic component (A.D. 200–600) but can also represent a very short time of settlement of the Late Woodland peoples (A.D. 600–1000). However, no ceramic assemblages of this cultural component were found throughout the midden, hence our OSL age should not be associated with this cultural period. Moreover, the OSL age is much older than the overlying Fort Walton component. The deposition of our sample between A.D. 505–705 most likely corresponds to the end stages of the Middle Woodland occupation of the site, when the land surface contained elements of the current human activities mixed with ceramic elements from the older, apparently far smaller occupation (Deptford). Even later occupations by the Fort Walton peoples added to the complexity of the ceramic assemblage from 20-30 cm (excavation Level 3), which contains all three types of ceramic elements.

Our shell-midden layer age is also in rough agreement with the first published uncalibrated radiocarbon date of about 2000 years B.P. (Stapor, 1975) assigned to Richardson’s Hammock. The recently reported Firetower South site (8Gu139) has been investigated only by surface collection, and produced only plain, indeterminate incised, and check-stamped prehistoric ceramics. We rather not associate this site to a particular time period yet, not until further more detailed analyses are completed.

It is important to note that an OSL age reflects the time elapsed since the last burial of the sand grains analyzed (in this case, the time until which a heavily utilized surface was buried). With this perspective in mind and by analyzing the spread of cultural deposits within Test Unit E, it may be said that in sites of extensive habitation (*i.e.* by different cultures), archaeological materials can be moved throughout the strata. Care has been taken in this case to avoid erroneous age assignment to various ceramic elements. Hence, our calibrated value of 1400 ± 100 years ago is a fairly good date for the end of the Middle Woodland period in coastal sites of the Apalachicola area.

The relict beach ridge underlying the archaeological site dated to about 3000-3600 years ago based on samples RH-TUE-2 and RH-GEO-1. These are the oldest ages to be reported on beach ridges from the St. Joseph Peninsula and Cape San Blas area (López, 2007). This new OSL chronology indicates that Richardson’s Hammock is much older than previously believed (*e.g.* Stapor, 1975; Rizk, 1991) and in rough accordance with Otvos (2005) proposed OSL age of 2900 years for Richardson’s Hammock. The RH-GEO-1 sample yielded an OSL age of 2700 ± 400 years ago, and occurred at a lower elevation (40 ± 5 cm lower) than the exposure of the relict beach ridge sand in the lower level of Test

Unit E (RH-TUE-2). However, its relatively younger age compared to RH-TUE-2 may be due to the bay's influence as it is located on the eastern edge of the ridge (see **Figure 5.3.**). RH-TUE-2 yielded a much better constrained age of deposition of 3300 ± 300 years for this eastern ridge, the oldest on Richardson's Hammock. An important aspect of this sample is that it occurs near the top of the clean quartz aeolian sand section (**Figures 5.5.** and **5.6.**), which means that the formation of the relict beach ridge had to occur prior to this aeolian layer. Thus the 3300 ± 300 years ago age is considered a *terminus ante quem* (i.e. time before which) age for the formation of the emergent land on which the archaeological site sits. Considering the uncertainty in the age this means that the emergent land on the north-eastern area of Richardson's Hammock could not have formed any later than about 3000 years ago, implying that the relict ridges forming the vast south and south-eastern area of the hammock may have emerged long before 3000 years ago (see **Figure 5.2.**). In any case we can be reasonably certain that the relict beach ridge on this north-eastern edge of Richardson's Hammock was formed sometime between 2300 and 3600 years ago (i.e. between 295 and 1595 B.C.).

Not much later after the development of Richardson's Hammock's north-eastern edge, the central-west area around RH's core location also emerged. RH-A, taken at a depth of 3.18 m below ground surface shows an OSL age of 3100 ± 300 years. This age is in agreement with the general lateral evolution of the hammock from south-east to north-west, based on the morphological patterns of ridges depicted throughout the hammock's surface (see **Figure 5.2.**). We suggest this value to be a *terminus ante quem* age for the formation of emergent land on the south-west area of Richardson's Hammock. Hence, land on this area of the hammock could not have formed any later than about 2800 years ago.

It is important to note that Richardson's Hammock has at least four marked sets of ridges, depicting different littoral accretion direction periods, contrary to only two noted by Rizk (1991). From southeast to northwest these sets are (**Figure 5.2.**): a) rh-1, around the salt marsh, with a major ridge trend N 60° W; b) rh-2, which truncates rh-1 and where Firetower South site (8Gu139) lies, has a ridge trend N 45° W; c) rh-3, the largest set with a general trend N 80° W to EW, showing a major change in longshore direction, is host to the Richardson's Hammock site (8Gu10); and d) rh-4, the newest and easternmost set which truncates rh-3, with a general trend EW.

Even though there seems to be only 200 years between the formation of the north-eastern edge of rh-3 and the south-west edge of rh-4, it is important to locate the samples in geographical perspective: RH-TUE-2 is located at the northern end of the easternmost ridge within the large set rh-3, and RH-A is found at the southern end of the third youngest ridge of the last and westernmost ridge set of the hammock, rh-4. Hence, the former is found at the termination of a ridge whereas the latter is found at the beginning of a different set of ridges, making

their ages in correct accretion order. The shallowest geological sample dated in this study, RH-B, revealed an age of 2300 ± 200 years, stratigraphically younger than the deeper RH-A. This age suggests in fact that land was emergent on the south edge of rh-4 at least 2500 years ago (*i.e.* A.D. 495), but no archaeological findings are to be encountered on this side of the hammock, even though it pre-dates the Middle Woodland shell-midden dated in this study. The OSL ages obtained in this study coupled with the geomorphological setting of Richardson's Hammock suggest that it may have been an emergent small island at least 2800 years ago with a protective hammock on its eastern side that favoured cultural settlement and an open, unsheltered, still evolving, beach environment on its western side.

5.5. CONCLUSIONS

This study demonstrates that optical dating is a credible method to date coastal shell-middens rich in quartz grains, but caution must be used when interpreting whether the age estimates can be applied to ceramic components which have experienced mixing through repeated occupation. Due to the various cultural chronologies proposed for northwest Florida, it is important to determine the absolute ages associated with coastal archaeological sites vs. interior ones for the same culture as such chronologies might be off by a few hundreds of years. In this study, we showed that the emergent land upon which the midden was deposited could not have formed any later than 3300 ± 300 years ago (1595–995 B.C.), and that the shell midden age of 1400 ± 100 years ago (A.D. 505–705) represents a time during which Middle Woodland-age occupation was ending in this coastal area of the Apalachicola region. Despite the almost complete emergence of Richardson's Hammock as a small island some 2300 ± 200 years ago (495–95 B.C.), prehistoric people did not find the beautiful white sands suitable for occupation until about 1900 years after the hammock's north-eastern bay-side first came into existence, and about 900 years after its Gulf shores came afloat. One question remains: why?

ACKNOWLEDGEMENTS

This research was possible thanks to the permissions granted by the Apalachicola National Estuarine Research Reserve (ANERR) and resource manager Roy Ogles and by the Florida Department of State, Bureau of Archaeological Research, which issued research permit No. 9900.39 allowing White's test excavations on the state lands of Richardson's Hammock. Special thanks to Jimmy Moses III, Captain Patrick Millender, and Jason Isbell from ANERR for their great assistance and help during this fieldwork, especially in the reopening of backfilled Test Unit E in 2003. Improvement of this manuscript was possible thanks to constructive comments provided by E.G. Otvos.

REFERENCES

- Adamic, G., & Aitken, M. J. (1998). Dose-rate conversion factors: update. *Ancient TL*, 16, 37-50.
- Aitken, M. J. (1985). *Thermoluminescence Dating*. London: Academic Press.
- Aitken, M. J. (1998). *An introduction to Optical Dating: The Dating of Quaternary Sediments by the Use of Photo-Stimulated Luminescence*. Oxford: Oxford University Press.
- Benchley, E. D., & Bense, J. A. (2001). *Archaeology and History of St. Joseph Peninsula State Park: Phase I Investigations*. Jacksonville: University of West Florida Archaeology Institute.
- Bøtter-Jensen, L., & Duller, G. A. T. (1992). A New System for Measuring Optically Stimulated Luminescence from Quartz Samples. *Nuclear Tracks and Radiation Measurements*, 20, 549-553.
- Cooke, C. W. (1939). Scenery of Florida, interpreted by a geologist. *Florida Geological Survey Bulletin*, 17, 1-118.
- Donoghue, J. F., & White, N. M. (1995). Late Holocene sea level change and delta migration, Apalachicola River region, northwest Florida, U.S.A. *Journal of Coastal Research*, 11(3), 651-663.
- Feathers, J. K. (1997a). The application of Luminescence Dating in American Archaeology. *Journal of Archaeological Method and Theory*, 4, 1-66.
- Feathers, J. K. (1997b). Luminescence Dating of Early Mounds in Northeast Louisiana. *Quaternary Science Reviews (Quaternary Geochronology)*, 16, 330-340.
- Forrest, B. M., Rink, W. J., Bicho, N., & Ferring, C. R. (2003). OSL ages and possible bioturbation signals at the Upper Paleolithic site of Lagoa do Bordoal, Algarve, Portugal. *Quaternary Science Reviews*, 22(10-13), 1279-1285.
- Huntley, D. J., Godfrey-Smith, D. I., & Thewalt, M. L. W. (1985). Optical dating of sediments. *Nature*, 313, 105-107.
- López, G. I. (2007). *Optical Dating of Barrier Island Sequences along the North-Western Florida Gulf Coast, near Apalachicola, U.S.A.* Ph.D. Dissertation, McMaster University, Hamilton.
- López, G. I., & Rink, W. J. (2007a). Characteristics of the burial environment related to Quartz SAR-OSL dating at St. Vincent Island, NW Florida, U.S.A. *Quaternary Geochronology*, in press (available online as of 13 July 2006).
- López, G. I., & Rink, W. J. (2007b). New Quartz-OSL ages for Beach Ridges on the St. Vincent Island Holocene Strandplain, Florida, U.S.A. *Journal of Coastal Research*, in press (accepted 2 December 2005).
- Madsen, A. T., Murray, A. S., Thorbjorn, J. A., Pejrup, M., & Breuning-Madsen, H. (2005). Optically Stimulated Luminescence Dating of Young Estuarine

- Sediments: a Comparison with ^{210}Pb and ^{137}Cs Dating. *Marine Geology*, 214, 251-268.
- Milanich, J. T. (1994). *Archaeology of Precolumbian Florida*. Gainesville: University Press of Florida.
- Munsell. (1975). *Soil Color Charts*. Baltimore: MacBeth Division of Kollmorgen Corp.
- Murray, A. S., & Wintle, A. G. (2000). Luminescence dating of quartz using an improved single-aliquot regenerative-dose procedure. *Radiation Measurements*, 32, 57-73.
- Murray, A. S., & Wintle, A. G. (2003). The single aliquot regenerative dose protocol: potential for improvements in reliability. *Radiation Measurements*, 37(4-5), 377-381.
- Otvos, E. G. (1992). Apalachicola coast Quaternary evolution, NE Gulf of Mexico. In C. H. Cletcher & J. F. Wehmiller (Eds.), *Quaternary Coasts of the United States: Marine and Lacustrine Systems* (Vol. Special Publication No. 48, pp. 221-232). Tulsa: Society of Economic Paleontologists and Mineralogists.
- Otvos, E. G. (2005). Coastal Barriers, Gulf of Mexico: Holocene Evolution and Chronology. *Journal of Coastal Research, Special Issue 42*, 141-163.
- Prescott, J. R., & Hutton, J. T. (1988). Cosmic Ray and Gamma Ray dosimetry for TL and ESR. *Nuclear Tracks and Radiation Measurements*, 14, 223-227.
- Rink, W. J., & Odom, A. L. (1991). Natural Alpha Recoil Particle Radiation and Ionizing Radiation Sensitivities in Quartz Detected with EPR: Implications for Geochronometry. *Nuclear Tracks and Radiation Measurements*, 18(1-2), 163-173.
- Rizk, F. F. (1991). *The Late Holocene development of St. Joseph Spit*. Ph.D. Dissertation, Florida State University, Tallahassee.
- Roberts, R. G. (1997). Luminescence Dating in Archaeology: from origins to optical. *Radiation Measurements*, 27, 819-892.
- Stapor, F. W. (1975). Holocene beach ridge plain development, Northwest Florida. *Zeitschrift für Geomorphologie*, 22, 116-144.
- Stewart, R. A., & Gorsline, D. S. (1962). Recent sedimentary history of St. Joseph Bay, Florida. *Sedimentology*, 1, 2516-2286.
- Thompson, J., Rink, W. J., & López, G. I. (2007). Optically-Stimulated Luminescence age of the Old Cedar Midden, St. Joseph Peninsula State Park, Florida. *Quaternary Geochronology*, in press (available online as of 19 June 2006).
- White, N. M. (2003). Late Archaic in the Apalachicola / Lower Chattahoochee Valley, Northwest Florida, Southwest Georgia, and Southeast Alabama. *The Florida Anthropologist*, 56(2), 69-90.
- White, N. M. (2005). *Archaeological Survey of the St. Joseph Bay State Buffer Preserve, Gulf County, Florida*. East Point and Tallahassee: Apalachicola

National Estuarine Research Reserve and Division of Historical Resources.

- White, N. M., Rodriguez, N. D., Smith, C., & Fitts, M. B. (2002). *St. Joseph Bay Shell Middens Test Excavations, Gulf County, Florida, 2000-2002: Richardson Hammock site, 8Gu10, and Lighthouse Bayou site, 8Gu114*. Tallahassee: Division of Historical Resources.
- White, W. A. (1970). The Geomorphology of the Florida Peninsula. *Florida Geological Survey Bulletin*, 51, 1-167.
- Willey, G. R. (1949). *Archaeology of the Florida Gulf Coast*. Washington D.C.: Smithsonian Institution.

CHAPTER 5 – FIGURES

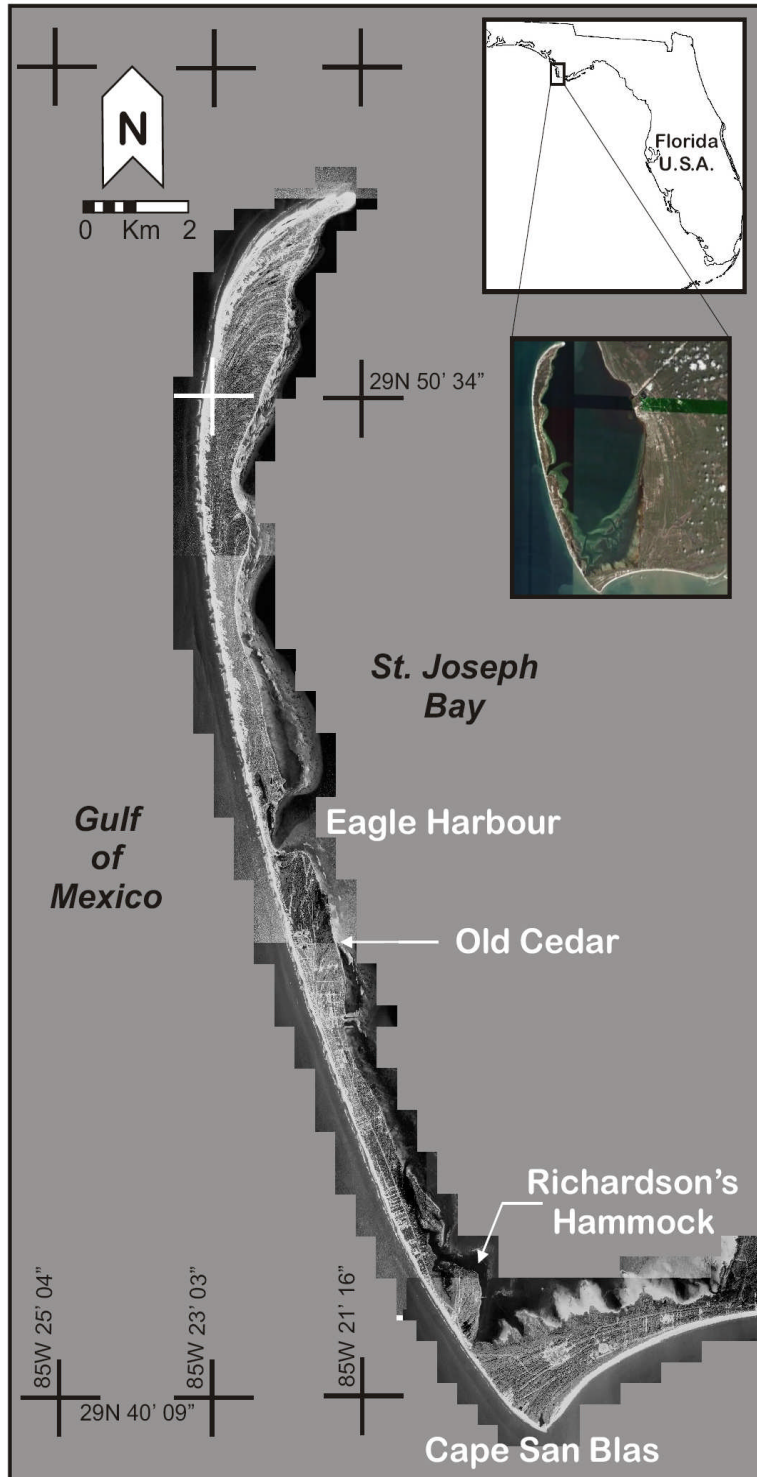


Figure 5.1. Site location map of St. Joseph Peninsula, northwest Florida, U.S.A. with Richardson's Hammock marked. Image source: Digital Ortho-Quadrangle images by U.S. Geological Survey (January 10th, 1999), <http://terraserver-usa.com/default.asp> .

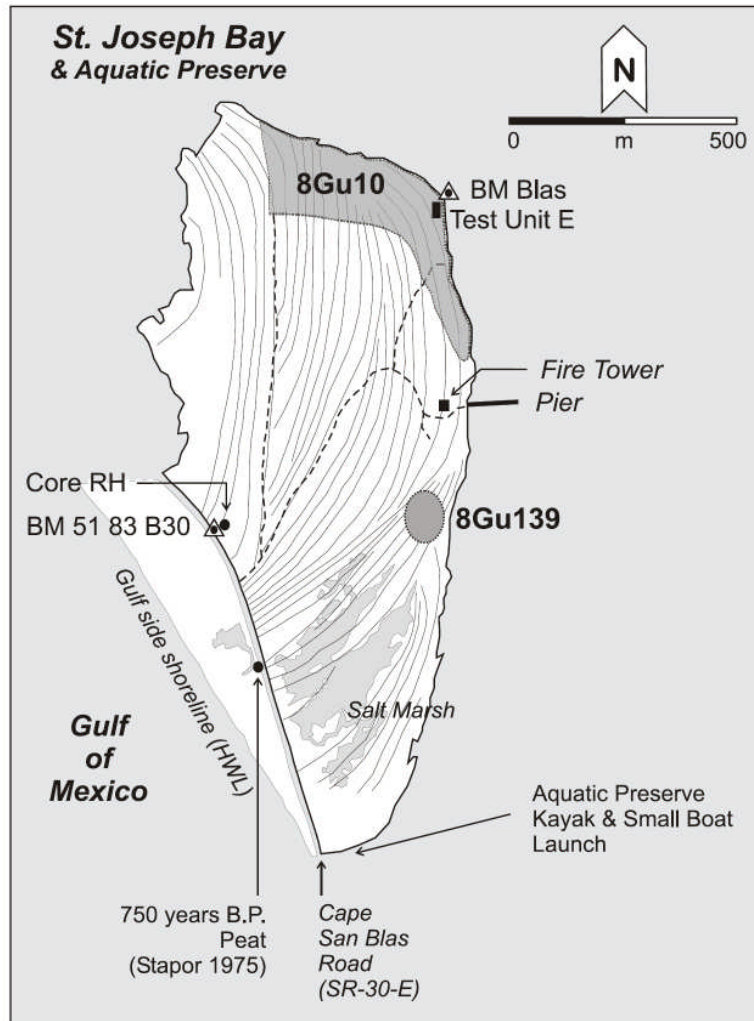


Figure 5.2.

Site location map of Richardson's Hammock. Beach ridges are shown as black curved lines. The Richardson's Hammock archaeological site, 8Gu10, is marked as the gray area within the dotted line along the hammock's northeastern-most end. Test Unit E is shown by a black rectangle and core RH is marked by black circle next to the southern benchmark 51 83 B30. The archaeological site 8Gu139 recently reported (White, 2005) is also shown and Stapor's (1975) peat age locale. Salt marsh areas are indicated in light gray and dirt roads by short-dashed lines. The contours of the hammock, beach ridges and salt marshes have been traced from Digital Ortho-Quadrangles (U.S. Geological Survey, March, 2005). The four proposed sets of ridges (rh-1, rh-2, rh-3, and rh-4) described in the text can be depicted using the different general trends of ridges seen throughout Richardson's Hammock.

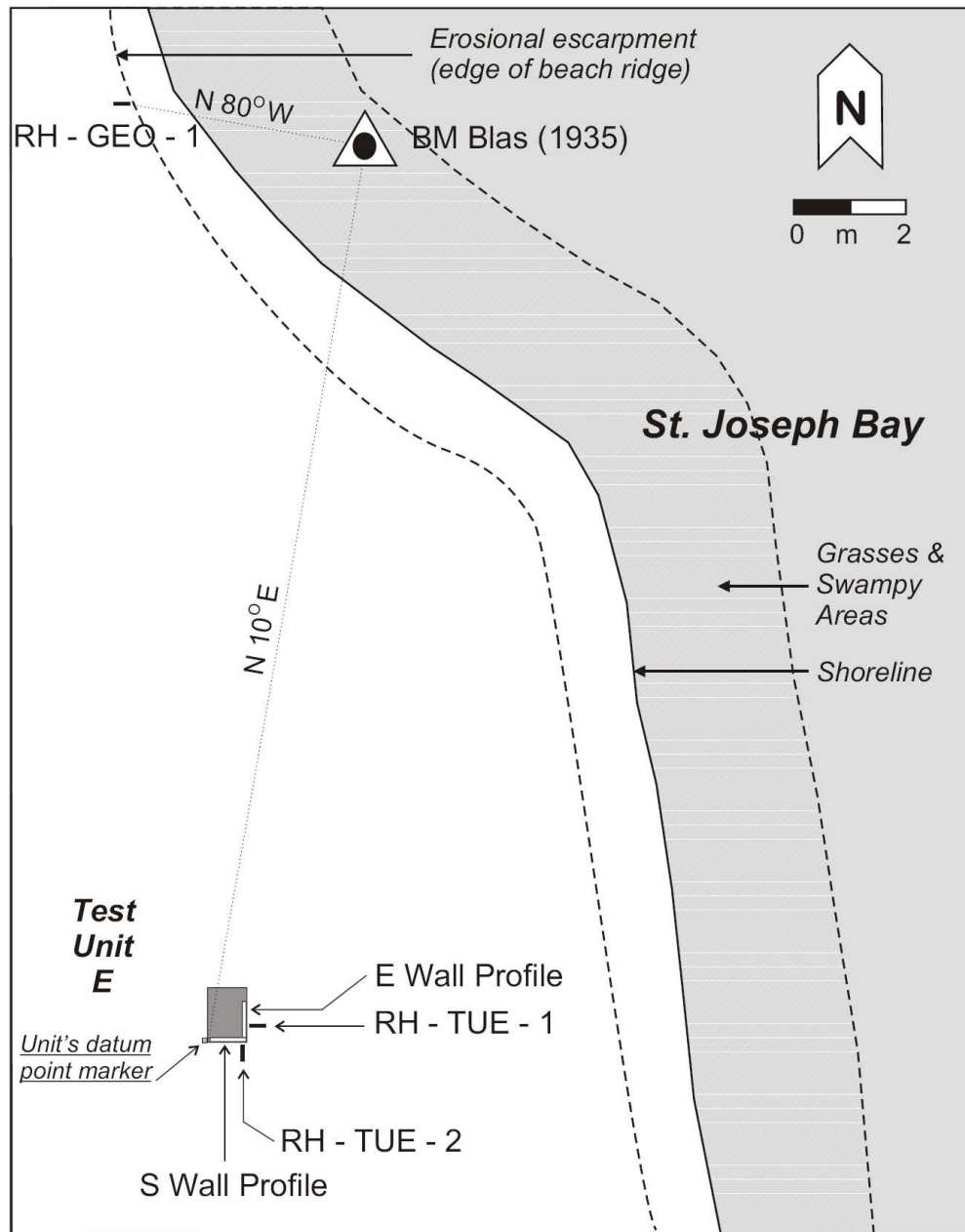


Figure 5.3.

Schematic drawing showing position of dated samples and stratigraphic profiles taken within trench TUE and the beach ridge located at the edge of the St. Joseph Bay. The core samples are marked by black rectangles and the profiles by white rectangles.



Figure 5.4.

Test Unit E, Floor 3 (30 cm depth below the surface), showing distribution of artifacts and far fewer large shells, characteristic of the Middle Woodland component at the site. Trowel points north. The large horse conch shell sticking out of the southeast corner (lower right of photo) is roughly above the area re-excavated for the later core samples.

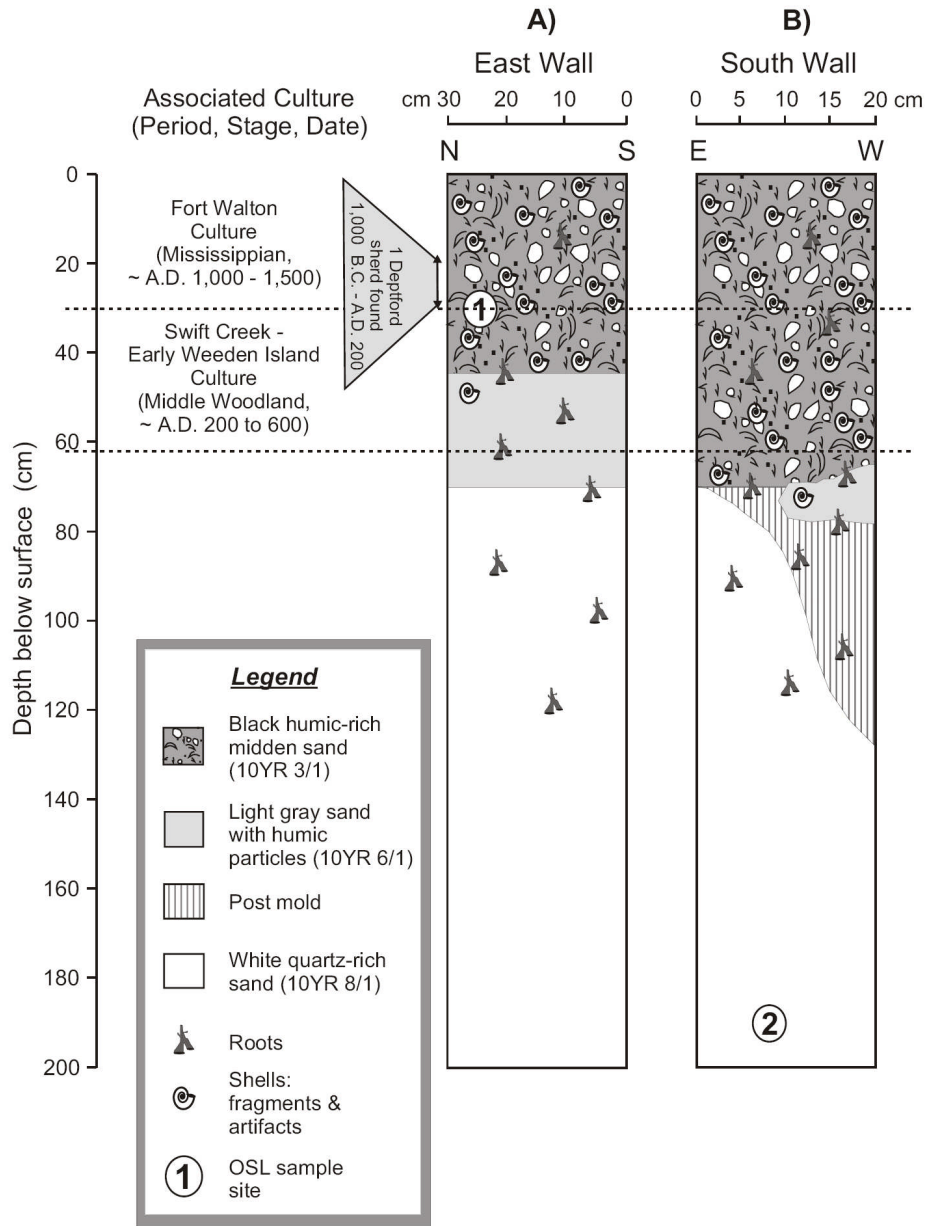


Figure 5.5.

Stratigraphic profiles showing the OSL samples taken within Test Unit E in July 2003: A) sample location 1 on the East Wall corresponds to sample RH-TUE-1; and B) sample location 2 on the South wall corresponds to sample RH-TUE-2.

A)



B)



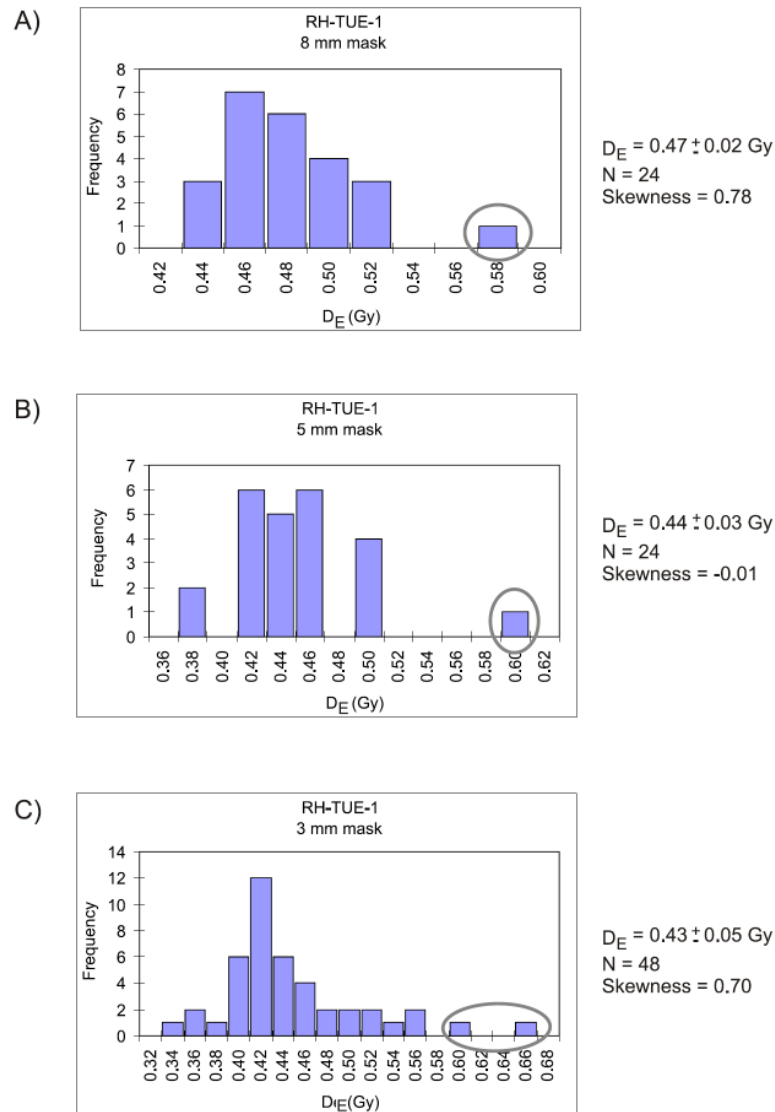
Figure 5.6. Photographs of Test Unit E: A) East Wall and OSL sample RH-TUE-1 being taken by Dr. W. Jack Rink and Jimmy Moses III assisting the operation; B) South Wall and position of OSL sample RH-TUE-2 (pointed by arrow) ready to be retrieved (at 2 m depth).



Location of
RH-GEO-1

Figure 5.7.

Photograph of the beach ridge on the bay-shore where sample RH-GEO-1 was taken. The gamma spectrometer is seen here inside the hole left after the sample was retrieved.

**Figure 5.8.**

D_E distributions of sample RH-TUE-1 at different mask sizes: A) 8mm; B) 5mm; and C) 3mm. The aliquots outside $D_E \pm 2\sigma$ are circled in each histogram and were not taken into the calculation of the final mean D_E used to obtain the OSL age (the same applies for figures 5.9. through 5.12.). The final mean D_E value and its associated 1σ error are given for each mask size as well as the number (N) of aliquots measured per mask size and the skewness associated to each distribution (the same applies for figures 5.9. through 5.12.).

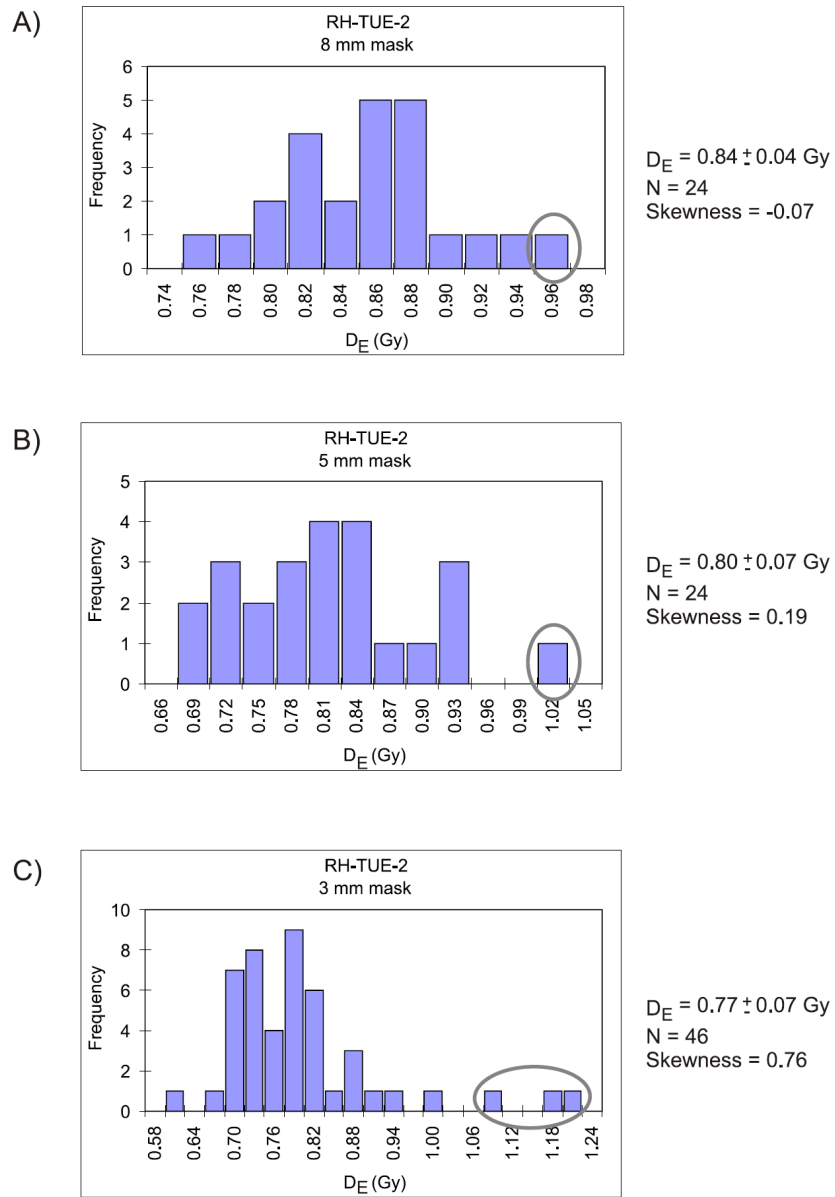


Figure 5.9.

D_E distributions of sample RH-TUE-2 at different mask sizes: A) 8mm; B) 5mm; and C) 3mm.

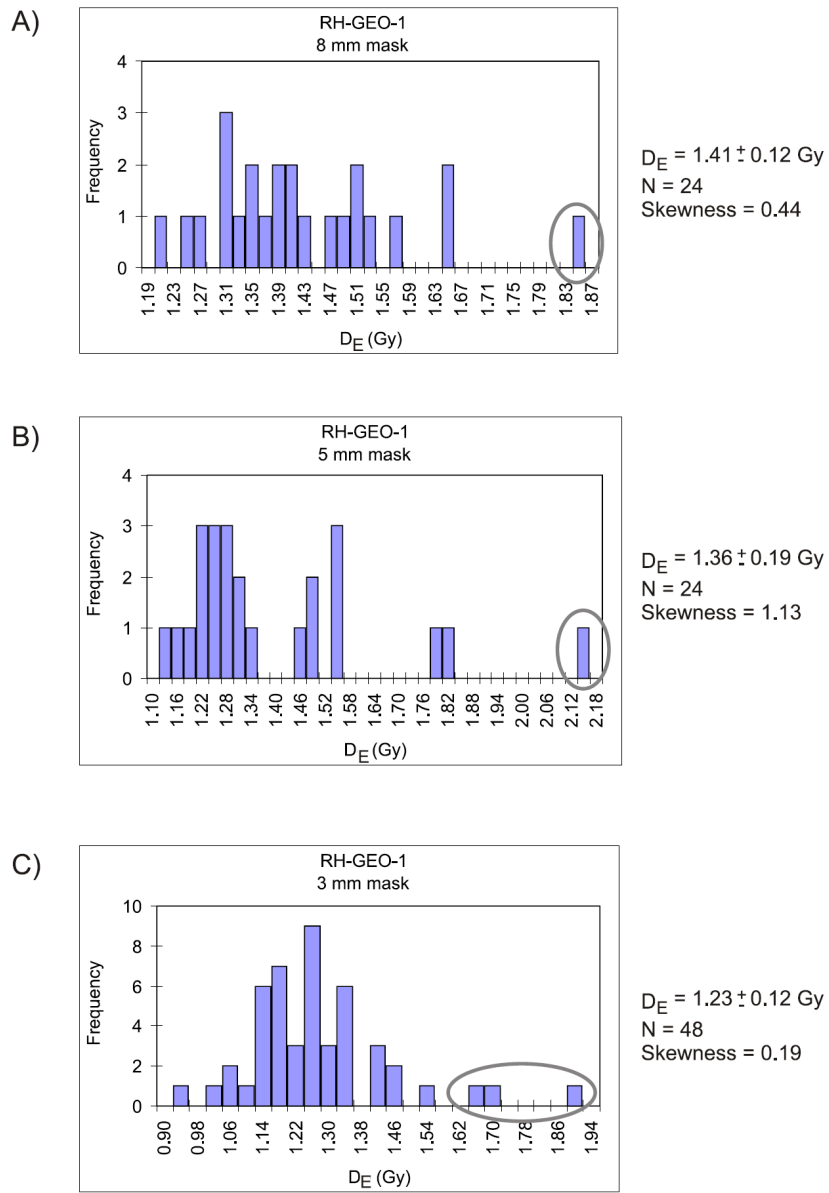


Figure 5.10. D_E distributions of sample RH-GEO-1 at different mask sizes: A) 8mm; B) 5mm; and C) 3mm.

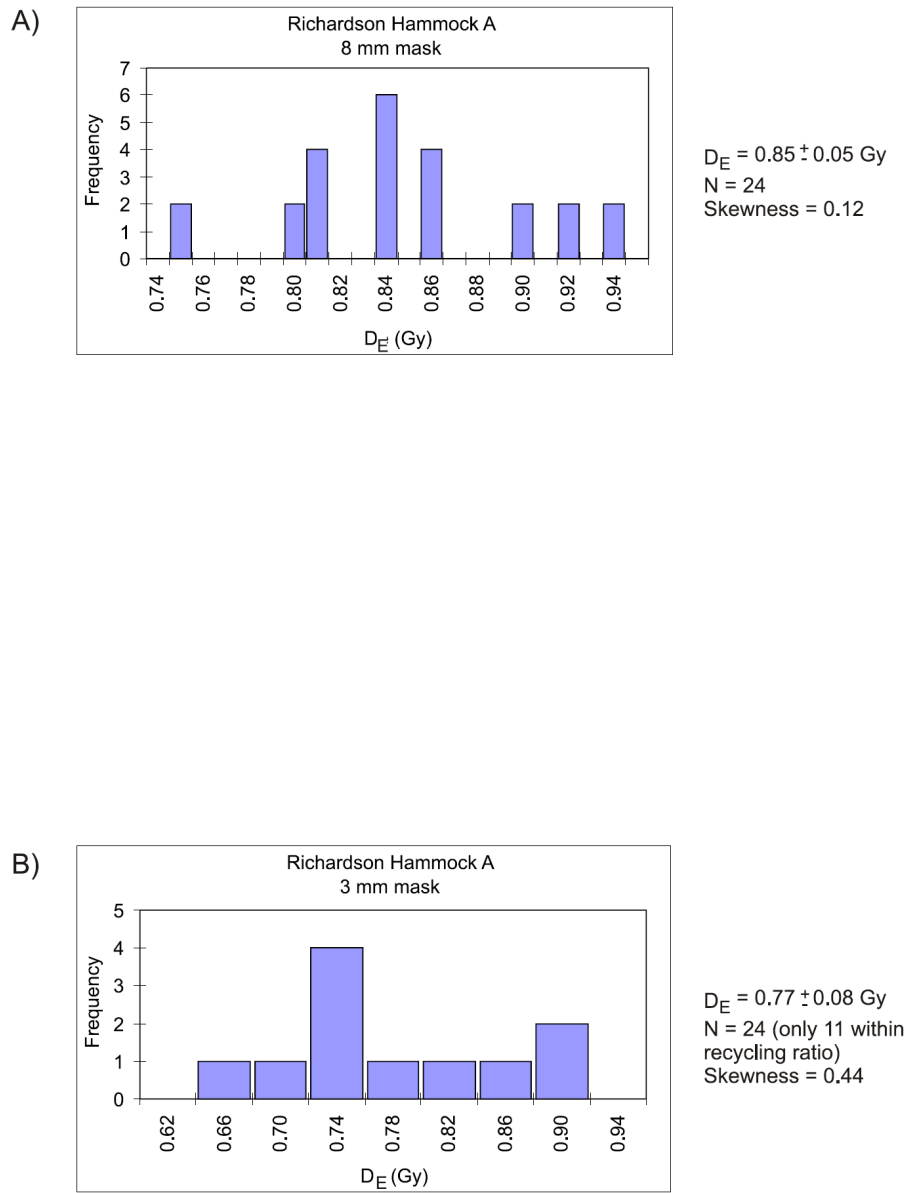


Figure 5.11.

D_E distributions of sample RH-A (bottom of long vertical core) at different mask sizes: A) 8mm; and B) 3mm.

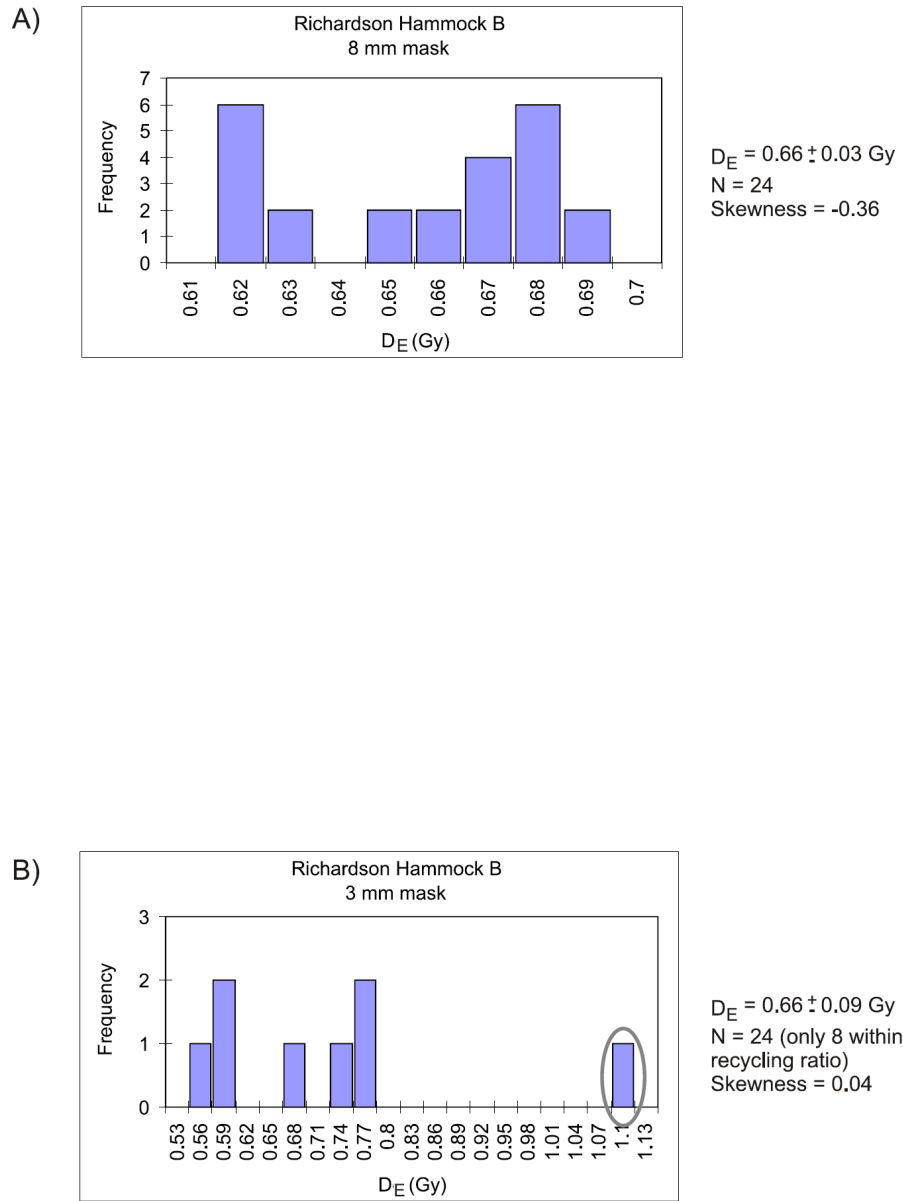


Figure 5.12.

D_E distributions of sample RH-B (top of long vertical core) at different mask sizes: A) 8mm; and B) 3mm.

CHAPTER 5 – TABLES**Table 5.I.**

Generalized Prehistoric cultural chronology for the Apalachicola area.

Period & Stage	Culture / Ceramic Series	Age (years ago)	Age Range
	Palaeoindian	12,000 – 9500	10,000 – 7500 B.C.
Early	Archaic	9500 – 7000	7500 – 5000 B.C.
Middle	Archaic	7000 – 5000	5000 – 3000 B.C.
Late	Archaic	5000 – 3000	3000 – 1000 B.C.
Early Woodland	Deptford	3000 – 1800	1000 B.C. – A.D. 200
Middle	Swift Creek	1800 – 1700	A.D. 200 – 300
Woodland	Early Weeden Island	1700 – 1400	A.D. 300 – 600
Late Woodland	Late Weeden Island	1400 – 1000	A.D. 600 – 1000
Mississippian	Fort Walton	1000 – 500 (?)	A.D. 1000 – 1500 (?)

Sources of different dates: Milanich (1994), White (2003, 2005).

All dates are based on uncalibrated radiocarbon ages except for the time range attributed to the Late Archaic culture (White 2003).

Table 5.II.
Results of Tests done on all Richardson Hammock samples prior to the final D_E estimation.

	Core Sample				
	RH-TUE-1	RH-TUE-2	RH-GEO-1	RH-B	RH-A
IRSL/OSL ratio Test [a]	0.001	0.002	0.001	0.001	0.001
Preheat Plateau Test [b]					
160 °C	0.49 ± 0.04	0.79 ± 0.07	1.39 ± 0.03	0.64 ± 0.05	0.76 ± 0.03
200 °C	0.49 ± 0.05	0.78 ± 0.08	1.33 ± 0.07	0.74 ± 0.06	0.74 ± 0.03
240 °C	0.50 ± 0.02	0.84 ± 0.07	1.59 ± 0.30	0.70 ± 0.03	n/a
280 °C	0.49 ± 0.06	0.84 ± 0.11	1.41 ± 0.03	n/a	n/a
Thermal Transfer Test [c]					
160 °C	-0.01 ± 0.01	-0.04 ± 0.01	-0.05 ± 0.01	-0.02 ± 0.01	-0.01 ± 0.01
200 °C	0.00 ± 0.01	-0.02 ± 0.01	-0.04 ± 0.01	-0.01 ± 0.00	0.00 ± 0.01
240 °C	-0.01 ± 0.01	-0.01 ± 0.01	-0.02 ± 0.01	-0.01 ± 0.01	0.00 ± 0.00
280 °C	0.00 ± 0.00	0.00 ± 0.00	0.00 ± 0.00	0.00 ± 0.00	0.00 ± 0.01
Dose Recovery Test [d]					
Given dose	0.62	1.15	2.12	0.35	0.44
160 °C	0.62 ± 0.01	1.19 ± 0.03	2.17 ± 0.04	0.34 ± 0.01	0.43 ± 0.01
200 °C	0.62 ± 0.01	1.20 ± 0.02	2.16 ± 0.04	0.35 ± 0.01	0.44 ± 0.00
240 °C	0.62 ± 0.01	1.19 ± 0.02	2.13 ± 0.02	0.37 ± 0.00	0.46 ± 0.01
280 °C	0.62 ± 0.00	1.15 ± 0.03	2.12 ± 0.03	0.37 ± 0.01	0.46 ± 0.00

With the exception of the IRSL/OSL ratio, all other tests were done by applying the SAR protocol to each aliquot at the different shown preheats.

[a] Average value of analysis made in three aliquots of the sample. It is the ratio between the signals measured by the infrared (IRSL) and blue light (OSL) stimulations. Values smaller than 0.003 indicate the absence of feldspar contaminating the sample.

[b] The resulting value is an equivalent dose (units are Gy). The "n/a" values are due to errors in the recycling ratio, hence, no equivalent doses could be determined at these specific preheats for these particular samples.

[c] The resulting value is an equivalent dose (units are Gy). The closest result is to zero, the smaller the chances for thermal transfer.

[d] The resulting value is an equivalent dose (units are Gy). The closest the obtained equivalent dose is to the given dose, the better the preheat temperature.

Table 5.III.
SAR - OSL ages and data for quartz sand samples taken at Richardson Hammock.

Core sample	AGE Laboratory No.	De (Gy)	238-U (ppm) [a]	232-Th (ppm) [a]	K (%) [a]	Water Content (%) [b]	Cosmic Dose Rate ($\mu\text{Gy/a}$) [c]	Annual Dose ($\mu\text{Gy/a}$) [d]	SAR-OSL age (a) [e]	SAR-OSL age range (at 1 σ)
RH-TUE-1	GL04075-076-080	0.47 ± 0.02	0.22 ± 0.1	0.64 ± 0.08	0.0049 ± 0.0011	7.10	218.99	324.9 ± 16.5	1400 ± 100 *	A.D. 505 A.D. 705
RH-TUE-2	GL04075-076-082	0.84 ± 0.04	0.12 ± 0.1	0.45 ± 0.05	0.0046 ± 0.0007	2.61	184.17	257.6 ± 16.8	3300 ± 300 **	1595 B.C. 995 B.C.
RH-GEO-1	GL04077-083	1.41 ± 0.12	0.59 ± 0.1	2.73 ± 0.18	0.0053 ± 0.0009	2.46	179.24	518.2 ± 19	2700 ± 400 **	1095 B.C. 295 B.C.
RH-B	GL04062-148	0.66 ± 0.03	0.27 ± 0.1	0.37 ± 0.06	0.0034 ± 0.0010	5.49	186.70	286.1 ± 16.4	2300 ± 200 **	495 B.C. 95 B.C.
RH-A	GL04062-148	0.85 ± 0.05	0.29 ± 0.1	0.49 ± 0.05	0.0038 ± 0.0009	14.33	168.94	273.7 ± 15.2	3100 ± 300 **	1395 B.C. 795 B.C.

[a] U, Th and K values determined by NAA .

[b] Water content as a fraction of dry weight determined from laboratory measurements.

[c] Cosmic dose rate value calculated using an overburden density of 2 g/cm³.

[d] All β and γ dose rates were calculated based on U, Th and K concentrations of each sample accounting for moisture values of the sample.

[e] Datum for SAR-OSL ages is A.D. 2005. The values have been rounded to nearest sensible number of precision.

* Age was calculated assuming instant sediment accumulation rates.

** Ages were calculated assuming constant (i.e. linear) sediment accumulation rates.

CHAPTER 6

PENINSULAR EVOLUTION AND OPTICAL DATING OF YOUNG COASTAL RIDGES ALONG THE GULF OF MEXICO

Gloria I. López *

W. Jack Rink

Archaeometry & Geochronology (AGE) Laboratory
School of Geography and Earth Sciences, McMaster University.
1280 Main Street West, Hamilton, Ontario, Canada, L8S 1M5

* Corresponding author: lopezgi@mcmaster.ca
glopez@eafit.edu.co

Prepared for:

Quaternary Geochronology: Elsevier Science, Oxford, ISSN 1871-1014 (Imprint: Elsevier).

Status: ready for submission (July, 2007).

ABSTRACT

This study evaluates the progradational history of a transgressive barrier spit using quartz optically stimulated luminescence (OSL) dating. Long-vertical sediment cores were taken sequentially from different beach and dune ridges located throughout St. Joseph Peninsula (Florida, U.S.A.), located on the north-eastern shores of the Gulf of Mexico. Multiple samples were extracted from the cores at different depth intervals to evaluate sedimentation rates. The OSL ages presented for the peninsula itself have a time span of ~ 2,000 years, which is in excellent agreement with the time of formation of the island precursor to the peninsula, some 3,000 years ago. Moreover, equivalent dose analyses of multiple large- and small-sized aliquots indicate the samples were well-zeroed prior to deposition and do not present post-depositional disturbances. A good spatial evolutionary chronology exists for the peninsula based on a few ancient maps and geomorphological surveys, and has been incorporated in this study. Some attempts have been previously made at dating this coastal system, and are analyzed in depth in terms of their significance as some lack sufficient spatial details to be assuredly compared with our results. Based on our OSL ages, we propose a new hypothesis of supra-tidal formation for this barrier spit, based at least on five initial sedimentary nuclei, contrary to previous beliefs.

6.1. INTRODUCTION

Strandplains and barrier islands with pristine progressions of ridge lineations are regarded as coastal progradation wonders by many geoscientists. Their development on diverse continental platforms is intrinsically related to several factors including sediment availability, ocean dynamics, basin geometry, bathymetry and sea level. Geomorphological, sedimentological and palaeontological analyses may only give a relative estimate of their place in time, as opposed to the more assertive absolute radiogenic or radioisotopic age estimates.

This paper presents new OSL data and ages from one of such coastal barrier system, St. Joseph Peninsula, Florida (U.S.A.), and examines its Holocene evolution. We outline parameters extracted from the various optically stimulated luminescence (OSL) measurements that can also be useful in the interpretation of the depositional and burial history of young coastal sediments. Some of these parameters have been previously used in other depositional settings to determine partial zeroing of the optical signal and post-depositional disturbances (e.g. Bateman et al., 2007a; Bateman et al., 2007b; Forrest et al., 2003).

Some of the first studies along the Gulf Coast of north-west Florida (U.S.A.) were reported by Price (1954). Detailed studies of the coastal surficial geology (both sub-aerial and sub-aqueous), mineralogy, supra-tidal

geomorphology and bathymetric characteristics of the continental shelf and slope have been published for the region (e.g. Donoghue and Tanner, 1992; Rizk, 1991; Stapor, 1973; Stapor, 1975; Tanner et al., 1989). Rizk (1991) divided St. Joseph Peninsula into 14 ridge sets based on individual ridge morphological characteristics such as orientation, curvature and truncation, as a result of detailed analysis of ancient nautical charts and air photographs. Moreover, he explains the supra-tidal progradation and general evolution of the peninsula based on these assigned ridge sets, following Stapor's (1973, 1975) original hypothesis that the peninsula had grown from two pre-existing islands, separated by a narrow inlet presently observed at Eagle Harbor (**Figures 6.1.** and **6.2.**). Most previously published materials are focused on the still existent sea level history controversy, but they are not targeted in this paper. Nonetheless, little is known about the absolute chronological evolution of this peninsula, as numerous beach and dune ridges that decorate the peninsula are vastly depleted in organic materials used for e.g. radiocarbon dating. Only a handful of dates have been published from the area, usually associated with relative determinations based on archaeological findings (Benchley and Bense, 2001; White, 2005; White et al., 2002) and basically one ^{14}C age on a peat unit found at St. Joseph Peninsula's southern end (Stapor, 1975).

More recently, a few studies, including this one, have targeted the barrier islands protecting the Apalachicola region (**Figure 6.1.**) to further understand, in a more accurate approach, their chronologies, hence the patterns of evolution of this local Floridian coastal system (e.g. Forrest, 2003; López and Rink, 2007a; López and Rink, 2007b; López et al., under review 2007; Otvos, 2005a). These studies have mostly used OSL or thermoluminescence (TL) (c.f. Otvos, 2005a) to determine the age of multiple pristine, vegetated or not, mature and young, ridges located throughout St. Joseph Peninsula, Cape San Blas, St. Vincent Island and Little St. George Island. Despite providing a more accurate estimate of the moment of burial of inorganic materials (e.g. quartz), OSL is may be also used to understand the evolution characteristics of the deposit itself (i.e. dosimetry histories, possible sediment sources, pre- and post-depositional disturbances).

6.2. STUDY AREA AND SAMPLING SITES

St. Joseph Peninsula is located in a region known as the Florida Panhandle (**Figure 6.1.**), within Gulf County, at a general latitude of $29^{\circ} 50'$ and longitude of $85^{\circ} 20'$. It is a long and narrow spit that seems to have evolved sequentially from south to north (**Figure 6.2.**). However, the intricate patterns of the hundreds of ridges which decorate its surface may suggest otherwise. Nonetheless, the peninsula exhibits a magnificent panorama of interlocking and truncated ridges that have evolved through time from beach-laid ridges to tall aeolian-capped dune ridges mostly towards its north end. Even though private, commercial and military development exists on the southern section of the peninsula, its central

and northern sections are protected recreational and wilderness areas within the T.H. Stone Memorial St. Joseph Peninsula State Park (Florida Department of Environmental Protection). Where development has not overcome nature, woodland (i.e. mostly pine), scrub oak and palmetto species thrive, with increasing vegetation density towards the St. Joseph Bay side of the peninsula. No rivers or streams drain into the bay. The closest fluvial system in the region is the Apalachicola River, postulated principal source of sediment for the barrier systems pertaining to this complex, with the exception of offshore to onshore and longshore drift (see **Figure 6.1.**).

The ridges along St. Joseph Peninsula can be divided into three general categories, based on geometry, height, and geographical position:

- a) Beach ridges: Located predominantly within the central and southern sections of the peninsula. Maximum heights of three meters and a moderate aeolian cap.
- b) Dune ridges: Predominantly along the Gulf-side of the peninsula within the central and north sections. These are ridges with heights exceeding three meters and with a thick aeolian input.
- c) Modern foredunes: The existent present-day foredunes located on the backshore edge of the beach, throughout the peninsula.

All three ridge types were targeted for this study as key ingredients for the understanding of the evolution of the peninsula. Moreover, we also wanted to see any potential differences regarding OSL data possibly characterizing the targeted depositional environments. Three ridges pertaining to the first type of system (a) were targeted: Rish Park, Harvey and Deer Ridge. Another three were chosen based on ridge type b: Haven, Wild and GPR1. Finally, three other ones fulfilled descriptions for c: White Sands, SJ002 1 and SJ002 2 (**Figure 6.2.**).

A total of 11 cores were retrieved from several ridges along St. Joseph Peninsula. While coring, sample tubes were rotated as little as possible to maintain alignment with geographical north, which was carefully marked on each sediment core. Three to six meter-long conventional aluminium irrigation pipes served as light-tight coring vessels, each thoroughly cleaned prior to insertion into the ground with a portable gas-powered vibra-coring system, adapted with a custom-made coupling to hold down each aluminium pipe. As depicted in **Figure 6.2.**, from south to north, the sediment cores retrieved are: Haven, Rish Park, White Sands, Harvey, Deer Ridge SJ201, Deer Ridge 1, Deer Ridge 2, Wild, SJ002 1, SJ002 2, and GPR 1. The maximum unconsolidated coring depth reached was 345 cm (Harvey) while the minimum was 125 cm (Deer Ridge SJ201). Nonetheless, 73% of the cores attained depths > 200 cm, in an attempt to

get as close to the base of each ridge as possible, i.e. the most realistic time of individual ridge formation at each geographical position along St. Joseph Peninsula. There was no clear sedimentological or visual structural evidence indicating the base of each ridge was reached. However, where visual structural evidence was present indeed, laboratory sampling at the very bottom of the core was avoided due to the sample location selection criteria detailed in the subsequent section. Thus, we propose our OSL age values to be *terminus ante quem* ages for the time of formation of each ridge, i.e. each ridge had to be formed no later than the ages presented in this paper.

Besides the geochronological objective of this research, a detailed geomorphological analysis of St. Joseph Peninsula was completed, and the same was accomplished for the other targeted barrier systems in this Apalachicola complex. Previously published bathymetric and topographic maps (e.g. USGS, 1982), high resolution satellite images (e.g. USGS, 1999; USGS, 2004), historical nautical charts and air photographs and field observations were combined to obtain a better understanding behind the historical morphological evolution and shoreline changes throughout the peninsula. Moreover, individual ridge sets were also depicted based on our own interpretation/observation as well as by comparisons with Rizk's (1991) and Stapor's (1973, 1975) data sets. **Figure 6.3.** shows the resulting ridge sets established for this research as well as all the targeted coring sites. Some of the historical shorelines are also shown, as well as ancient topographic survey markers (i.e. survey benchmarks) and light houses as important reference points, some of which are presently not existent.

6.3. OSL DATING

The unconsolidated-sediment cores were split-opened under subdued orange lighting at the AGE Laboratory (McMaster University, Canada). Each core was strategically split-opened perpendicular to the direction of the ridge from which it was extracted, consequently permitting the observation of any potential syndepositional sedimentary structures. Following stratigraphical analysis of one split-half of each individual core under bright light, the locations for collection of OSL samples were selected. Two and a half centimetre-long slabs of sediment were taken for OSL dating from the non-exposed split-half sections of each sediment core. Material close to the edges of the pipes (i.e. ~0.3 cm) was rejected to avoid any contamination from the coring itself (i.e. downward penetration).

The number of OSL samples extracted from each core and the selection of their location within each core depended on the following criteria: a) overall length of the core; b) sedimentological homogeneity around 30 cm of the centre of the sample, which also accounts for radioisotopic homogeneity of the targeted sample; c) the ridge's geographical position and relationship with other cores within proximity; and d) overall importance of the core in terms of the peninsula's

evolution. Furthermore, sections of core with intricate patterns of heavy mineral- and/or organically-rich layers/horizons (e.g. varying thicknesses and number of layers), were avoided for sampling to comply with selection criteria b. In some cases (e.g. the lowermost 50 cm of Rish Park core), even though the area evidenced water-laid deposition (i.e. very close to the base of the ridge), no sample was taken here to avoid dosimetry problems.

In all cases, an OSL sample was selected from the lower part of the core (i.e. sample A), while a second one was extracted from the upper part of the core (i.e. sample B), at least 50 cm below the surface of the core (i.e. topographical surface) to avoid the soft cosmic rays input. Samples A and B were generally at least 50 cm apart. Deer Ridge SJ201 and Deer Ridge 2 were the only cores with only one sample (i.e. A) taken for OSL dating. All sediment cores (hence, samples depths) were corrected for compaction by comparing the total lengths of both the original core vessel and the sediment core recovered. In all cases, linear compaction was assumed as no material was lost during extraction because core catchers were always used and the bottom part of the cores was inspected immediately after recovery. A total of 20 samples were subjected to OSL dating. **Table 6.1.** summarizes the locations, environment assigned, ridge sets and burial depths of the OSL samples recovered from St. Joseph Peninsula and presented in this paper.

Coarse-grain quartz separates (i.e. 150-212 μm) were obtained after preparing each OSL sample under subdued orange lighting following standard laboratory protocols (i.e. chemical and mechanical treatments) highlighted in López and Rink (2007b). The estimated present-day moisture content was obtained from oven-drying each sample at a temperature < 60 °C. In general and based on sedimentological and mineralogical analyses of this coastal setting and experience with previous samples (see López and Rink, 2007b), slabs of sediment ~ 2.5 cm-long x ~ 7 cm-wide x ~ 3.5 cm-deep, taken from only one split-half section of a core, contain enough quartz to get at least ~ 5 g of grains of this mineral in the targeted 150-212 μm grain-size fraction, i.e. enough separate to complete all necessary OSL tests and measurements at the designated aliquot sizes required for the purposes of this research.

Prior to the measurement of each sample's palaeodose, i.e. the final equivalent dose (D_E) used in the determination of the age of each individual sample, a series of luminescence tests were performed on several single aliquots of each sample to determine the following (see López and Rink, 2007a) for details):

- a) Initial assessment of the D_E value (3 to 6 large-sized aliquots) was estimated by comparing the natural OSL vs. the OSL signal obtained after a dose selected between the values of 0.26 and 0.89 Gy was given (OSL with 220 °C pre-heat for 10 s at a rate of 10 °C/s). This range of doses was

chosen based on the estimated young age of the peninsula and the values depended on each sample's location (e.g. White Sands samples were given a 0.26 Gy dose while Rish Park samples were given a 0.89 Gy dose). The determination of the best laboratory dose and test dose values to use in the regeneration cycles was done based on the initial assessment value.

- b) Contamination by feldspar in the same run used for the initial D_E assessment, using the same dose value for IRSL as for OSL (IRSL with 220 °C pre-heat for 10 s at a rate of 10 °C/s) (3 to 6 large-sized aliquots). An IRSL/OSL ratio < 0.03 was taken to indicate insignificant levels of feldspar contamination.
- c) Best preheat temperature to use during the measurement of the OSL signal. This value was selected among four different values (160, 200, 240 and 280 °C), after three tests were performed on three sets of 12 large-sized aliquots: pre-heat plateau test (PHP), dose recovery test (DRT), and thermal transfer test (TTT). The doses given for DRT varied between 0.29 and 0.87 Gy, depending on the obtained initial D_E (test a). The pre-heat value with best response at all three tests was chosen as pre-heat for 10 s prior to each OSL measurement. A standard cut-heat of 160 °C for 0 s was given after each test dose, at 10 °C/s increments.

The final D_E was measured using the single aliquot regenerative (SAR) protocol (Murray and Wintle, 2000) at two different aliquot sizes (large: 8 mm mask size; and small: 3 mm mask size) on 18 to 48 aliquots per sample (see **Table 6.2**). A total of six regeneration doses (including one zero dose and one repeat of the lowest dose) were used in all D_E measurements. In general, the minimum regeneration dose administered was of 0.26 Gy while the maximum was 2.60 Gy on the much older sample. The test doses usually ranged between 0.35 and 0.45 Gy, depending on the sample.

All measurements were done using an automated RISØ TL-DA-15 reader with blue light-emitting diodes (emission centered at 470 ± 30 nm) for OSL stimulation (at 125 °C for 100 s), which was measured through a 6 mm-thick Hoya U-340 filter. An infrared laser diode unit (emission centered at 830 ± 30 nm) was used for infrared stimulation. The first 0.4 s of the stimulation were used as the OSL signal, whereas the average value of 10 channels in the last 4 s was subtracted as background.

For the final D_E estimation, hence the age calculation, any aliquots with values falling within the following criteria were excluded: a) natural signal smaller than three times the background noise (i.e. to avoid low signal to noise ratios as young samples tend to have low natural OSL signals (c.f. Ballarini et al., 2003; Stokes, 1992); b) recycling ratios outside 0.90 to 1.10 range; c) test dose

error > 10%; d) D_E uncertainties > 20%; e) D_E values greater than two standard deviations of the mean (i.e. outliers). The final D_E value of each sample was calculated by obtaining the mean D_E value of the accepted aliquots, similar to the central age model of Galbraith et al. (1999). The final D_E error was calculated as one standard deviation (i.e. $\pm 1\sigma$) of the D_E values for distributions with skewness coefficients < -0.65 and > +0.65 (i.e. slightly to highly skewed distributions), and one standard error of the mean for distributions with skewness coefficients between -0.65 and +0.65 (i.e. symmetrical distributions) (see **Table 6.2.**). Frequency distribution plots with corresponding cumulative frequency (%) curves were built to assess the degree of dispersion and modality of each D_E distribution, as well as radial plots (**Figure 6.4.**). The size of the bins used for each histogram was obtained by calculating the median of the aliquots' D_E uncertainties for each individual sample (usually < 0.02 Gy for the large-sized aliquots and < 0.04 Gy for the small-sized aliquots).

The gamma and beta dose rates were calculated based on sediment geochemistry. Sub-samples of each original whole core sample extracted for OSL were sent to the McMaster University Nuclear Reactor, where the thorium and potassium contents were determined using neutron activation analyses (NAA) while uranium was measured using delayed neutron counting (**Table 6.3.**). Cosmic-ray dose rate values were obtained using the program ANATOL (v. 0.72 B, provided by N. Mercier, CNRS, Paris) which uses the calculations by (Prescott and Hutton, 1988) and also incorporates energy release data of (Adamiec and Aitken, 1998).

In addition to the measured laboratory values' errors, the following additional systematic errors were incorporated into each age calculation: a) $\pm 25\%$ for moisture content; b) $\pm 2\%$ for etching; c) $\pm 5\%$ for cosmic-ray dose rate; d) $\pm 10\%$ global systematic error (which accounts for any other changes in environmental dose rates not accounted for elsewhere). The ages are quoted in years before a *datum*, depending on the sample's measurement date which spanned between 2004 and 2006 (see **Table 6.3.**).

Once the ages were obtained, vertical accretion rates were calculated for individual cores containing two samples (i.e. lower sample A and upper sample B), and for the Old Cedar and RH-TUE sites, as both contained lower and upper samples taken at the same locale. All cores were corrected for compaction which was assumed linear throughout the sediment core. The average sediment accumulation rate (ASAR) was calculated for two portions of each core (and sites) using the SAR-OSL ages as follows (see **Table 6.4.**):

$$\text{Lower ASAR} = (\text{A vs. B depth difference}) / (\text{A vs. B age difference})$$

Upper ASAR = (Ground surface vs. B depth difference) / (Ground surface [age = 0] vs. B age difference)

6.4. RESULTS

6.4.1. OSL CHARACTERISTICS OF THE SAMPLES

All IRSL/OSL ratios obtained for these coastal sediments ranged between 0.001 and 0.004, indicating the high level of purity obtained during mineralogical separatory procedures in the laboratory. Hence, a standard IRSL/OSL ratio of < 0.01 is possible to be obtained when dealing with samples taken from quartz-rich coastal environments such as these ones with almost no feldspar component. Interestingly, the lowest values are associated with the samples believed to be among the oldest on the peninsula (Rish Park, Haven, and Deer Ridge), while the highest values are associated with modern frontal coastal systems (SJ002 1 and White Sands), probably indicative of sediment source being the modern Apalachicola River outflow as opposed to the origin of sediments forming the older ridges on the peninsula.

The preheat temperatures used to measure the final D_E of each of the 20 samples analyzed for this study ranged from 160 to 280 °C and were chosen according the best common results obtained for the PHP, DRT and TTT tests. Interestingly, the youngest samples (i.e. based on OSL age, geographical position and a geomorphological assessment of the progradation of the St. Joseph spit) were measured using relatively high preheat temperatures (i.e. 240 and 280 °C), while the oldest samples used low preheats (i.e. 160 and 200 °C). In theory, geologically young samples should be associated with relatively low preheats whereas older ones should respond better to elevated temperatures (c.f. Bøtter-Jensen et al., 2003), in order to avoid potential thermal transfer problems, which in turn may lead to age under- or over-estimations. Lower preheats are usually associated with negligible or low transfer (e.g. Bailey et al., 2001; Rhodes, 2000).

No convincing evidence for partial zeroing was ever observed in any of the samples measured for this study. As no evidence of incomplete zeroing was found when analyzing D_E values and the spread in D_E distributions with decreasing aliquot size (from 8 and 5 to 3 and 1mm mask sizes), the ages were calculated using D_E values obtained from the large-sized aliquots.

D_E frequency distributions, cumulative frequency (%) curve and radial plot diagrams as well as analyses of multiple statistical parameters were performed on each sample at each aliquot size measured. **Figure 6.4.** is a typical example of OSL data obtained for the samples used in this study. As observed in the majority of the frequency plots, the data obtained from the large-sized aliquot is encompassed by the one obtained at the 3 mm size, with the exception of the

average one or two outliers, normally located towards the high D_E end. The comparison between the frequency plots of large- and small-sized aliquots is further evidence of full luminescence signal zeroing. The cumulative frequency curve may help elucidate population modes when clear evidence is not observed in the histogram. As in all cases, only one aliquot was found as outlier (i.e. $> \pm 2\sigma$). This is normal for the vast majority of the samples from neighbouring young barrier coastal settings analyzed, not only pertaining to this study but also to previous ones by the same authors.

For more details regarding the D_E frequency distributions and cumulative frequency curves analyses, see the appendix section in López (2007).

6.4.2. OSL DATING RESULTS

For the ages reported herein, we assume (**Table 6.3**): a) measured water content similar to moisture content throughout sample's burial history, within error; b) no disequilibrium in the uranium decay chain basically due to the very low (< 0.5 ppm) uranium concentrations (thus no significant dose contribution); and c) constant sediment accumulation since burial. The latter, i.e. linear accumulation model, uses a cosmic-ray dose rate value calculated for half of the sample's burial depth, to account for variations in overburden thicknesses since the original emplacement of the sample (see also López and Rink (2007b) and Thompson et al. (2007)). The results, both final D_E values and OSL ages, associated with the samples analyzed in this study, are all in stratigraphical order within each core. Moreover, stratigraphical and temporal correlations can also be applied and are evidenced among cores taken within proximity of each other, i.e. both cores SJ002 and all three Deer Ridge cores, as seen in **Figures 6.5.** and **6.6.**

In general, the samples recovered from St. Joseph Peninsula can be grouped into three main sets based on their D_E values: a) those showing high D_E values (between 0.25 and 0.57 Gy), which are basically isolated into two regions of the spit (here after referred as nuclei); b) those showing lower D_E values (between 0.20 and 0.25 Gy), essentially located throughout the interior of the peninsula; and c) those with D_E 's of < 0.07 Gy, located along the frontal region (Gulf side) and the northern end of the spit. These D_E groups reflect the ages associated with the different samples, grouped below by time of formation (i.e. age range) and overall evolutionary and geomorphological position on the peninsula. The OSL ages for all sets of samples are reported below, and results are discussed from south to north along the peninsula. Please refer to **Table 6.3.** for all data regarding age calculations of individual samples.

6.4.2.1. SAR-OSL AGES OF ST. JOSEPH PENINSULA PRECURSOR NUCLEI

In a previous study done on Richardson's Hammock (see **Table 6.1.** and **Figures 6.2.** and **6.3.** for location and **Table 6.3.** for general data and results), the

authors OSL-dated two ridges on the northeast and southwest edges of this hammock (López et al., under review 2007) and obtained what are suggested as the oldest general ages for the St. Joseph Peninsula region. RH-GEO-1 was a horizontal sediment core taken on a ridge exposed on the northeast bay-shore edge of Richardson's Hammock, which showed a SAR-OSL age of $2,700 \pm 400$ years ago. Another two horizontal sediment cores RH-TUE-1 and RH-TUE-2 were recovered from the untouched clean walls of a two metres-deep trench, some 20 m south of RH-GEO-1 and on the same ridge. The trench was re-opened with permission post previous archaeological investigations in the area. Sample RH-TUE-1, taken from inside a shell midden layer, showed an age of $1,400 \pm 100$ years ago. RH-TUE-2 was taken from the underlying clean quartz-sands pertaining to the same ridge as RH-GEO-1, and was assigned a SAR-OSL age of $3,300 \pm 300$ years, *terminus ante quem* for the formation of that ridge. On the southwest edge of Richardson's Hammock, a long vertical core was retrieved from the morphologically youngest set of ridges associated to the hammock. The lower and upper samples retrieved from the RH core showed ages of $3,100 \pm 300$ and $2,300 \pm 200$ years ago, respectively (see **Table 6.3.**). Overall, the *terminus ante quem* age of formation of Richardson's Hammock is associated with the bay-shore ridge (i.e. samples RH-TUE-2 and RH-GEO-1), hence its shallow precursor had to form prior to at least $\sim 3,300$ years ago. Hence, we consider Richardson's Hammock the oldest and first sedimentary nucleus to form in the area, whose growth continued to $\sim 2,300$ years ago, precursor to the formation of St. Joseph Peninsula (López et al., under review 2007), and referred to hereafter as the Richardson's Hammock nucleus.

Besides the samples recovered from Richardson's Hammock, essentially three sample locations along St. Joseph Peninsula showed high D_E values: Rish Park, Deer Ridge (all three cores) and Harvey (see **Figures 6.2.** and **6.3.** for locations and **Tables 6.1.** and **6.2.**). Rish Park is located five kilometres north of Richardson's Hammock and about three kilometres south of the Harvey core, which in turn is only 500 m to the southeast of Deer Ridge. For practical purposes, the area surrounding Rish Park will be named hereafter the Rish Park nucleus, whereas the area around Deer Ridge and Harvey will be named hereafter the Eagle nucleus.

According to sedimentological analyses performed on the Rish Park core and a 1.5 m-wide x 3 m-long trench opened in 2002 adjacent to the core, sample A was taken just 30 cm above in low angle ($< 10^\circ$) parallel stratification shown by the intercalation of heavy mineral and quartz-rich laminae, suggesting a swash deposition environment. Thus, sample A is stratigraphically close to, but must likely be slightly younger than what we believe is the base of the Rish Park ridge. A $2,200 \pm 200$ years age was obtained for Rish Park A, the oldest age found in this study for the peninsula. The upper sample from Rish Park, sample B, is related to a wind-laid environment. Aeolian sediments commonly cap the ridges

that decorate the coastal barrier systems near Apalachicola, but their thicknesses vary depending on the position of the ridge referent to the prevailing winds and local topography. Located at 63 cm below surface (**Table 6.1.**), Rish Park B showed an age of $1,600 \pm 100$ years (**Table 6.2.**), making it contemporaneous to Deer Ridge 2 A, the lowermost sample on that particular ridge (see below). The Rish Park nucleus encompasses the second oldest ages throughout St. Joseph Peninsula, thus we suggest it to be the second oldest of the nuclei in the area.

The Harvey core was extracted from an elongated N10°E ridge located just 500 m and two ridges southeast of Deer Ridge, immediately south of the Eagle Harbor embayment, on the St. Joseph Bay side (**Figures 6.1., 6.2. and 6.3.**). Its lowermost sample A, from a depth of 330 cm, shows a *terminus ante quem* age of $1,700 \pm 100$ years ago for the initial formation of this ridge (**Table 6.3.**). Sample B, at 90 cm depth, gave an age of $1,300 \pm 200$ years ago (**Table 6.3.**). Even though the depths of Harvey samples seem greater than those from Rish Park, the calculated lower ASAR at Harvey is four times greater than the former: 0.60 cm/yr compared to 0.13 cm/yr respectively (**Table 6.4.**).

Deer Ridge is a relatively narrow ridge running N10°E and culminating on the south shore of Eagle Harbor (**Figure 6.2.**). Three cores were recovered from this ridge and its immediate surroundings (**Figure 6.4.**): Deer Ridge 1 located by the crest of the ridge; Deer Ridge 2 on the west flank of the ridge and 1.25 m below the top of the former; and Deer Ridge SJ201 situated on the west trough (or runnel) of the ridge, 1.85 m below the top of Deer Ridge 2. As seen in **Figure 6.5.**, the lowermost sample of the triplets is Deer Ridge SJ201 A, but it is also the youngest one with a $1,000 \pm 80$ years age (**Table 6.3.**). In such a case, it is important to understand the geomorphological positioning of the sample, as depth alone may not explain its age but its relative burial history. As seen in **Figure 6.5.**, Deer Ridge SJ201 A was taken in the swale, hence, depicting a story post-formation of the ridge itself. As for the ridge itself, sample Deer Ridge 2 A, which is associated with a water-lain environment (i.e. parallel laminations at $< 10^\circ$), is the oldest with an age of $1,600 \pm 100$ years (hence a *terminus ante quem* of formation of this ridge) and Deer Ridge 1 B, pertaining to the aeolian cap, is the youngest at $1,300 \pm 100$ years (**Table 6.3.**). Due to their similar lower and upper ages and relative closeness, both ridges, Harvey and Deer Ridge, seem to be contemporaneous, making this area of the peninsula the third oldest nucleus (i.e. Eagle nucleus) to Rish Park, only ~500 years younger.

6.4.2.2. SAR-OSL AGES OF INTERIOR RIDGES

Within more interior regions of St. Joseph Peninsula, we have two coring sites, both presently protected from any present day direct influence from St. Joseph Bay or the Gulf of Mexico. Core Haven, located south of Eagle Harbor, northwest of RH and at the same latitude as the northern edge of Pig Island

(**Figures 6.1., 6.2. and 6.3.**), was retrieved from the first ridge west of Cape San Blas road. It is oriented N5°W. The ridge does not continue east of the main road but does extend towards the Gulf side of the peninsula, culminating in a beach-housing development area, roughly one kilometre south of the coring site. Both Haven samples, A and B, even though from depths 1.40 m apart, are almost statistically undistinguishable from each other, 950 ± 80 and 840 ± 60 years respectively, making this one of the fastest grown (i.e. rapid vertical accretion) interior ridges on St. Joseph Peninsula (i.e. lower ASAR of 1.27 cm/yr) (see **Table 6.4.**).

A similar rapid vertical growth rate of 0.85 cm/yr (lower ASAR; **Table 6.4.**) applies to the ridge which held the sediments from core Wild, located and named after the protected wilderness area in northern St. Joseph State Park, which is located in the northern end of the peninsula (**Figures 6.1., 6.2. and 6.3.**). The lowermost sample (**Table 6.1.**), Wild A, showed an age of 930 ± 70 years, while an age of 690 ± 60 years (**Table 6.3.**) was obtained for the upper sample Wild B. Even though core Wild is located towards the northern end of an elongated N20°E ridge, north of Eagle Harbor, ~10.5 km north of core Haven, it has striking similarities with the latter in terms of both samples depths (i.e. A and B within both cores), ages and overall calculated ASAR (**Table 6.4.** and **Figure 6.7.**). Both cores, Wild and Haven, are located within similar distances from the Gulf shoreline and are in similar geomorphological positions, which may also explain their contemporaneous character. This westward progradation along the Gulf of Mexico was occurring after initial ridge formation had built earlier ridges to the east.

6.4.2.3. SAR-OSL AGES ALONG THE PENINSULA'S WESTERN MARGIN AND SPIT TERMINUS

The last four sediment cores and related ridges are grouped into the category of modern coastal frontal systems, i.e. those which are still evolving. These four cores are: GPR 1, SJ002 1, SJ002 2 and White Sands (see **Figures 6.1., 6.2. and 6.3.**) each with two associated OSL ages (i.e. samples A and B – see **Tables 6.1., 6.2. and 6.3.**). The only core taken closest to the northern terminus of St. Joseph Peninsula was GPR 1. This northern spit end region, encompassing over 90 km², is decorated with about seven consecutive beach ridges, all concave towards the southeast. Core GPR 1 was taken within the fifth ridge inland from the modern ephemeral foredune ridge present along the spit end, which has an N70°E direction (**Figure 6.6.**). The lowermost sand layers of this 2.41 m-long core showed planar to sub-planar lamination, evidencing water-laid deposition. An age of 250 ± 20 years was obtained for bottom sample GPR 1 A. Some 1.19 m above A, sample GPR 1 B was taken from sands with $< 10^\circ$ sub-horizontal laminations and showed an age of 220 ± 40 years (**Table 6.3.**), statistically indistinguishable from the deeper sample. The calculated lower ASAR value for

this ridge reaches an astonishing 3.96 cm/yr, surpassing any other accumulation rate calculated in this study for the more interior ridges (**Table 6.4.** and **Figure 6.7.**).

The Gulf-side beach front of St. Joseph State Park, north of Eagle Harbor, is decorated by many elongated massive foredunes, following the direction of the modern shoreline, cut by intermittent blow-out and washover areas that have broken through some inland mature ridges. This intricate but magnificent coastal scenery has prone intermittent parabolic dune development, which intensifies with increasing north latitude (**Figures 6.2.** and **6.3.**). About 4.30 km north of Eagle Harbor, but only ~700 m north of core Wild, along the beach, is the SJ002 site, a massive blow-out and presumably washover area with an impressive 12.32 m above mean sea level (a.m.s.l.) high dune at the rear of this 107 metre-wide system (**Figure 6.6.**). Two cores were taken from this site: SJ002 1, on what is believed to be an isolated remnant of a 6.40 m-high a.m.s.l. ex-foredune, which had developed prior to the modern one (~4 m-high a.m.s.l.), where SJ002 2 was retrieved, just a few meters east of the presently forming incipient dunes. According to geographical position and logical accretion evolution, SJ002 1 was considered older than SJ002 2. This was confirmed by the ages obtained and also by the relative depths a.m.s.l. of each of the samples. A 190 ± 30 years ago age was obtained from the bottom of SJ002 1 while a 140 ± 20 years old one from its top. As for SJ002 2, even though both samples are 82 cm apart, the ages obtained are statistically undistinguishable from each other: 120 ± 8 and 110 ± 8 for sample A and B respectively. Such chronological proximity may suggest an extremely rapid sediment input, but it would be equivocal to provide ASAR values for statistically indistinguishable ages. For SJ002 1 the calculated lower ASAR of 1.82 cm/yr is similar to the majority of vertical accretion rates associated with the peninsula's history (**Table 6.4.** and **Figure 6.7.**).

The youngest of all the ridges grouped in this category is the one named White Sands. This impressive 1 km-long x 160 m-wide x 9 m-high (a.m.s.l.) active foredune, parallel to the modern St. Joseph Peninsula shoreline (N10°W), was located south of Eagle Harbor, just south of a beach housing area along White Sands road (**Figures 6.1., 6.2.** and **6.3.**). Parts of a unit containing remnants of massive heavy mineral layers intercalated with quartz-rich sands interpreted as sediment deposited during the waning stages of Hurricane Opal's storm surge in October 1995 (Forrest, 2003). An optical age of 8 ± 1 years ago was obtained on a sample collected within this heavy mineral-rich deposit in the summer of 2003 (**Figure 6.8.**). Unfortunately, and as of summer 2006, landward erosion due to the hurricane season of 2004, and some subsequent beach-front housing development, had destroyed any evidence of the hurricane-deposited sediments. The White Sands core was taken, during the summer of 2004, on a depression within this system, ~ 3 m below and ~ 2 m inland of the crest of the foredune and reached a depth of 258 cm (**Table 6.1.**). The lowermost sample, White Sands A,

showed an age of 170 ± 10 years ago, while an age of 24 ± 1 years was obtained for White Sands B (**Table 6.2.**). No evidence of the ~ 20 cm-thick heavy mineral deposit, exposed in 2002, was found within the core, and the relative position of Forrest's (2003) 8 ± 1 OSL age with our ages cannot be established. The calculated lower ASAR for this foredune (i.e. 1.28 cm/yr) is in accordance with the growth rate calculated for the Wild core (**Table 6.4.** and **Figure 6.7.**).

6.5. DISCUSSION

In this study, the evolution of St. Joseph Peninsula was based on extensive field work, sedimentological and geomorphological analyses, OSL ages, ancient maps and recent satellite imagery, as well as the interpretation of previously published data (i.e. ^{14}C and OSL dating, and sedimentological and geomorphological analyses).

Concordant with the geomorphology and vegetation, we found that the ridges located near St. Joseph Bay are older than their interior and subsequent Gulf side counterparts. Moreover, the ages obtained in this study also agree with the longshore dynamics surrounding the peninsula, inferring a general growth tendency from south to north, as evidenced by the shape and direction of the spit (**Figures 6.1.** and **6.2.**). However, determining the specific localities that served as potential precursor littoral shallows in both space and time, which in turn served as accretion platforms in a coastal environment such as this one, can only be achieved by geochronology. Furthermore, in coastal clastic-rich environments such as this barrier spit, where organic materials are scarce, the most reliable dating method to use is OSL due to the overwhelming amount of quartz grains, readily available.

As OSL measures the last moment of burial of any given sediment, and to better comprehend any chronologies obtained from this type of coastal environment, it is key to understand the importance and implications of the different geomorphological and sedimentological processes associated with the overall evolution of the barrier system. Basically, it is important to recognize that the rate of both vertical and horizontal growth of any given ridge and/or foredune is intrinsically related to: a) morphological processes affecting the area; b) sediment supply; c) geographical location within the system; and d) oceanic and atmospheric factors. Hence, and as stated before, in this kind of environment, the deeper the sample does not necessarily yield the older the age relative to nearby cores (e.g. Deer Ridge). However, the age obtained may help elucidate and/or constrain the evolution hypotheses established for that particular environment. Nonetheless, our core samples did show in each case ages in correct stratigraphical order, so, statistically indistinguishable ages relative to one another, within individual ages; no statistically indistinguishable inversions were found.

For organizational and logical purposes, we divide the discussion of this research into two different sections: one dealing with the findings obtained from the analyses of the OSL data; and the other focused on the chronologies for the overall surficial evolution of St. Joseph Peninsula.

6.5.1. ASSESSING THE RELATIONSHIP BETWEEN OSL AND THE DEPOSITIONAL ENVIRONMENT

It has been suggested that the best aliquot sizes to use when estimating the age of a sediment deposit (i.e. the burial D_E) are the smaller ones (Olley et al., 1998), hence aliquots containing around 100 grains or less. In smaller aliquots, the probability of measuring incompletely-zeroed grains diminishes whereas that of including basically well-zeroed ones increases. However, large size aliquots can also provide good estimates of an age when all the grains pertaining to that aliquot have received the same amount of sunlight exposure prior or during deposition, hence all the grains will show similar sensitivities (see explanation on better resolved normal distribution of D_E values in following paragraph). This must be the case for the samples measured in this study as they are in general agreement with the expected chronology. Furthermore, checking for inconsistencies in the OSL history of the sample may be done by comparing large-sized aliquots with small-sized to single grain aliquots. However, and as seen in this study (e.g. **Figure 6.4.**), a simple 8 mm versus 3 mm or 5 mm versus 1 mm size aliquots comparison may be sufficient to attest for evidences of incomplete zeroing, post-depositional disturbances, among others. Further studies in this direction have been suggested by Bateman et al. (2007a, 2007b).

As seen in the samples measured for OSL in this study, with decreasing mask sizes, there is increasing manifestation of both lower (but not zero values) and higher D_E values towards both ends of the distribution but maintaining most of the D_E values in the center (i.e. statistically similar mean D_E for all mask sizes –within error–). As mask size decreases, the amount of grains contributing to the OSL signal also decreases. However, the luminescence signal at lower mask sizes is given by grains with D_E values encompassing the initial distribution obtained with the 8 mm mask size. Hence, a higher resolution of the distribution is being obtained and not incomplete zeroing and/or any post-depositional disturbance.

We propose that this manifestation of spreading D_E distribution with decreasing mask size is evidence only for increasing resolution of D_E within the grain population. Hence, the spreading may be due to inhomogeneities in the beta doses to small numbers of grains. Thus, the larger mask sizes better represent the overall natural dose rate distribution due to all sources of dose rate.

6.5.2. PENINSULAR EVOLUTION OF ST. JOSEPH

St. Joseph Peninsula appears to be a textbook example of simple single bidirectional spit growth. However, and according to our OSL age results and some previously published data, its evolutionary history is more complicated than that. The first one to suggest a nuclei-derived evolution for the peninsula was (Stapor, 1973, 1975). According to him, the first nuclei to form were Richardson's Hammock and the area just north of Eagle Harbor, and later in Holocene history, they connected by longshore drift accretion. This general hypothesis has been accepted by (Rizk, 1991) in his geomorphological and sedimentological study of St. Joseph Peninsula, and more recently by (Otvos, 2005a) based on four reported TL ages along the peninsula (**Figure 6.8.**), one on Richardson's Hammock (**Figure 6.8.**) and two on Cape San Blas. The evolution of Richardson's Hammock is discussed in (López et al., under review 2007), and in agreement with Otvos' (2005a) TL age, this highly vegetated small area started to evolve no later than $3,300 \pm 300$ years ago (OSL *datum* A.D. 2005, (López et al., under review 2007) and was fully emergent as a small island no later than $2,300 \pm 200$ years ago (OSL *datum* A.D. 2005, (López et al., under review 2007). Archaeological evidence suggest that its easternmost edge was used by the Middle Woodland peoples only some $1,400 \pm 100$ years ago (OSL *datum* A.D. 2005, (López et al., under review 2007). Without doubt, Richardson's Hammock may be considered as the first nucleus from where St. Joseph Peninsula started its projection into the Gulf of Mexico waters (i.e. our ridge set As in **Figure 6.3.**). Our *terminus ante quem* age of $3,300 \pm 300$ years ago for the easternmost ridge on Richardson's Hammock is concordant with our previously reported ages for the emergence of the northwest margin of St. Vincent Island, another Apalachicola barrier island further to the east (López and Rink, 2007a, 2007b).

In geomorphological terms, the peninsula may be divided into ridge sets, based on the general similar direction, curvature and shape of groups of ridges, hence providing evidence for palaeo-accretion patterns and truncations, which in turn may elucidate the longshore drift and wave-front directionality at the time of formation of each set. **Figure 6.3.** details the set dividers based on a detailed study of multiple-year air photographs, satellite images and nautical/topographic maps. In general, St. Joseph Peninsula oldest areas neighbour St. Joseph's Bay, while the youngest are closer to the Gulf shores and progressively to the north. Moreover, Highway 30E seems to be a good marker to divide the peninsula in younger versus older sets, south of Eagle Harbor (**Figure 6.2.**). Rizk (1991) further suggested that there may exist a third peninsula-forming nucleus (his ridge set nc; c.f. Figure 6 in Rizk, 1991) which coincides with our ridge set Bn, marking a prominent protrusion of the peninsula towards St. Joseph Bay, with concave-eastward ridges (**Figure 6.3.**). Tanner (1987) also suggested this ridge set Bn as one of the precursor nuclei, in addition to our ridge sets En and Es (**Figure 6.3.**), as they depict similar easterly protrusions, believed to be the remnants of ancient

individual islands. However, it is equivocal to solely base evolution histories on geomorphological data, as re-curvatures may also indicate simple hydrodynamic changes in the longshore drift rather than previously existing sedimentary precursors. To further attest such hypotheses, absolute chronologies are to be required. Geochronologically, Rizk (1991) and Tanner (1987) may only have had available three dates to constraint their findings: Stapor's (1975) peat age (**Figure 6.8.**) and two other relative ages associated with the archaeological sites at Old Cedar and Richardson's Hammock eastern edge (8Gu85 and 8Gu10 Florida Master Site File, respectively). The latter only suggesting that these bay side areas had to be already fully emerged prior to the arrival of Ancient Peoples, so they could have inhabited them (c.f. López et al., under review 2007; Thompson et al., 2007).

Based on the geomorphology (e.g. ridges morphologies and directionalities), our OSL ages and previous ages, we suggest herein that St. Joseph Peninsula did not evolve from two but rather five nuclei, each strategically located along the spit trend, each a key shallow area or “sedimentary island” constrain to the supply of sand from the neighbouring Apalachicola River and offshore. From south to north, the proposed nuclei are: Richardson's Hammock, Rish Park, Eagle Harbor, and Pompano (**Figure 6.9.**). Rish Park covers the area determined as ridge set Ds (see **Figure 6.3.**), around the Rish Park core (it is inferred that the area around the 1910 San Pedro survey benchmark is contemporaneous to the Rish Park nucleus); the Eagle nucleus contains the ridges which held all three Deer Ridge and Harvey cores; the Harbor nucleus is the area immediate to the old 1934 survey benchmark, as the Pompano nuclei (see **Figure 6.3.** for details and **Figure 6.9.** for general overview). The area by the 1838 Old brick Light House (destroyed in 1851), on the north end of St. Joseph Peninsula, has been given a TL age of 1,700 years by Otvos (2005), which is not in agreement with the geomorphological reconstruction of the spit terminus based on ancient maps. As no details of depth of the sample were given by Otvos in his 2005 paper, this age is not taken into consideration for the general evolution of the peninsula in this study. In general, TL has a tendency to overestimate burial ages due to inaccurate determination of incompletely zeroed luminescence signals. Nonetheless, and as a suggestion for future optical studies, and to maintain the credibility of this dating technique, precise geographical location should be given for any OSL-dated sample, including elevation and most critically, burial depth. These basic details are fundamental when constraining, associating or co-relating OSL ages, as optical ages depict, more precisely, the timing since the last burial, i.e. the deposition of the sediments forming the targeted environment. Hence, in active dynamic coastal clastic-rich environments such as this one, formed by continuous “landscape inhomogeneities” such as beach and dune ridges, exact positioning of the sample (i.e. [x,y,z]) is required if any comparison/constraint among consecutive ridges is to be made.

Each one of these five nuclei emerged at different times but subsequent to the preceding. Based on our OSL ages and the ridge set patterns and truncations, we have estimated the time frames of formation of each nuclei and consequent progradation of St. Joseph Peninsula (**Figure 6.9.** and **Table 6.5.**): Time 1 (T1) is given a *terminus ante quem* age range of *ca.* 3,600 to 2,400 years ago which encompasses the entire time interval of formation of Richardson's Hammock, from east to west, as it is treated as one nucleus; Time 2 (T2) at least between *ca.* 2,400 and 1,400 years ago; Time 3 (T3) at least between *ca.* 1,400 and 1,000 years ago; Time 4 (T4) at least between *ca.* 1,000 and 700 years ago; Time 5 (T5) at least between *ca.* 700 and 300 years ago; Time 6 (T6) a *terminus ante quem* earlier than *ca.* 300 years; and Time 7 (T7) associated to all the modern on-going shore processes. The same time intervals have been depicted and used in the interpretation of the overall evolution of the Apalachicola Complex Barrier Islands as seen in López (2007). The estimated direction of accretion (as a result of net longshore drift) from each nucleus is noted on **Figure 6.9.** and is based in the general ridge set progradation direction, i.e. from the estimated initial point of formation (where the ridges are most close to each other), towards the ridges' curvature terminus. T4 and T5 (and arrows pointing west) represent general historical times and the modern accretion/re-shaping of the present shoreline (i.e. White Sands, SJ002 1, SJ 002 2 and GPR1 cores).

As mentioned before, the first nucleus was Richardson's Hammock which emerged at T1. By the time Richardson's Hammock was culminating its formation as an island, the Rish Park and Eagle nuclei may have been emerging shallows, with ridges accreting from east to west (**Figures 6.3.** and **6.8.**). In the meantime and throughout the development of the peninsula, sediment had to be readily available to continue providing material to support the other nuclei shallows to the north, as well as any further offshore accretion (as subsequent platforms for future prograding ridges). Post T1 and concurrent to T2, the bay side between the 1910 survey markers San Pedro and Eagle evolved. Unfortunately, we have no geochronological evidence yet for the time of formation of Pig Island. Interestingly, there are at least two ridge sets decorating this small island north of Richardson's Hammock (**Figures 6.2.** and **6.3.**). The orientations of these ridge sets are somewhat concordant to those of Richardson's Hammock, which may only suggest, rather than assert, some contemporaneous setting. Moreover, the westernmost ridges along Pig Island seem to be submerged, similar to those on the St. Joseph Bay side of the western lower mainland and the Apalachicola Bay side of St. Vincent Island and Little St. George Island, further evidencing possible subsidence of the Holocene cap due to potential compaction of parts of the Pleistocene platform in this region (López and Rink, 2007b; Otvos, 1985).

The Eagle nucleus had to be emerged completely < 1,000 years ago based on the archaeological evidence found at the Old Cedar archaeological site. An

OSL age of 940 ± 100 years (*datum* A.D. 2005) for the shell-midden (Thompson et al., 2007) indicates occupation during the Late Weeden Island culture phase of coastal Florida. Moreover, the dating of the underlying ridge (*terminus ante quem* age of $1,780 \pm 130$ years ago; OSL *datum* A.D. 2005 (Thompson et al., 2007)), which geographically is the one ridge east of Haven, concurs with our hypothesis for the emergence of the Eagle nucleus at T2.

The Eagle Harbor embayment may have remained an inlet throughout T2 and T3. Based on geomorphological evidence, it is proposed that the sediment that formed on the bay-side area between Eagle Harbor and the 1934 Harbor survey marker (i.e. ridge set As in **Figure 6.3.**) was deposited towards the end of T3, as the Harbor nucleus accreted both south- and north-ward. Contrary to Rizk (1991), both Harbor and Pompano nuclei are not contemporaneous, and the bridge that formed on the Gulf-side of Eagle Harbor, which now unites both the south and north sections of St. Joseph Peninsula, may have only emerged post T3 and probably during T4. After the complete emergence of Harbor and Pompano nuclei, ridges started to form northward and seaward during T4, evidenced by the ridges hosting the Haven and Wild cores. This ~ 800 year-long period (and counting) may be considered the most productive in terms of the spit's end and westward growth (**Figures 6.3., 6.8.** and **6.9.**) as well as the evolution of Cape San Blas (which will be discussed in a future manuscript; c.f. López, 2007).

In general, along St. Joseph Peninsula, ridge patterns are basically divided by the Cape San Blas road (Highway 30E), the main north-south trend road (**Figure 6.3.**). To the east of Hwy 30E, the ridges have terminal curvatures concaving towards the east, evidencing palaeo-directions of land growth. On the western Gulf side, the ridges tend to be more rectilinear (e.g. ridge at Haven core site), except at the northern spit end of the peninsula, which shows multiple re-curvatures of the ridges due to longshore drift engulfing the sedimentary terminus. The former ridges have no evident continuum on the west side of the road. The ridges west of the highway pertain to the so-called frontal system, which is mainly composed of elongated active foredunes of varying heights and some ephemeral blow-out areas mostly closer to Eagle Harbor, basically as a result of intensive erosion during more historical times. Nonetheless, these rectilinear ridge growth patterns may be associated with the closure of the Eagle Harbor inlet sometime during formation of ridge sets Fs and Cn. North of the harbour, large blow-out and washover areas, with increasing parabolic dune development towards the spit end, also pertain to this frontal system.

There is no evidence for development of extensive dune fields on St. Joseph Peninsula. However, some active unstable foredune systems, constricted principally to blow-out areas towards the northern region of the peninsula (north of SJ002 – see **Figures 6.2.** and **6.3.**), show the development of large transverse

dunes, sometimes exceeding heights of 20 m, that are accreting inland, disrupting the system of beach ridges immediately east.

Some of those systems are believed to have formed at least < 300 years ago, e.g. SJ002, as indicated by the age obtained by Forrest (2003) on the stable mature backdune, located at the end of the throat of the blow-out on SJ002 (**Figure 6.6.**). Forrest's (2003) OSL age F3 (**Figure 6.8.**) suggests that this massive backdune had to have formed no prior to at least ~ 90 years ago, as F3 is not at the base of the dune. The ages provided by the samples dated in this study from SJ002 1 and 2 show older values in settings that are seaward of Forrest's (2003) sample F3 (see **Figure 6.6.**). Nonetheless, the OSL ages associated with the remnant knob at SJ002 1 are in correct stratigraphical order compared to Forrest's (2003) sample F3, suggesting a) a possible link between the backdune and the knob at one point in time (i.e. attached together), or b) very rapid dune (hence previous beach ridge) consecutive formation. To assert which hypothesis is the correct one, a much higher resolution sampling for OSL-dating would have to be done both on the backdune (i.e. below sample F3) and on the remnant knob (above sample SJ002 1 B). This is an example of the dynamism of this coastal setting and the difficulties presented before researchers in geomorphologically-complex environments, ameliorated here by the use of OSL in a variety of environments on the peninsula.

The frontal-systems along St. Joseph Peninsula (> T4) are in a continuous battle against wind, water and natural erosion, in addition to any anthropogenic unrest. Unfortunately, and with the exception of its section north of Eagle Harbor, which is protected by the T.H. Stone Memorial St. Joseph State Park, the southern section of St. Joseph Peninsula is highly prone to erosion, there where development is at its highest (see **Figures 6.2.** and **6.3.**). An example of the latter are the large quantities of perpendicular-to-the-beach roads throughout the southern peninsula, which, in moments of natural high-energy release such as storm surges, facilitate erosion and reach to more secluded/vegetated ancient areas.

6.6. CONCLUSIONS

Young littoral and aeolian sediments from St. Joseph Peninsula (Florida, U.S.A.) spanning the past *ca.* 3,300 years have been successfully dated using SAR-OSL. There is no doubt that this Holocene coastal barrier system quickly emerged and developed due to a continuous supply of sediment from a south provenance. The direction of the spit growth certainly points to a prevailing south-to-north longshore drift existent throughout the history of this peninsula.

Based on our observations, we propose five nuclei as the precursors to the progradation and formation of this peninsula. This hypothesis is concurrent with

previously published archaeological findings and OSL dating also done by the authors among other colleagues.

Bulk unconsolidated sediments, sampled from small constricted areas within long-vertical sediment cores, can provide credible SAR-OSL ages for the various depositional systems targeted throughout the peninsula. The depositional ages presented herein are consistent with the depositional processes and burial histories of each site. Despite all being unconsolidated sandy deposits, no evidence of significant post-depositional disturbances are seen. Furthermore, samples collected from the upper layers of the sediment cores that could be more prone to present-time biological activity at the surface, show no evidence of re-working.

We also propose a new observational analysis model for OSL data: increasing resolution may be obtained with decreasing aliquot size when D_E values are obtained equally on both sides of the distribution. Such phenomenon may be due to dosimetry distributions at the micro-scale, rather than due to pre- or post-depositional complications.

Last but not least, when publishing OSL ages for dynamic coastal environments constituted by multiple ridges and/or ridge sets, such as St. Joseph Peninsula and environs, it is important to provide accurate geographical positioning of the samples (i.e. [x,y,z] data) so more precise constraints and correlations can be established between various authors' datasets and the credibility of the OSL ages maintained for specific burial depths, i.e. sedimentary depositional environments.

ACKNOWLEDGEMENTS

This research was made possible thanks to the unquestionable and great logistic, financial and personal support of the T.H. Stone Memorial St. Joseph Peninsula State Park and the Apalachicola National Estuarine Research Reserve (both Florida Department of Environmental Protection). Exploratory, sampling and coring permissions were granted by the former entities as well as the Wm. J. Rish Recreation Park (on St. Joseph Peninsula), the St. Joe Municipality (Gulf County) and individual land owners. Financial support was provided through a Natural Science and Engineering Research Council of Canada (NSERC) grant to WJR. Field assistances throughout the various field seasons, from 2002 to 2005, by Dr. J. Boyce, J. Etherington, K. Keizars, J. Pilarczyk, K. Moretton, M. Kossak, J. Thompson, and S. Collins (all from McMaster University) are immensely appreciated.

REFERENCES

- Adamiec, G. and Aitken, M.J., 1998. Dose-rate conversion factors: update. *Ancient TL*, 16: 37-50.
- Bailey, S.D., Wintle, A.G., Duller, G.A.T., and Bristow, C.S., 2001. Sand deposition during the last millennium at Aberffraw, Anglesey, North Wales as determined by OSL dating of quartz. *Quaternary Science Reviews*, 20: 710-704.
- Ballarini, M., Wallinga, J., Murray, A. S., van Heteren, S., Oost, A. P., and Bos, A. J. J., 2003. Optical dating of young coastal dunes on a decadal time scale. *Quaternary Science Reviews*, 22(10-13): 1011-1017.
- Bateman, M.D. et al., 2007a. Detecting post-depositional sediment disturbance in sandy deposits using optical luminescence. *Quaternary Geochronology*, 2: 57-64.
- Bateman, M.D. et al., 2007b. Preserving the palaeoenvironmental record in Drylands: Bioturbation and its significance for luminescence derived chronologies. *Sedimentary Geology*, 195(1-2): 5-19.
- Benchley, E.D. and Bense, J.A., 2001. *Archaeology and History of St. Joseph Peninsula State Park: Phase I Investigations*, University of West Florida Archaeology Institute, Jacksonville.
- Bøtter-Jensen, L., McKeever, S.W.S. and Wintle, A.G., 2003. *Optically Stimulated Luminescence Dosimetry*. Elsevier, Amsterdam, 355 pp.
- Donoghue, J.F. and Tanner, W.F., 1992. Quaternary terraces and shorelines of the Panhandle Florida region. In: C.H. Cletcher and J.F. Wehmiller (Editors), *Quaternary Coasts of the United States: Marine and Lacustrine Systems*. Society of Economic Paleontologists and Mineralogists, Tulsa, pp. 233-241.
- Forrest, B.M., 2003. *Applications of Luminescence techniques to Coastal Studies, St. Joseph Peninsula, Gulf County, Florida*. M.Sc. Thesis, McMaster University, Hamilton, 209 pp.
- Forrest, B.M., Rink, W.J., Bicho, N. and Ferring, C.R., 2003. OSL ages and possible bioturbation signals at the Upper Paleolithic site of Lagoa do Bordoal, Algarve, Portugal. *Quaternary Science Reviews*, 22(10-13): 1279-1285.
- Galbraith, R.F., Roberts, R.G., Laslett, G.M., Yoshida, H. and Olley, J.M., 1999. Optical dating of single and multiple grains of quartz from Jinmium rock shelter, northern Australia. Part I: experimental design and statistical models. *Archaeometry*, 41: 339-364.
- López, G.I., 2007. *The Late Quaternary evolution of the Apalachicola Barrier Island Complex, North-East Gulf of Mexico, as determined from optical dating*, McMaster University, Hamilton, 300 pp.

- López, G.I. and Rink, W.J., 2007a. Characteristics of the burial environment related to Quartz SAR-OSL dating at St. Vincent Island, NW Florida, U.S.A. *Quaternary Geochronology*, 2: 65-70.
- López, G.I. and Rink, W.J., 2007b. New Quartz-OSL ages for Beach Ridges on the St. Vincent Island Holocene Strandplain, Florida, U.S.A. *Journal of Coastal Research*, in press (accepted 2 December 2005).
- López, G.I., Rink, W.J. and White, N.M., (under review 2007). Optical dating of an ancient coastal occupation site and underlying land on the northwest Gulf Coast of Florida, near Apalachicola, U.S.A. *Geoarchaeology*: (submitted December 2006; 42 pp).
- Murray, A.S. and Wintle, A.G., 2000. Luminescence dating of quartz using an improved single-aliquot regenerative-dose procedure. *Radiation Measurements*, 32: 57-73.
- Otvos, E.G., 1985. Barrier Island Genesis - Questions of alternatives for the Apalachicola coast, north east Gulf of Mexico. *Journal of Coastal Research*, 1(3): 267-278.
- Otvos, E.G., 2005a. Coastal Barriers, Gulf of Mexico: Holocene Evolution and Chronology. *Journal of Coastal Research*, Special Issue 42: 141-163.
- Prescott, J.R. and Hutton, J.T., 1988. Cosmic Ray and Gamma Ray dosimetry for TL and ESR. *Nuclear Tracks and Radiation Measurements*, 14: 223-227.
- Rhodes, E.J., 2000. Observations of thermal transfer OSL signals in glacial quartz. *Radiation Measurements*, 32: 595-602.
- Rizk, F.F., 1991. The Late Holocene development of St. Joseph Spit, Florida State University, Tallahassee.
- Stapor, F.W., 1973. Coastal sand budgets and Holocene beach ridge plain development - Northwest Florida, Florida State University, Tallahassee, 221 pp.
- Stapor, F.W., 1975. Holocene beach ridge plain development, Northwest Florida. *Zeitschrift für Geomorphologie*, 22: 116-144.
- Stokes, S., 1992. Optical dating of young (modern) sediments using quartz: results from a selection of depositional environments. *Quaternary Science Reviews*, 11: 153-159.
- Tanner, W.F., 1987. The Beach: Where is the "River of Sand"? *Journal of Coastal Research*, 3(3): 377-386.
- Tanner, W.F., Dermipolat, S., Stapor, F.W. and Alvarez, L., 1989. The Gulf of Mexico Late Holocene sea level curve. *Transactions Gulf Coast Association of Geological Societies*, 39(553-562).
- Thompson, J., Rink, W.J. and López, G.I., 2007. Optically-Stimulated Luminescence age of the Old Cedar Midden, St. Joseph Peninsula State Park, Florida. *Quaternary Geochronology*, 2: 350-355.
- USGS, 1982. Indian Pass, Florida 29085-F2-TB-024 7.5 minute series Orthophotomap, Florida.

- USGS, 1999. Digital Orthographic Quarter-Quads Q4642 and Q4641; Indian Pass - West Pass, Florida; 1 m resolution; UTM projection, NAD 83; 8 quarter-quads. FDEP.
- USGS, 2004. Northwest Florida Water Management District (NFWFMD) ADS40 Digital Imagery Acquisition and Natural Color and Color Infrared Orthophoto Production (remote-sensing images). FDEP.
- White, N.M., 2005. Archaeological Survey of the St. Joseph Bay State Buffer Preserve, Gulf County, Florida, Apalachicola National Estuarine Research Reserve and Division of Historical Resources, East Point and Tallahassee.
- White, N.M., Rodriguez, N.D., Smith, C. and Fitts, M.B., 2002. St. Joseph Bay Shell Middens Test Excavations, Gulf County, Florida, 2000-2002: Richardson Hammock site, 8Gu10, and Lighthouse Bayou site, 8Gu114, Division of Historical Resources, Tallahassee.

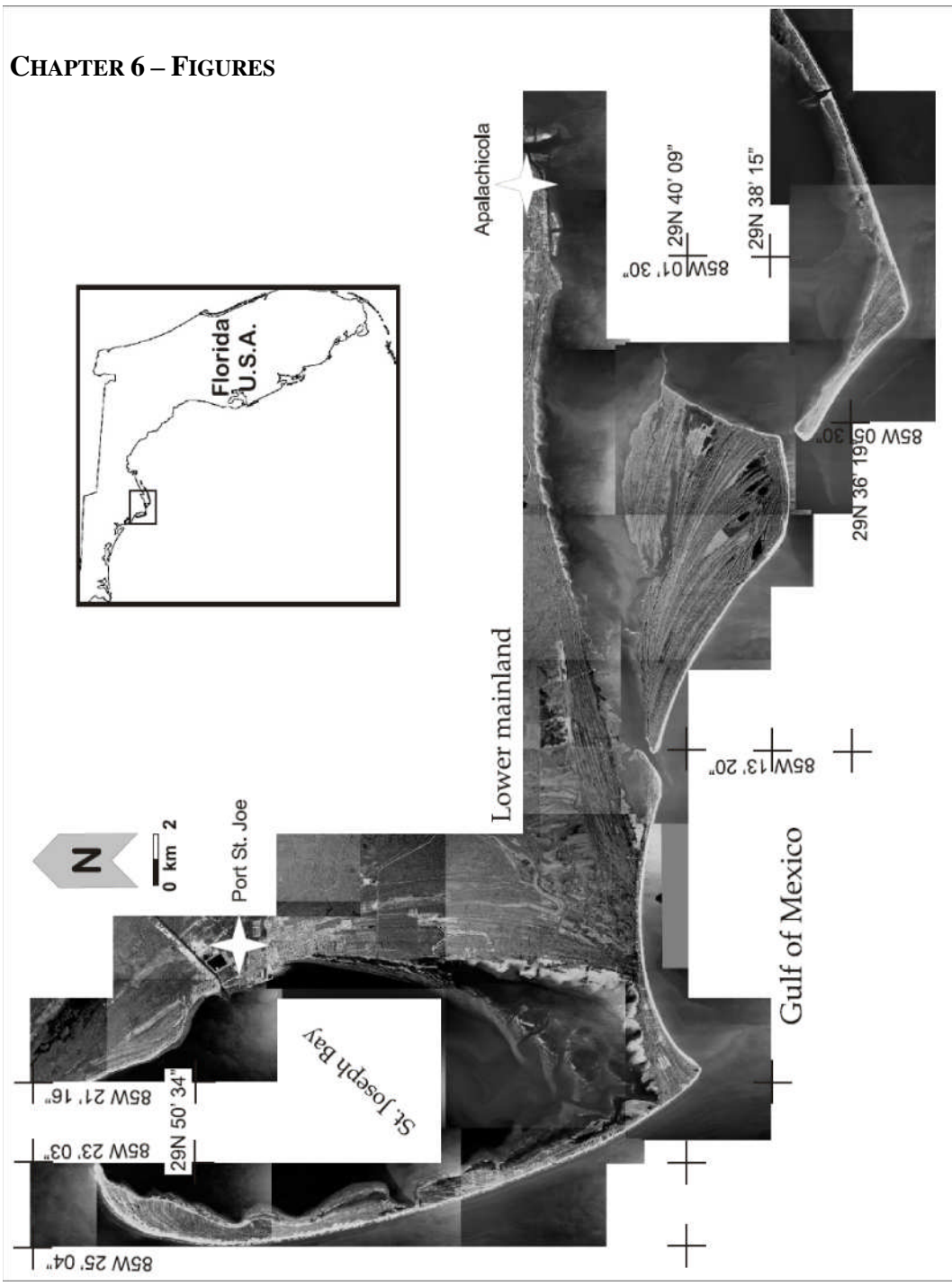


Figure 6.1. General location of St. Joseph Peninsula within the Apalachicola Barrier Island Complex, north-eastern Gulf of Mexico, U.S.A.

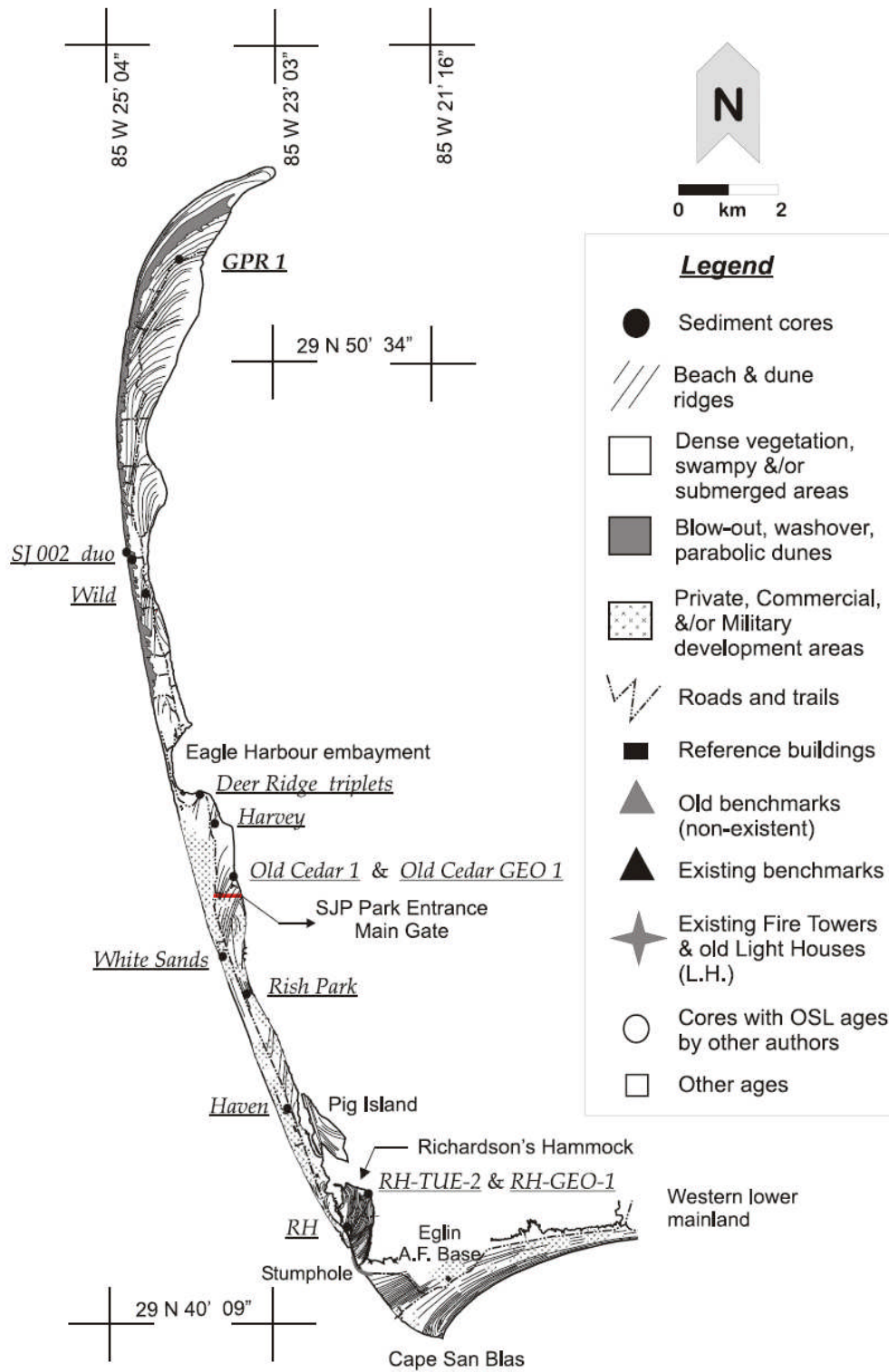
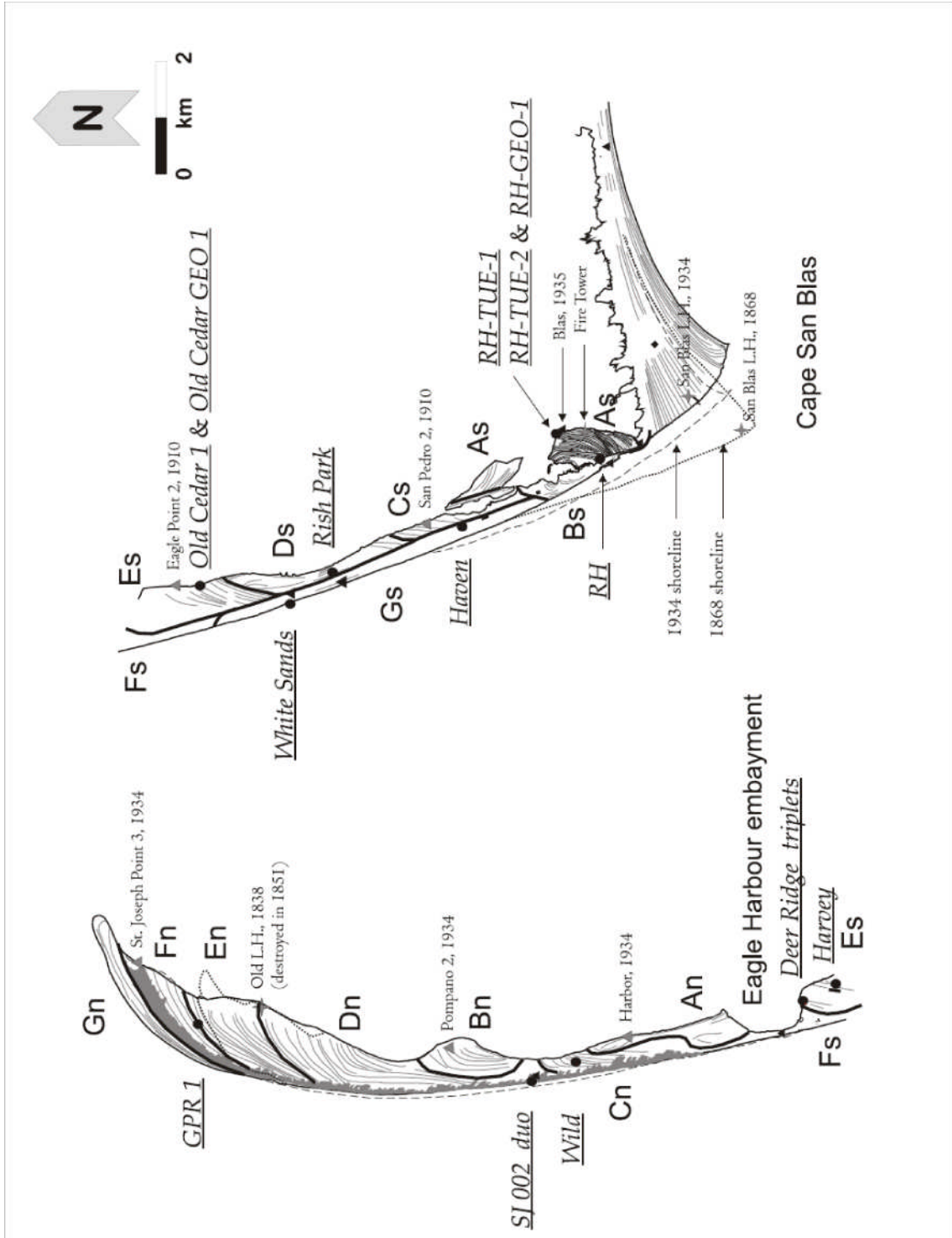


Figure 6.2.

Geomorphological map of St. Joseph Peninsula depicting all the core locations selected for this study. The legend applies to the remainder figures involving the peninsula. Shoreline traced at MHWL from DOQQ images from USGS (2004) as well as ridges. Details are based on topographic/bathymetric map USGS (1982) and DOQQ images from USGS (1999, 2004). Geographical coordinates are NAD 83. Even though Cape San Blas is known to have started forming at least some 630 years ago (López, 2007), it is shown here, and maintained throughout the remainder figures, as a reference area to depict shoreline changes affecting southern St. Joseph Peninsula.

Figure 6.3.

St. Joseph Peninsula ridge sets and previous historical shorelines. Ridge set delineations are based on detail analyses of ridge morphologies and truncations based USGS DOQQ images, nautical and topographic maps. Location of old topographical survey points (i.e. benchmarks) and previously existing light houses as well as remaining ones is marked for general reference.



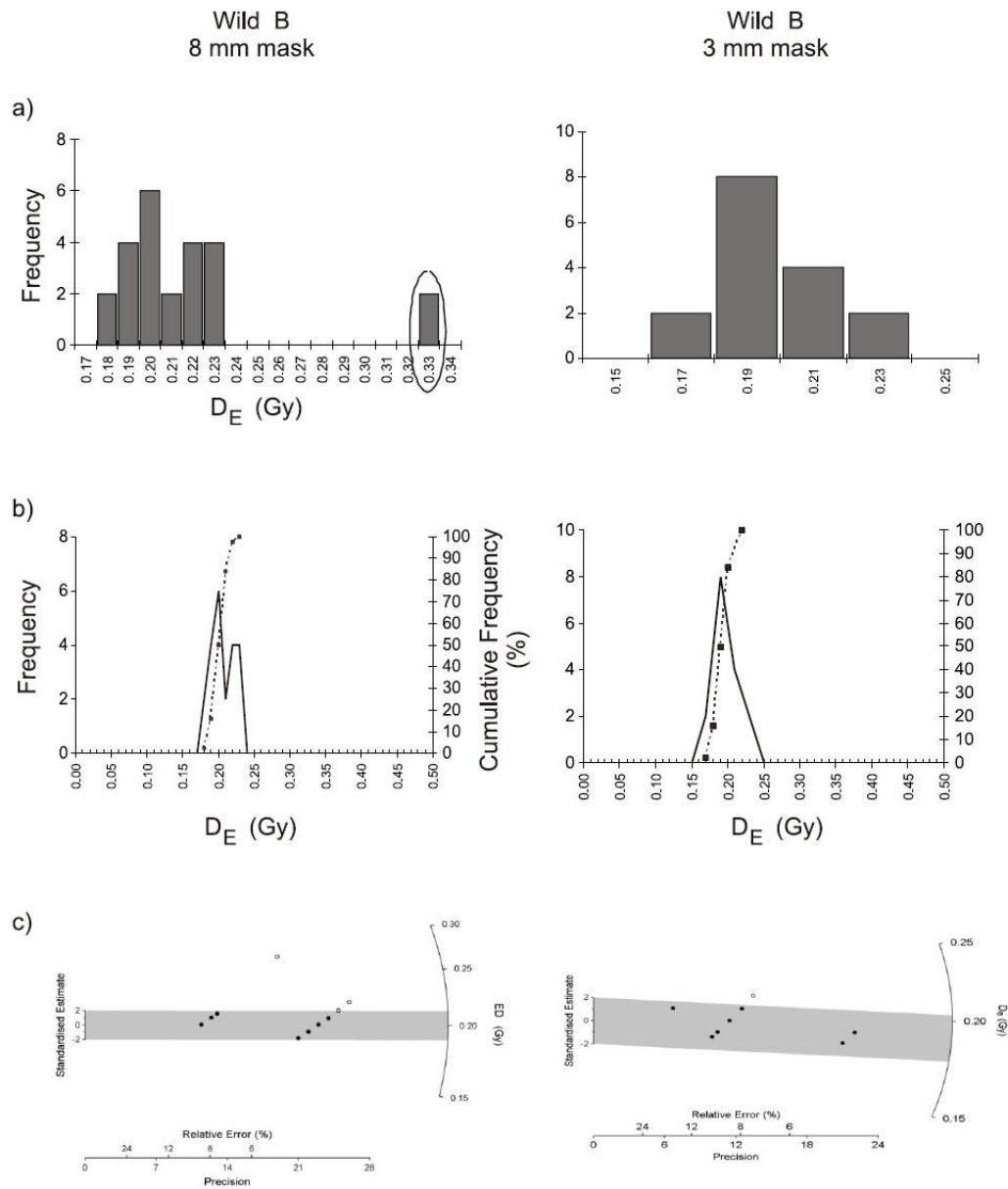


Figure 6.4.

Example of D_E frequency histograms for both large and small sized aliquots. Associated cumulative frequency (%) curves and radial plots were also analyzed to determine the symmetry of the distribution to further constraint the error associated to each calculated OSL age.

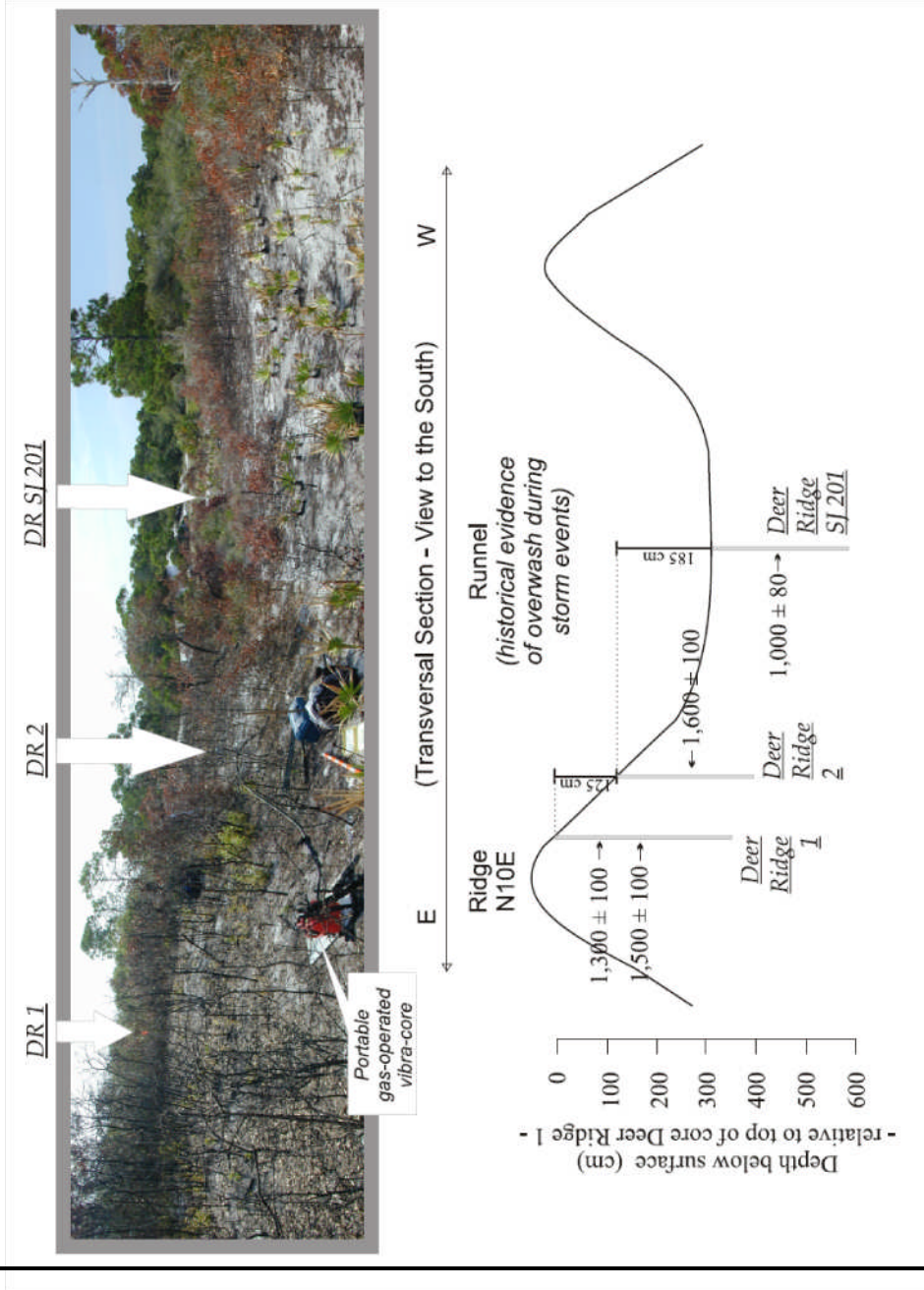


Figure 6.5.

Transversal section and associated photo-mosaic of the Deer Ridge area where cores Deer Ridge 1, Deer Ridge 2 and Deer Ridge SJ201 were taken. Note the positioning of each core and their OSL age relation. In the photo-mosaic, the gas-operated vibra-core is depicted for scale. Arrows point to the exact locations of the cores within this ridge-runnel system. All photographs by G.I. López (2003).

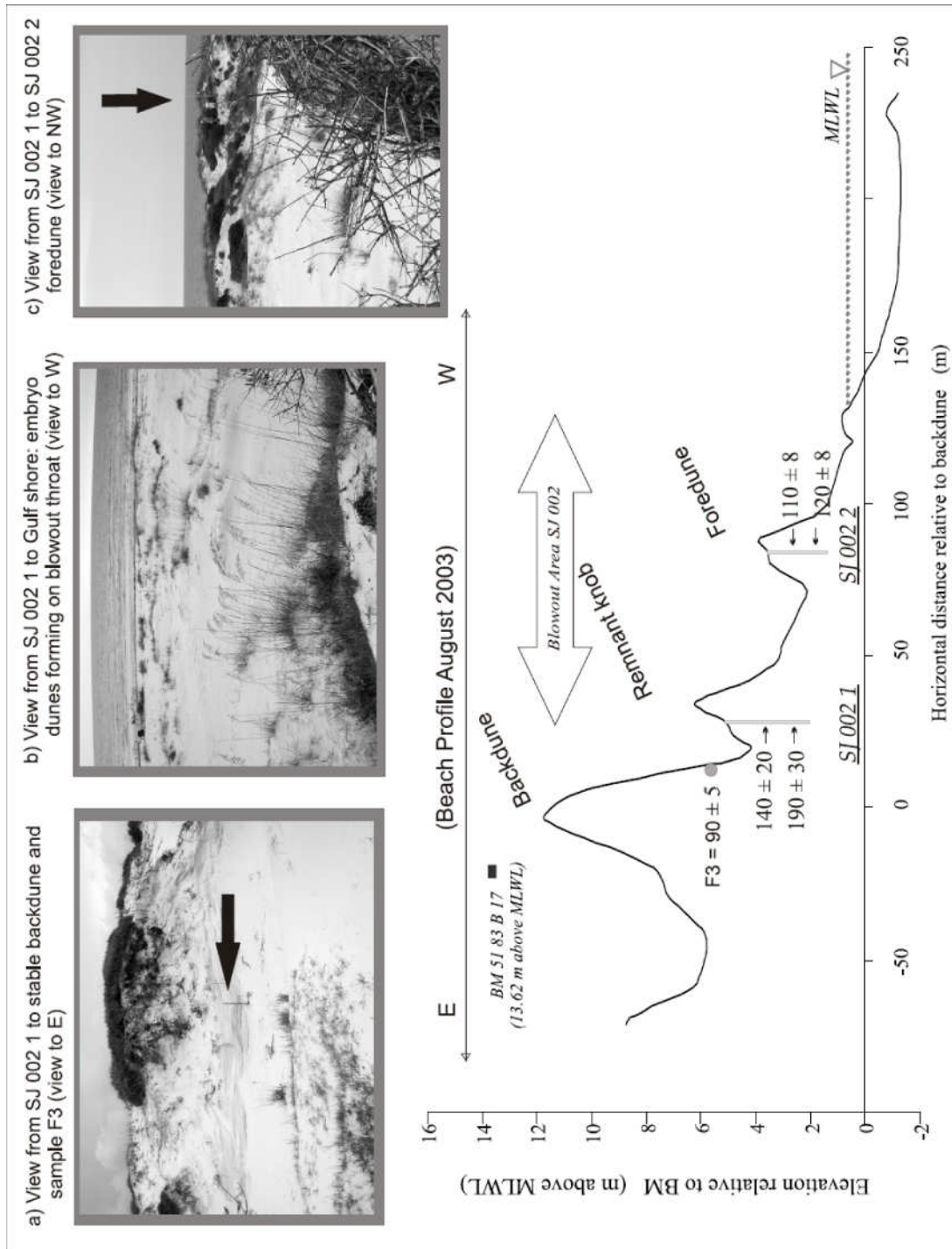


Figure 6.6.

Transversal section and associated photographs of the SJ002 area where cores SJ002 1 and SJ002 2 were taken. The exact location of Forrest's sample F3 (taken in 2001) is also shown. The area is considered a blow-out with a wide throat ending at the mature stable backdune, currently eroding. The arrows on the photographs point to the exact locations of the cores and F3 sample. The transversal section is an actual beach profile surveyed in August 2003. All photographs by G.I. López (2003).

Calculated ASAR based on OSL ages

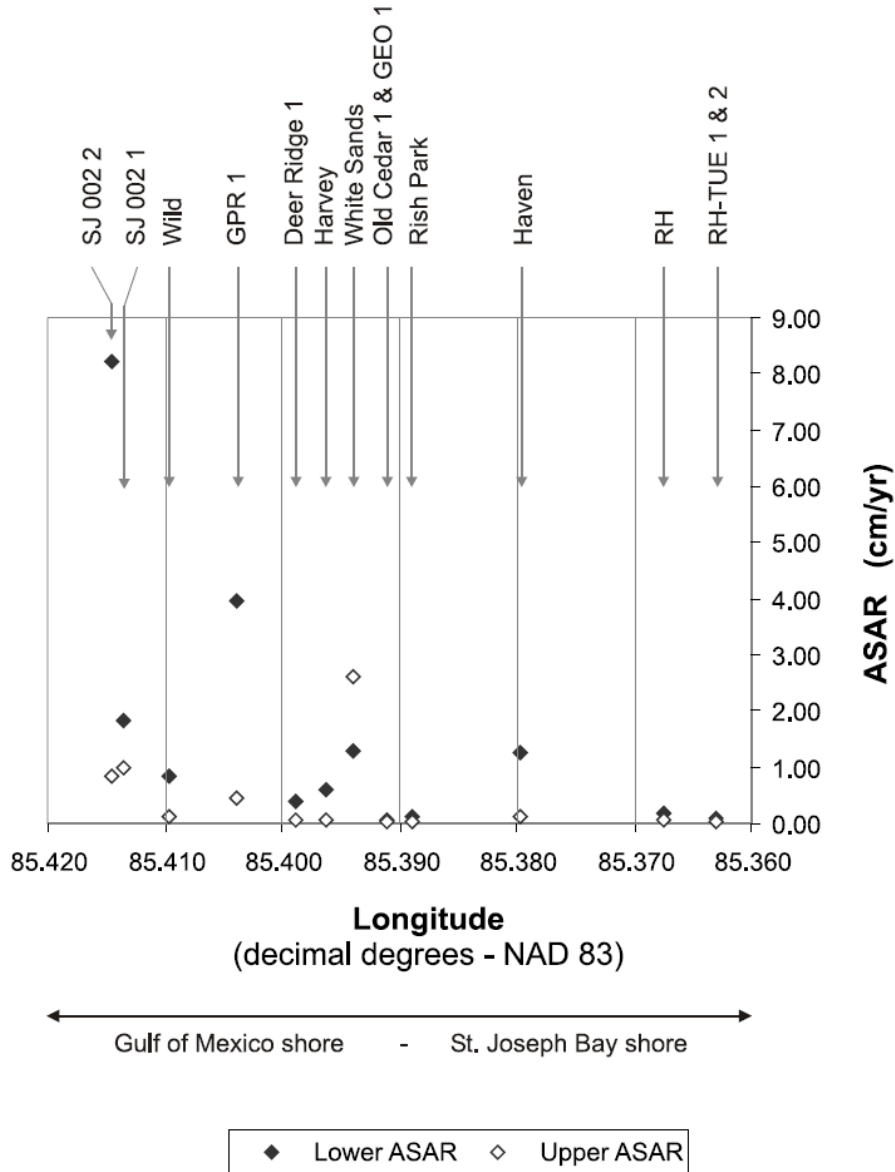


Figure 6.7.

Average sediment accumulation rate (ASAR) plot of all cores corresponding to Table 6.4. ASAR is slowest for the initial four nuclei if compared to the rates of the modern frontal coastal systems.

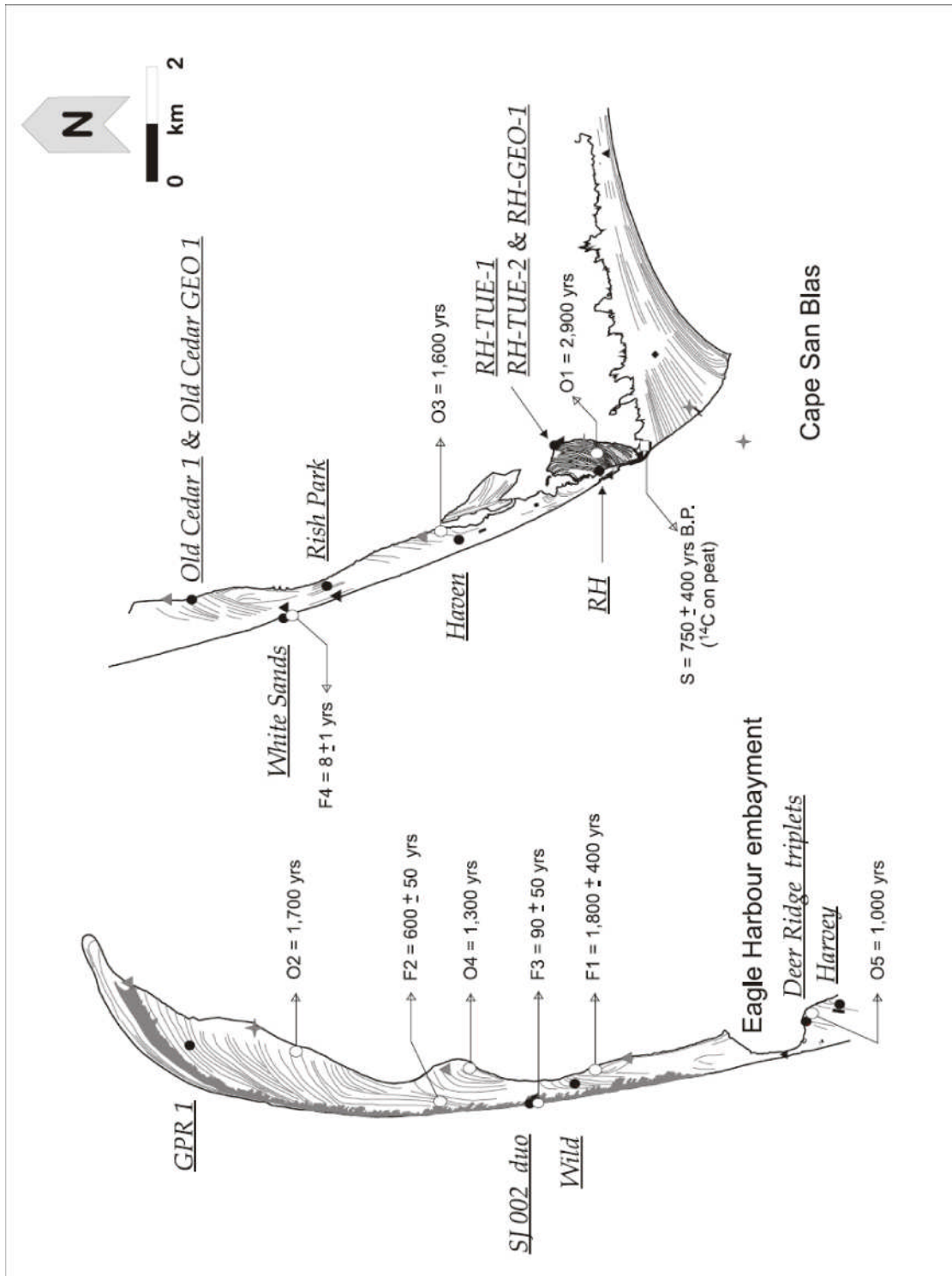
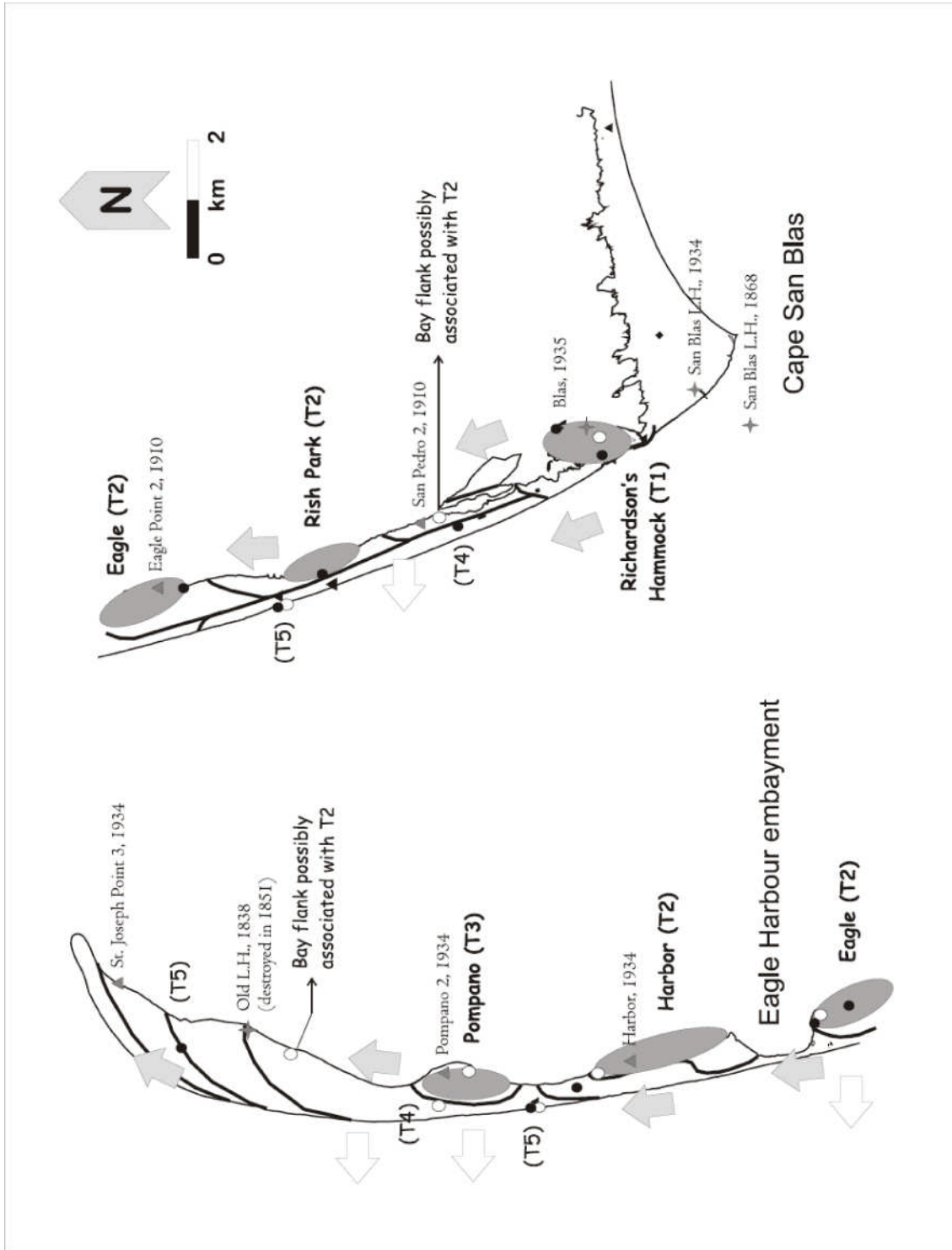


Figure 6.8.

Previous chronologies reported for St. Joseph Peninsula. Samples O1 to O5 correspond to the TL ages obtained by Otvos (2005a). Locations for these samples are based solely on the locations depicted in his Figure 18 (Otvos, 2005a). Samples F1 to F4 correspond to the OSL ages obtained by Forrest (2003) between 2001 and 2003. Locations for these samples were obtained from precise geographical coordinates. Sample S1 corresponds to the only ^{14}C date available for the peninsula (Stapor, 1975, on peat layer). Sediment cores recovered for this study are shown by black-filled circles for reference.

Figure 6.9.

Proposed multiple-nuclei positioning and evolution for St. Joseph Peninsula based on this study. Grey ellipses depict the estimated five nuclei positions (note that the Eagle nucleus is repeated for practical purposes). Grey arrows indicate most probable direction of growth to the north (i.e. accretion/progradation direction due to longshore drift), whereas white ones indicate growth direction to the west (i.e. as per onshore-offshore aggradation). Time intervals (T1, T2, etc.) are pointed for each nucleus and estimated for some of the beach ridge sets as per Table 6.5. and Figure 6.3., respectively. Other symbols are explained in Figure 6.2.



CHAPTER 6 – TABLES

Table 6.1.
Location of cores taken on St. Joseph Peninsula (NW Florida, U.S.A.) and details regarding samples OSL-dated.

Core	Latitude N [a]	Longitude W [a]	Environment [b]	Associated Ridge Set [c]	Total Length of Sediment Core (cm) [d]	Sample [e]	Original Core Sample [f]	Laboratory Number [g]	Burial Depth of Sample (cm) [h]
RH-TUE-1	29° 41' 25.66"	85° 21' 46.82"	shell midden (archaeological site, Florida Master Site File 8Gu10)	As (sub-set rh-3*)	[i]	[i]	[i]	GL04075-076-080	30.00
RH-TUE-2	29° 41' 25.66"	85° 21' 46.82"	hardwood hammock	As (sub-set rh-3*)	[i]	[i]	[i]	GL04075-076-082	190.00
RH-GEO-1	29° 41' 26.70"	85° 21' 46.80"	hardwood hammock	As (sub-set rh-3*)	[i]	[i]	[i]	GL04077-083	230.00
RH	29° 41' 03.95"	85° 22' 03.12"	slash pine flatwoods	As (sub-set rh-4*)	377.96	B	OSL 1	GL04062-148	170.08
						A	OSL 2	GL04062-148	317.83
Haven	29° 42' 21.90"	85° 22' 47.22"	slash pine flatwoods	Gs	305.77	B	OSL 1	GL04123	108.93
						A	OSL 2	GL04120	248.97
Rish Park	29° 43' 39.06"	85° 23' 19.86"	scrub oak	Ds	243.84	B	OSL 2	GL04060-061	63.26
						A	OSL 1	GL04060-061	143.77
White Sands	29° 44' 03.36"	85° 23' 38.40"	sea oat + coastal low scrub oak	Gs	257.61	B	OSL 7	GL04144-152	62.38
						A	OSL 1	GL04141	249.50
Old Cedar 1	29° 44' 55.36"	85° 23' 27.87"	shell midden (archaeological site, Florida Master Site File 8Gu85)	Es	[i]	[i]	[i]	JT05005	25.00
Old Cedar GEO 1	29° 44' 55.36"	85° 23' 27.87"	scrub oak	Es	[i]	[i]	[i]	JT05006	70.00
Harvey	29° 42' 28.39"	85° 23' 46.44"	scrub oak	Es	344.73	B	OSL 1	GL04144-152	89.54
						A	OSL 2	GL04144-152	329.51
Deer Ridge S1201	29° 45' 48.18"	85° 23' 55.56"	slash pine flatwoods	Es	125.00	A	OSL 1	GL04013-014	135.14
Deer Ridge 1	29° 45' 48.90"	85° 23' 55.68"	scrub oak	Es	225.30	B	OSL 1	GL04121-122	90.57
						A	OSL 2	GL04121-122	169.82
Deer Ridge 2	29° 45' 48.96"	85° 23' 55.80"	scrub oak	Es	182.30	A	OSL 1	GL04121-122	151.92
Wild	29° 47' 55.96"	85° 24' 34.96"	scrub oak	Ch	300.50	B	OSL 1	GL04130	86.71
						A	OSL 2	GL04130	290.78
S1002 1	29° 48' 23.92"	85° 24' 48.50"	coastal low scrub oak	Dn	269.80	B	OSL 2	GL04107-108	139.99
						A	OSL 1	GL04107-108	230.91
S1002 2	29° 48' 24.90"	85° 24' 52.08"	sea oat + coastal low scrub oak	Dn	159.30	B	OSL 2	GL04093-101	91.67
						A	OSL 1	GL04092	173.88
GPR 1	29° 51' 39.29"	85° 24' 14.19"	scrubby flatwoods	En-Fn	240.80	B	OSL 2	GL04107-108	99.05
						A	OSL 1	GL04107-108	217.94

[Notes for Table 6.1.]

- [a] GPS Geographic Coordinates (NAD 83).
 - [b] Names refer to both shore and coastal inland plant communities as characterized in Myers and Ewel (1990) with the exception of the archaeological sites.
 - [c] Revised after analysis of 1999 and 2004 DOQQ's for the area (USGS, 1999, 2004), topographic map of the area (USGS, 1982), and Rizk's ridge sets (Rizk, 1991).
 - [d] Depth values have been corrected for compaction.
 - [e] Names assigned to samples to standardize, among all cores, the general location of each sample within each core.
A = sample taken towards the bottom of the core; B = sample taken towards the top of the core. Both are at least 1 m apart.
 - [f] Original name given while sampling one split half of core for OSL-dating.
 - [g] All AGE Laboratory. File names of final D_E measurement on 18 to 48 aliquots of each sample.
 - [h] Actual burial depth of center of the sample, considering compaction during coring.
 - [i] Horizontal sediment cores (~ 20 cm-long): sample for OSL-dating came from the central region of each core.
- * Richardson's Hammock has four ridge set patterns, all described in López and Rink (under review); here they are treated as one in terms of general evolution of St. Joseph Peninsula.

Table 6.2.

SAR - OSL Equivalent Dose data for quartz sand samples taken from St. Joseph Peninsula, Florida, U.S.A.

Core [a]	Sample [b]	Aliquot Size (mm)	n [c]	ED Value (Gy)	ED Error (Gy)	Skewness
Haven	B	8	22	0.22	0.00	-0.61
		3	20	0.21	0.01	0.48
	A	8	24	0.24	0.01	0.48
		3	18	0.21	0.01	0.62
Rish Park	B	8	23	0.52	0.02	0.68
		3	12	0.47	0.01	0.03
	A	8	22	0.57	0.04	0.75
		3	11	0.51	0.04	1.06
White Sands	B	8	22	0.03	0.00	0.00
		3	16	0.04	0.02	1.47
	A	8	17	0.07	0.00	-0.15
		3	17	0.08	0.03	1.11
Harvey	B	8	16	0.39	0.04	1.45
		3	11	0.37	0.07	1.08
	A	8	18	0.51	0.01	0.49
		3	17	0.47	0.01	0.48
Deer Ridge SJ201	A	8	46	0.25	0.00	-0.36
		3	n/a	n/a	n/a	n/a
Deer Ridge 1	B	8	22	0.38	0.02	0.87
		3	22	0.34	0.01	0.52
	A	8	20	0.42	0.01	-0.11
		3	14	0.38	0.02	-0.39
Deer Ridge 2	A	8	22	0.39	0.01	0.57
		3	14	0.35	0.01	0.34
Wild	B	8	22	0.20	0.01	0.09
		3	16	0.19	0.01	0.64
	A	8	23	0.25	0.00	0.33
		3	18	0.23	0.03	0.79
SJ002 1	B	5	22	0.04	0.01	-1.40
		1	19	0.03	0.02	1.00
	A	5	22	0.05	0.01	1.22
		1	16	0.09	0.02	-0.72
SJ002 2	B	8	22	0.03	0.00	0.21
		3	19	0.04	0.00	0.01
	A	8	23	0.03	0.00	0.18
		3	19	0.03	0.00	-0.07

GPR 1	B	5	20	0.06	0.01	-0.90
		1	15	0.07	0.00	0.43
	A	5	22	0.06	0.00	-0.50
		1	15	0.05	0.00	0.43

[a] A = sample taken towards the bottom of the core; B = sample taken towards the top of the core.
Both are at least 1 m apart.

[b] Depth values have been corrected for compaction.

[c] Number of aliquots accepted for calculation of the equivalent dose after all criteria was met (e.g. within recycling ratio; excluding 2σ outliers).

^ Values rounded off to sensible number of precision.

Note: Each age's error corresponds to either $\pm 1\sigma$ or ± 1 standard error of the final mean D_E , depending on each sample's distribution.

Table 6.3.
SAR - OSL ages and data for quartz sand samples taken from St. Joseph Peninsula, Florida, U.S.A.

Core	Sample [a]	ED Value (Gy) [b]	Analytical Error (Gy) [b]	238-U (ppm) [c]	232-Th (ppm) [c]	K (ppm) [c]	Water Content (%) [d]	Cosmic Dose Rate ($\mu\text{Gy/a}$) [e]	Annual Dose ($\mu\text{Gy/a}$) [f]	SAR-OSL age (a) [g]	SAR-OSL error (a) [g]	Datum [g]
RH-TUE-1	-	0.47	0.02	0.22 ± 0.1	0.64 ± 0.08	49 ± 11	7	219	325 ± 17	1,400	100	2005
RH-TUE-2	-	0.84	0.04	0.12 ± 0.1	0.45 ± 0.05	46 ± 7	3	184	258 ± 17	3,300	300	2005
RH-GEO-1	-	1.41	0.12	0.59 ± 0.1	2.73 ± 0.18	53 ± 9	3	179	518 ± 19	2,700	400	2005
RH	B	0.66	0.03	0.27 ± 0.1	0.37 ± 0.05	34 ± 10	6	187	286 ± 16	2,300	200	2005
	A	0.85	0.05	0.29 ± 0.1	0.49 ± 0.05	38 ± 9	14	169	274 ± 15	3,100	300	2005
Haven	B	0.22	0.00	0.10 ± 0.1	0.39 ± 0.05	58 ± 9	5	197	262 ± 17	840	60	2006
	A	0.24	0.01	0.14 ± 0.1	0.41 ± 0.06	44 ± 9	3	177	252 ± 17	950	80	2006
Rish Park	B	0.52	0.02	0.21 ± 0.1	0.72 ± 0.07	24 ± 12	3	216	327 ± 17	1,600	100	2005
	A	0.57	0.04	0.15 ± 0.1	0.25 ± 0.05	20 ± 10	5	191	254 ± 17	2,200	200	2005
White Sands	B	0.03	0.00	2.08 ± 0.1	7.88 ± 0.51	16 ± 10	3	218	1247 ± 31	24	1	2006
	A	0.07	0.00	0.60 ± 0.1	1.34 ± 0.11	49 ± 11	8	177	412 ± 17	170	10	2006
Old Cedar 1	-	0.38	0.03	0.36 ± 0.1	2.81 ± 0.18	139 ± 40	3	215	407 ± 9	940	100	2005
Old Cedar GEO 1	-	0.47	0.03	0.16 ± 0.1	0.29 ± 0.05	112 ± 30	1	209	264 ± 5	1,800	130	2005
	B	0.39	0.04	0.22 ± 0.1	0.50 ± 0.06	60 ± 11	18	203	293 ± 15	1,300	200	2006
Harvey	A	0.51	0.01	0.29 ± 0.1	0.71 ± 0.07	46 ± 11	3	168	297 ± 17	1,700	100	2006
	A	0.25	0.00	0.10 ± 0.1	0.20 ± 0.00	62 ± 6	19	192	239 ± 15	1,000	80	2004
Deer Ridge SJ201	B	0.38	0.02	0.16 ± 0.1	0.51 ± 0.06	71 ± 9	4	202	290 ± 17	1,300	100	2006
	A	0.42	0.01	0.21 ± 0.1	0.38 ± 0.06	44 ± 9	3	187	276 ± 17	1,500	100	2006
Deer Ridge 2	A	0.39	0.01	0.10 ± 0.1	0.25 ± 0.05	60 ± 7	7	189	244 ± 16	1,600	100	2006
	B	0.20	0.01	0.21 ± 0.1	0.34 ± 0.06	51 ± 9	3	204	291 ± 17	690	60	2006
Wild	A	0.25	0.00	0.25 ± 0.1	0.35 ± 0.06	49 ± 10	3	172	269 ± 17	930	70	2006
	B	0.04	0.01	0.26 ± 0.1	0.39 ± 0.04	58 ± 6	3	191	295 ± 17	140	20	2006
SJ002 1	A	0.05	0.01	0.17 ± 0.1	0.38 ± 0.04	30 ± 5	4	179	257 ± 17	190	30	2006
	B	0.03	0.00	0.15 ± 0.1	0.24 ± 0.03	47 ± 4	4	202	268 ± 17	110	8	2006
SJ002 2	A	0.03	0.00	0.17 ± 0.1	0.30 ± 0.03	43 ± 5	5	186	260 ± 17	120	8	2006
	B	0.06	0.01	0.17 ± 0.1	0.29 ± 0.03	44 ± 5	5	199	272 ± 16	220	40	2006
GPR 1	A	0.06	0.00	0.15 ± 0.1	0.16 ± 0.03	52 ± 5	13	181	238 ± 15	250	20	2006

[Notes for Table 6.3.]

- [a] A = sample taken towards the bottom of the core; B = sample taken towards the top of the core. Both are at least 1 m apart.
- [b] Equivalent doses and errors from large aliquots: all 8 mm mask except for samples from cores GPR1 and SJ002 1 which were 5 mm masks.
- [c] U, Th and K values determined by NAA at Nuclear Reactor facility, McMaster University.
- [d] Water content as a fraction of dry weight determined from laboratory measurements.
- [e] Cosmic-ray dose rate value calculated using an overburden density of 2 g/cm³ and accounting for ridge geometry.
- [f] All β and γ dose rates were calculated based on U, Th and K concentrations of each sample accounting for moisture values of the sample.
- [g] Datum values (i.e. measurement year) for SAR-OSL ages are given in column.
- * Ages were calculated assuming constant sediment accumulation rates (i.e. linear sediment accumulation), with the exception of the two shell midden sites (Old Cedar 1 and RH-TUE-1) which ages were calculated assuming instant sedimentation (i.e. using half of the burial depth value to calculate the cosmic-ray dose rate).
- ^ Values rounded off to sensible number of precision.

Table 6.4.

Average sediment accumulation rates (ASAR) between OSL samples at different depth intervals within individual core or sites.

Core [a]	Sample [b]	Burial Depth of Sample (cm)	SAR-OSL age (a)	SAR-OSL error (a)	Lower ASAR (cm/a) [c]	Upper ASAR (cm/a) [d]	Longitude [e]
RH-TUE-1	*	30.00	1,400	100	0.08	0.02	85.36301
RH-TUE-2	*	190.00	3,300	300			
RH	B	170.08	2,300	200	0.18	0.07	85.36753
	A	317.83	3,100	300			
Haven	B	108.93	840	60	1.27	0.13	85.37978
	A	248.97	950	80			
Rish Park	B	63.26	1,600	100	0.13	0.04	85.38885
	A	143.77	2,200	200			
White Sands	B	62.38	24	1	1.28	2.60	85.39400
	A	249.50	170	10			
Old Cedar 1	**	25.00	940	100	0.05	0.03	85.39107
Old Cedar GEO 1	**	70.00	1,800	130			
Harvey	B	89.54	1,300	200	0.60	0.07	85.39623
	A	329.51	1,700	100			
Deer Ridge 1	B	90.57	1,300	100	0.40	0.07	85.39880
	A	169.82	1,500	100			
Wild	B	86.71	690	60	0.85	0.13	85.40971
	A	290.78	930	70			
SJ002 1	B	139.99	140	20	1.82	1.00	85.41347
	A	230.91	190	30			
SJ002 2	B	91.67	110	8	8.22	0.83	85.41447
	A	173.88	120	8			
GPR 1	B	99.05	220	40	3.96	0.45	85.40394
	A	217.94	250	20			

All cores have been corrected for compaction which was assumed linear throughout each core.

[a] Only cores with two samples at different intervals or sites with two consecutive samples.

[b] A corresponds to sample taken towards the bottom of the core and B to the one taken towards the top of the core.

[c] Values corresponding to the lower part of the core: calculations for depth interval between samples A and B.

[d] Values corresponding to the upper part of the core: calculations for depth interval between sample B and the ground surface.

[e] Geographical Coordinates in decimal degrees (NAD 83).

* RH-TUE-1 overlies RH-TUE-2, within the same excavated trench and ridge.

** Old Cedar 1 overlies Old Cedar GEO 1, within the same exposed bay-shore ridge.

Table 6.5.

Proposed time intervals for the formation and evolution of St. Joseph Peninsula.

Time Interval [a]	Age Range (a) [b]	Associated Nucleus	Associated Ridge Set	Comment
T1	3,600 - 2,400	Richardson's Hammock	As	The earliest "island" nucleus in the region is formed during this time. The western edge of this nucleus (i.e. cores RH-TUE-2 and RH-GEO-1) formed before the eastern portion (i.e. core RH).
T2	2,400 - 1,400	Rish Park / Eagle / Harbor	Ds / Es / An	Formation of at least three other separate nuclei from pre-existing shallows, north of Richardson's Hammock. The highest average sediment accumulation rates are seen between prior than and during T2.
T3	1,400 - 1,000	Pompano	Bn	This fifth nucleus, north of Harbor, is based on Otvos (2005a) age, the morphology of the bay-shore protrusion and the orientation of the ridges which depicts an enclosed system (i.e. nucleus).
T4	1,000 - 700	n/a	Gs; Cn	Continuous ridge development northward and westward around and from nuclei formed in time T2. It is hypothesized that continuous vertical aggradation and lateral progradation occurred even after the full development of the first four nuclei.
T5	700 - 300	n/a	Fs, Gs; Cn to Fn	Further continuous ridge development northward and westward occurred along SJP. It is hypothesized that continuous vertical aggradation and lateral progradation occurred even after the full development of the first four nuclei.
T6	≤ 300	n/a	Gs; Gn	SJP northern terminus continuous aggradation and formation of presently mature foredunes and backdunes along SJP.
T7	≤ 10	n/a	Fs, Gs; Gn	All actively forming shoreline environments on the Gulf side of SJP, which may or may not be eroding previous ridge set components (e.g. embryo dunes, incipient foredunes, hurricane deposits, blowouts, berms).

[a] This same time interval is proposed for the overall supra-tidal evolution of the Apalachicola Complex Barrier Islands (López, 2007).

[b] Our SAR-OSL ages are *terminus ante quem* for the time of formation of the ridges sampled.

CHAPTER 7

EVOLUTION AND OPTICAL LUMINESCENCE DATING OF A PLEISTOCENE AND HOLOCENE COASTAL BARRIER COMPLEX, NE GULF COAST, FLORIDA, U.S.A.

Gloria I. López *

W. Jack Rink

Archaeometry & Geochronology (AGE) Laboratory
School of Geography and Earth Sciences, McMaster University.
1280 Main Street West, Hamilton, Ontario, Canada, L8S 1M5
Phone: 1-905-525 91 40 extension 27686/24180
Fax: 1-905-546 04 63

* Corresponding author: lopezgi@mcmaster.ca
 glopez@eafit.edu.co

Prepared for:

Earth-Science Reviews: Elsevier Science, Oxford, ISSN 0012-8252 (Imprint: Elsevier).

Status: ready for submission (July 2007).

ABSTRACT

This paper summarizes the late-Holocene supra-tidal evolution of the central-west barrier islands pertaining to the Apalachicola Complex, situated on the NE Gulf of Mexico, NW Florida (U.S.A.). The evolution is primarily based on optical dating ages obtained by the authors during the past four years of research in the area. They are related to the archaeological, sedimentological, geomorphological and geological history of this region. Constraints with other independent chronologies were attempted, only if well-documented publication of results was in order available. Lateral progradation and vertical accretion rates, as well as a more generalized evolution history of any given clastic-rich coastal system are possible to obtain and constrain only if accurate and precise chronologies are obtained or in existence. We present Optically Stimulated Luminescence (OSL) ages in this study. Due to both the increasing understanding of the protocols and the reliability of this geochronometric technique, we can improve earlier estimates that utilized radiocarbon dating in an environment where organic remains are less conveniently preserved or not existent. Four main barrier systems, as well as a minor one, all within this coastal complex, were studied to obtain a regional horizontal and vertical OSL chronology, including a thin barrier island, a strandplain, a spit, and a cusped foreland, which were also analyzed in terms of geomorphology and sedimentology. Long vertical vibracores were recovered from multiple beach and dune ridges throughout the study area. Holocene OSL ages ranged from 22 ± 4 to $3\,300 \pm 300$ years ago, in addition to two much older Pleistocene ages of $24\,200 \pm 5\,800$ and $154\,200 \pm 10\,400$ years ago from the neighbouring lower mainland strandplain. The latter is considered to be the oldest absolute age ever obtained for relict barrier ridges pertaining to the Gulfport Formation in Florida. A progressive Holocene-time evolution over the past ca. 3 000 years is inferred from coupled OSL and geomorphological analyses.

Keywords: optical dating, quartz, OSL, geochronology, barrier island, beach ridge, coastal evolution, Holocene, Pleistocene, Apalachicola, Florida.

7.1. INTRODUCTION

The rate at which coastal environments evolve (i.e. vertical accretion and lateral progradation) has been determined by optical stimulated luminescence (OSL) dating, but also using constraints from a detailed geomorphological and geological study of their environmental setting. Without absolute dating, these methods are only relative, based on series of comparisons between different dated materials. Radiocarbon dating is the most widely spread geochronometric technique used to date relatively young (< 50 000 years B.P.) sediments

associated with a diversity of depositional environments. However, dating Quaternary sediments which lack delicate and decomposable organic materials has always been a problem. The accuracy of the age determination of any given deposit is intrinsically related to how well the material used for dating portrays the specific time of deposition of the sediment, hence formation of the deposit. We have overcome these problems using OSL.

Different minerals release different luminescence signals of specific wavelengths when stimulated by heat (as in the case of thermoluminescence – TL –) or light (Aitken, 1998; Bøtter-Jensen et al., 2003). In the mid 1980's (Huntley, 1985) pioneered optical dating while looking for a method to determine when sediments were last exposed to sunlight. OSL measures energy (i.e. trapped charge) accumulated over geological time in minerals with light-sensitive defects and structural impurities in their crystal lattice, such as quartz or feldspar. The trapped charge is due to the absorption of naturally occurring ionizing radiation. The luminescence emission (or signal) is a measure of such trapped charges. Combined with radioisotope concentrations of U, Th, and K in the bulk sediment and the calculated cosmic radiation, it can be used to determine the last light exposure, i.e. age of any given siliciclastic deposit. Since optical dating is a measure of the last burial episode, it is particularly interesting for active sedimentary systems. However, it is critical to carefully select the location of OSL samples to avoid distortion of OSL signals: e.g. sedimentologically complex layers/units showing inhomogeneous distributions of heavy minerals; the possibility of total or partial zeroing of some grains due to turbation within the deposit. Even though natural bioturbation, soil formation and internal sediment re-working may affect OSL ages, it is possible to avoid such problematic effects while analyzing the optical signal, hence selectively enabling reliable age estimates (e.g. Bateman et al., 2007a; Bateman et al., 2007b; López and Rink, 2007a).

Over the past 20 years, the increasing development of the accuracy of results has made it a reliable and applicable method to clastic-rich coastal sedimentary environments, with increasingly successful results in a variety of depositional environments (e.g. aeolian, fluvial, lacustrine, etc.). Although the natural zeroing mechanism is the same in all environments (i.e. natural sunlight), the extent (i.e. consistency) of the zeroing is different and dependent on transport/burial processes and/or conditions. Correct optical ages from several lithostratigraphic units from a variety of coastal environments (e.g. coastal linear and parabolic dunes, beach ridges, boulder deposits) of known age, have lent credibility to OSL over the past six years, proving the precision and accuracy of quartz OSL dating (e.g. the early works of Banerjee et al., 2003; Jungner et al., 2001; Murray-Wallace et al., 2002; Sommerville et al., 2003). Moreover, since the development of the single-aliquot regenerative-dose (SAR) protocol (Murray

and Wintle, 2000) the range of ages obtained for clastic coastal environments as well as the reliability of such ages has been rapidly increasing. The first attempt to quantify coastal progradation rates using solely OSL dating was done by Murray-Wallace et al. (2002), demonstrating a relatively rapid but variable beach ridge development and strandplain progradation over the past 6 000 years. In a different study, Banerjee et al. (2003) demonstrated the efficacy of OSL dating in coastal evolution reconstructions when comparing the OSL ages obtained from eight dune ridges with historical maps.

More recently, five neighbouring, poorly dated, coastal barrier systems along the NE Gulf of Mexico (**Figure 7.1.**), with diverse successions of beach and dune ridges, have been targets of investigation since 2002, with results compiled in (López, 2007). Vertical accretion and lateral progradation rates of a pristine strandplain located along the NE waters of the Gulf of Mexico, were determined (López and Rink, 2007a; López and Rink, 2007b), by attempting, for the first time in OSL dating, the usage of long vertical sediment cores recovered from several beach ridges across St. Vincent Island. A better understanding of rates of beach and dune ridge development and barrier island accretion can be obtained from a detailed OSL dating survey. In addition, the development of St. Joseph Peninsula (López and Rink, submitted 2007; Thompson et al., 2007) and an earlier smaller barrier island called Richardson's Hammock (López et al., under review 2007) have provided a regional context to the results summarized here. However, in this paper, we integrate the major geochronological findings related to all the studied barrier islands and present new OSL data for the remaining two barrier systems (Little St. George Island – also known as Cape St. George – and Cape San Blas) as well as a much older contiguous mainland relict ridge, west of the modern Apalachicola river, delta, and estuary. We examine their late Holocene chronological history as a group, in terms of coastal surficial development by means of OSL, and review previously proposed evolutions for these central-west barrier systems pertaining to the Apalachicola Barrier Island Complex.

Our view in this regional study is that a key to understanding coastal progradation in relatively passive tectonic environments (such as the NE region of the Gulf of Mexico) is to investigate all growing dimensions (i.e. vertical, lateral) as a function of sediment volume and base level availability. Thus thickness and geometry of a coastal environment would be defined as a function of a) sediment supply/volume; b) existing bathymetric surface; c) coastal hydrodynamics (i.e. longshore drift, wave energy, wave base, wave refraction/reflection); and d) water depth (i.e. relative sea level position). The final geometrical arrangement of a deposit within the coastal wedge would be defined by its efficiency to manage erosive or transport processes such as wave action, littoral and tidal currents and most of all, relative sea level fluctuations.

7.1.1. PREVIOUS STUDIES

The generally fine- to medium-sized sands composing the Apalachicola Complex barrier islands are mainly comprised of quartz (> 90 %) and heavy minerals (5 – 10 %), small quantities of feldspar (< 5 %) and little or no organic matter. Scattered marine shells (complete and/or fragmented) are only found on the berm, foredunes and incipient dunes that constitute the < 200 year-old frontal coastal systems along the beachface and backshore areas of modern shoreline environments. Older shells, primarily gastropods and some pelecypods, are only found in and around quite surficial shell middens and archaeological sites located on the more protected bay- and marshy-shores of some Apalachicola barrier islands (e.g. St. Vincent Island, Little St. George Island, Richardson's Hammock and St. Joseph Peninsula) (as also evidenced by Stapor (1975) and White (2003)).

Debate regarding the source of the barrier-forming minerals goes back as early as 1845 (Kwon, 1969). For such reason, several studies related to the surface bottom sediments and sub-bottom stratigraphy of the inner shelf around the Apalachicola Complex have been undertaken (Donoghue, 1992; Donoghue, 1993; Donoghue and Tanner, 1992; Schnable and Goodell, 1968; Stewart and Gorsline, 1962; Tanner, 1961). The latter represent some of the earliest works in the area, besides the characterization of coastal energy levels (Gorsline, 1966). This region of the Florida Panhandle, fringed by clastic barrier islands and beaches, contains one of the four major sandy coastlines of Florida, but is actually the only one where quartz is the dominant (> 80 %) sandy mineral. This quartz is igneous and volcanic in origin, ultimately derived from the Appalachian Mountain Range by way of one of Florida's and Georgia's major drainage systems (~ 800 km-long), the Apalachicola River.

During Late Quaternary lowstands, poly-mineral sands from the Apalachicola River are believed to have been deposited on the inner shelf of the NE Gulf of Mexico (Donoghue and Greenfield, 1991). The same regime is inferred to exist throughout the Quaternary, being the river the main contributor of clastic sediment to this part of the Gulf (Donoghue, 1993; Kwon, 1969). The barrier islands are believed to have been formed by continuous deposition of sediments out-flowing the Apalachicola River in favourable low to moderate energy littoral conditions (Gorsline, 1966; Tanner, 1995). However, sedimentological and mineralogical studies (Hsu, 1960; Kwon, 1969; Schnable and Goodell, 1968) have shown that the actual mineral composition of the barrier islands is similar to that of the lower mainland (i.e. Apalachicola Pleistocene ridges) rather than the modern material presently flowing out of the river. In fact, during the Pleistocene the river emptied directly onto the Gulf, forming a classic large cusped delta (Schnable and Goodell, 1968), of unknown marginal

extension, as the palaeo-delta grew atop a pre-Pleistocene open-space offshore platform, during at least 80 000 to ~ 6 000 years ago.

Following the last major sea level rise (~ 5 000 years ago), re-working of submerged deltaic features and sediment sorting by littoral processes constituted the main source of barrier island sediments. It was estimated that the modern barrier island rim of the Apalachicola River delta (**Figure 7.1.**) would have formed ~ 6 000 years ago (Donoghue and Tanner, 1992; Donoghue and White, 1995; Stapor, 1973). Moreover, the Apalachicola Barrier Island Complex is believed to fully enclose its rim in the near future, resulting in an inland migrating delta front, if infilling of the Apalachicola estuary (Apalachicola Bay) continues at the previously estimated rate of 8 mm/a (Donoghue and Tanner, 1992), and erosion of the coastal barriers intensifies (failing any major change in sea level).

The first to have proposed a generalized evolution of the central-western barrier islands pertaining to the Apalachicola Complex was Stapor (1973, 1975). In his work, he estimated, with very limited absolute chronological control that, the first barrier islands emerged somewhere in between 6 500 and 4 000 years B.P. (i.e. two sedimentary nuclei at the south end and central region of St. Joseph Peninsula and the northern ridges of St. Vincent Island). Beach ridge development in all barriers, as a result of continuous sediment supply and shallow platform accretion, made progradation possible in several directions, until the present day geography was reached. Stapor's (1973, 1975) evolution was mostly based in detailed sedimentological (i.e. internal structure and granulometry) and morphological studies of the ridge patterns as, at the time, only six relative ages of archaeological provenance and three ^{14}C ages on geological materials were available for the barrier islands.

Continuing with a similar detailed sub-bottom stratigraphical work to that of Schnable and Goodell (1968) and Donoghue and Tanner (1992), Otvos (1992) stipulated a generalized Quaternary evolution of the Apalachicola coast based on beach ridge generations (i.e. sets or groups), their morphologies (orientations and heights) and a few ^{14}C ages obtained for the Holocene-Pleistocene contact on deep sediment cores. His interpretation of the initial stages of development of the barrier systems differed quite dramatically from that of Stapor (1973, 1975) but was similar towards the final stages of evolution. No ages were associated with the proposed stages.

Over the past 40 years, various sedimentological and geomorphological studies have been conducted on the lower relict mainland, the modern Apalachicola River delta, but the emphasis has been St. Vincent Island, a magnificent pristine strandplain example (Otvos, 1985; Otvos, 2005a; Otvos, 2005b; Stapor, 1973; Stapor, 1975; Tanner, 1995). Analyses of barrier island progradation, sea level history and beach/dune ridge formation and periodicity

have also been assessed from the sedimentological, stratigraphical and geomorphological point of view, with quite differing perspectives (e.g. Donoghue and Tanner, 1992; Otvos, 1992; Otvos, 2005a; Otvos, 2005b; Tanner et al., 1989). Rizk (1991) studied in detail the geomorphological and sedimentological characteristics of St. Joseph Peninsula in an attempt to portray in more detail its evolution, but with no other chronologies than those published by Stapor (1973, 1975). In more recent years, four ridges on St. Joseph Peninsula were dated by OSL (Forrest, 2003) to better visualize some of Rizk's (1991) observations.

In the absence of relevant absolute ^{14}C dates, two forms of assessing barrier island and delta formation/evolution have been evaluated: geomorphologically (e.g. Stapor, 1973) and archaeologically (e.g. Donoghue and Tanner, 1992; Donoghue and White, 1995). The distribution of archaeological sites along the Apalachicola River valley and neighbouring barrier shores shows no evidence of occupation prior to ~ 7 000 years B.P. It has to be noted that these archaeological sites have only been encountered along the bay-shores of some of the barrier islands targeted in this study: at least five sites on St. Vincent Island, one site on Little St. George Island, two sites Richardson's Hammock and one site on central St. Joseph Peninsula. Most of these coastal and estuarine sites are shell middens, sometimes mounded, enriched in a variety of coastal and freshwater faunal specimens and ceramic artifacts, portraying the diversity of aboriginal groups that once inhabited these lands (White, 2003; White et al., 2002). Despite the richness and importance of these coastal prehistoric archaeological sites, they are mostly poorly understood and/or ambiguously-dated. To date, the oldest coastal occupational sites are found on the northwest edge of St. Vincent Island, with approximate ages of 3 000 – 4 000 years B.P (Donoghue and White, 1995). The other few coastal sites along these barrier islands are younger in age. Little St. George Island has some archaeological evidence on its central-north edge, but only dating back as far as 300 – 800 years B.P. (Donoghue and White, 1995; Stapor 1975). Remnants of at least two ancient occupational sites exist on the bay side of St. Joseph Peninsula: a) one dating back to 1 400 years ago lies on what is considered to be the first island-nucleus (Richardson's Hammock) from which the peninsula emerged about 3 300 years ago (López et al, under review 2007); and b) the other as old as 940 years ago (Thompson et al, 2007) overlying a 1 800 year old beach ridge, considered part of another peninsula-forming nucleus on the central region of St. Joseph Peninsula (López and Rink, (submitted 2007)).

The only three existing recent / surficial ^{14}C ages that may be used in the supra-tidal evolution of these barrier islands are: a) an age of $1\,545 \pm 500$ years B.P. on a peat layer underlying the Little St. George Island archaeological site previously mentioned (Stapor, 1975); b) a $2\,110 \pm 130$ years B.P. age on shell (*Mulinia* sp.) located 15 cm above the top of a silty layer comparable to a modern intertidal marsh environment along the central eastern shore of St. Vincent Island

(Stapor, 1975); and c) a 754 ± 400 years B.P. age on an exposed peat layer “immediately north of the oldest ridge” on Cape San Blas (Stapor, 1975).

During the course of this four year long research, a set of at least 25 OSL and TL ages were published for the St. Vincent Island, Cape San Blas, Indian Pass Peninsula, and St. Joseph Bay eastern ridge flank by Otvos (2005a, 2005b). However, only 16 of those ages have been reported somewhat compatible with earlier proposed evolutions (e.g. (López and Rink, 2007b; Otvos, 1992; Rizk, 1991; Stapor, 1973; Stapor, 1975), even though their duplicates and other individual samples have given yet unexplainable highly unrealistic values (Otvos, 2005a). For a detailed revision of Otvos (2005a) OSL ages, please refer to López and Rink (2007a; submitted 2007).

7.2. STUDY AREA AND METHODOLOGIES

7.2.1. APALACHICOLA BARRIER ISLAND COMPLEX

The Apalachicola Barrier Island Complex is situated on the NE margin of the Gulf of Mexico, in a region known as the Florida Panhandle (U.S.A.). It is composed of a series of barrier islands which from East to West are: Dog Island, St. George Island, Little St. George Island, St. Vincent Island, and St. Joseph Peninsula (**Figure 7.1.**). One cape and a small peninsula are also part of the complex: Cape San Blas and Indian Pass Peninsula. Each of the barrier islands is decorated by a series of parallel to sub-parallel beach and dune ridges and swells that may or not be truncated in some areas. St. Vincent Island is a magnificent strandplain example, the best in the region. The St. George islands are the narrower ones, depicting fewer successions of ridges mostly oriented N45°W on Little St. George Island. St. Joseph Peninsula is a classic example of a barrier spit, growing almost due north, with active ridge and inter-tidal flat progradation at the spit-end. Cape San Blas connects the peninsula to the lower mainland, which in turn, depicts pristine successions of both north-south and east-west trending ridges believed to be Pleistocene in age (i.e. Gulfport Formation; Schnable and Goodell, 1968; Otvos, 1992). Indian Pass Peninsula is a minor protrusion extending eastward from the foot of Cape San Blas tombolo.

The barriers studied were St. Joseph Peninsula (SJP), St. Vincent Island (SVI) and Little St. George Island (LSGI). Cape San Blas (CSB), a mainland protrusion with east-west concave-seaward ridges was also studied. The study area stretches over ~ 60 km of beaches along the Gulf Coast. The northern half of SJP is owned by the State of Florida and covers the area within the T.H. Stone Memorial St. Joseph Peninsula State Park while the southern half houses a multitude of mostly vacationing complexes. The central-north and southern areas of CSB are owned by the Eglin Air Force Base (U.S. Air Force). SVI is a National Wildlife Refuge and is part of the U.S. Fish and Wildlife Service. LSGI

is managed by the Apalachicola National Estuarine Research Reserve (ANERR) and encompasses 246 000 acres of land and water around the Apalachicola River.

7.2.2. SAMPLE LOCATIONS

Twenty six long vertical unconsolidated sediment cores were recovered from 23 individual beach and dune ridges located throughout LSGI, SVI, CSB, and SJP, as well as one palaeo-ridge on the lower mainland, considered to be Pleistocene in age. The maximum depth reached was 3.60 m (Romanelli core) while the minimum was 1.22 m (SVI #2b core) – both uncompacted values – using a portable gas-operated vibra-core with an adapted custom-made coupling (**Figure 7.2.**). The ridges were cored close to their crests and almost all cases, low-angle parallel to sub-parallel laminations were observed towards the bottom of the cores, indicating closeness to the base of the ridge (i.e. inferring to the initial ridge-forming water-laid lithosome). All cores were corrected for compaction, which was assumed linear throughout each sediment core.

In addition to the long vertical cores, five short (~ 20 cm-long) horizontal unconsolidated sediment cores were recovered from and around two archaeological sites on SJP. Two cores were taken at the Old Cedar (8Gu85 Florida Master Site File) archaeological site: one from the surficial shell midden and the other from the underlying exposed relict beach ridge (see (Thompson et al., 2007) for details). At the Richardson's Hammock (8Gu10 Florida Master Site File) archaeological site, two cores (surficial shell midden and underlying beach ridge) were recovered from a fresh wall of a re-opened previously excavated trench, while a third was recovered from the same relict beach ridge exposed on the bay-side (see López et al. (under review 2007) for details). The exact geographical coordinates for all the cores recovered from the studied barrier systems are detailed in **Table 7.1.**

Vertical cores were sampled for OSL dating at two different depth intervals in an attempt to get two distinct lithosomes: the lower water-lain sedimentological units and the upper aeolian component (usually capping the majority of the ridges in the region). The bottommost sample was usually labelled "OSL 1" or "A" and the uppermost one "OSL 2" or "B" (see **Table 7.1.**). It is important to note that the number of OSL samples extracted from the vertical cores was mostly dependent on length of the core and sedimentological homogeneity of the 30 cm contiguous to the centre of each sample (i.e. in order to avoid radioisotopic inhomogeneity). Only two vertical cores were sampled at one depth interval (Deer Ridge SJ201 and Deer Ridge 2). Sampling details for individual cores can be seen in López and Rink (2007b), Thompson et al. (2007), López et al. (under review), and López, (2007).

The exact location of the sediment cores is shown in **Figures 7.3. to 7.6.**, each depicting an individual or a group of the barrier systems studied: LSGI (**Figure 7.3.**); Richardson's Hammock, CSB and the western lower mainland area (**Figure 7.4.**); SJP (**Figure 7.5.**); and SVI (**Figure 7.6.**). The sediment core recovered from the lower mainland (i.e. Oak Ridge core) was utilized as the oldest time marker for the evolution of this barrier complex, as it pertains to the former initial deltaic ridge plain that once dominated the area. A total of 55 samples were collected from 31 cores and were all OSL dated.

Loose surface sand (i.e. top of crest) from two ridges (a modern foredune and a relict ridge) was also taken as control samples: they were both analyzed for OSL to demonstrate that sediment from these barrier islands had been fully zeroed by natural sunlight prior (or during) deposition.

7.2.3. DATING METHODOLOGY

Core splitting and sampling, as well as all laboratory treatments (chemical and mechanical), sample handling and measurements were done under subdued orange lighting conditions at the AGE Laboratory (McMaster University, Canada). For vessel handling prior to coring, coring and core-splitting methodologies as well as laboratory treatments see López (2007). All sediment cores were corrected for compaction, which in turn was assumed linear throughout each core.

It had been demonstrated that only ~ 50 g of bulk sediment (i.e. a 2.5 cm-long x 7 cm-wide x 3.5 cm-deep slab of sediment from one half of a split core) is sufficient to obtain between 3 and 30 g of the 150-212 μm quartz grain fraction for OSL-dating purposes in these quartz-rich barrier systems (López, 2007): the smaller the sampling area, the better the lithological and local radioisotopic constraint.

Multiple aliquots were prepared to determine the luminescence characteristics of all 55 samples and controls: quartz grains were mounted on 9 mm diameter aluminium discs after being sprayed with silicone oil at four different mask sizes (8, 5, 3 and 1 mm diameters). In general, between 18 and 48 aliquots were utilized for the final determination of the equivalent dose (D_E) of each sample, each at two or more mask sizes (i.e. aliquot size). However, prior to the determination of this final D_E estimate of each individual sample, which was the value used in the calculation of the final age, a series of tests were performed on 40 different single aliquots of large size (i.e. 8 mm), to estimate an initial D_E , and to determine, verify and correct for feldspar contamination, pre-heat temperature, thermal transfer and regeneration dose cycle (see details in López, 2007).

The SAR protocol (Murray and Wintle, 2000) was utilized to determine the final D_E of each OSL sample with six regeneration doses (including a zero dose and a repeat dose) and one test dose. With the exception of the Oak Ridge samples, the minimum dose given to the samples was 0.26 Gy, while the maximum was 4.33 Gy. For Oak Ridge, the minimum dose was 4.34 Gy and the maximum 173.62 Gy (see **Table 7.1.**). All OSL measurements were done in an automated RISØ TL-DA-15 reader with blue light-emitting diodes and a single 6 mm-thick Hoya U-340 filter, at a temperature of 125 °C for 100 s. The OSL signal accounted for was integrated from the first 0.4 s of the stimulation, while the subtracted background was integrated from the last 10 channels (~ 4 s) of the decay curve. Details for final D_E selection criteria (i.e. aliquot by aliquot basis) are given in López (2007). A central age model, excluding aliquots with D_E 's falling outside a $\pm 2\sigma$ range, was used to calculate the final D_E . The final D_E error calculation was dependent on the symmetry of the D_E distribution, hence the D_E skewness coefficient of each sample. **Table 7.1.** details the skewness coefficients obtained for samples from CSB, LSGI and Oak Ridge. One standard error of the mean D_E was attributed to symmetrical distributions, whereas one standard deviation of the D_E values was the error associated to asymmetrical distributions (normally only slightly \pm skewed distributions) (see López (2007) for details).

Radiation dose rates were calculated from measured concentrations of radioisotopes (neutron activation analyses and delayed neutron counting of the bulk sediment), cosmic-ray dose rate calculations (dependent on the accurate estimation of the overburden atop each sample), and water contents (measured in the laboratory). For all samples, uranium and thorium concentrations are relatively low (most < 1 ppm), thus no effect consequences of secular disequilibrium were assumed. Radioisotope concentrations and total dose rates are shown in **Table 7.2.** for samples recovered from CSB, LSGI and Oak Ridge (new data presented in this paper). For additional details regarding all other samples, refer to López and Rink (2007b), Thompson et al. (2007), López et al. (under review), and López and Rink, (submitted 2007).

For consistency purposes, we consider all of our ages to be terminus ante quem for the time of formation of each individual ridge dated, as we are not certain to have reached the absolute base of the ridges (even less the Pleistocene platform under the cored barrier islands). Hence, each ridge had to have emerged no later than the OSL ages obtained during this research. Moreover, the OSL ages shown here are reported as years ago, with a reference datum established as the year when the luminescence measurements for a given sample were completed (i.e. A.D. 2004, A.D. 2005 or A.D. 2006).

7.3. RESULTS

7.3.1. OSL CHARACTERISTICS AND DATA

In terms of OSL characteristics, the samples analyzed showed the following general trends: a) IRSL/OSL ratios < 0.01 ; b) pre-heat temperatures ranged between 160 and 280 °C, with lowest values being best for the oldest samples and vice-versa (with the exception of the Oak Ridge samples); c) no thermal transfer observed; d) dose recovery pre-heat temperatures were included within the pre-heat plateaus; e) no evidence of fully zeroed aliquots (i.e. aliquots with zero D_E values) ; f) no evidence of incomplete zeroing (i.e. long tail of high D_E values); f) generally, D_E values obtained using large-sized aliquots (8 or 5 mm) are included within those obtained at the smaller sizes (3 or 1 mm); g) only one or maximum two aliquots were found as outliers (i.e. $> \pm 2 \sigma$) in each D_E distribution and excluded from the final D_E calculation.

All samples analyzed and dated from the four major coastal barrier systems pertaining to the Apalachicola Complex (i.e. LSGI, SVI, CSB and SJP), as well as the samples retrieved from the lower mainland Oak Ridge core were all in correct stratigraphical order within and among consecutive cores. New D_E (with associated final errors) and OSL age results specific of LSGI, CSB and Oak Ridge (lower mainland) are given in **Table 7.2**. **Table 7.3**. displays the OSL ages of previously reported samples measured throughout this study. As expected, the maximum D_E values and ages arise from the Oak Ridge core; however, but even though concordant to the Pleistocene, they are unexpectedly old relative to their stratigraphical positioning if compared to other Pleistocene studies in the region (c.f. Schnable and Goodell, 1968).

The oldest samples associated to any of the coastal barriers are to be found on Richardson's Hammock (samples RH A, RH-TUE-2 and RH-GEO-1) and SVI (cores SVI # 5 and SVI #6). Continuous vertical accretion is manifested in all cores, even though rates vary among ridges. Continuous lateral progradation is evident throughout LSGI, SVI, and CSB, but occurs to both the north and west on SJP, evidencing its growth in more than one direction at the same time. However, our SAR-OSL ages depict several groups of ages indicative of different stages of evolution as indicated by López (2007).

As for the modern analogues analyzed, they both showed D_E values of 0 Gy, indicating a zero age, hence demonstrating that the quartz grains being deposited in these coastal barriers are completely exposed to sunlight prior to or during deposition.

7.3.2. OSL AGE RESULTS IN THE CONTEXT OF BARRIER GEOCHRONOLOGY AND DEVELOPMENT PHASES

A generalized schematic interpretation of the supra-tidal evolution of these Apalachicola barrier islands was possible to be generated, based mostly on our OSL age results and the geomorphological analysis of the different barriers (**Tables 7.2.** and **7.3.**) and is displayed in **Figure 7.7**. Five successive stages of development are portrayed in **Figures 7.7a.** through **7.7e.**, showing the potential palaeo-geography for the former palaeo-cusate Pleistocene Apalachicola delta and the Late Holocene development of the complex's barrier islands since at least ca. 3 000 years ago until present time. The location of our cores is given throughout the different evolutionary stages as points of reference. This interpretation also accounts for the geomorphological and geometrical analyses done for each barrier system. Further to our analyses, all other previous studies and chronologies were also taken into consideration and assessed prior to our final interpretation.

In all sub-sets of **Figure 7.7.**, inferred principal longshore drift, tidal currents and the main outflow of the fluvial sediment contribution directions are shown. A generalized Late Pleistocene cusate palaeo-foreland is inferred as one of the potential initial sources of subsequent barrier island sediment (**Figure 7.7a.**). In general, and while this ancient shoreline was continuously being eroded and/or taken over by the potential development of ancestral island-nuclei, the northern part of SVI emerged while the Richardson's Hammock, Rish Park and Eagle nuclei were already existent (**Figure 7.7a.**). At least some 1 500 years later, SVI continued to build up its pristine, mainly concave-seaward ridge sets southward, while the widest elbow-shaped area of LSGI started to develop as more ridges emerged probably associated to the existence of an initial island-nucleus known as Sand Island in old nautical charts (c.f. Tanner, 1975) (**Figure 7.7b.**). In the mean time, SJP continued its northward progradation as two sets of spits growing out from the ancestral nuclei, possibly maintaining the existent deep Eagle Harbor inlet. At least ca. 500 years ago, most of the barrier systems were very close to present-day shape (**Figure 7.7c.**), with the exception of the West Pass margins of both SVI and LSGI, the Indian Pass Peninsula and the northern tip of SJP spit. By now, the Eagle Harbor inlet may have been closed by continuous longshore action and seaward ridge accretion. Presumably ca. 1 000 years ago, CSB started its seaward growth, from the lower mainland. For ~ 500 years, CSB rapidly evolved until complete enclosure of St. Joseph Bay (**Figure 7.7c.**). The rapid tombolo-like progradation of CSB can be noted between **Figures 7.7c.** and **7.7d.**, in which the cape's extension is inferred from 1800's nautical charts, depicting it as the fastest accreting barrier system studied in the region so far, contrary to previous beliefs.

Figure 7.7e. portrays the present-day geometry and full exposure of the barrier systems targeted for this study. The multitude of individual ridge and ridge sets orientations throughout these coastal barriers deserves particular attention. There are no generalized trends to cluster them all. Instead, an array of displays in several directions suggests a highly hydrodynamic system, allowing changes in longshore drift through time over a relatively small geographical area. Such dynamism may also be the cause for the intensive erosion seen since the mid 1800's (c.f. Coastal Tech. and Preble-Rish Inc., 1998; Lamont et al., 1997; Rizk, 1991; Stapor, 1975), mostly affecting CSB, the seaward apex of LSGI and the southern portion of SJP (noted in **Figure 7.7e.** as “+” and “-” symbols for accretion and erosion, respectively), most likely because they are the most protruded geometries of the complex. Due to the scale used and the schematic character of **Figure 7.7.**, such historical shoreline changes could not be depicted herein but have been detailed in López and Rink (2007b), López et al. (under review) and López and Rink (submitted 2007).

Some of the sediment forming these barrier islands may have a Pleistocene provenance as the lower mainland coastal relict ridges eroded through time. The only core retrieved from the lower mainland, west of the Apalachicola River (**Figures 7.4.** and **7.7a.**), is Oak Ridge, recovered from NS-trending concave-seaward broad parallel relict ridges. The terminus ante quem age of formation for this ridge was calculated to be at least $154\,200 \pm 10\,400$ years ago, based on the bottommost sample OSL-dated (Oak Ridge A – see **Table 7.2.**). The upper sample, Oak Ridge B, showed an age of $24\,200 \pm 5\,800$ years ago at only 1.18 m below actual ground surface (**Tables 7.1.** and **7.2.**). The average sediment accumulation rate (ASAR) between these two samples is 0.0007 cm/a (assuming constant sediment accumulation) (**Table 7.4.**), suggesting a very slow formation for this Pleistocene landform, value which could also be masked by extended sediment compaction and landscape evolution through time. Nonetheless, the uppermost age could also represent an aeolian reactivation surface. The Oak Ridge core is presently being dated at a higher resolution to determine any potential sedimentary hiatuses. Furthermore, some other ridges in this lower mainland area are being cored for future OSL studies.

The Late Holocene Apalachicola Barrier Island Complex has been a relatively rapidly prograding system since about, in general terms, the last major sea level change some 5 000 years ago. **Figure 7.8.** depicts the ages obtained for all the bottommost samples retrieved from cores and archaeological sites, which show the terminus ante quem time of formation of the cored ridges. Evidence of such rapid platform and supra-tidal sedimentary build up can be found on the calculated rates of lateral progradation (assuming constant both sediment supply and lateral accretion) based on our OSL ages for the barrier systems studied: a) SVI evolved at least over the past $2\,730 \pm 400$ years (sample SVI #5 OSL1) and

its estimated progradation rate is ~92 m / 100 years, as calculated between samples SVI #3 OSL1 and SVI #0 OSL1 (López and Rink, 2007b); b) LSGI shows an average progradation rate of ~209 m / 100 years (as calculated between the bottommost samples of cores LSGI 1 and LSGI 3); while c) CSB shows a average progradation rate of ~433 m / 100 years (as calculated between samples Roy Eglin A and Hogan A).

While SVI grew as a classic strandplain, with a continuous sedimentary accretion at its frontal edge (i.e. Gulf shore), LSGI and SJP evolved from ancestral nuclei, probably in the form of pre-existing sedimentary shoals before the supra-tidal ridge formation and progradation. Moreover, Richardson's Hammock could be considered a small island strandplain on itself, due to the high concentration of continuous beach ridges, which in turn form at least four ridge sets (see **Figure 7.4.**). Nonetheless, the fastest growing system is without a doubt the CSB tombolo.

The suite of results presented below are for each individual barrier system studied during the past four years of research, in sequential manner, from the relatively oldest to the relatively youngest system, even though all may be considered concurrent, at some point in time, among each other.

7.3.2.1. RICHARDSON'S HAMMOCK OSL AGES

From our OSL ages, it is evident that the evolution of this barrier complex started at Richardson's Hammock (see **Tables 7.1.** and **7.3.** and **Figure 7.7.**). Shortly thereafter, SVI started to emerge on its northernmost side. Such ridges, corresponding to cores SVI #5 and SVI #6 are presently at sea level (López and Rink, 2007b), as well as some of the oldest ridges on both the Apalachicola Bay side of LSGI and the south-eastern St. Joseph Bay edge (see **Figures 7.3.** through **7.6.**), concordant to suggestions of slow submergence (presumably due to compaction of Pleistocene underlying clays) of some barrier shorelines and sinkhole formation on the lower mainland by Otvos (1992). In general, and according to our OSL ages, a relative continuous rapid progradation is evident for at least CSB and SJP (**Figure 7.8.**). SVI and LSGI may have endured an intermittent, however continuous, progradation as seen by the time lapses between samples. Richardson's Hammock abruptly stopped any further progradation just after ~ 2 500 years ago, apparently mainly due to the initiation of SJP sea- and north-ward, which truncated its growth.

7.3.2.2. ST. VINCENT ISLAND (SVI) OSL AGES

Undoubtedly, the most interesting coastal system of all is SVI, due to its magnificent, yet pristine ridge decorations. López and Rink (2007b) studied it in detail based on the SAR-OSL ages obtained on 14 samples from seven cores

(**Table 7.3.**). In general, D_E values obtained ranged between 1.04 ± 0.13 and 0.11 ± 0.01 Gy, for the oldest and youngest samples analyzed, respectively. For more details please check López and Rink (2007b).

Even though the bottommost samples of cores SVI #5 and SVI #6 (**Figure 7.6.**) showed statistically indistinguishable ages, the terminus ante quem age of time of formation of this northern section of SVI is considered to be $\sim 2\,800$ years ago. The youngest age obtained from SVI associated to time of ridge formation is 410 ± 60 years ago (sample SVI #0 OSL1). It is interesting to note that a great portion of SVI, i.e. ridge sets C-D-E-F (see **Figure 7.6.**), emerged over only ~ 900 years (see **Figure 7.8.**), while ridge sets G through K evolved at an approximate rate of ~ 92 m / 100 years, equivalent to one ridge forming every ~ 82 years (López and Rink, 2007b). It is interesting to note the elevated values of Lower ASAR (i.e. calculated between samples A and B) for the cores closer to the Gulf shoreline as opposed to those further away (**Table 7.4.** and **Figure 7.9.**), suggesting a rapid vertical accretion, i.e. ridge formation, for samples younger than $\sim 2\,000$ years old.

7.3.2.3. ST. JOSEPH PENINSULA (SJP) OSL AGES

Based on ridge morphology, peninsulas may be seen as environments showing continuous systematic progradation from a single point of origin, both in the prevailing longshore drift direction and seaward, perpendicular to shore, building the sedimentary platform (i.e. shallow) from which they subsequently emerge. As evidenced by our SAR-OSL ages, SJP did not evolve from a single system. As seen in **Figures 7.8.** and **7.9.**, SJP tends to show some age clustering, i.e. a marked difference is seen between the older samples (which also show a smaller Lower ASAR value) and the younger samples (e.g. Rish Park and Old Cedar Geo 1 bottommost samples compared to the other cores – see **Table 7.4.**). López and Rink (submitted 2007) have identified at least four sedimentary nuclei along SJP, i.e. shallows or “islands” conceived as precursors to the peninsula, being Richardson’s Hammock the first, as described above. Such nuclei emerged from previously formed shallows along the length of the peninsula, each at different stages in time. Rish Park is considered the second oldest nucleus, named after the core of the same name, and corresponds to the southernmost area of SJP (see **Figure 7.5.**), showing a terminus ante quem age of $2\,200 \pm 200$ years ago (**Table 7.3.**). A third nucleus named “Eagle”, due to its location just south of Eagle Harbor (see **Figure 7.5.**), is comprised by the ridges where the Deer Ridge triplets, Old Cedar duo and Harvey cores were recovered. It is considered to be at least $1\,800 \pm 130$ years old (**Table 7.3.**). “Harbor” (named after a former benchmark location) is the fourth spit-forming nucleus. It was depicted from detailed morphological studies, and assigned a SAR-OSL age of $1\,800 \pm 400$ from a previous study by Forrest (2003). Moreover, there is a potential fifth nucleus

named “Pompano”, as discussed in López and Rink (submitted 2007), with an assigned TL age of 1 300 years based on a previous study by Otvos (2005a).

Six other ridges located among the frontal and spit end ridges, corresponding to the youngest ridge sets of SJP (see López and Rink, submitted 2007), allow us to determine the relative ages of lateral formation of the peninsula post nuclei emergence. Wild core depicted a terminus ante quem age of ridge formation of 930 ± 70 years ago, contemporaneous to the Haven ridge site. GPR 1, SJ 002 1, SJ 002 2 and White Sands (see **Figure 7.5.**) are < 300 years in age, representing historical times of ridge formation which depict the highest Lower ASAR values throughout SJP (**Table 7.4.** and **Figure 7.9.**).

7.3.2.4. LITTLE ST. GEORGE ISLAND (LSGI) OSL AGES

It has been previously suggested that this barrier island (**Figure 7.3.**) evolved similarly to SJP, from a pre-existing sedimentary nuclei known as “Sand Island” (Stapor, 1975), according to historical nautical charts (**Figure 7.7.**). Unfortunately, no sedimentary cores were taken at this location. At its widest area, LSGI is decorated by a succession of pristine ridges with no geomorphological evidence of truncation. Three long vertical sedimentary cores were taken throughout this widest area: LSGI 1, LSGI 2 and LSGI 3. The terminus ante quem ages of formation of the ridges host to these cores are respectively: $1\ 900 \pm 200$, 500 ± 50 , and 32 ± 3 years ago (see **Table 7.2.**), showing a general lateral progradation rate of 208.8 m / 100 years (assuming constant sediment supply and aggradation). Only LSGI 1 and LSGI 2 allow us to determine correct Lower ASAR values as samples A and B taken from LSGI 3 are statistically indistinguishable from each other (**Table 7.4.** and **Figure 7.9.**), suggesting extremely rapid sediment accumulation.

It is yet unknown if the ridges to the east of the old lighthouse (see **Figure 7.3.**), now abandoned and on the surf zone, are evidently older or contemporaneous to our LSGI 1 and LSGI 2 bottommost core samples. The presence of submerged ridges on the bay-shore along the eastern arm of the island may suggest an old character to at least this bay-side area of the island, similar to the submerged ridges on the northern end of SVI.

7.3.2.5. CAPE SAN BLAS (CSB) OSL AGES

Undoubtedly, the youngest barrier system in the complex is CSB. Its rapid strandplain-like progradation suggests constant and abundant, readily available, sediment supply (**Figures 7.4., 7.7e.** and **7.7f.**). It formed as a tombolo structure, progressively linking the lower mainland to the southern edge of Richardson’s Hammock and SJP, presumably emerging atop a continuously aggrading shoal.

Core Roy Eglin showed a bottommost age of 630 ± 40 years, terminus ante quem for the formation of the northernmost ridge cored on CSB (**Table 7.2.** and **Figure 7.8.**). Subsequently, the ridge host to the Romanelli core, located to the east and south of Roy Eglin, emerged around at least 530 ± 40 years ago. Interestingly, the Lower ASAR values are higher for the Roy Eglin core (0.92 cm/a) than for the Romanelli core (0.61 cm/a), most probably due to their geographical location: the latter may have needed more time to form as the tombolo accreted westward (**Table 7.4.** and **Figure 7.9.**). The terminus ante quem age of formation for the ridge host to Hogan is only 330 ± 20 years ago, suggesting a lateral progradation rate of ~ 433 m / 100 years for the cape terminus. The presence of the CSB lighthouse (moved to its present location in A.D. 1934) may provide a relative lateral progradation rate of ~ 10 m/a, compared to the time of deposition of sample Hogan B.

7.4. DISCUSSION

A detailed stratigraphical Pleistocene-recent study of this Apalachicola Coast was conducted by Schnable and Goodell (1968) and Otvos (1992) using borings ≤ 50 m-long. Several ^{14}C -derived ages were obtained on mollusc shells mostly around the Holocene-Pleistocene contact (c.f. Schnable and Goodell, 1968). The Pleistocene sediments vary in thickness throughout the Apalachicola Complex, thinning towards the east and being maxima at CSB (~ 40 m). They are generally divided into three main sequences: the upper Prairie (mostly alluvial) and Gulfport (coastal barrier ridges) formations, and the lower Biloxi Formation (neritic to estuarine deposits) (Otvos, 2005b). The barrier forming ridges presently seen on the western lower Apalachicola mainland are associated to the Gulfport Formation (see **Figures 7.1.** and **7.4.**) which corresponds to the Sangamon Interglacial (i.e. Marine Isotope Stage 5) (Otvos, 2005b). To date, the general Gulf Coast age range attributed to the Gulfport Formation has been 116 to 124 Ka (Otvos, 1992; Otvos, 2005b). Our results (i.e. sample Oak Ridge A – see **Tables 7.1.** and **7.2.**) show a slightly older OSL age (~ 154 Ka) associated to this formation, the oldest age ever published for these linearly-oriented relict barrier-forming ridges seen throughout the mainland shores of the Gulf of Mexico. Nonetheless, the maximum extension of this lower mainland strandplain is still unknown, so the authors are only speculating its position relative to sea level in the figures depicting the supra-tidal evolution of the Apalachicola barrier islands targeted in this study (see **Figure 7.7.**). As for future research, it would be interesting to date the east-west trending relict ridges neighbouring Oak Ridge (**Figure 7.1.**) to determine how old are some of the “younger” Pleistocene remnants of the Gulfport Formation in this area.

Atop the generally muddy to fine-sized Pleistocene sands lay the recent Holocene mixed siliciclastic sands that form the modern platform and supra-tidal

barrier bodies, which are probably < ~ 15 m-thick, and emerged as sea level rose from the last interglacial (Schnable and Goodell, 1968; Donoghue and Tanner, 1992; Otvos, 1992). Some authors have suggested SVI as the oldest Holocene coastal barrier in the region (with its northernmost ridges at least some 3 000 years old) and that, based on archaeological coastal midden sites and a few surficial peat ^{14}C ages, the rim of barrier islands cannot be older than 3 500 years B.P. (Stapor, 1973, 1975; Donoghue and Tanner, 1992; Donoghue and White, 1995). As evidenced by our SAR-OSL results, the oldest ages associated with the barriers pertain to both Richardson's Hammock and SVI, which are indeed at least 3 000 years old (**Figure 7.10.**), as their corresponding oldest ages are statistically indistinguishable from each other. These ages suggest that sea level must have been stable at that time to allow continuous progradation and accretion of the barrier islands.

Arguments regarding the formation of these older ridges being coeval with sea level high-stands have been a continuum for the past 20 years. According to various authors, sea level may have stabilized some 5 000 to 6 000 years ago in order to allow initiation of this barrier complex. Without entering into an intrinsic sea level discussion, our results suggest that such sea level stabilization could not have occurred prior to ~ 3 000 years ago. In fact, the oldest ages obtained on both Richardson's Hammock and SVI are located some two meters below present mean sea level. Detailed investigations related to past sea level interpretations based on our OSL ages and their precise location within these inorganic sea level markers (i.e. the lithosomes/sedimentary facies they pertain to within the beach/dune ridges) are currently taking place. Nonetheless, the purpose of this paper is to interpret our OSL ages as well estimated chronologies to infer the general supra-tidal barrier progradation and compare them with previously correctly published ages, as well as geomorphological analyses of ridge distribution patterns and historical maps/images.

The earliest proposed evolution for some of the barrier islands of this Apalachicola Complex was made by Stapor (1973, 1975), an interpretation mostly based on the sedimentological characteristics of the coastal barrier deposits and the geomorphological analysis of the different ridge orientations and truncations (**Figure 7.11.**). Surprisingly, and mainly due to the minimal number of ages he presented, mostly archaeologically related and believed no earlier than 3 500 to 3 000 years B.P., Stapor's (1973, 1975) interpretation is still very similar to the one we propose herein, which is based on a total of 55 SAR-OSL ages obtained throughout the lower mainland, LSGI, SVI, CSB, SJP and Richardson's Hammock. In his interpretation, the former cusped pre-Holocene Apalachicola delta (Schnable and Goodell, 1968) started to erode away some 6 500 years ago (its maximum extension sea-ward is still unknown) after sea level stabilized, while the northernmost part of SVI was already emerged, and two

island-nuclei were littoral shallows on either side of Eagle Harbor as the predecessors of SJP. Our results suggest that this occurred at least 3 000 years ago (**Figure 7.10.**), as per the terminus ante quem character of the ages of our bottommost samples on Richardson's Hammock, SJP and SVI (see **Figure 7.7a.**). Furthermore, Stapor (1973, 1975) suggests almost fully emergent SVI and LSGI ~ 2 000 years ago, which is partly contraire to our findings (see **Figure 7.7b.**). A peat layer on the northern edge of LSGI, close to the location of our core LSGI 1 (see **Figure 7.3.**), has been assigned a ^{14}C -age of $1\,545 \pm 500$ years B.P. by Stapor (1975), and is concordant with the terminus ante quem age we assign to the northernmost cored ridge on LSGI. Nonetheless, the Gulf shoreline of LSGI at that time could not have been as developed as Stapor proposes due to our terminus ante quem age assigned to LSGI 2 of only 500 ± 50 years ago.

As for SJP, he suggests only two precursor nuclei and fully developed spits growing north and south of Eagle Harbor, contrary to our findings of at least five nuclei throughout the eastern bay margin of SJP (including Richardson's Hammock) (see **Figures 7.7a. through 7.7d.**). Rizk (1991) proposed a similar evolution for SJP to that of Stapor (1973, 1975), based on geomorphological and sedimentological studies. He divided SJP into 14 ridge sets that evolved from those two to three precursor sedimentary nuclei, similar to our proposed 14 ridge sets (López and Rink, submitted 2007). While the modern complex took shape and the barrier islands acquired their present-day morphologies, CSB only emerged < 1 000 years (Stapor, 1973), which is concordant to our findings but we were able to constrain its emergence as a bay-locking tombolo to at least 630 ± 40 years ago (terminus ante quem age of formation of the ridge where core Roy Eglin was taken). Furthermore, Stapor's (1975) only ^{14}C -age of 750 ± 400 years B.P. for SJP and CSB, taken from a peat layer on the northwest corner of CSB, north of the geographically oldest ridge on CSB, concurs with our Roy Eglin A age. This peat age may only help us constrain the time of closure of St. Joseph Bay, hence complete formation of the northward section of the CSB tombolo.

Unfortunately, we were unable to obtain OSL ages for the Indian Pass Peninsula, located just east of the foot of CSB tombolo. Its location in time, as seen in **Figure 7.7.**, is merely speculative. Evidently, future coring of these ridges is strongly encouraged to further constrain the sub-aerial evolution of these barrier systems. Furthermore, areas such as Pig Island, just north of Richardson's Hammock, "Sand Island" and the eastern arm of SJP are also to be dated in the future, to obtain more constraints on the evolution of the complex.

Following Stapor's original interpretation, Otvos (1992) suggested that CSB and Richardson's Hammock were involved in the early development of SJP and SVI, mainly based on the ridge morphologies (c.f. his Figure 7; Otvos, 1992) and a few ^{14}C -ages from the Pleistocene-Holocene contact. Its first interpretation

suggested that CSB, Richardson's Hammock and the Indian Pass Peninsula were continuous and attached, being the first barriers to form attached to the lower mainland. Subsequently, and through continuous ridge emergence, SVI and SJP accreted southwest-ward and northward, respectively. Based on our results, this interpretation is certainly equivocal and erroneous.

During the course of this research, some TL and OSL ages obtained from SJP, CSB, SVI and parts of the lower mainland shores were published by Otvos (2005a, 2005b), suggesting a different supra-tidal evolution interpretation to that he suggested in 1992 (**Figure 7.12.**). Intriguingly, Otvos (2005a and pers. com.) considers some of his TL and OSL ages, especially those related to SVI, a failure for yet unknown reasons, as they do not correspond with the expected ridge chronologies (see López and Rink, 2007b). TL may indeed depict older burial age estimates as it may inaccurately determine un-zeroed luminescence signals. As for his OSL ages, and despite the fact that not all have listed among the tables provided, no precise depth is given within the ridges sampled, making the correlation with our samples difficult. Nevertheless, our proposed interpretation is quasi-concordant with Otvos (2005a) geochronological and geomorphological interpretations of the supra-tidal evolution of SVI, CSB, SJP and Richardson's Hammock, despite the fact of his assumed unrealistic OSL and TL ages. Nonetheless, we only considered six of his 25 OSL and TL ages to be consistent with both our own SAR-OSL ages and overall evolution interpretation of the Apalachicola Complex: two for SJP, one for Richardson's Hammock, one for CSB, and two for SVI. The ages we believe are reasonable are (c.f. his Figures 16 and 18, Otvos, 2005a): a) a 2 900 years ago OSL age (no details provided) located on the core area of Richardson's Hammock and associated with our time interval T1 (see **Figure 7.10.**); b) a 1 600 years ago TL age on the southern portion of SJP (no details provided) possibly associated with our time interval T2; c) a 1 300 years ago TL age associated to our "Pompano" nucleus on SJP (López and Rink, submitted 2007), associated to our time interval T3; d) a 600 years ago TL age on the central northern region of CSB, associated with our time interval T5; e) a 3 950 years ago OSL age on the north-west edge of SVI may be the closest approximate to our oldest ages on the same island, and associated with our time interval T1; and f) a 602 years ago OSL age close to the Gulf shore of SVI, probably between Tanner's (1992) set G and K, which corresponds to our time interval T5. More details are given in López and Rink (2007b) regarding the OSL age comparisons among Otvos' (2005a) samples from SVI.

In general, SVI and LSGI evolved throughout a relative large time frame, contrary to CSB, SJP and Richardson's Hammock (**Figures 7.8.** and **7.9.**), the latter being the oldest barrier system so far dated in the Apalachicola Complex. A generalized evolution of all the targeted barrier systems can be synthesized by six consecutive time intervals spanning from at least 3 000 years ago to present time

(**Figure 7.10.**). CSB shows a fast progradation, spanning only over five centuries. However, and most interestingly, SJP shows a consistent assemblage of OSL values, inferring the multiple-nuclei hypothesis suggested by López (2007). At present, no major lateral progradation is occurring throughout the barrier system, with the exception of the northern terminus of SJP (**Figure 7.7e.**). This is probably due to the almost full enclosure of the Apalachicola River sediment supply by the barrier island rim, resulting on drift starvation and increasing erosion which could also be a reflection of rising sea level. Major erosion is occurring along the beaches facing the south and west Gulf shores, with southern SJP, CSB and the LSGI elbow being the most affected, since historical times. For the latter two (i.e. LSGI and CSB), the presence of extensive offshore shoals may be related to the elevated hydrodynamics and erosion they witness. For example, it has been estimated that between 1973 and 1997, $\sim 40\,000\text{ m}^3 / \text{a}$ of sediment have been deposited around CSB western terminus, while $\sim 180\,000\text{ m}^3 / \text{a}$ of sediment have been eroded on SJP and CSB from Richardson's Hammock southward (Coastal Tech. and Preble-Rish Inc., 1998). Based on historical nautical maps, CSB has eroded $\sim 1.5\text{ km}$ on its western Gulf shore but accreted $\sim 1\text{ km}$ on its southern shore since the mid 1800's until 2004. Similar erosion rates apply to the southern elbow of LSGI. The ever-changing shoal morphology around CSB western terminus may be a proxy of the influence of tidal and longshore currents. As a matter of fact, CSB is considered a tidal current divergent point (Gorsline, 1966), refracting the strong tidal currents eastward and northward, as depicted in **Figure 7.7**. In addition, to the west of CSB, longshore drift directions are generally to the west and north and the coast is classified as a moderate wave energy coast. East of CSB and encompassing LSGI, the drift is to the east and the wave energy is still moderate. However, east of LSGI, the coast turns into a low wave energy system (Gorsline, 1966; Myers and Ewel, 1990).

Plots of OSL ages and ASAR values against distance from shore exhibit our ridge formation rates, thus time elapsed between different stages of development of a coastal system. If the relation is highly linearly concordant, a system may have been formed in a short period of time over an evenly sloping pre-existing platform and vice-versa (**Figures 7.8.** and **7.9.**). Such analyses are of particular importance when dealing with coastal environments that are believed to have undergone multiple relative sea level fluctuations. If the progradation rates are indisputably linear and the consecutiveness as well as inter-distance between ridges is regular, the ridge plain progradation may had been formed during still-stand sea level, sediment supply permitting.

Palaeo-geographies of coastal barrier islands may be reconstructed using ridge / ridge set morphologies, as they represent palaeo-shoreline positions and may be used as proxies for morpho- and hydro-dynamics. However, the interpretation of the evolution of a system gains more accuracy when such

analyses are coupled with absolute chronologies. As with any other absolute geochronometric technique, specifics such as depth of the sample, elevation and geographical location should be regarded with great care in order to establish any type of correlation and/or constraint with other or the same dating method when assessing the same environment. Even though optical dating has been increasingly accepted as an accurate and precise geochronometric technique, it is important to maintain specifics such as geographical location, depth of sample and datum (i.e. year of measurement) in publications (mostly those colleagues outside the geochronological community) to facilitate interpretations and make constraints as correctly as possible, such as intra-ridge or inter-ridge correlations, in our case.

7.5. CONCLUSIONS

The central-west barrier island system of the Apalachicola Complex evolved relatively rapidly over a period of at least ca. 3 000 years, contrary to previously published data, developing some of the most pristine and interesting ridge sequences in the Gulf of Mexico. At least two barrier systems began to evolve simultaneously around 3 000 years ago (Richardson's Hammock and SVI), presumably just after sea level stabilized in the region. This new data contradicts previous hypotheses that suggested the barrier complex emerged between 5 000 to 6 000 years ago (based on archaeological evidences) as sea level stabilized in the Gulf of Mexico, while the nearby Pleistocene mainland strandplain eroded away. Current work is being done by the authors to tackle the sea level history of the region in greater detail.

Longshore dynamics and tidal currents played an important role in the continuous evolution of this coastal barrier complex, as evidenced by the intricate patterns and directionality of the multiple ridge set systems. Moreover, sediment supply may have been abundant and somewhat constant, at least from around 3 000 to 300 years ago, to concur with the different rates obtained for barrier formation, progradation and accretion. Such speculation could be linked to greater erosion rates in the neighbouring mainland, probably due to changes in climate, but is to be further investigated.

This study demonstrates the validity of optical dating in appraising not only accurate chronologies but also the evolution of sub-aerial coastal siliciclastic environments. The optical dating protocols utilized in this study appear to be suitable for the type of quartz forming these successions of barrier-forming beach and dune ridges, allowing the estimation of reliable vertical accretion rates and lateral progradation estimates. Optical dating is being increasingly accepted and used as an established geochronometric technique. Nonetheless, the results obtained have to be backed up with a thorough account of the experimental procedures utilized. It is important to adequately present and discuss optical

dating results (as previously stated by e.g. Prescott and Robertson, 1997; Lian and Roberts, 2006), but also try to standardized some parameters to ensure a continuity in the quality of optical dating results.

7.6. ACKNOWLEDGEMENTS

This research was made possible thanks to the continuous logistic, financial and personnel support of the T.H. Stone Memorial St. Joseph Peninsula State Park and the Apalachicola National Estuarine Research Reserve (both Florida Department of Environmental Protection). Exploratory, sampling and coring permissions were granted by the former entities as well as the Eglin Air Force Base on Cape San Blas (U.S. Air Force), Wm. J. Rish Recreation Park (on St. Joseph Peninsula), Port St. Joe Municipality (Gulf County), St. Vincent National Wildlife Refuge (U.S. Fish and Wildlife Service), Dr. Nancy Marie White (University of South Florida), and individual land owners. We also acknowledge financial support through a Natural Science and Engineering Research Council of Canada (NSERC) grant provided to WJR. Intermittent logistical and field assistance provided by the Fish and Wildlife Research Unit (University of Florida) and the Florida Geological Survey are greatly appreciated. Last but not least, and throughout the various field seasons from 2002 to 2005, the authors acknowledge the great assistances in the field provided by Dr. J. Boyce, J. Etherington, K. Keizars, J. Pilarczyk, K. Moreton, M. Kossak, J. Thompson, and S. Collins (all from McMaster University). The authors are also grateful to E.G. Otvos and J.F. Donoghue for discussions held and information provided and interchanged over the course of this research.

7.7. REFERENCES

- Aitken, M.J., 1998. An introduction to Optical Dating: The Dating of Quaternary Sediments by the Use of Photo-Stimulated Luminescence. Oxford University Press, Oxford, 267 pp.
- Banerjee, D. et al., 2003. New quartz SAR-OSL ages from the stranded beach dune sequence in south-east South Australia. *Quaternary Science Reviews*, 22(10-13): 1019-1025.
- Bateman, M.D. et al., 2007a. Detecting post-depositional sediment disturbance in sandy deposits using optical luminescence. *Quaternary Geochronology*, 2: 57-64.
- Bateman, M.D. et al., 2007b. Preserving the palaeoenvironmental record in Drylands: Bioturbation and its significance for luminescence derived chronologies. *Sedimentary Geology*, 195(1-2): 5-19.
- Bøtter-Jensen, L., McKeever, S.W.S. & Wintle, A.G., 2003. *Optically Stimulated Luminescence Dosimetry*. Elsevier, Amsterdam, 355 pp.

- Coastal Tech. and Preble-Rish Inc., 1998. Hurricane Evacuation Route and Beach Management on St. Joseph Peninsula: Feasibility and Design Study.
- Donoghue, J.F., 1992. Late Quaternary Coastal and Inner Shelf Stratigraphy, Apalachicola Delta Region, Florida. *Sedimentary Geology*, 80: 293-304.
- Donoghue, J.F., 1993. Late Wisconsinian and Holocene depositional history, northeastern Gulf of Mexico. *Marine Geology*, 112(185-205).
- Donoghue, J.F. and Greenfield, M.B., 1991. Radioactivity of heavy mineral sands as an indicator of coastal sand transport processes. *Journal of Coastal Research*, 7(1): 189-201.
- Donoghue, J.F. and Tanner, W.F., 1992. Quaternary terraces and shorelines of the Panhandle Florida region. In: C.H. Cletcher and J.F. Wehmiller (Editors), *Quaternary Coasts of the United States: Marine and Lacustrine Systems*. Society of Economic Paleontologists and Mineralogists, Tulsa, pp. 233-241.
- Donoghue, J.F. and White, N.M., 1995. Late Holocene sea level change and delta migration, Apalachicola River region, northwest Florida, U.S.A. *Journal of Coastal Research*, 11(3): 651-663.
- Forrest, B.M., 2003. Applications of Luminescence techniques to Coastal Studies, St. Joseph Peninsula, Gulf County, Florida. M.Sc. Thesis, McMaster University, Hamilton, 209 pp.
- Gorsline, D.S., 1966. Dynamic Characteristics of West Florida Gulf Coast Beaches. *Marine Geology*, 4: 187-206.
- Hsu, K.J., 1960. Texture and mineralogy of the recent sands of the Gulf Coast. *Journal of Sedimentary Petrology*, 30(3): 380-403.
- Huntley, D.J., 1985. On the zeroing of the thermoluminescence in sediments. *Physics and Chemistry of Minerals*, 12: 122-127.
- Jungner, H., Korjonen, K., Heikkinen, O. and Wiedman, A.M., 2001. Luminescence and radiocarbon dating of a dune series at Cape Kiwanda, Oregon, U.S.A. *Quaternary Science Reviews*, 20: 811-814.
- Kwon, H.J., 1969. Barrier Islands of the Northern Gulf of Mexico Coast: Sediment Source and Development.
- Lamont, M.M. et al., 1997. The Cape San Blas Ecological Study, Florida Cooperative Fish and Wildlife Research Unit.
- López, G.I., 2007. The Late Quaternary evolution of the Apalachicola Barrier Island Complex, North-East Gulf of Mexico, as determined from optical dating,, McMaster University, Hamilton, 300 pp.
- López, G.I. and Rink, W.J., 2007a. Characteristics of the burial environment related to Quartz SAR-OSL dating at St. Vincent Island, NW Florida, U.S.A. *Quaternary Geochronology*, 2: 65-70.
- López, G.I. and Rink, W.J., 2007b. New Quartz-OSL ages for Beach Ridges on the St. Vincent Island Holocene Strandplain, Florida, U.S.A. *Journal of Coastal Research*, in press (accepted 2 December 2005).

- López, G.I. and Rink, W.J., (submitted 2007). Peninsular Evolution and Optical Dating of Young Coastal Ridges along the Gulf of Mexico. *Quaternary Geochronology*: (50 pp).
- López, G.I., Rink, W.J. and White, N.M., (under review 2007). Optical dating of an ancient coastal occupation site and underlying land on the northwest Gulf Coast of Florida, near Apalachicola, U.S.A. *Geoarchaeology*: (submitted December 2006; 42 pp).
- Murray-Wallace, C.V., Banerjee, D., Bourman, R.P., Olley, J.M. and Brooke, B.P., 2002. Optically stimulated luminescence dating of Holocene relict foredunes, Guichen Bay, South Australia. *Quaternary Science Reviews*, 21(8-9): 1077-1086.
- Murray, A.S. and Wintle, A.G., 2000. Luminescence dating of quartz using an improved single-aliquot regenerative-dose procedure. *Radiation Measurements*, 32: 57-73.
- Myers, R.L. and Ewel, J.J., 1990. *Ecosystems of Florida*. University of Central Florida Press, Orlando, 765 pp.
- Otvos, E.G., 1985. Barrier Island Genesis - Questions of alternatives for the Apalachicola coast, north east Gulf of Mexico. *Journal of Coastal Research*, 1(3): 267-278.
- Otvos, E.G., 1992. Apalachicola coast Quaternary evolution, NE Gulf of Mexico. In: C.H. Cletcher and J.F. Wehmiller (Editors), *Quaternary Coasts of the United States: Marine and Lacustrine Systems*. Society of Economic Paleontologists and Mineralogists, Tulsa, pp. 221-232.
- Otvos, E.G., 2005a. Coastal Barriers, Gulf of Mexico: Holocene Evolution and Chronology. *Journal of Coastal Research*, Special Issue 42: 141-163.
- Otvos, E.G., 2005b. Numerical Chronology of the Late Quaternary Gulf Coastal Plain; Barrier Evolution and an Updated Holocene Sea-Level Curve. *Gulf Coast Association of Geological Societies Transactions*, 55: 629-641.
- Rizk, F.F., 1991. *The Late Holocene development of St. Joseph Spit, Florida State University, Tallahassee*.
- Schnable, J.E. and Goodell, H.G., 1968. *Pleistocene-Recent Stratigraphy, Evolution, and Development of the Apalachicola Coast, Florida., Boulder, Colorado*.
- Sommerville, A.A., Hanson, J.D., Sanderson, D.C.W. and Housley, R.A., 2003. Optically stimulated luminescence dating of large storm events in Northern Scotland. *Quaternary Science Reviews*, 22(10-13): 1085-1092.
- Stapor, F.W., 1973. Coastal sand budgets and Holocene beach ridge plain development - Northwest Florida, Florida State University, Tallahassee, 221 pp.
- Stapor, F.W., 1975. Holocene beach ridge plain development, Northwest Florida. *Zeitschrift für Geomorphologie*, 22: 116-144.

- Stewart, R.A. and Gorsline, D.S., 1962. Recent sedimentary history of St. Joseph Bay, Florida. *Sedimentology*, 1: 256-286.
- Tanner, W.F., 1961. Offshore shoals in area of energy deficit. *Journal of Sedimentary Petrology*, 31(1): 87-95.
- Tanner, W.F., 1992. Three thousand years of sea level change. *Bulletin American Meteorological Society*, 73(3): 297-303.
- Tanner, W.F., 1995. Origin of beach ridges and swales. *Marine Geology*, 129: 149-161.
- Tanner, W.F., Dermipolat, S., Stapor, F.W. and Alvarez, L., 1989. The Gulf of Mexico Late Holocene sea level curve. *Transactions Gulf Coast Association of Geological Societies*, 39(553-562).
- Thompson, J., Rink, W.J. and López, G.I., 2007. Optically-Stimulated Luminescence age of the Old Cedar Midden, St. Joseph Peninsula State Park, Florida. *Quaternary Geochronology*, 2: 350-355.
- USGS, 1982. Indian Pass, Florida 29085-F2-TB-024 7.5 minute series Orthophotomap, Florida.
- USGS, 1999. Digital Orthographic Quarter-Quads Q4642 and Q4641; Indian Pass - West Pass, Florida; 1 m resolution; UTM projection, NAD 83; 8 quarter-quads. FDEP.
- USGS, 2004. Northwest Florida Water Management District (NFWFMD) ADS40 Digital Imagery Acquisition and Natural Color and Color Infrared Orthophoto Production (remote-sensing images). FDEP.
- White, N.M., 2003. Late Archaic in the Apalachicola / Lower Chattahoochee Valley, Northwest Florida, Southwest Georgia, and Southeast Alabama. *The Florida Anthropologist*, 56(2): 69-90.
- White, N.M., Rodriguez, N.D., Smith, C. and Fitts, M.B., 2002. St. Joseph Bay Shell Middens Test Excavations, Gulf County, Florida, 2000-2002: Richardson Hammock site, 8Gu10, and Lighthouse Bayou site, 8Gu114, Division of Historical Resources, Tallahassee.

CHAPTER 7 – FIGURES

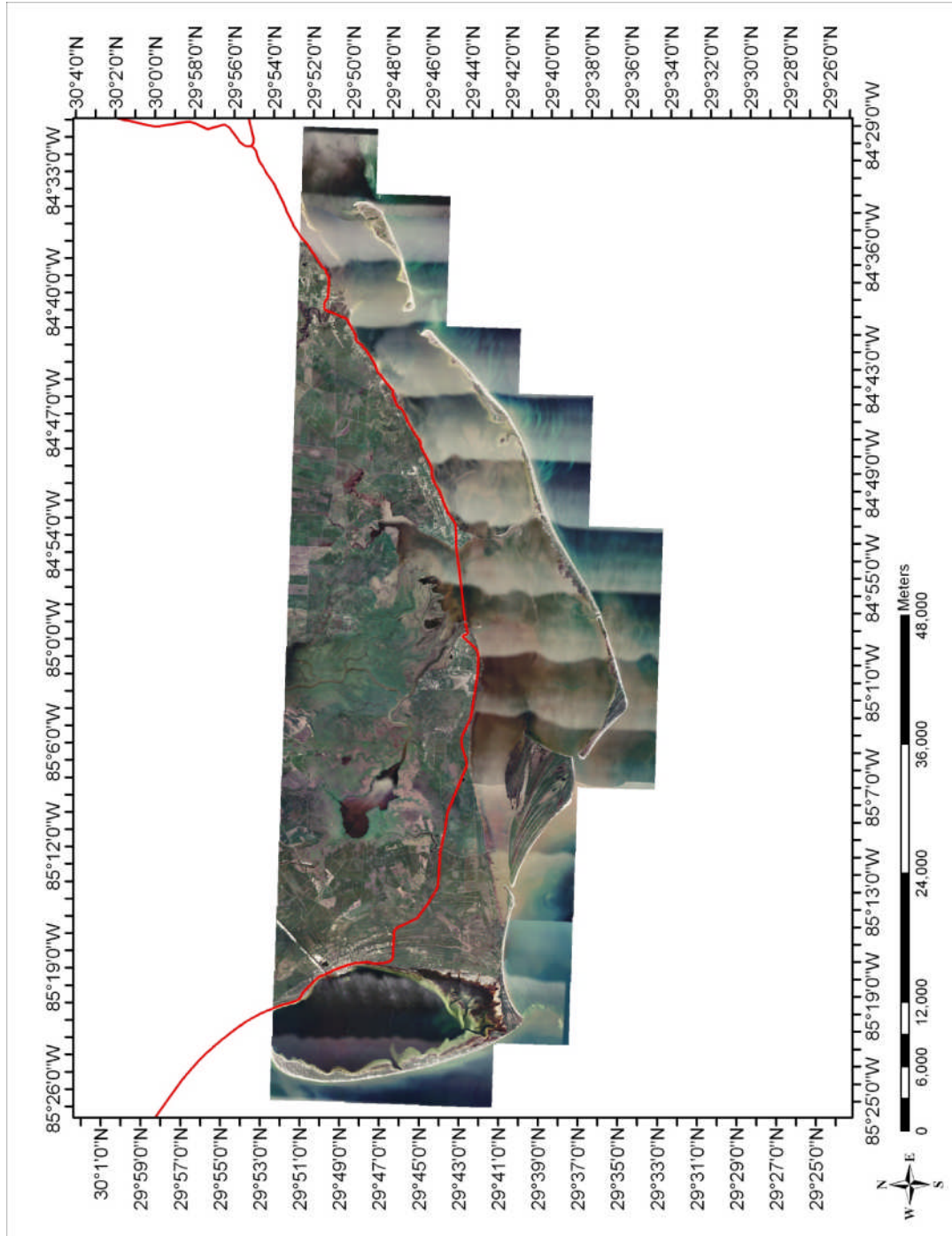


Figure 7.1.

General location of the Apalachicola Barrier Island Complex on the Florida Panhandle, U.S.A. Multiple long-vertical sediment cores were extracted from multiple ridges decorating St. Joseph Peninsula, Cape San Blas, St. Vincent Island and Little St. George Island, as well as Oak Ridge, on the mainland. Image source: FDEP – Natural Colour 2004 Digital Orthographic Quarter-Quad (DOQQ), geographic projection NAD83 (USGS, 2004), <http://data.labins.org/2003/MappingData/DOQQ/doqq.cfm>

Figure 7.2.

Coring the Apalachicola Barrier Islands: a) submerged ridge at SVI #5 site at the end of Road 5, on the northern edge of St. Vincent Island – the dense vegetation in the background corresponds to a small emergent remnant of the same submerged ridge (July 2003, Dr. W.J. Rink and K. Moretton on photo); b) retrieving core with a truck-jack on the northern flank of the SJ002 1 dune (view to the Gulf shore – west –, July 2003, G.I. López and K. Moretton on photo). All photographs by G.I. López.

a)



b)



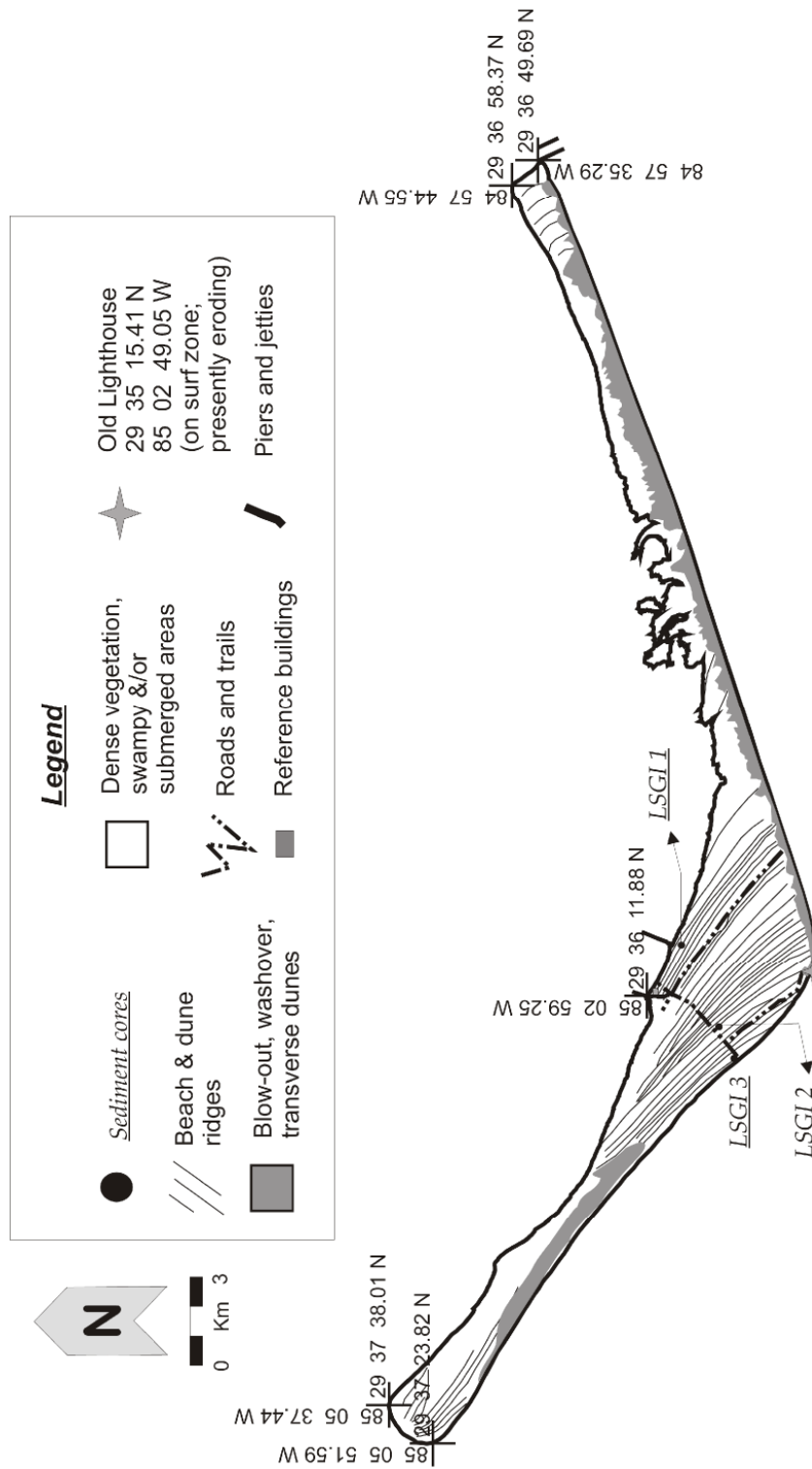
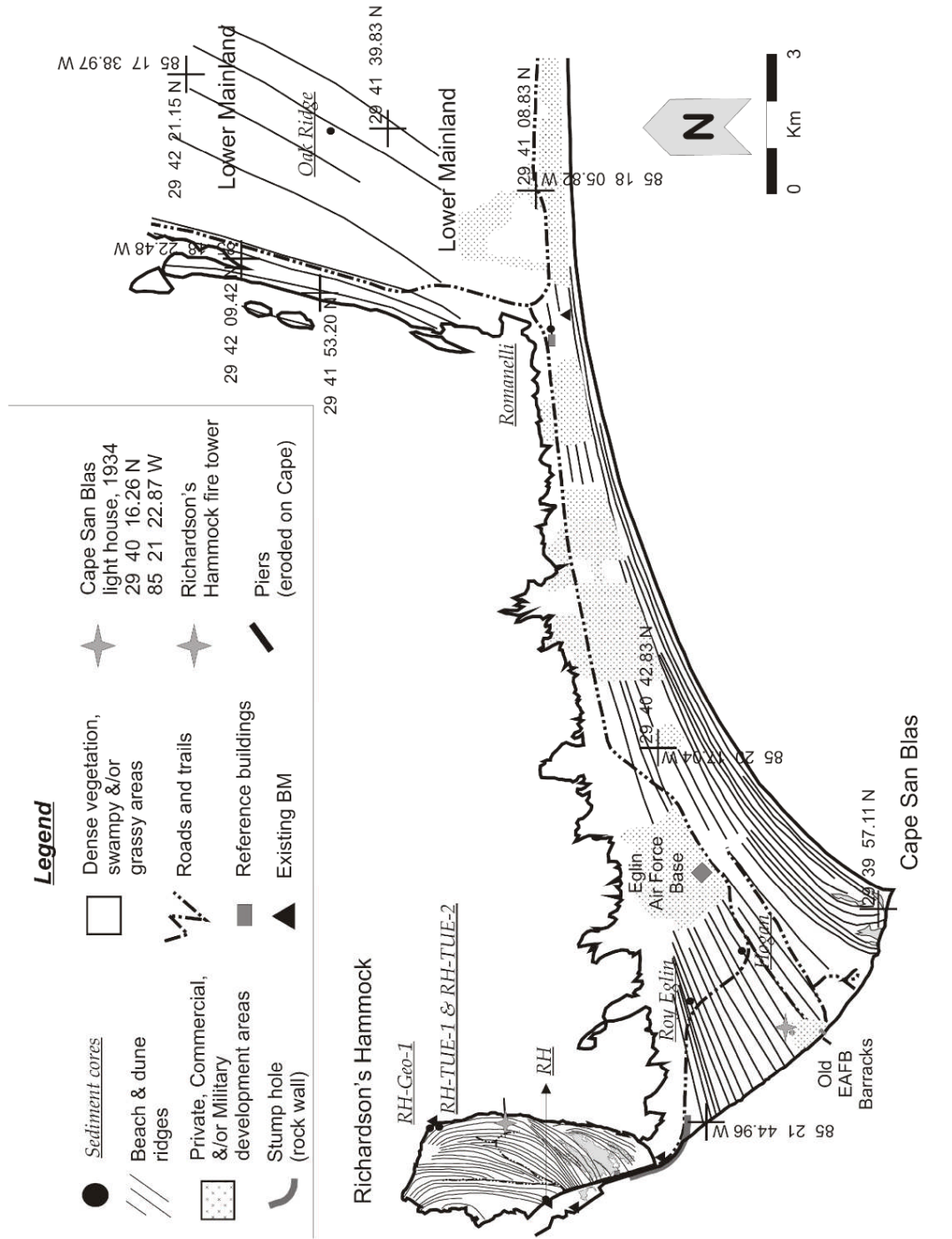


Figure 7.3.

Little St. George Island preserve (administered by ANERR). Location of the three sediment cores, all recovered from different ridges, is marked by black circles with corresponding names and Arabic numbers. The old lighthouse, now on the surf zone, has been severely eroded and has been out of commission since ~ 1970. Island and ridges have been traced from Natural Colour DOQQ images (USGS, 2004); geographic coordinates (NAD 83).

Figure 7.4.

Richardson's Hammock, Cape San Blas and western lower mainland area (see Figure 7.1. for reference). Location of sediment cores is marked by black circles with corresponding names with Arabic numbers (if any): one long vertical (western side) and three short horizontal cores (near and at the Florida 8Gu10 archaeological site) were recovered from Richardson's Hammock (López et al., (under review 2007)); three long vertical cores on Cape San Blas (results in this paper) and one long vertical core on the western lower mainland area (results in this paper). Shorelines and ridges have been traced from Natural Colour DOQQ images (USGS, 2004); geographic coordinates (NAD 83).



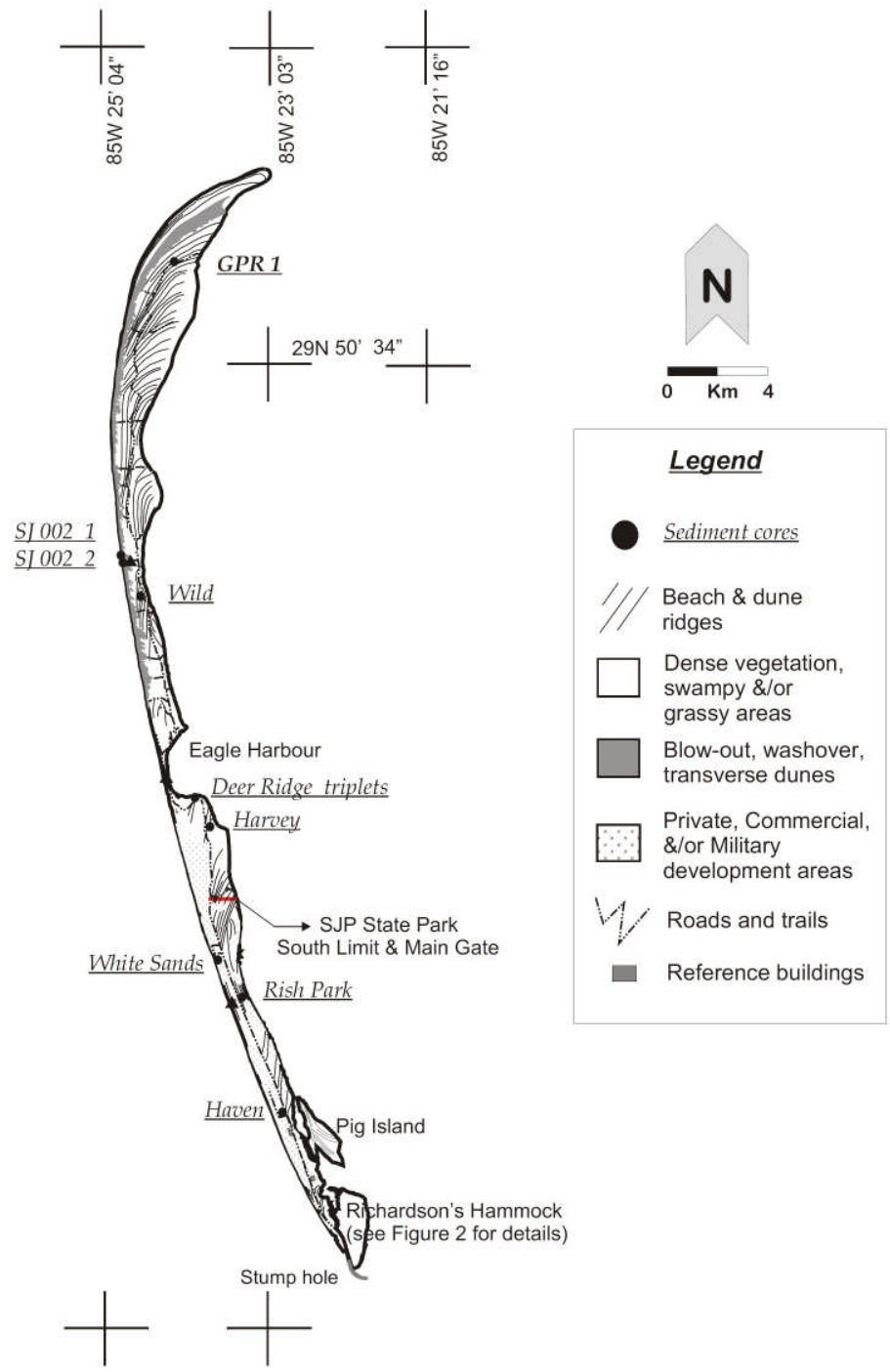
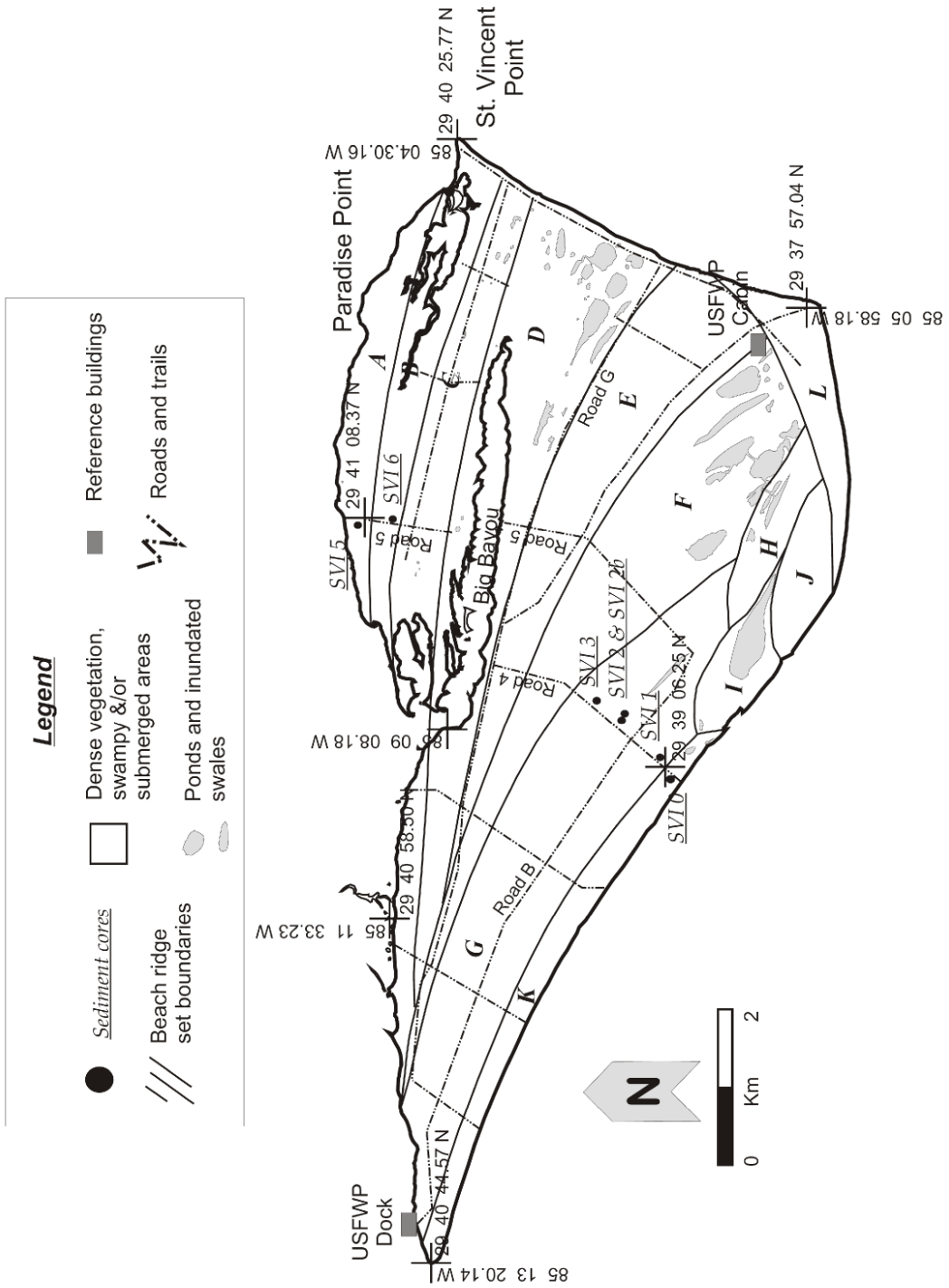


Figure 7.5.

St. Joseph Peninsula. The central-northern part of the peninsula is part of the T.H. Stone Memorial St. Joseph State Park (FDEP) whereas the southernmost region is heavily privately inhabited. Black circles depict the location of coring sites. A total of 11 long vertical sediment cores were recovered from different ridges throughout the peninsula as well as two short horizontal ones at the Florida 8Gu85 Old Cedar archaeological site (López, 2007). Shorelines and ridges have been traced from Natural Colour DOQQ images (USGS, 2004); geographic coordinates (NAD 83).

Figure 7.6.

Site location map of St. Vincent Island (U.S. National Wildlife Refuge). Even though individual ridges have been delimited based on DOQQ images (USGS, 1999) and topographic map data (USGS, 1982), they are not shown here due to their high number. Instead, ridge sets are depicted here. They have been delimited similarly to the proposed division by Tanner: capital letters A through L indicate the chronological sequence of sets (modified from (Tanner, 1992; Tanner et al., 1989)). Dotted line along northern shoreline is an attempted correlation of ridges between east and west portions of this northern coastline as inferred from air-photographs (López and Rink, 2007b). Black circles depict the location of the seven sediment cores recovered from ridges along Roads 4 and 5. Shoreline has been traced from Natural Colour DOQQ images (USGS, 1999; USGS, 2004); geographic coordinates (NAD 83).



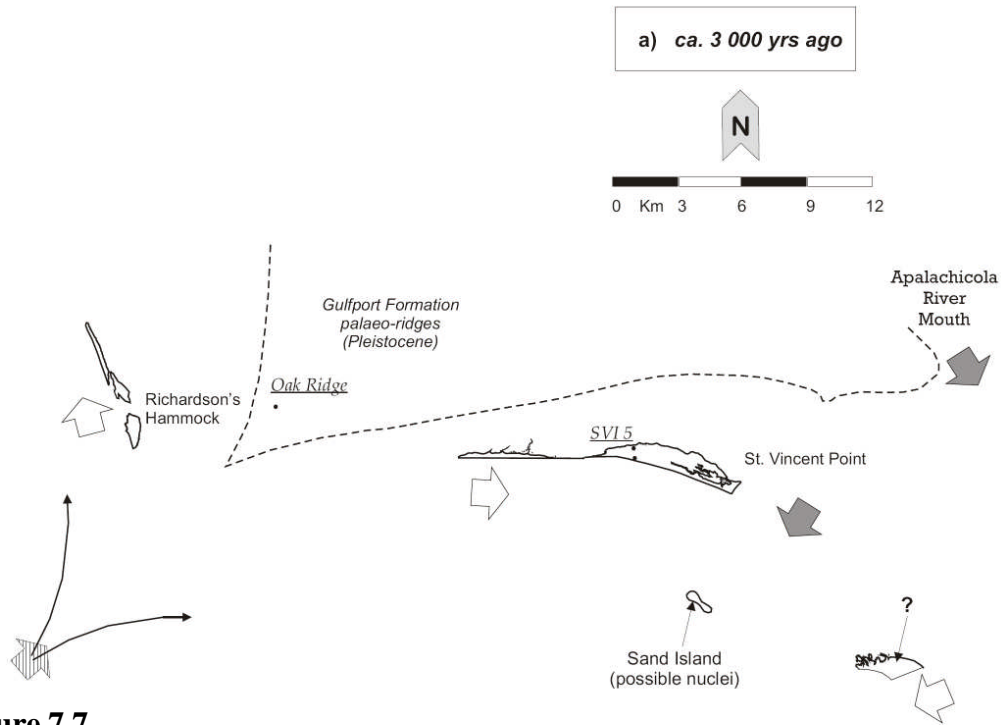
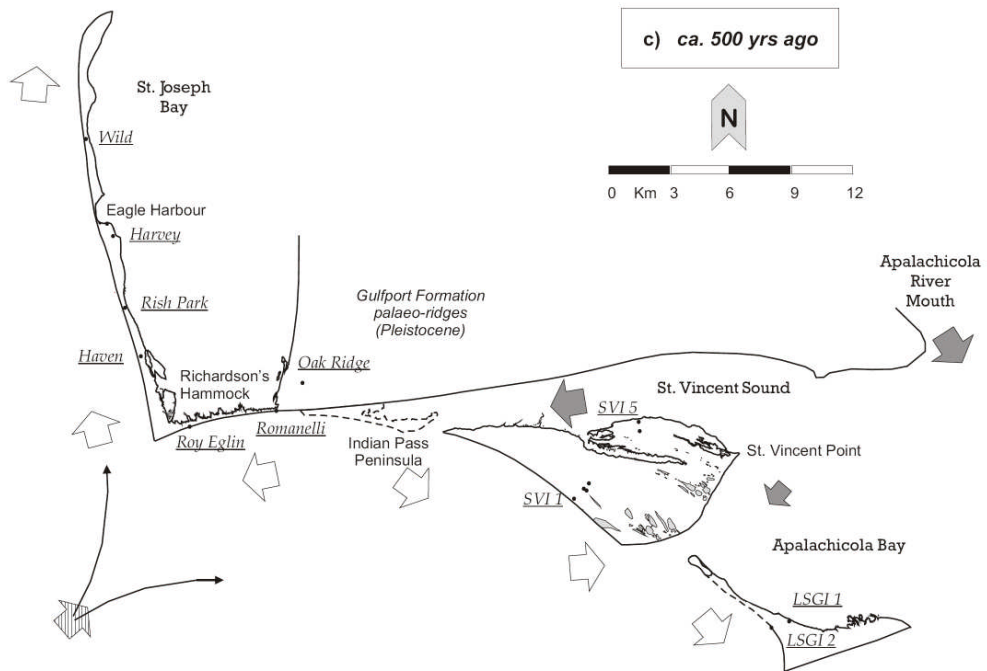
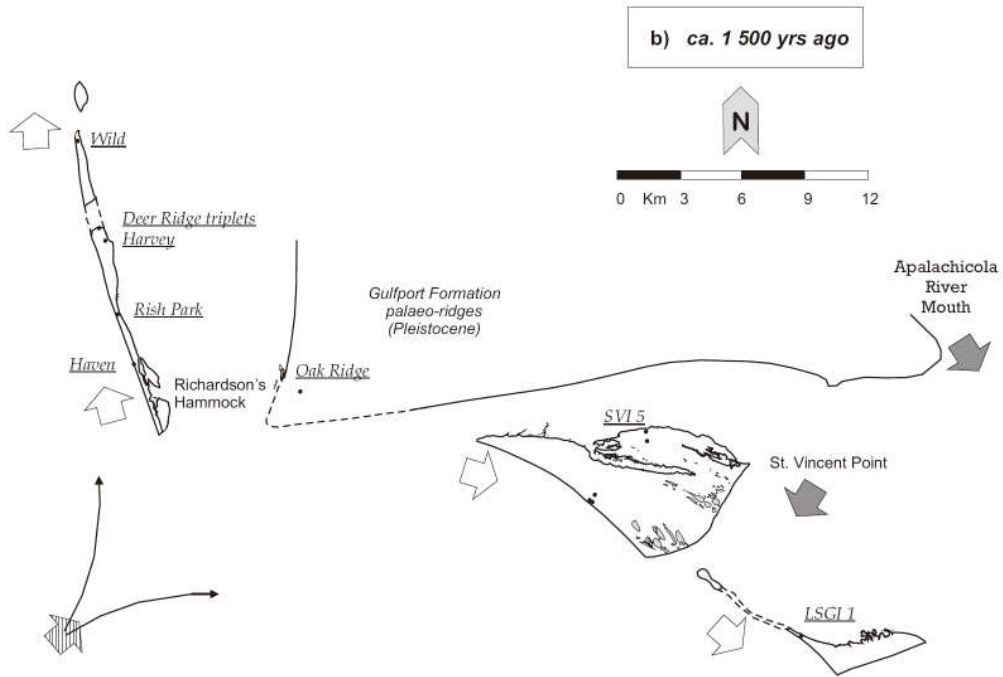
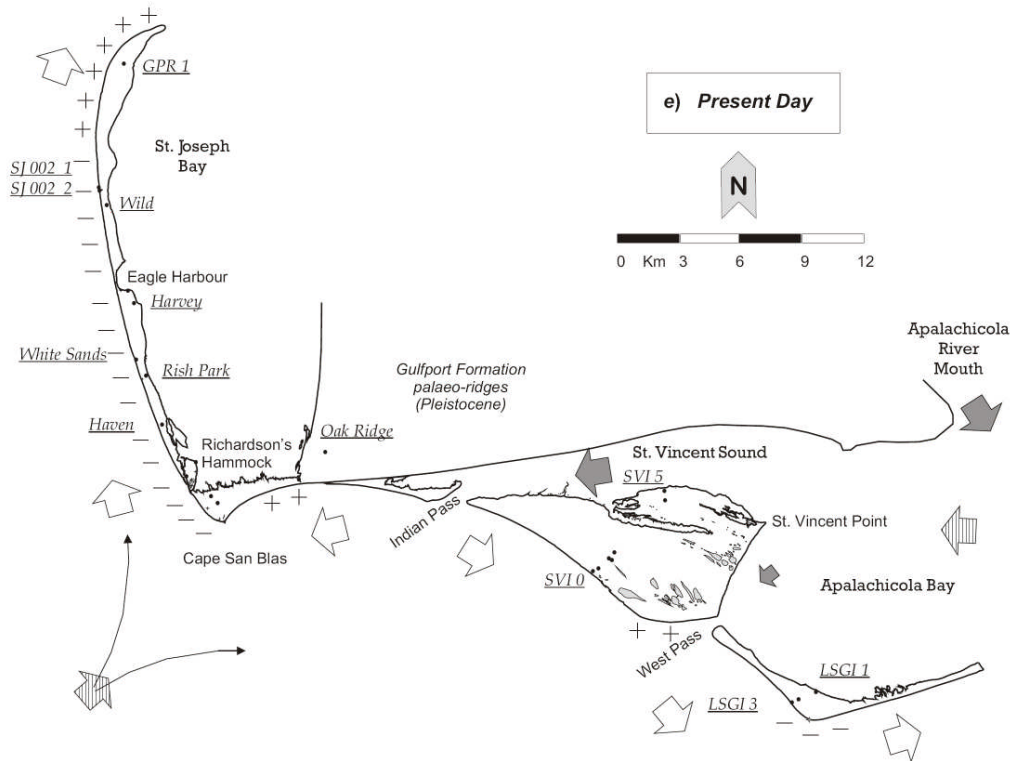
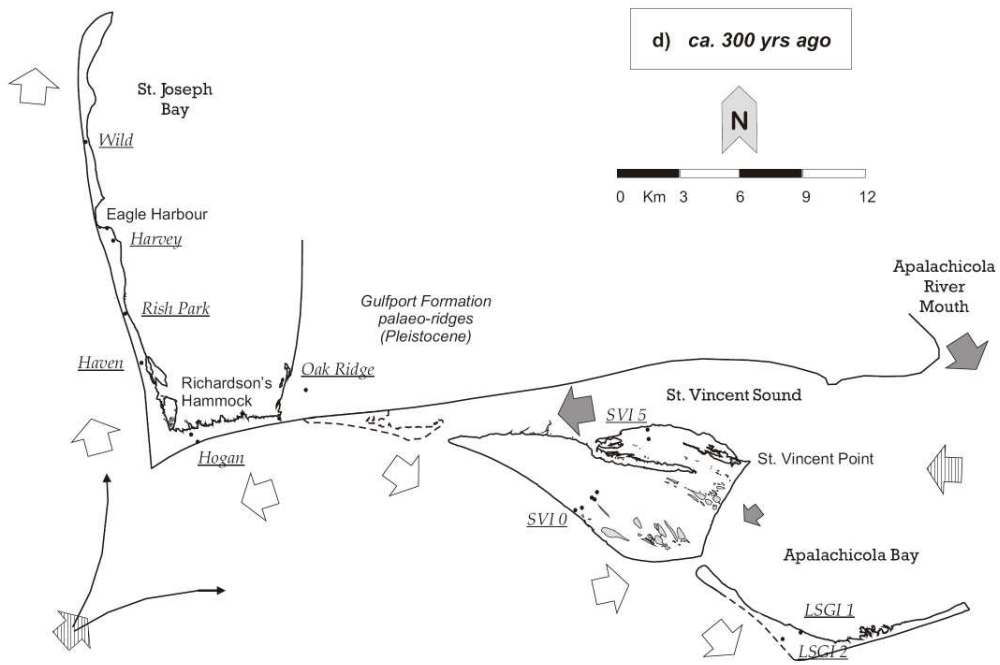


Figure 7.7.

Chronological evolution of the central-eastern barriers pertaining to the Apalachicola Complex based on optical ages obtained by López (2007). Only the estimated surficial progradation of the four barrier systems targeted for this study is shown. Inferred shorelines are shown by dashed lines. Six different time stages are detailed in figures 7.7a. through 7.7e., from ca. 3 000 years ago to present day. Black circles depict sediment core positions. Shorelines shown in figures 7.7a. through 7.7e. are inferred based on our optical ages and ridges/ridge sets geometries and truncations. Shorelines shown in figure 7.7e. were defined based on FDEP 2004 DOQQ images for the area (at MHWL). The barriers' geographical position is maintained as shown in previous figures (see Figures 7.1. through 7.6.). Thick white arrows depict the most probable net longshore drift direction. Thick dashed arrows depict modern tidal currents as evidenced by Gorseline (1966). Thick grey arrows depict the most probable plumes (i.e. sources) of sediment (size of arrow simulates preferential direction). In figure 7.7e., the latter have been constraint to the actual sediment discharge as seen by satellite imagery from April 2004. The positive and negative symbols (+ and -) seen in figure 7.7e. refer to the stretches of coastline that are presently showing progradation and erosion, respectively, based on four years of field observations, comparisons among different years of DOQQ's (USGS, 1999, 2004) and shoreline analyses done by Coastal Tech. and Preble-Rish Inc. (1998)

Figures 7.7b. to 7.7e. continue in the following two pages.





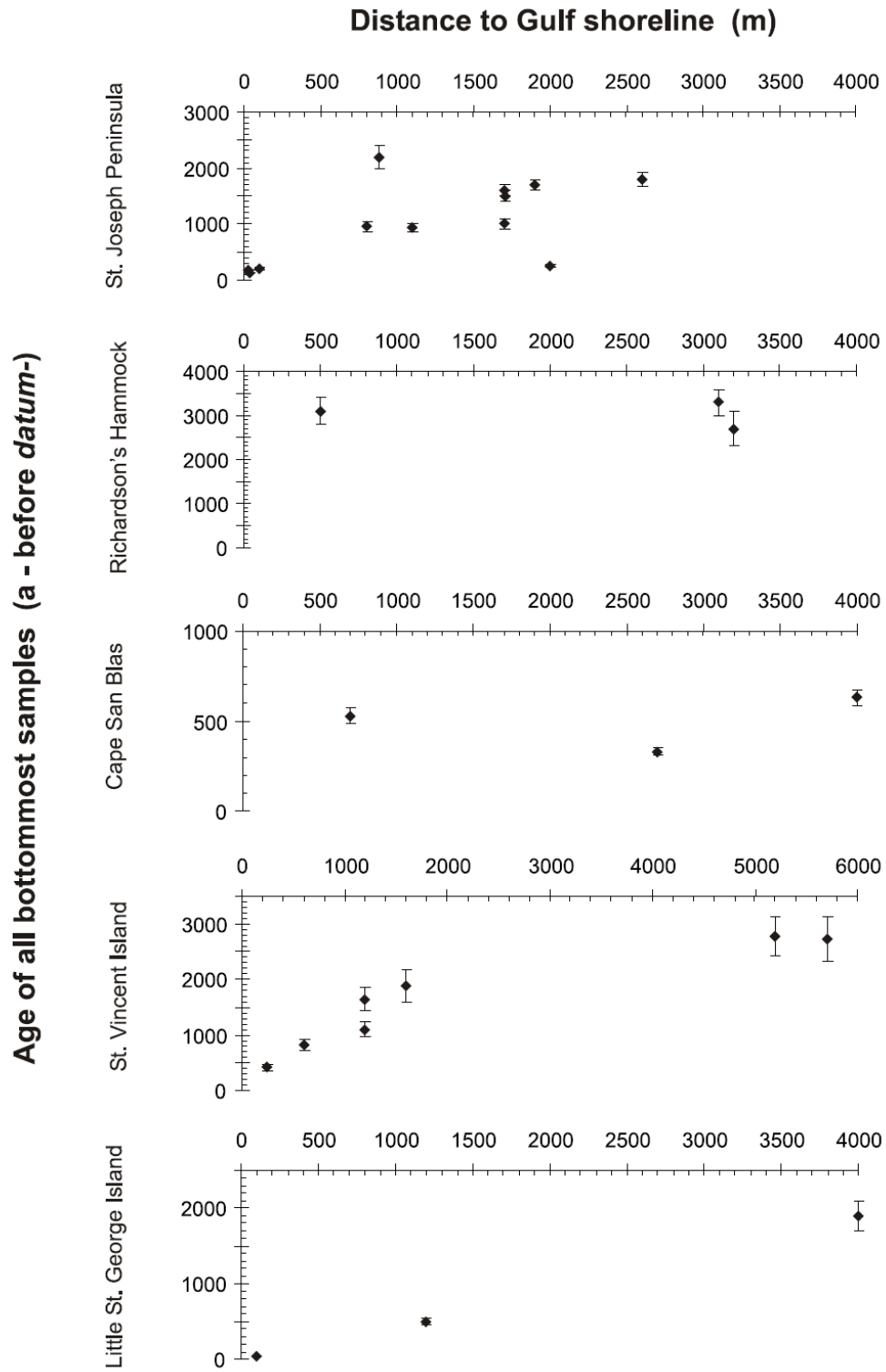
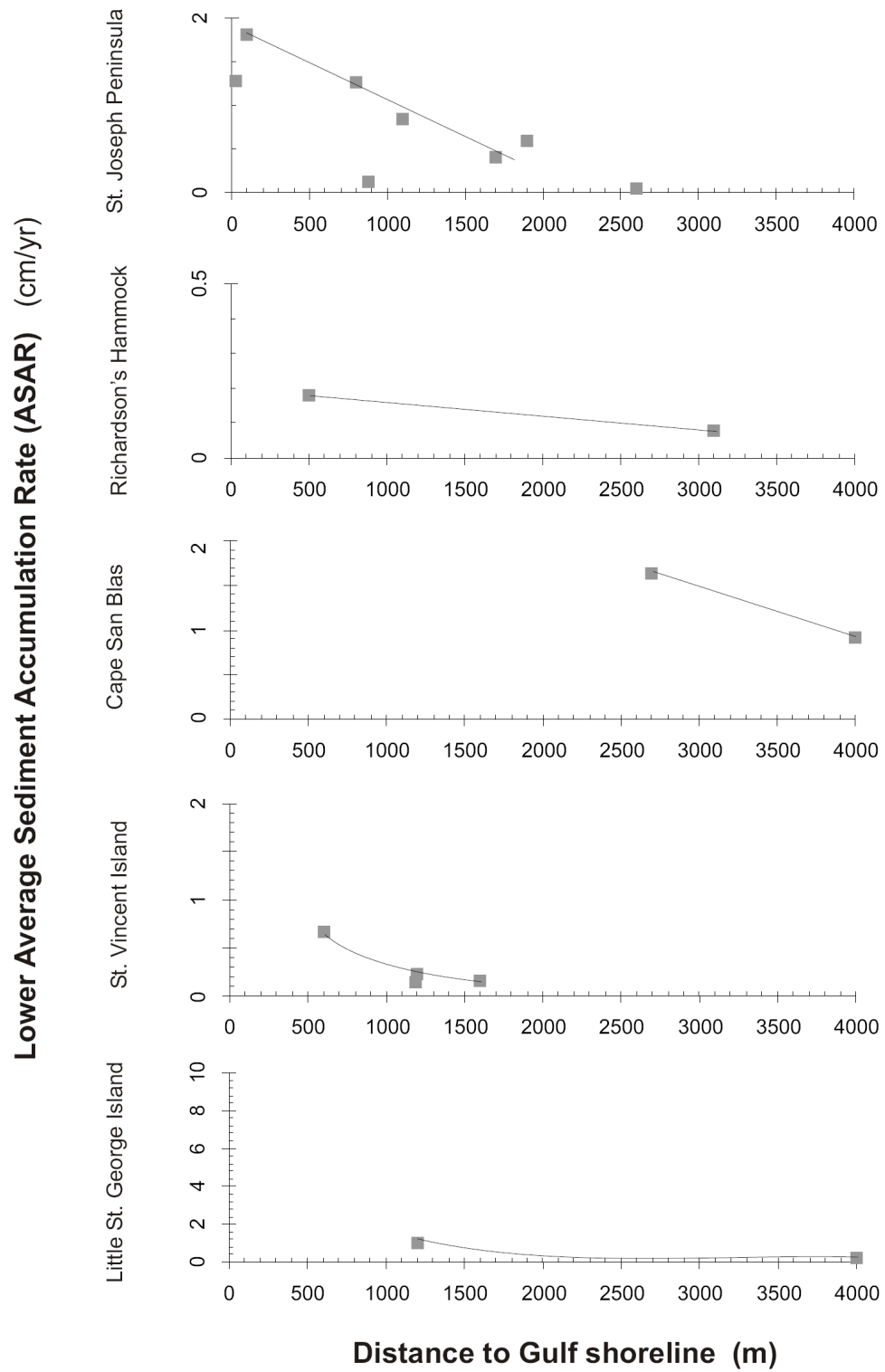


Figure 7.8.

Optical ages of 28 individual quartz fractions retrieved from the ridges decorating the central-western Apalachicola Barrier Island Complex: 25 long vertical cores and three short horizontal cores. The filled diamonds correspond to the ages obtained from the samples taken from the bottommost sections of the vertical cores and the horizontal geological samples collected from archaeological sites (Old Cedar GEO 1, RH-TUE-2 and RH-GEO-1), depicting the terminus ante quem time of formation of those ridges. Samples are organized according to their distance to the modern shoreline (i.e. based on traced maps using 2004 DOQQ's). All the samples taken within Richardson's Hammock are considered to be part of one nucleus. Optical ages shown are years ago relative to their datum, with their individual final errors also plotted (see Tables 7.2. and 7.3.).

Figure 7.9.

Lower Average Sediment Accumulation Rate (ASAR) vs. distance from the Gulf shorelines, calculated from the two consecutive samples within each core or site (i.e. between A and B and OSL1 and OSL2). Only those samples that are in correct stratigraphical order and are distinguishable from each other are shown (see Table 7.4. for details and values). Trend lines were drawn to facilitate overall comparison between all five systems. Higher ASAR values are seen in ridges closer to the shoreline except for CSB which has a reversed trend, due to the different geographical location of the samples (see Figure 7.4.).



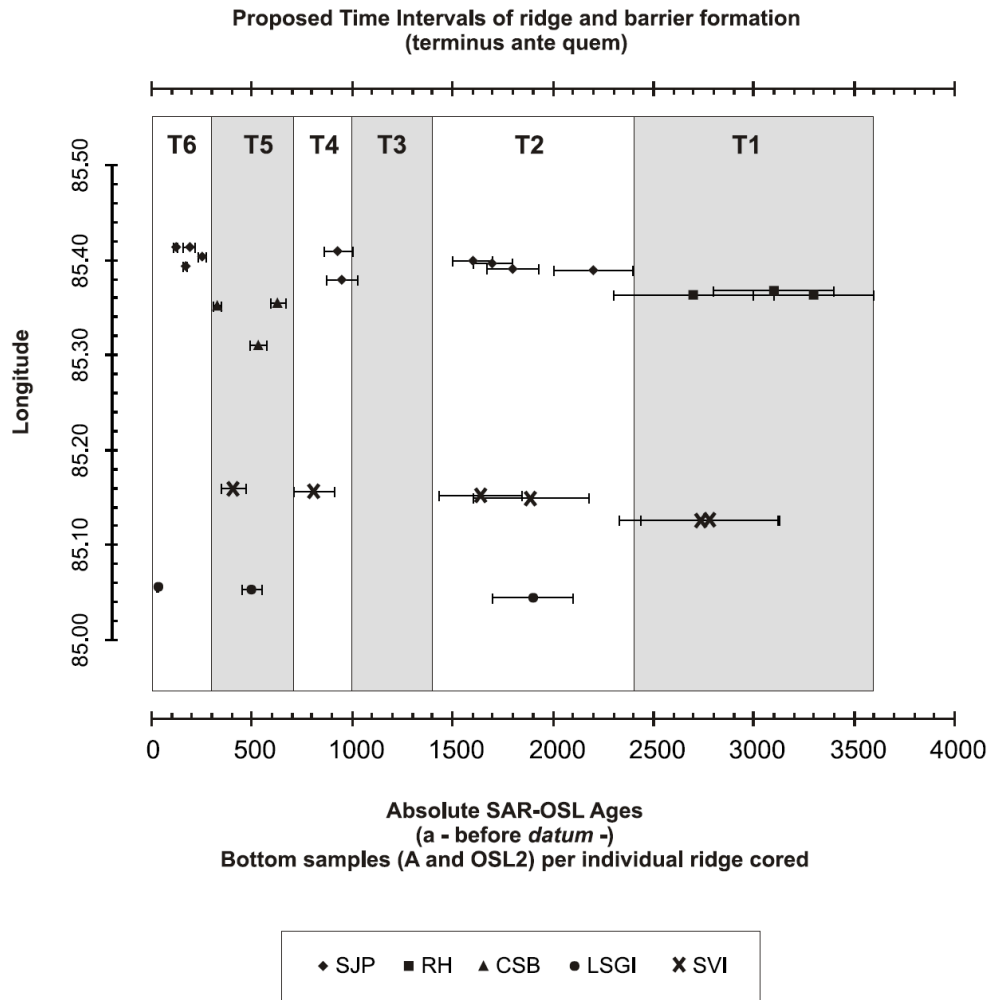


Figure 7.10.

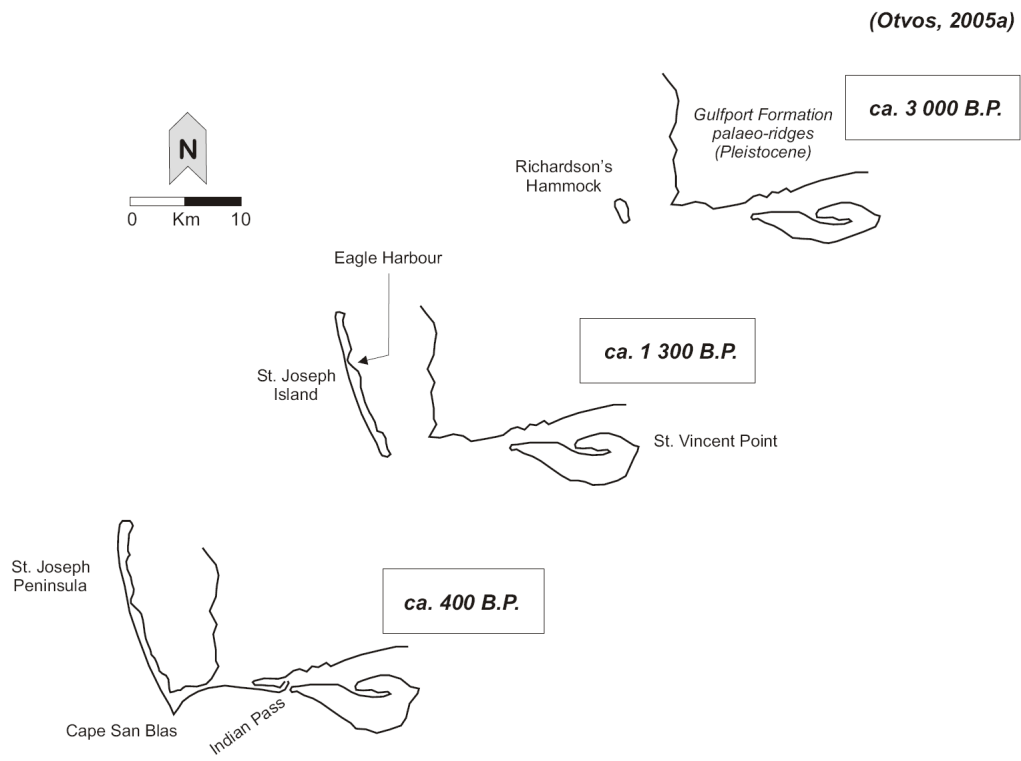
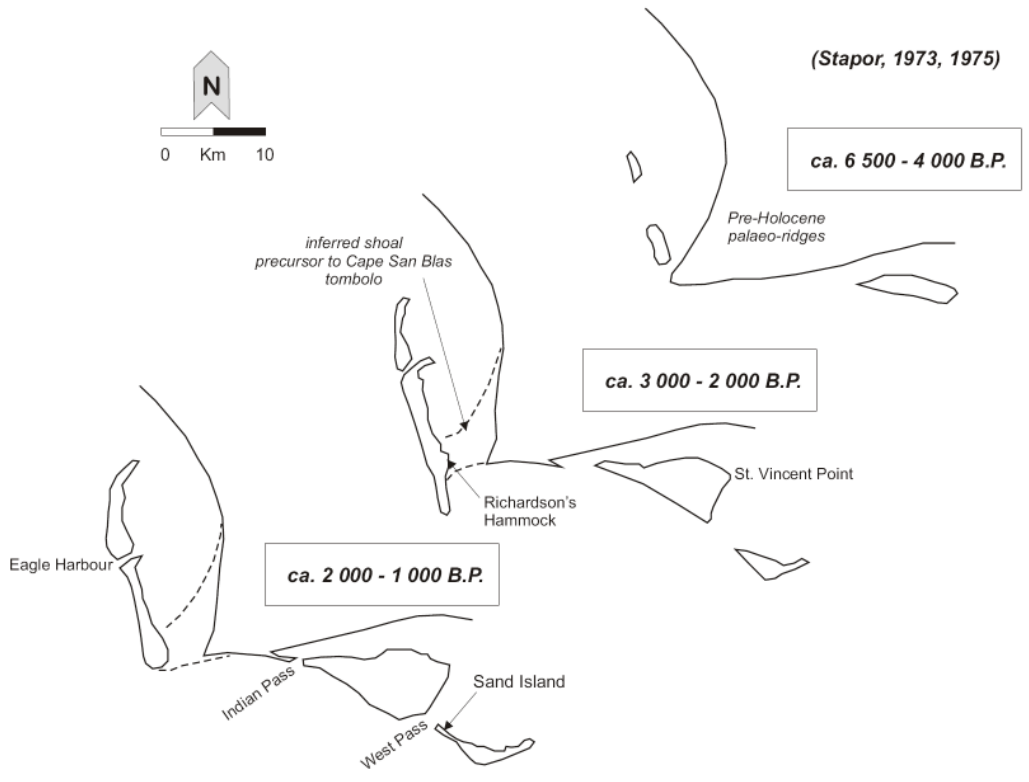
Optical ages versus Longitude positioning (Geographical NAD 83) for all five barrier systems studied: SJP = St. Joseph Peninsula; RH = Richardson’s Hammock; CSB = Cape San Blas; SVI = St. Vincent Island; LSGI = Little St. George Island. Only the bottommost samples from each ridge cored are shown, hence the terminus ante quem moment of ridge formation (i.e. for Deer Ridge, only sample Deer Ridge 2 A is shown). Several “age clusters” can be noted and six different time intervals of formation are proposed: T1 to T6. Such age ranges also correspond to the intervals of formation proposed for Richardson’s Hammock and St. Joseph Peninsula, which concur with the multiple-nuclei-derived hypothesis presented by López (2007). Note that the cluster between present time and 300 years ago does not correspond to a nucleus but rather the much younger samples recovered from foredunes and the northern tip of the peninsula.

Figure 7.11.

General interpretation of the supra-tidal evolution of the western portion of the Apalachicola Barrier Island Complex as suggested by Stapor (1973, 1975). Modified from Stapor (1973). His “present day” complex dates back to 1970 and is very similar to the one depicted in Figure 7.7f. (i.e. Cape San Blas tombolo is fully formed at that stage in time). All shorelines are inferred as per Stapor (1973).

Figure 7.12.

General interpretation of the supra-tidal evolution of the western portion of the Apalachicola Barrier Island Complex as suggested by Otvos (2005a). Modified from his figure 18 (Otvos, 2005a). His “present day” figure is similar to the one depicted in Figure 7.7f. All shorelines are inferred as per Otvos (2005a). He assumes a continuous progradation of St. Joseph Peninsula from the original Richardson’s Hammock precursor nuclei.



LIST OF TABLES

Table 7.1.

Geographical coordinates (NAD 83) and SAR-OSL equivalent dose (D_E) data for quartz fractions recovered during this study from the lower mainland, Cape San Blas and Little St. George Island, Florida, U.S.A.

Core	Latitude N [a]	Longitude W [a]	Sample [b]	Total Length of Sediment Core (cm) [c]	Burial Depth of Sample (cm) [c]	Aliquot Size (mm)	n [d]	ED Value (Gy)	Analytical ED Error (Gy)	Skewness
Oak Ridge	29° 41' 51.29"	85° 17' 52.01"	B	239.23	118.43	8	16	8.52	2.02	0.68
			A		213.18	3	24	5.83	1.09	0.97
			B		90.14	8	24	52.28	1.26	0.08
			A		301.56	3	22	41.65	8.16	1.60
Roy Eglin	29° 40' 35.95"	85° 21' 16.15"	B	331.88	90.14	8	23	0.11	0.00	0.17
			A		301.56	3	23	0.11	0.00	0.58
			B		112.23	8	22	0.21	0.00	0.06
			A		209.77	3	24	0.19	0.00	0.17
Hogan	29° 40' 25.39"	85° 21' 04.89"	B	218.00	112.23	8	22	0.08	0.01	0.94
			A		209.77	3	20	0.07	0.00	-0.23
			B		84.96	8	22	0.10	0.00	-0.33
			A		349.19	3	20	0.11	0.01	0.25
Romanelli	29° 41' 05.57"	85° 18' 38.39"	B	360.23	84.96	8	24	0.04	0.00	0.19
			A		349.19	3	16	0.05	0.01	-0.15
			B		95.86	8	22	0.49	0.02	-0.09
			A		214.38	3	22	0.49	0.10	1.08
LSGI 1	29° 36' 00.07"	85° 02' 38.23"	B	272.77	95.86	8	17	0.47	0.03	0.98
			A		214.38	1	14	0.48	0.02	-0.50
			B		84.30	8	24	0.65	0.05	0.83
			A		192.69	3	24	0.59	0.05	0.80
LSGI 2	29° 35' 47.11"	85° 03' 10.87"	B	222.80	84.30	8	22	0.12	0.01	1.00
			A		192.69	3	22	0.16	0.06	0.84
			B		90.72	8	17	0.14	0.01	-0.66
			A		158.76	1	12	0.13	0.02	1.53
LSGI 3	29° 35' 41.71"	85° 03' 22.57"	B	226.80	90.72	8	10	0.01	0.00	0.18
			A		158.76	3	12	0.02	0.00	0.00
			B		90.72	8	17	0.01	0.00	0.99
			A		158.76	1	12	0.02	0.00	0.26

[a] Geographic Coordinates (NAD 83).

[b] A = sample taken towards the bottom of the core; B = sample taken towards the top of the core. Both are ~1 m apart or greater.

[c] Depth values have been corrected for compaction.

[d] Number of aliquots accepted for calculation of the equivalent dose after all criteria was met (e.g. within recycling ratio; excluding 2σ outliers, etc.)

Table 7.2. SAR-OSL ages and data obtained for quartz fractions (150-212µm) from the long vertical sediment cores recovered from the lower mainland, Cape San Blas and Little St. George Island, Florida, U.S.A.

Core	Sample		Analytical		U (ppm) [c]	Th (ppm) [c]	K (ppm) [c]	Water Content (%) [d]	Cosmic Dose Rate (µGy/a) [e]	Annual Dose (µGy/a) [f]	SAR-OSL		Datum [g]
	[a]	(Gy) [b]	ED Value (Gy) [b]	ED Error (Gy) [b]							age (a) [g]	error (a) [g]	
Oak Ridge	B	8.52	2.02	0.32 ± 0.1	1.04 ± 0.09	176 ± 13	14	195	352 ± 16	24 200	5 800	2006	
	A	52.28	1.26	0.37 ± 0.1	1.11 ± 0.09	38 ± 8	16	181	339 ± 15	154 200	10 400	2006	
Roy Eglin	B	0.11	0.00	0.17 ± 0.1	0.20 ± 0.04	176 ± 17	14	203	277 ± 15	400	30	2004	
	A	0.21	0.00	0.41 ± 0.1	0.87 ± 0.07	78 ± 15	8	171	336 ± 16	630	40	2004	
Hogan	B	0.08	0.01	0.18 ± 0.1	0.40 ± 0.10	328 ± 14	18	197	295 ± 15	270	30	2006	
	A	0.10	0.00	0.25 ± 0.1	0.50 ± 0.10	380 ± 17	22	182	301 ± 15	330	20	2006	
Romanelli	B	0.04	0.00	0.37 ± 0.1	0.90 ± 0.10	357 ± 16	3	205	396 ± 17	100	6	2006	
	A	0.49	0.02	1.53 ± 0.1	5.70 ± 0.40	148 ± 12	4	165	927 ± 26	530	40	2006	
LSGI 1	B	0.47	0.03	0.16 ± 0.1	0.35 ± 0.05	988 ± 35	19	201	346 ± 15	1 400	100	2006	
	A	0.65	0.05	0.25 ± 0.1	0.93 ± 0.08	364 ± 18	3	181	348 ± 17	1 900	200	2006	
LSGI 2	B	0.12	0.01	0.16 ± 0.1	0.52 ± 0.06	222 ± 15	3	206	309 ± 17	390	40	2006	
	A	0.14	0.01	0.16 ± 0.1	0.56 ± 0.06	146 ± 13	8	184	279 ± 16	500	50	2006	
LSGI 3	B	0.01	0.00	0.36 ± 0.1	1.87 ± 0.14	284 ± 16	5	202	446 ± 18	22	4	2006	
	A	0.01	0.00	0.18 ± 0.1	0.68 ± 0.07	262 ± 16	7	188	307 ± 16	32	3	2006	

[Notes for Table 7.2.]

- [a] A = sample taken towards the bottom of the core; B = sample taken towards the top of the core. Both are at least 1 m apart.
- [b] Equivalent doses and errors from large aliquots: all 8 mm mask.
- [c] U, Th and K values determined by NAA at Nuclear Reactor facility, McMaster University.
- [d] Water content as a fraction of dry weight determined from laboratory measurements.
- [e] Cosmic-ray dose rate value calculated using an overburden density of 2 g/cm³ and accounting for ridge geometry.
- [f] All β and γ dose rates were calculated based on U, Th and K concentrations of each sample accounting for moisture values of the sample.
- [g] Datum values (i.e. measurement year) for SAR-OSL ages are given in column.
- * Ages were calculated assuming constant sediment accumulation rates (i.e. linear sediment accumulation).
- ^ Values rounded off to sensible number of precision.

Table 7.3.

Compilation of SAR-OSL ages obtained for previously reported barriers of the Apalachicola Complex, Florida, U.S.A. Geographical coordinates (NAD 83) are also given.

- [a] GPS Geographic Coordinates (NAD 83).
- [b] A and OSL1 correspond to samples taken towards the bottom of the core and B and OSL2 towards the top of the core, at least 1 m above A or OSL1.
- [c] Depth values have been corrected for compaction.
- [d] Datum for SAR-OSL ages is: [04] for A.D. 2004; [05] for A.D. 2005; [06] for A.D. 2006.
- ^ Values have been rounded to nearest sensible number of precision.
- * Only ages showing this symbol were calculated assuming instant sediment accumulation rates. Otherwise, all other ages were calculated assuming constant (i.e. linear) sediment accumulation rates.
- + Horizontal sediment cores: sample was taken from the most central region of each core.

Table 7.3. is on following page.

[Table 7.3.]

Core	Latitude N [a]	Longitude W [a]	Sample [b]	Burial Depth of Sample (cm) [c]	SAR-OSL Age Value	(a) ^ error	Datum [d] *
St. Joseph Peninsula:							
Haven	29° 42' 21.90"	85° 22' 47.22"	B	108.93	840	60	[06]
			A	248.97	950	80	[06]
Rish Park	29° 43' 39.06"	85° 23' 19.86"	B	63.26	1600	100	[05]
			A	143.77	2200	200	[05]
White Sands	29° 44' 03.36"	85° 23' 38.40"	B	62.38	24	1	[06]
			A	249.50	170	10	[06]
Old Cedar 1	29° 44' 55.36"	85° 23' 27.87"	+	25.00	940	100	[05] *
Old Cedar Geo 1	29° 44' 55.36"	85° 23' 27.87"	+	70.00	1800	130	[05]
Harvey	29° 42' 28.39"	85° 23' 46.44"	B	89.54	1300	200	[06]
			A	329.51	1700	100	[06]
Deer Ridge SJ201	29° 45' 48.18"	85° 23' 55.56"	A	135.14	1000	80	[04]
Deer Ridge 1	29° 45' 48.90"	85° 23' 55.68"	B	90.57	1300	100	[06]
			A	169.82	1500	100	[06]
Deer Ridge 2	29° 45' 48.96"	85° 23' 55.80"	A	151.92	1600	100	[06]
Wild	29° 47' 55.96"	85° 24' 34.96"	B	86.71	690	60	[06]
			A	290.78	930	70	[06]
SJ 002 1	29° 48' 23.92"	85° 24' 48.50"	B	139.99	140	20	[06]
			A	230.91	190	30	[06]
SJ 002 2	29° 48' 24.90"	85° 24' 52.08"	B	91.67	110	8	[06]
			A	173.88	120	8	[06]
GPR 1	29° 51' 39.29"	85° 24' 14.19"	B	99.05	220	40	[06]
			A	217.94	250	20	[06]
Richardson Hammock:							
RH-TUE-1	29° 41' 25.66"	85° 21' 46.82"	+	30.00	1400	100	[05] *
RH-TUE-2	29° 41' 25.66"	85° 21' 46.82"	+	190.00	3300	300	[05]
RH-GEO-1	29° 41' 26.70"	85° 21' 46.80"	+	230.00	2700	400	[05]
RH	29° 41' 03.95"	85° 22' 03.12"	B	170.08	2300	200	[05]
			A	317.83	3100	300	[05]
St. Vincent Island:							
SVI #0	29° 39' 01.41"	85° 09' 32.62"	OSL 2	102.41	370	50	[04]
			OSL 1	180.88	410	60	[04]
SVI #1	29° 39' 06.98"	85° 09' 23.04"	OSL 2	100.75	710	70	[04]
			OSL 1	167.40	810	100	[04]
SVI #2	29° 39' 22.98"	85° 09' 06.06"	OSL 2	99.93	780	100	[04]
			OSL 1	217.09	1640	210	[04]
SVI #2b	29° 39' 23.34"	85° 09' 05.58"	OSL 2	98.50	840	100	[04]
			OSL 1	159.57	1100	130	[04]
SVI #3	29° 39' 32.58"	85° 08' 57.30"	OSL 2	103.76	920	130	[04]
			OSL 1	246.43	1890	290	[04]
SVI #5	29° 41' 08.28"	85° 07' 33.96"	OSL 2	103.58	2860	340	[04]
			OSL 1	222.62	2730	400	[04]
SVI #6	29° 40' 53.34"	85° 07' 34.86"	OSL 2	88.88	2790	290	[04]
			OSL 1	156.09	2780	340	[04]

Table 7.4.

Compilation of Average Sediment Accumulation Rate (ASAR) for cores and archaeological sites having been sampled at two different depth intervals. Distances of cores to the modern shoreline are also given as well as whether or not the samples' ages are statistically distinguishable from each other.

Core	Distance from Gulf shoreline (m) [a]	Sample [b]	Lower ASAR (cm/a) [c]	Upper ASAR (cm/a) [d]	OSL Age Range (a) [e] ^		Ages Statistical Distinction [f]
					Min.	Max.	
St. Joseph Peninsula:							
Haven	800	B	1.27	0.13	780	900	y
		A			870	1030	
Rish Park	880	B	0.13	0.04	1500	1700	y
		A			2000	2400	
White Sands	30	B	1.28	2.6	23	25	y
		A			160	180	
Old Cedar 1	2600	+	0.05	0.03	840	1040	y
Old Cedar Geo 1		+			1670	1930	
Harvey	1900	B	0.6	0.07	1100	1500	y
		A			1600	1800	
Deer Ridge SJ201	1700	A	*	*	920	1080	*
Deer Ridge 1	1700	B	0.4	0.07	1200	1400	y
		A			1400	1600	
Deer Ridge 2	1700	A	*	*	1500	1700	*
Wild	1100	B	0.85	0.13	630	750	y
		A			860	1000	
SJ 002 1	100	B	1.82	1	120	160	y
		A			160	220	
SJ 002 2	40	B	8.22	0.83	102	118	n
		A			112	128	
GPR 1	2000	B	3.96	0.45	180	260	n
		A			230	270	
Lower Mainland & Cape San Blas:							
Oak Ridge	n/a	B	0.0007	0.0049	18400	30000	y
		A			143800	164600	
Roy Eglin	4000	B	0.92	0.23	370	430	y
		A			590	670	
Hogan	2700	B	1.63	0.42	240	300	y
		A			310	350	
Romanelli	700	B	0.61	0.85	94	106	y
		A			490	570	

[cont. Table 7.4.]

Core	Distance from Gulf shoreline (m) [a]	Sample [b]	Lower ASAR (cm/a) [c]	Upper ASAR (cm/a) [d]	OSL Age Range (a) [e] ^		Ages Statistical Distinction [f]
					Min.	Max.	
Richardson Hammock:							
RH-TUE-1	3100	+	0.08	0.02	1300	1500	y
RH-TUE-2		+			3000	3600	
RH-GEO-1	3200	+	*	*	2300	3100	*
RH	500	B	0.18	0.07	2100	2500	y
		A			2800	3400	
St. Vincent Island:							
SVI #0	240	OSL 2	1.96	0.28	320	420	n
		OSL 1			350	470	
SVI #1	600	OSL 2	0.67	0.14	640	780	y
		OSL 1			710	910	
SVI #2	1190	OSL 2	0.14	0.13	680	880	y
		OSL 1			1430	1850	
SVI #2b	1200	OSL 2	0.23	0.12	740	940	y
		OSL 1			970	1230	
SVI #3	1600	OSL 2	0.15	0.11	790	1050	y
		OSL 1			1600	2180	
SVI #5	5700	OSL 2	**	0.04	2520	3200	n'
		OSL 1			2330	3130	
SVI #6	5200	OSL 2	**	0.03	2500	3080	n'
		OSL 1			2440	3120	
Little St. George Island:							
LSGI 1	4000	B	0.24	0.07	1300	1500	y
		A			1700	2100	
LSGI 2	1200	B	0.99	0.22	350	430	y
		A			450	550	
LSGI 3	100	B	6.80	4.12	18	26	n
		A			29	35	

[Notes for Table 7.4.]

Burial depths for each sample are given in Tables 7.1. and 7.3.

- [a] Actual perpendicular distance to Gulf shoreline based on DOQQ images (USGS, 2004) and Geographic Coordinates (NAD 83).
- [b] A and OSL1 correspond to samples taken towards the bottom of the core and B and OSL2 towards the top of the core.
- [c] Values corresponding to the lower part of the core: calculations for depth interval between samples OSL1 and OSL2.
- [d] Values corresponding to the upper part of the core: calculations for depth interval between sample OSL2 and the ground surface.
- [e] For calculated OSL ages, please refer to Tables 7.2. and 7.3.
- [f] OSL ages for samples A and B, within a given core or site, are in correct stratigraphical order and:
 - y = their values are distinguishable from each other; n = their values are indistinguishable from each other, so ASAR is false and indicates very rapid sedimentation;
 - n' = Lower ASAR cannot be calculated due to their indistinguishable and reverse character.
- + Horizontal sediment cores: sample was taken from the most central region of each core.
- ^ Values have been rounded to nearest sensible number of precision.
- * Sample stands alone, so no ASAR calculation is possible.
- ** OSL ages for samples A and B are statistically indistinguishable from each other and/or in reverse order.

CHAPTER 8

GENERAL CONCLUSIONS AND FUTURE RESEARCH

This dissertation involved a geomorphological, sedimentological and geochronological assessment of a multitude of beach and dune ridges forming four major coastal barrier systems, in order to provide a comprehensive understanding of the general evolution of the Apalachicola Barrier Island Complex. Four major coastal barriers and one minor system perched along 60 km of Gulf shoreline were targeted in this study: St. Joseph Peninsula (SJP), Cape San Blas (CSB), St. Vincent Island (SVI), Little St. George Island (LSGI) and Richardson's Hammock, respectively. The Late Quaternary supra-tidal evolution of this coastal complex situated in the north-western Gulf coast of Florida was successfully determined from optical dating chronologies and detailed coastal geomorphological and historical analyses. Both, lateral progradation and vertical accretion rates were obtained and utilized to better appraise the overall evolution of these systems.

The only viable method able to provide such detailed chronologies was optical dating due to the lack of organic materials (i.e. carbonates and carbonaceous) in the clastic quartz-rich coastal sedimentary deposits forming these barrier islands. A total of 55 optical ages were obtained using the protocols established for single-aliquot regenerative-dose (SAR) optically stimulated luminescence (OSL) dating.

This research has proven to be a valuable contribution to the general knowledge of barrier island development in this region of the Gulf of Mexico, especially in geochronological terms, as previously published age information is sparse, erroneous in some cases, or non-existent. Only a few poorly constrained radiocarbon ages exist for the region as well as some archaeological data, rendering the optical ages obtained during this research important for the general understanding of the timing of formation of these barrier islands and their evolution through geological time. Hence, the most significant contribution that this dissertation provides is the understanding of the supra-tidal evolution of the central-west region of the Apalachicola Barrier Island Complex.

Even though this research does not provide more detailed specifics in terms of sea level fluctuations for this region of the Gulf of Mexico, the oldest optical ages obtained for the studied area suggest that sea level may have been stable at around 3,000 years ago rather than 5,000 to 6,000 as stated in previous publications. This new evidence may have implications in the previous

understanding of the evolution of coastal systems and Late Holocene sea level changes in the Gulf of Mexico. However, more detailed research is needed, so it can be compared with already proposed sea level curves for the region.

As for future research, detailed investigations regarding the relationship between ridge formation/stratigraphy, optical ages and sea level should be appraised in order to better constrain, if possible, the sea level interpretations already published for this region of the Gulf of Mexico. For this, precise elevations have to be obtained from each one of the samples believed to represent water-lain lithosomes (i.e. closest to sea level at the time of deposition), in order to link their ages to present mean sea level and, hence, better hypothesize past fluctuations. Even though this was contemplated by the candidate during her research, a series of unfortunate events occurred to the elevation data collected for the majority of the cored sites, and this goal could not be achieved during the present study, however it is still being considered for the immediate future.

In the same line of thought and for this type of coastal environments, one should always try to collect samples as deep as possible within beach/dune ridges to enable tackling the base of formation of each individual ridge. Samples at this depth would provide better information relevant to sea level studies. This could be achieved only if deep coring is possible and/or achieved. Even though vibro-coring is an inexpensive and simple method to recover sediment cores, it may not always be the most effective method to use when the goal is to reach those deeper ridge layers.

Detailed studies of erosion rates both on the barrier islands and the mainland should be obtained as there are presently few available (mostly for St. Joseph Peninsula). The latter in order to elucidate possible sediment supply histories that would help better comprehend the barrier islands' progradation and almost constant evolution over the past 3,000 years. If erosion rates are known for the mainland, it could be possible to calculate the amount of sediment supplied by the Apalachicola River during different time periods, and be able to link them to potential climatic fluctuations.

This research demonstrated the feasibility of obtaining good estimates of coastal barrier evolution based on detailed geochronological, geomorphological and sedimentological work. However, much precise time intervals of individual ridge, ridge sets and barrier formation could have been obtained if, for example, more ridges (e.g. within all the individual ridge sets) would have been targeted and more sediment cores recovered, so more optical ages could have been obtained. This enormous task was impossible to achieve during this dissertation do to obvious time and economic constraints and the extent of the candidate's study area. Nonetheless, when detailed depositional evolutions are the target, more sediment cores should be collected in order to cover as much of the potential

study area as possible. Such strategy may reduce sources of error in the chronologies established for the evolution of any given coastal barrier system. Moreover, and in terms of vertical accretion rates, more samples should be dated per sediment core, so high-resolution chronologies and sediment accumulation rates could be obtained, reducing, yet again, any sources of error in those calculations.

The luminescence protocols utilized to obtain the optical ages presented throughout this dissertation have been proven successful and adequate for the type and conditions of the quartz found and extracted from the coastal barriers forming the Apalachicola Complex. Even though such protocols are standard, they were the best suited to study in detail these depositional environments.

The specific conclusions obtained from this research may be better divided into three main categories according to the different contributions obtained for the different relevant scientific fields. Hence, in general, there are conclusions pertaining to the geological (i.e. coastal evolution, sedimentology, etc.), archaeological and methodological (i.e. OSL characteristics and dating) studies completed during this Ph.D. research.

8.1. GEOLOGICAL AND GEOCHRONOLOGICAL

Optical dating was applied to a variety of beach and dune lithosomes pertaining to a multitude of ridges throughout the Apalachicola Barrier Island Complex, on its central and western regions. Quartz grains, at the 150-212 μm fraction, extracted from those ridges were used to determine the luminescence signal at various levels.

Enough quartz separate (≤ 5 g) can be obtained from sediment slabs ~ 2.5 cm-long x ~ 7 cm-wide x ~ 3.5 cm-deep, taken from only one split-half section of a long vertical sediment core. The thinner the slab, the better appraisal of the lithostratigraphic unit being analyzed, hence the more accurate the estimate of the last burial.

All cores were corrected for compaction by calculating the difference between the lengths of the original coring vessels to those of the recovered sediment cores. Because core catchers were used and visual inspection was done in all instances, sediment loss during extraction is not considered an issue. This calculation implies a linear compaction throughout the sediment cores and does not account for differences (if any) in porosity, packing (i.e. loose unconsolidated upper sediments vs. lower ones) and water content of the different sediment layers/facies composing each core. Hence, if there are to be any errors associated

with this compaction calculation, they would be also attributed to the sediment accumulation rates as only two sample depths were used in their calculation. Therefore, any errors due to core compaction, but also precision on the optical ages themselves, would be propagated directly into the average sediment accumulation rates (ASAR). Further investigations in this area (i.e. volume reduction due to coring and consequent accumulation rates), as well as calculations using exponential compactions should be done in order to minimize errors, if any, in the sedimentation rates presented throughout this dissertation.

The ages obtained ranged from 22 ± 4 to $3,300 \pm 300$ years ago, for the coastal barriers, and $24,200 \pm 5,800$ and $154,200 \pm 10,400$ years ago for the relict Pleistocene Oak Ridge on the lower mainland. This range of values is consistent with earlier studies as to the efficacy of OSL when dating continuously prograding coastal environments.

The minimum age error obtained was 1 year while the maximum was 400 years (excluding the Oak Ridge samples), making the calculated errors $< 15\%$ of the overall age values.

I have found at least five spit-forming, peninsula-growing, island-nuclei at SJP. Previous beliefs stated only two.

Lateral progradation and vertical accretion rates have been obtained by using OSL dating in multiple samples extracted from vertical cores retrieved from successive ridges. Moreover, the lower ages provide *terminus ante quem* limits for ridge formation and the closest interpretation to the geographical evolution of the barrier islands, as they are the best available minimum ages for the formation of individual ridges. The upper ages illustrate the rate of formation and preservation of the aeolian components capping the ridges, and are interpreted to portray the actual environmental stability of the systems. These vertical accretion rates are the first ever derived in the area and provide new information on the sedimentary dynamics of aeolian deposition, which continues to date, even on ridges stranded well inland of the modern shorelines (as seen on SVI). This data might provide a new paradigm in our understanding of stabilization and continuing vertical growth of older beach ridges. Furthermore, our understanding of rates of vertical accretion by aeolian processes on nearshore dune ridges has been greatly advanced. These new observations, coupled with further studies of shoreline behaviour, could have major implications for coastal zone management.

As previously believed, but never asserted due to the lack of reliable absolute chronologies and suitable materials for other dating methods, the first coastal systems to fully emerge among these Apalachicola barriers were undoubtedly Richardson's Hammock (the small island-peninsula at the southern foot of SJP and at the westernmost attachment of CSB) and the north-eastern area of SVI. Emergence of these systems and later barriers suggest both a stabilized

sea level and a constant supply of sediment infilling the pre-existing submerged palaeo-deltaic platform of Apalachicola. The numerous ridges existent throughout the barriers are indicative of active longshore drift as the main ridge-building process in the region. Moreover, the multitude of different ridge orientations and truncations suggest several changes in the longshore directionality, proving the complexity of the hydrodynamics in this Panhandle region.

Care must be taken when evaluating and correlating ages obtained via the same (i.e. luminescence) or other independent methods. In coastal studies such as this one, it is important to know the precise location of samples previously published, so a better correlation and comparison among individual ridges and lithosomes can be established. Such parameters are vital to each individual OSL age, as optical dating measures the time elapsed since the last burial, hence, it is specific to a precise lithostratigraphic unit within a sedimentary package. Moreover, the precision of such parameters (i.e. geographical coordinates, altitude and overburden thickness) are needed to calculate environmental dose rates. Suggestions regarding this standardized control of publication values are reported herein to raise awareness among colleagues outside the geochronological community regarding the state-of-the-art of reporting optical ages. This “standardized etiquette” should be maintained even more now due to the increasing acceptance and reliability of optical ages.

The major geological results obtained from this research may be summarized as follows:

- ❖ Richardson’s Hammock grew from $3,300 \pm 300$ to $2,300 \pm 200$ years ago.
- ❖ SJP started growing its southernmost nucleus around $2,200 \pm 200$ years ago and its northern spit terminus is still prograding.
- ❖ SVI grew from $\sim 2,800 \pm 300$ to at least 370 ± 50 years ago.
- ❖ LSGI grew from $1,900 \pm 200$ to at least 22 ± 4 years ago.
- ❖ CSB grew from 630 ± 40 years ago to at least the mid 1800’s when its south-western cape terminus reached its maximum known position, being the fastest growing coastal system in the Apalachicola Complex.
- ❖ The five studied coastal systems evolved during six time intervals, since $\sim 3,000$ years ago to present time, each spanning over $1,200 - 1,000 - 400 - 300 - 400$ and 300 years, from oldest to youngest as depicted in Figure 7.10. (Chapter 7).
- ❖ SJP most probably evolved from five sedimentary “island” nuclei rather than two.

- ❖ Inland aeolian dune caps accumulate at a slower rate than nearshore ones.
- ❖ Rates of vertical accretion were determined for different coastal settings and depend on the geographical location of the ridges with respect to shore (as seen in Chapters 6 and 7).
- ❖ A continuous aeolian accumulation has been observed on vegetated inland relict beach ridges (e.g. SVI).

8.2. ARCHAEOLOGICAL

Despite the inferred activity surrounding a settlement (i.e. intense traffic; permanent/temporal settlement daily activities; re-working of the surficial soil/deposit; transporting, burial and re-burial of allochthonous materials; post-depositional mixing; etc.), it is possible to date with confidence coastal occupational sites using OSL, as seen for the shell-rich middens dated at Old Cedar (central SJP – Chapter 4) and at Richardson’s Hammock (southern SJP – Chapter 5).

Re-working of surficial sediments might not be possible to detect by eye in the field but may well be identified with OSL. In both cases studied, the activity surrounding these archaeological sites, did not affect the optical signal of the quartz grains retrieved from each of these coastal middens. In other words, the possible post-depositional anthropogenic processes responsible for the movement of artifacts inside the middens (as in the case of Richardson’s Hammock), did not affect the OSL homogeneity of these anthropogenic layers. Such remark can be evidenced by analyzing the single aliquot D_E distributions obtained from the different aliquot sizes measured (i.e. 8, 5, 3, 1 mm mask sizes): no over-dispersion or shift in the D_E distribution was seen with decreasing mask sizes; rather, distributions with higher resolution (i.e. symmetrical spread towards both ends of the curve from a common central D_E value) were observed with decreasing mask sizes. No evidence of bioturbation was seen either.

Is this relevant only to coastal shell-rich midden sites? This may be of interesting research potential in the fields of both archaeology and geoarchaeology. Moreover, if sampling is done at high resolution, OSL may shine some light into one of archaeology’s precious questions: how often a site was re-occupied, if ever abandoned for periods of time, rather than a sole estimate of the life time of any given settlement site.

8.3. METHODOLOGICAL

This research has demonstrated the value of using long vertical coring in OSL dating, as the technique does not affect the sediment being cored, and multiple samples may be analyzed for the same ridge.

Details surrounding some of the parameters and analyses, relevant to the methodological conclusions here presented, can be found in the Appendices, where the author makes sufficient interpretation of the analyses that should be accounted for in this type of research and this type of quartz grains (i.e. sediment).

The IRSL/OSL ratios obtained for all the samples measured during this research showed values ranging from 0.001 to 0.004. It would then be safe to establish an IRSL/OSL ratio of < 0.01 when dealing with this specific type of siliciclastic samples, i.e. environments.

Even though all the barrier samples obtained during this research are considered geologically young (i.e. $< 4\ 000$ years), it is interesting to note that, as a general trend, the oldest samples measured in this study tended to behave better to both dose recovery test and pre-heat plateau test when low pre-heat temperatures (i.e. 160 and 200 °C) were administered. On the contrary, the youngest samples measured herein behaved their best at higher pre-heat temperatures (i.e. 240 and 280 °C).

Despite the active dynamics of these modern coastal barrier systems, not a single fully zeroed aliquot was ever observed in any of the young samples measured, suggesting no turbation/contamination from upper layers or surficial deposits. This in turn, suggests that these ridges, once formed, maintain a relative depositional equilibrium with the external environment, allowing for a continuous burial rather than chaotic re-mixing of sediment on the surface. The latter indicates possible rapid burial conditions, hence preservation of the lithosome, and little bioturbation.

Modern analogues extracted from the active crests of modern foredunes, at a depth of only 2 cm, showed D_E values of 0.0 ± 0.001 Gy, indicating complete zeroing of quartz grains in this type of coastal environment. Hence, it can be said that in this study area, all the quartz grains get fully exposed to sunlight during transport and/or prior to burial.

When using frequency diagrams to analyze D_E distributions, the calculation of the skewness coefficient may be used as a valid assessment of the degree of symmetry of the distribution. Even though the difference between the standard deviation of the aliquots' D_E values and the standard error of the mean for the same distribution was small for the majority of the samples measured, it may signify a greater or smaller age error once the age calculation is computed. Hence, for symmetrical distributions, the best associated D_E error may be the standard error, whereas for asymmetrical ones, it would be the standard deviation. As there are no established values determining the ranges of symmetry for skewness coefficients in optical dating, the candidate determined those values by comparing differently calculated skewness coefficients from multitude of distributions with the general behaviour of a) the frequency distributions

themselves, b) the cumulative frequency (%) curves associated to those distributions, and c) the radial plots drawn from those distributions. The final skewness values determined for D_E distribution analyses (as detailed in the Appendices) are: a) values between -0.65 and $+0.65$ represent symmetrical distributions; b) values < -0.65 and $> +0.65$ are slightly to highly skewed as the number diminishes or increases, respectively.

As in sedimentological grain size analyses, the usage of the cumulative frequency (%) curve may be a valuable tool in the analyses of the distribution of D_E values in a sample. Such curve characterizes the different sub-populations existent in the data. As seen in the Appendices, the more “S”-shaped curve, with symmetrical tails, the more unimodal, hence symmetrical the D_E distribution. The verticality of the curve portrays similar statute. However, the more horizontal the curve or the more difference in tail-size, the more asymmetrical the distribution, hence the more poly-modal the population. The cumulative frequency (%) curve could be further used to better visualize any incomplete zeroing or bioturbation in any given sample, if any of these factors are present.

In a large set of aliquots (i.e. > 20) and with single aliquot measurements done at the 8 and 3 mm mask sizes (or at 5 and 1 mm mask sizes), it is possible to detect post-depositional disturbances and radiogenic heterogeneity of a sample. If such analysis is necessary in any given investigation, using single aliquot measurements in both large and small aliquots may help the researcher in time and effort to achieve this goal, rather than going into the deeper and tedious single-grain measurements. This research has proven that it is not necessary, for this particular type of depositional environments, to go to extensive lengths to detect such inconsistencies in the OSL behaviour of a sample.

Within the similar trend of thoughts, comparison of frequency distributions among large and small aliquot sizes (i.e. 8 and 3 or 5 and 1 mm mask sizes) has proven that, for the vast majority of the samples measured during this research, the larger aliquot size values tend to be always encompassed within the range of values obtained for the smaller aliquot sizes. This particular discovery has been named “increasing resolution”, and may well be a new luminescence proxy to determine inhomogeneities in the dose rate within the sedimentary deposit at the micro-scale (see Appendix V).

A correlation between sediment accumulation patterns of different coastal sub-environments and the behaviour of the optical luminescence signal was attempted in order to further understand the relationship between depositional / transport processes and optical signals. I believe the complexity of the burial environment (i.e. the deposit on itself and the distribution of minerals within it) is an important factor to consider in future studies, to better comprehend optical signal signatures.

I only hope the much needed detailed investigations regarding the intrinsic relationship between sedimentology, dynamic processes (e.g. deposition and transport) and optical dating will continue in the future, as luminescence may not only be useful for geochronology but could also be used as a proxy to further understand sedimentary processes.

APPENDIX I

List of all cores taken during this Ph.D. Research

All cores were taken with permission granted by the following agencies and/or persons:

- | | |
|---|--|
| St. Joseph Peninsula:
(<i>SJP</i>) | St. Joseph Peninsula State Park
Anne Harvey & Cynthia Emrich (SJP State Park Managers at the time)
Wm. J. Rish Recreation Park - Billy C. Quinn Jr., resident Park Manager
Private owners of land &/or residential areas: David and Marsha Harrell (Haven road)
Port St. Joe Municipality
Florida Department of Environmental Protection <i>FDEP</i>
Apalachicola National Estuarine Research Reserve <i>ANERR</i> - Roy Ogles |
| Richardson Hammock:
(<i>RH</i>) | Dr. Nancy Marie White (University of South Florida) for the archaeological site
Florida Department of State, Bureau of Archaeological Research
Florida Department of Environmental Protection <i>FDEP</i>
Apalachicola National Estuarine Research Reserve <i>ANERR</i> - Roy Ogles |
| Cape San Blas:
(<i>CSB</i>) | Florida Department of Environmental Protection <i>FDEP</i>
Roy Ogles <i>ANERR</i>
Port St. Joe Municipality - Salinas Park
Eglin Air Force Base (U.S. Air Force, Department of Defence) |
| Mainland (Buffer Preserve): | Florida Department of Environmental Protection <i>FDEP</i>
Apalachicola National Estuarine Research Reserve <i>ANERR</i> - Roy Ogles |

St. Vincent Island: St. Vincent National Wildlife Refuge (US Fish and Wildlife Service)
(SVI) Terry Peacock (Refuge Manager)

Little St. George Island: Florida Department of Environmental Protection *FDEP*
(LSGI) Apalachicola National Estuarine Research Reserve *ANERR* - Roy Ogles

On SJP & RH - Field Season August 2002

	Core Name [a]	Date Taken	Latitude N [b]	Longitude W [b]	Location Comments
1	Deer Ridge (SJ201)	Aug 5 2002	29° 45' 48.18"	85° 23' 55.56"	Inside SJP State Park; Deer Ridge test core; taken on a washover fan area at base of ridge; N side of road on curve before Shop; stake left at base of dune ridge.
2	Rish Park (SJ235)	Aug 9 2002	29° 43' 39.06"	85° 23' 19.86"	Inside Rish Park; E side of road; S of boardwalk to Bay front; stake left on top of dune ridge.
3	RH (SJ258)	Aug 12 2002	29° 41' 03.95"	85° 22' 03.12"	Inside Richardson Hammock; E side of road; ~ 100 m N of main entrance gate; ~ 10m E of fence & BM; stake left on dune ridge.
4	Roy/Eglin (SJ263)	Aug 13 2002	29° 40' 35.95"	85° 21' 16.15"	Inside DEP property next to Eglin Air Force Base; named "Eglin/RoyOgles" site; E side of road 1st curve after Eglin's barracks entrance; ~200m E of fence; N side of trail; ~20m E of big oak tree; stake left on dune ridge.

On SJP & RH - Field Season July-August 2003

	Core Name	Date Taken	Latitude N [a]	Longitude W [a]	Location Comments
5	SJ 002 1	Jul 17 2003	29° 48' 23.92"	85° 24' 48.50"	Inside SJP State Park; SJ 002 is big blowout area 100 m S of park post 22; core #1 taken on the S side of the "island dune", a remnant knob in the middle of the blowout area; stake left.
6	SJ 002 2	Jul 17 2003	29° 48' 24.90"	85° 24' 52.08"	Inside SJP State Park; same as above but core 2 was taken on E slope/almost crest of the central area of the foredune system that forms the NW boundary of the blowout area; stake left.
7	Deer Ridge 1	Jul 17 2003	29° 45' 48.90"	85° 23' 55.68"	Inside SJP State Park; same area as SJ201Deer Ridge core taken in 2002 but this time closer to the bay shore; core 1 was taken on the W slope of the ridge; stake: WPT27.
8	Deer Ridge 2	Jul 17 2003	29° 45' 48.96"	85° 23' 55.80"	Same as above but core 2 was taken on the foot of ridge; ~ 10 m W of core 1; stake left.
9	Haven	Jul 19 2003	29° 42' 21.90"	85° 22' 47.22"	Haven Rd (W side of Cape San Blas Rd (Hwy 30E), N of BP Gas Station); core taken on crest of 1st ridge; on N side of Haven Rd.; ~ 10 m W of Hwy 30E; stake left.
10	GPR 1	Aug 6 2003	29° 51' 39.29"	85° 24' 14.19"	Inside SJP State Park, N of Army Camp Rd; northernmost site named GPR1 (1st GPR survey); core taken on NW corner of big ridge surveyed, between lines 1&2 just N of line 4; on NW side of main dirt road leading to SJP point; ~ 50m NW of big tree with Corona bottle cap that was used as backsight; stake & brick.
11	RH- TUE-1	Jul 29 2003	29° 41' 25.66"	85° 21' 46.82"	Richardson Hammock archaeological original site Florida 8Gu10 - Test Unit E; horizontal core taken in E wall; inside midden @ 25 cm N from SE corner of trench & 30 cm depth from present day land surface.
12	RH- TUE-2	Jul 29 2003	29° 41' 25.66"	85° 21' 46.82"	Same as above but S wall; horizontal core taken in white sand bellow midden @ 5 cm W from SE corner of trench & 190 cm depth from present day land surface.

13	RH-GEO-1	Jul 29 2003	29° 41' 26.70"	85° 21' 46.80"	Richardson Hammock archaeological area; beach ridge exposed on bay shore just E of Trench Unit E, near but W of survey marker Blas 1935; horizontal core taken inside ridge @ 90 cm below crest top.
----	----------	-------------	----------------	----------------	--

On SVI - Field Season July-August 2003

	Core Name	Date Taken	Latitude N [a]	Longitude W [a]	Location Comments
14	SVI #0	Jul 23 2003	29° 39' 01.41"	85° 09' 32.62"	Youngest mature ridge; closest to Gulf; rel. Tanner's set K.
15	SVI #1	Jul 22 2003	29° 39' 06.98"	85° 09' 23.04"	Young ridge; rel. Tanner's set G.
16	SVI #2	Jul 22 2003	29° 39' 22.98"	85° 09' 06.06"	Middle-south of island; crest of ridge; rel. Tanner's sets F-G.
17	SVI #2b	Jul 22 2003	29° 39' 23.34"	85° 09' 05.58"	Middle-south of island; N slope of ridge; rel. Tanner's sets F-G.
18	SVI #3	Jul 22 2003	29° 39' 32.58"	85° 08' 57.30"	Middle of island; rel. Tanner's set F.
19	SVI #5	Jul 23 2003	29° 41' 08.28"	85° 07' 33.96"	Northernmost swampy area (sunk ridge); Tanner's set A.
20	SVI #6	Jul 23 2003	29° 40' 53.34"	85° 07' 34.86"	North of island; muddy ridges; Tanner's set B.

On LSGI - Field Season July-August 2003

	Core Name	Date Taken	Latitude N [a]	Longitude W [a]	Location Comments
21	LSGI 1	Jul 25 2003	29° 36' 00.07"	85° 02' 38.23"	Bay side concave area of LSGI, at northernmost apex of NW-SE trending ridges; by old dock.
22	LSGI 2	Jul 25 2003	29° 35' 47.11"	85° 03' 10.87"	Road cut ridge on "Y" dirt road to beach; E side of dirt road; 3rd ridge from S to N from lighthouse road to cabin; ridge ~ N40°W.
23	LSGI 3	Jul 25 2003	29° 35' 41.71"	85° 03' 22.57"	Youngest mature ridge Gulf side; NW side of main dirt road to beach; ridge ~ N35°W parallel to shoreline; W beach arm of LSGI.

On SJP & CSB - Field Season July-August 2004

	Core Name	Date Taken	Latitude N [a]	Longitude W [a]	Location Comments
24	White Sands 1	Jul 22 2004	29° 44' 03.36"	85° 23' 38.40"	White Sands foredune system location; core taken just N of the original Total Station stake (the oldest one); it's in a trough protected by crests on the W N & S; @ 7.6m E of crest of foredune & 15.3m N of Opal sample stake; between GPR survey lines.
25	Romanelli 1	Aug 1 2004	29° 41' 05.57"	85° 18' 38.39"	Inside Salinas Park on CSB; core taken on the big ridge that has a boardwalk and gazebo, NW of playground; on the NW side of the ridge @ the crest; stake & brick.
26	Oak Ridge 1	Aug 2 2004	29° 41' 51.29"	85° 17' 52.01"	Inside the Buffer Preserve backcountry; entry by gate off Hwy 30, just SE of Preserve Centre; take Sand Ridge Rd, S to the triangle junction; core on E side of road by oak bushes; stake & brick.
27	Harvey 1	Aug 2 2004	29° 42' 28.39"	85° 23' 46.44"	Inside SJP State Park; ridge on E side of Park's office/entrance; core taken on crest looking towards E slope of ridge; stake.
28	Wild 1	Aug 2 2004	29° 47' 55.96"	85° 24' 34.96"	Inside SJP State Park; N of Well field gate; pass BF's core SJ252 location (old SJ14B); on W side of road @ a curve bending E; have to walk W inside bush ~ 50 m S of curve; stake & wood boards.
29	Hogan	Dec 2004	29° 40' 25.39"	85° 21' 04.89"	Inside Eglin Air Force Base on CSB; enter brush just NE of entrance to road leading to Gulf (towards the ols EAFB barracks), travel ~ 15 m E along crest to core location.
30	Old Cedar 1	Aug 1 2004	29° 44' 55.36"	85° 23' 27.87"	Inside SJP State Park - Marine Trail; ~ 100 m N of where trail emerges onto bayshore; Old Cedar archaeological site Florida 8Gu85; bayshore erosional scarp exposing shell midden.
31	Old Cedar Geo 1	Aug 1 2004	29° 44' 55.36"	85° 23' 27.87"	Same as above but location of core is in white sand ridge below shell midden.

Characters:

[a] Original core names.

[b] Geographical coordinates (NAD 83).

Special Notes:

a. Cores were collected using standard soft Aluminium irrigation pipes (7 cm diameter & max length 6 m).

b. Two types of cores were utilized: vertical and horizontal.

c. Most cores extracted were long vertical ones, with the exception of RH-TUE-1, RH-TUE-2, RH-GEO-1,

d. Old Cedar and Old Cedar GEO which were short horizontal ones.

e. For the vertical cores, coring was achieved using a portable gas operated vibracore with a custom-made coupling system that holds the pipe and allows for easier handling of the descending pipe.

f. The minimum and maximum lengths achieved with the vertical coring were 1 and 5 m, respectively.

g. A 1.2 m-long truck jack set on a small wood platform was used to retrieve each sediment core.

h. For the horizontal cores, coring was achieved by percussion, using a mallet on a piece of wood set before the core to prevent damaging the pipe.

i. The horizontal cores were 20 cm in length.

j. Pulling by hand was used to retrieve each horizontal core.

APPENDIX II

PROGRAMS USED FOR OSL MEASUREMENTS / ANALYSES AND AGE CALCULATIONS

The sequences of commands established to determine the natural and laboratory D_E values obtained for each quartz fraction of each individual sample were built using:

SEQUENCE EDITOR by RISØ National Laboratory, Denmark
TL/OSL program for Windows with LM Data I/S
Geoff Duller – v 1.15 – 1999
Type of file: seq
Provided by RISØ National Laboratory in 2000

Note: It is important to accurately type within “run info” (a sub-tab inside the OSL operation command) any information related to the irradiation dose at it will affect calculations within the raw data display in *ANALYST*.

The luminescence data obtained after each measurement is first loaded and checked using this next program. The resulting decay and growth curves as well as an initial frequency histogram obtained for each individual aliquot can be seen and analyzed. The raw data can then be accepted and saved as an “ascii” file for subsequent manual analysis (i.e. in Microsoft Excel).

Luminescence ANALYST by RISØ National Laboratory, Denmark
Program for Windows
Geoff Duller – v 3.07b – 2002
Aberystwyth Luminescence Laboratory, University of Wales, U.K.
Type of file: bin
Provided by RISØ National Laboratory in 2000

Both of these programs are compatible with the RISØ TL / OSL – DA 15 Reader, used for all luminescence measurements completed for this Ph.D. research.

Note: It is possible to change the values displayed as raw data (i.e. first window when a bin file is uploaded), to correct, for example, for any mistakes written

within the “run info” sub-tab in *SEQUENCE EDITOR*, but it is not possible to correct for irradiation doses given as an operation command.

All final analyses such as acceptance/rejection of aliquots based on recycling ratios, test dose errors and 2σ outliers for the final estimation of each D_E value are achieved by building a detailed spreadsheet using *MICROSOFT EXCEL* for Windows. Descriptive statistical analyses are done for each mask size and sample measured on the accepted aliquots: mean, standard deviation, standard error, skewness, Pearson’s skewness, mode, median, etc. Bar histograms and cumulative frequency (%) plots are also constructed and analyzed in *EXCEL*.

Another approach to analyze the distribution of D_E values for each mask size and sample measured is to build a radial plot. It allows inputting D_E values and their respective errors, and the D_E value to which the data is standardized (default 2σ range). This program only allows graph construction (which can be copied to the clipboard) but not storage within the program.

RADIAL PLOT

Program for Windows

Jon Olley and Michael Reed – v 1.3 – 1999-2003

CSIRO Land and Water, Australia

Provided by Richard ‘Bert’ Roberts, University of Wollongong,
Australia, March 2006 (personal communication)

All parameters pertaining to each individual sample are then input into the following program, used to calculate the OSL age in years:

ANATOL – Analyse Thermo Opto Luminescence

Program for Windows

Norbert Mercier and Christophe Gaugez – v 0.72B – 1998

LSCE – Domaine du CNRS, Gif-sur-Yvette, France

Type of file: age

Provided by N. Mercier in 2000

A detailed explanation of the parameters to input within *ANATOL* is described in Appendix VIII.

APPENDIX III

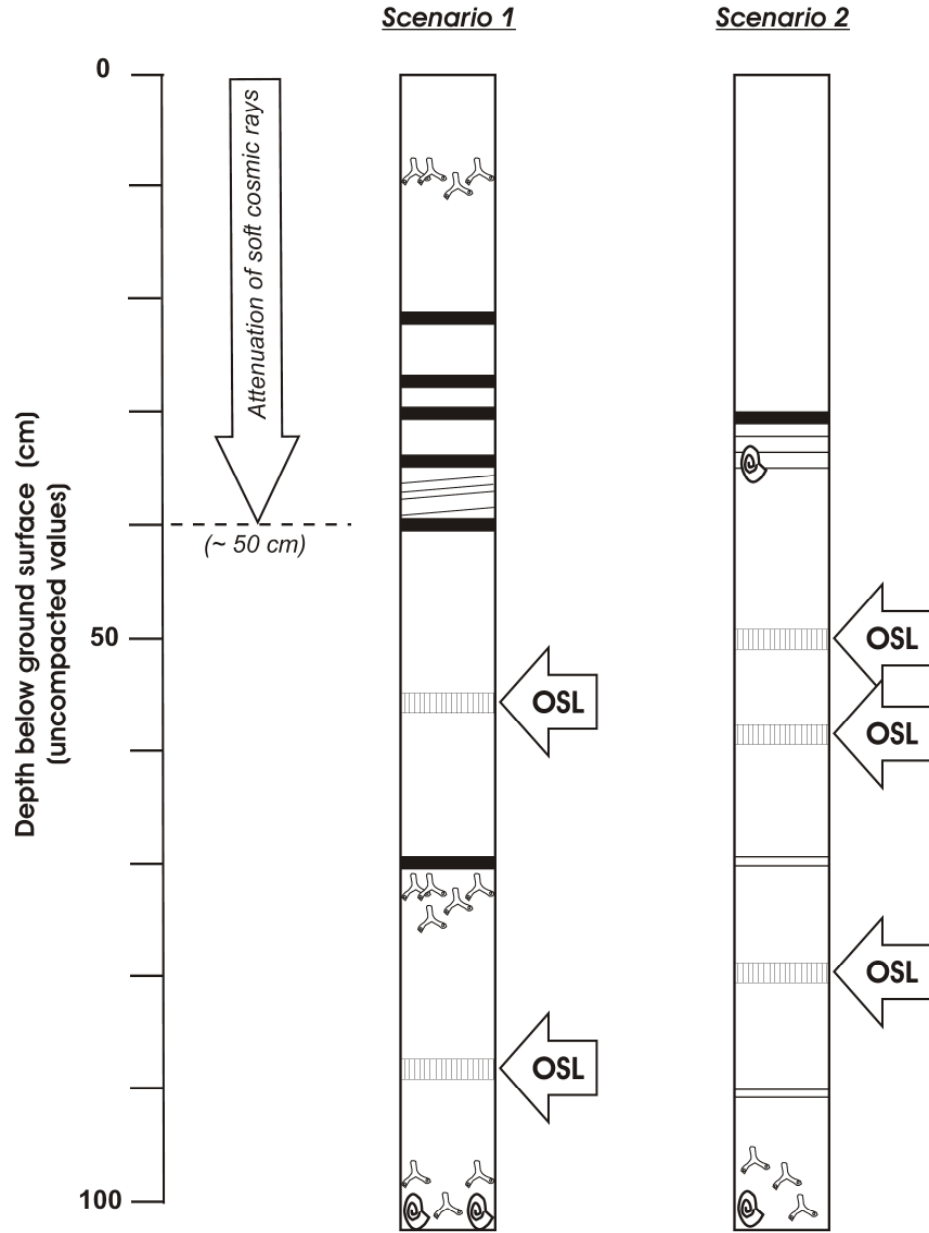
GUIDELINES FOR OSL SAMPLE COLLECTION AND LABORATORY PREPARATION

When collecting long vertical cores, it is possible to sub-sample the sediment core at multiple intervals. For this Ph.D. research, two intervals were targeted, each at a different depth and at least 50 cm to 1 m apart from each other. When using pipes 7 cm-in-diameter as coring vessels, as done in this study, and when dealing with unconsolidated fine to medium grain-sized sedimentary deposits composed of > 80% of quartz grains, it is possible to retrieve as little as 2 cm of sediment length-wise (and the width of the split core, i.e. 7 cm) to obtain enough quartz (i.e. ≥ 2 g) in the 90-150, 150-212 and 212-250 μm grain size fractions to OSL date. Two grams of quartz at the targeted fraction is the minimum amount required to complete all the OSL tests and measurements portrayed in this study.

Sampling Strategies: Sedimentological Homogeneity

In general, sampling for OSL has to be done with care. It is recommended that at least the 30 cm immediately surrounding the centre of the sample (i.e. 15 cm above and 15 cm below within a split-half core) are as lithologically homogeneous as possible. This is to avoid any radioisotopic inhomogeneity within the sedimentary package being sampled. For example, sections of a split-half core with intricate heavy mineral and organically-rich layers or patterns (i.e. varying thicknesses and number of layers) are to be avoided when sampling for OSL. Stratigraphical, hence compositional, complexity can complicate the calculation of the dose rate. Both vertical and horizontal complexities within any given sedimentary deposit should be avoided, if possible.

To better illustrate this sampling strategy, two stratigraphical scenarios are given below as examples that may be well possible to encounter when split-opening a sediment core retrieved from coastal environments such as the ones studied for this dissertation. The best locations for collecting OSL samples are given by the vertically-dashed areas pointed by thick arrows. The black layers and lamina are concentrations of heavy minerals. Shell and detritus materials are also depicted. Uppermost OSL samples should be taken at or below ~ 50 cm depths (uncompacted value) to reduce the cosmic radiation factor. In the figure, the sediment cores are ~ 7 cm in diameter.



Chemical and Mechanical Treatment of OSL Samples

The following table summarizes the preparation steps to follow for the initial chemical treatments to be done on all samples to be OSL-dated. These are those followed at the AGE Laboratory after the original sample extracted from one split-half of each core is oven dried (< 60 °C) and subsequently divided into both “work” and “archive” samples. Before any treatment starts, a small portion of the original sample (~2 g) has to be extracted for NAA (and subsequently sent to the Nuclear Reactor). Samples are to be weighted before and after each step. All chemical treatments are to be done under the fume hood, in the darkroom laboratory under subdued orange light. A complete and more detailed protocol was updated and written by the candidate in May 2003 and is available at the AGE Laboratory.

Step	Treatment	Length of treatment
1	10% HCl	Until reaction ceases (1 day)
	Change to 50% HCl if 10% HCl reaction continues for more than 1 day.	Until reaction ceases
2	10% H ₂ O ₂	Until reaction ceases (1 day)
	Change to NaOH if above reaction continues for more than 1 day.	
3	Oven-dry (< 60 °C)	(1 day)
4	Archive ~5g for Coulter Counter analyses	
5	Dry-sieve using small sieves & disposable nylon meshes: <90; 150; 212; 250; >250 µm	20 minutes per load using small sieves (each sample takes ~ 4 loads)
6	Archive all fractions but 150-212 µm	
7	Mineral separation using heavy liquid to get separates of Heavy Minerals, Quartz; K-feldspar.	1 day per sample
	Following treatment is only done in the quartz separates:	
8	40% HF	40 minutes
9	10% HCl	40 minutes
10	Dry in clean oven (< 60 °C)	½ day
11	Sample ready for OSL measurements	

Notes:

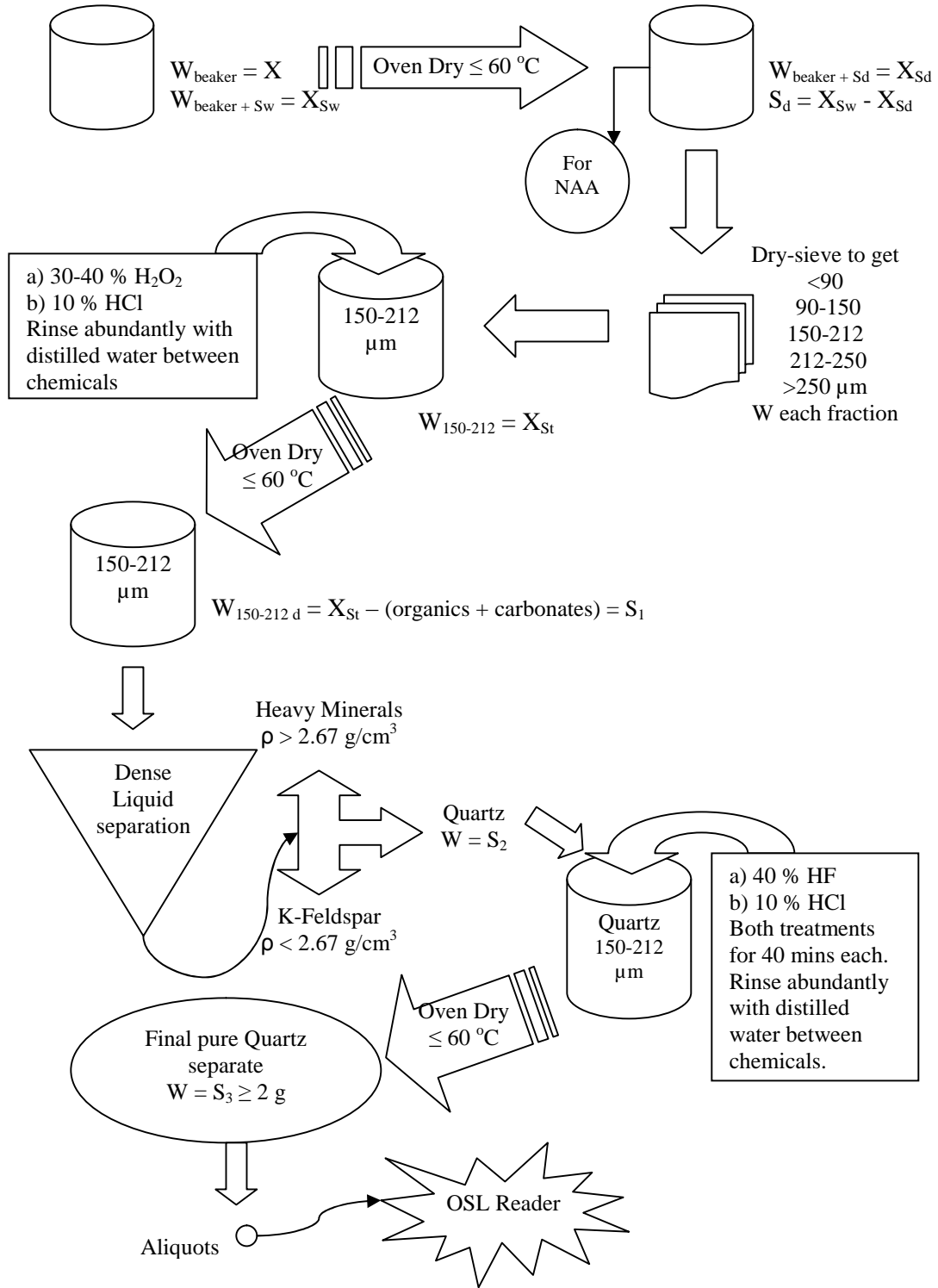
These steps may take up to 2 weeks per sample. However, a batch of up to 6 samples can be treated at the same time.

A clean environment (i.e. counter tops, beakers, utensils, etc.) is to be maintained at all times in the darkroom laboratory to avoid any external contamination of the samples and final quartz separates.

The following is a generalized flux diagram to quickly visualize the laboratory treatment steps required to obtain pure quartz separates from samples retrieved from long vertical cores collected along the coastal ridges of Apalachicola. The targeted grain size fraction for this study was 150-212 μm for all core samples.

Where:

W	weight (g)
S _w	wet sample
S _d	dry sample
For NAA	small sub-sample (< 2 g) of the whole dried original sample required to obtain the concentrations of U, Th, and K for each sample
S _t	targeted sample's fraction
S ₁	dry weight of targeted fraction after organics and carbonate removal
S ₂	dry weight of quartz separate of targeted fraction prior to etching
S ₃	dry weight of etched quartz sample (ready to be OSL measured)



APPENDIX IV

GENERAL SINGLE-ALIQUOT REGENERATIVE-DOSE (SAR) PROTOCOL

The SAR protocol came to life after Murray and Roberts (1998) first ideated a regenerative procedure for OSL signal measurement (i.e. that could be repeated numerous times) that could correct for sensitivity changes in quartz as seen in the past. It was then first improved by Murray and Wintle (2000) and subsequently by Murray and Wintle (2003) and Wintle and Murray (2006). It has essentially become the most applied protocol to optically date quartz so far.

A generalized description of the method and sequence are given below.

Generalized outline of a SAR measurement sequence used in this study:

-
1.
 - a. D_N (received during burial)
 - b. PH_T (selected between 160 ° and 280 °C)
 - c. OSL L_N
 2.
 - a. T_D
 - b. CH_T (160 °C, i.e. to empty the 110 °C TL trap)
 - c. OSL T_N
 3.
 - a. $R_{D1, D2, \dots, Di}$
 - b. PH_T (same value as for the natural)
 - c. OSL $L_{1, 2, \dots, i}$
 4.
 - a. T_D
 - b. CH_T
 - c. OSL $T_{1, 2, \dots, i}$
 5. Repeat steps 3 and 4 for: $R_{D2}, R_{D3}, R_{D4}, R_{D5},$ and R_{D6} .
-

Where:

Natural Dose	D_N
Natural OSL signal	L_N
Test Dose	T_D (usually $\leq R_{D1}$, $\frac{1}{2}$ of D_N or 10% of D_N)

The same value is repeated throughout the sequence.

Test Dose signal	T_N for the natural and $T_1, T_2 \dots T_i$ for the induced OSL T_D signals given after each regenerative dose R_D at $x = 1, 2, \dots, i$
Regenerative doses	$R_{D1}, R_{D2} \dots R_{Di}$
Regenerated signals	$L_1, L_2 \dots L_i$
PH _T	Pre-Heat Temperature (10 °C/s increments) held for 10 s. The same value is used throughout the sequence.
CH _T	Cut-Heat Temperature (10 °C/s increments) held for 0 s (i.e. cooled immediately). The same value is used throughout the sequence.
OSL	Measurement of the OSL signal using blue LED's at a temperature of 125 °C (i.e. to prevent re-trapping in the 110 °C TL trap) for 100 s.

The following measurement cycles (besides the initial measurement of the natural dose) were used and maintained for all samples dated in this research, bracketing the natural dose:

$$\begin{array}{ll}
 R_{D1} \approx \frac{1}{2} D_N & R_{D4} \approx 3 \text{ or } 4 D_N \\
 R_{D2} \approx D_N & R_{D5} = 0 \\
 R_{D3} \approx 2 D_N & R_{D6} = R_{D1}
 \end{array}$$

Each regeneration point is given by the values obtained from L_i/T_i (i.e. a sensitivity corrected value of the OSL signal as at each cycle, each measurement is divided by the test dose signal). To build a sensitivity corrected growth curve, the former values are plotted in the Y-axis and the given R_{Di} in the X-axis (both axes starting at 0). In general, the regeneration doses are given relatively closely spaced, as their aim is to encompass the natural dose and generate a growth curve with the best possible fitting (i.e. with the smallest divergence from linearity). As most of the D_E 's in this study were $\ll 20$ Gy, linearity (i.e. linear fitting curve) in the dose response was observed.

Incorporated within the SAR protocol are the following tests:

- Sensitivity
The test dose is administered to determine sensitivity changes within each cycle and throughout the sequence (i.e. independent of any R_{Di} , optical stimulation or thermal treatment). Sensitivity can be tested with R_{D6} which is the repeated value in the sequence. If there are no changes in sensitivity, hence $R_{D1} / R_{D6} = 1$, known as the Recycling Ratio.
- Recuperation
When administering $R_{D5} = 0$ (i.e. no dose), no detectable signal should be observed, hence $L_5/T_5 = 0$.

The appropriate PH_T was determined based on the following tests, each established as a SAR sequence, carried out for single aliquots of each individual sample (using 8-mm-mask-size aliquots), each at four different temperatures (160 °, 200 °, 240 °, and 280 °C):

- Pre-Heat Plateau
- Dose Recovery – to determine the ability and efficacy of the SAR protocol for a given known laboratory dose (c.f. Madsen et al., 2005).
- Thermal Transfer – to identify any dependency of R_{Di} to temperature (c.f. Madsen et al., 2005; Ballarini et al., 2003).

The PH_T that complied with all three tests was then used in the final sequence intended to measure between 18 and 48 single aliquots of each sample for the final D_E determination, at the 1, 3, 5 and 8 mm mask sizes.

A list of all PH_T , T_D and R_{Di} values selected for each sample measured during this study are given in Appendix XI.

APPENDIX V

PARAMETERS FOR ALIQUOT ANALYSIS AND GUIDELINES FOR D_E DETERMINATION

Initial Criteria

All the criteria mentioned below can be set and checked while analyzing the raw data of each aliquot (i.e. bin files) in *ANALYST*. It can be also done manually (i.e. on a spreadsheet), or a combination of both.

Aliquots that are to be part of the group of D_E values utilized to calculate the final mean D_E of any individual sample, and consequently the determination of the final age of each sample, are to follow the subsequent criteria:

Natural or Regenerated Signal Intensity	Value obtained from the integration of the first 2 (i.e. 0.4 s) of 250 channels (i.e. 100 s) used to construct the decay curve of each aliquot during each OSL measurement. > 90% of the OSL signal is contained in the first second of the signal (Bøtter-Jensen et al., 2003), corresponding to the fast component.
--	--

In the samples measured during this Ph.D. research, the older ones showed a fast component contained in the first 1 to 1.5 s of the signal, while all of the younger samples showed a fast component contained in the first 0.5 to 0.8 s of the signal.

Background Signal	Value obtained from the integration of the last 10 (i.e. 4 s) of 250 channels (i.e. 100 s) used to construct the decay curve for each aliquot during the OSL measurement. This value is subtracted from the overall luminescence signal.
-------------------	--

Natural vs. Background	The natural signal has to be at least 3 times higher than the background noise.
------------------------	---

Test Dose Error	If T_N error falls $\pm 10\%$ out of the value, the aliquot
-----------------	---

is excluded. It is automatically calculated by *ANALYST*.

Recycling Ratio Values between 0.90 and 1.10 are accepted.

Recycling Threshold Level $\pm 10\%$

D_E Error It is the individual aliquot uncertainty
< 20%

D_E Analysis and Determination

An example of calculation of a Final D_E value (and its error) for a sample with similar values of to those found on St. Joseph Peninsula is exemplified below.

It is to be noted that all luminescence measurements done in the RISØ Reader are input and given in seconds. To convert these values into Gray (Gy), each value has to be multiplied by the Reader's radioactive $^{90}\text{Sr}/\text{Y}$ β source dose rate dose rate for the day/month/year of the measurement, which is based on the radioactive decay of the initial dose rate value of the $^{90}\text{Sr}/\text{Y}$ β source.

After accepting the aliquots that fell into the proper values of the first four criteria described above, the rest of the selection was done manually in *EXCEL*. The first step is to select the aliquots that follow the criteria detailed above. In this example, only one aliquot (#8) has a recycling ratio (RR) outside the condition values. As for D_E errors < 20%, all other aliquots match that criterion.

All the subsequent calculations (i.e. averages, standard deviations, medians and standard error) will exclude aliquot 8.

Explanation of Calculated Values:

Average of distribution, excluding aliquots outside RR:

In table = RR Av D_E

Calculated average of all aliquots, excluding #8 in s and Gy:

It will be used to determine which D_E values fall outside the 2σ range.

Standard Deviation of distribution, excluding aliquots outside RR:

In table = RR StdD D_E

Calculated standard deviation of all aliquots, excluding #8 in s or Gy:

It will be used to determine which D_E values fall outside the 2σ range.

Disc#	ED (s) measured	ED_Err (s) measured	ED (Gy) calculated	ED_Err (Gy) calculated	RR measured	RR_Err measured	E1	E2
-------	-----------------	---------------------	--------------------	------------------------	-------------	-----------------	----	----

Linear Curve Fitting (Syst Error 0.0%)

1	0.6	0.1	0.05	0.01	1.08	0.04		
2	0.6	0.1	0.05	0.01	1.01	0.03		
3	0.7	0.1	0.06	0.01	0.99	0.04		
4	0.8	0.1	0.07	0.01	0.95	0.06		
5	0.7	0.1	0.06	0.01	0.97	0.04		
6	0.5	0.1	0.04	0.01	1.06	0.07		
7	0.7	0.1	0.06	0.01	1.08	0.06		
8	0.6	0.2	0.05	0.02	1.14	0.08		
9	0.6	0.1	0.05	0.01	1.04	0.06		
10	0.7	0.1	0.06	0.01	1.04	0.07		
11	0.7	0.1	0.06	0.01	1.05	0.04		
12	0.7	0.1	0.06	0.01	0.98	0.04		

Using suitable aliquots based on E1:			
RR Av De (s)	RR StdD "error" De (s)	RR Av De (Gy) *	RR StdD De (Gy) *
0.66	0.08	0.06	0.007

2σ range:	
De-2σ (s)	De+2σ (s)
0.50	0.82

Excluding aliquots outside 2σ based on E2:			
2σ Av De (s)	2σ StdD De (s)	2σ Av De (Gy) *	2σ StdD De (Gy) *
0.66	0.08	0.06	0.007

Manually analyzed criteria (in this case):

E1 Aliquots outside Recycling Ratio

E2 Aliquots outside 2σ range

BIN width:	
Median ED_Err (s)	Median ED_Err (Gy)
0.10	0.01

Std Error (Gy)
0.002

Results:

E1 1 aliquot outside Recycling Ratio

E2 includes all aliquots accepted within Recycling Ratio

Note that all ED errors are <20% of ED value.

Date measured: 1-Mar-06
 Reader Dose Rate used: 1-Mar-06
 Reader Dose Rate *: 0.08768

The “ 2σ range”:

It is the range of D_E values that contains those aliquots that will be used to calculate the final mean D_E .

The lower limit of this range is obtained by subtracting twice the “RR StdD D_E ” from the “RR Av D_E ” = $D_E - 2\sigma$.

The upper limit of this range is obtained by adding twice the “RR StdD D_E ” to the “RR Av D_E ” = $D_E + 2\sigma$.

The aliquots inside this 2σ range will be the only ones chosen to establish the Final Mean D_E and its standard deviation:

Final Mean D_E :

In table = 2σ Av D_E

It is the mean of the distribution of accepted values, hence, the calculated average of the D_E values within the 2σ range (i.e. the best statistical estimate of the average D_E for a group of values).

This final mean D_E value is the one used to calculate the final age of each individual sample.

It is similar to the “central age model” of Galbraith et al. (1999).

Note that each D_E value in Gy depends on the date the sample was measured (i.e. depends on the source’s dose rate). Hence, the age is also dependent on that date, reason why each individual age is given relative to a *DATUM*, which is the YEAR of the measurement of that particular sample.

Final D_E error or analytical error:

This final D_E error is the one used to calculate the error of the final age for each sample.

Two types of errors are calculated – standard deviation & standard error.

In table = 2σ StdD D_E

It is the standard deviation of the distribution of accepted D_E values. One calculated standard deviation of the D_E values within the 2σ range (i.e. the average uncertainty of the accepted individual D_E values of the sample).

In table = StdError

It is the standard deviation of the Mean D_E . Calculated standard error of the D_E values within the 2σ range.

Depending on the symmetry of the distribution (i.e. skewness analysis), one or the other errors is used as the final D_E error value for the age calculation:

- If the D_E distribution is symmetrical, the standard error may be used as the final D_E error value.
- If the D_E distribution shows some asymmetry, the standard deviation should be used as the final D_E error value.

Bin size width:

A frequency distribution diagram is then built to further analyze the spread of D_E values selected (i.e. accepted following the criteria) for each sample. The size of the bin for each histogram is calculated as follows:

In table = Median ED_Err

Calculated median of all the D_E uncertainties, excluding those aliquots with D_E error values > 20% and those that are outside the RR.

Other parameters are also calculated based on the values of the selected and accepted aliquots used to obtain the Final Mean D_E :

- Median of the distribution
- Skewness coefficient of the distribution (see Appendix VII)
- Pearson's coefficient of skewness (see Appendix VII)
- % D_E error (Final D_E error divided by the Final Mean D_E)

Size of Aliquots and Frequency Distribution Analysis

Histograms are built in order to visually analyze the spread of the D_E distribution obtained for any given size of aliquot utilized for each sample. The size of the aliquot is given by the number of grains that it can hold, provided the diameter of silicon-oil sprayed prior to mounting the grains. Such diameter is set by mask sizes usually of 8, 5, 3 and 1 mm.

In general, each mask size normally contains the following amounts of grains:

8 mm > 1,000 grains

5 mm ~ 500 grains

3 mm ~ 200 grains

1 mm ~ 60 grains

In general, large and small aliquots (i.e. mask sizes) are employed for each sample to further study the D_E behaviour as the amount of grains measured for OSL changes. The OSL signal of each aliquot, independent of size, is the average of the signals given by the grains. However, that signal may be due to a few “bright” grains and several “active” or “normal” grains (i.e. all other grains contributing to the OSL signal), or vice-versa. Aliquots might show a degree of dispersion in the D_E values due to the presence and/or absence of “bright” grains or incompletely-zeroed grains. Moreover, it is important to identify the degree of uncertainty associated with each aliquot, as it might also provide evidence of “bright” or incompletely-zeroed grains. Hence, grain-to-grain variations can only be detected as the amount of grains diminishes, i.e. the aliquot’s size decreases.

It has been suggested that the best aliquot sizes to use when estimating the age of a sediment deposit (i.e. the burial D_E) are the smaller ones (Olley et al., 1998), hence aliquots containing around 100 grains or less. In smaller aliquots, the probability of measuring incompletely-zeroed grains increases, as well of that of including basically well-zeroed. However, as seen in this research and further detailed below, large size aliquots can also provide good estimates of the age any given sample collected from this study area.

By analyzing the relationship between the D_E ’s values and histograms obtained with both large and small aliquots for the same sample, it is possible to determine:

- Incomplete zeroing
Seen as higher than usual D_E estimates. Incompletely-zeroed grains can mask the true average D_E of any given aliquot, resulting in an overestimation of the true burial dose (i.e. age) of a sample.
If a sample is contaminated with incompletely-zeroed grains, the spread in D_E values among aliquots of the same sample becomes larger as mask size decreases.
E.g. previous studies: Wallinga (2001); Li (1994).
- Turbation (biological and/or geological) from above
With decreasing mask sizes, there is increasing manifestation of lower D_E values (i.e. younger grains), resulting in a histogram with values concentrated towards the lower dose portion of the distribution.
This type of post-deposition turbation may be caused by flora (e.g. roots) and/or fauna (e.g. burrowing) existent in the overlying layers, or pedogenesis.
E.g. previous studies: Bateman et al. (2003, 2007); Forrest et al. (2003).
- Turbation (biological and/or geological) from below

With decreasing mask sizes, there is increasing manifestation of higher D_E values (i.e. older grains), resulting in a histogram with values concentrated towards the higher dose portion of the distribution.

This type of post-deposition turbation could be caused by fauna (e.g. burrowing), liquefaction (?), or may be compaction (?).

E.g. previous studies: unknown to date, i.e. potential for future studies.

- Increasing resolution

With decreasing mask sizes, there is increasing manifestation of both lower (but not zero values) and higher D_E values towards both ends of the distribution but maintaining a peak of D_E values in its center (i.e. statistically similar mean D_E for all mask sizes –within error–). The distribution tends to obtain a Gaussian shape with decreasing mask size.

As mask size decreases, the limited number of grains increases resolution of variability, compared to the D_E distribution obtained from the initial large mask size. This D_E distribution obtained with the small aliquots is no longer “masked” as a group contribution to the apparent D_E in the large aliquots. The luminescence signal at lower mask sizes is given by grains with D_E values that encompass the initial distribution obtained with the 8 mm mask size. Hence, a higher resolution of the distribution is being obtained.

It is hypothesized that this phenomenon occurs as a result of a natural environment aging in conditions with no affecting major external changes to the deposit but rather inhomogeneities in the dose rate at a micro-scale (i.e. some quartz grains being closer to or further away from readily radioactive grains).

Study compelled to this Ph.D. research.

For this research, diameters of 8 and 3 mm, 5 and 1 mm or a combination of all mask sizes were used to analyze the D_E 's of individual samples. Mask size diameters were selected based on the amount of quartz fraction left after all chemical and mechanical laboratory treatments were done in all core samples. In some cases, the quantity of quartz fraction was so small (i.e. < 1 g), that there was only enough sediment to use the 5 and 1 mm mask sizes (e.g. samples GPR1 A and B, and SJ002 1 A and B).

For all samples in this dissertation, optical ages were calculated using the Final Mean D_E (\pm Final D_E error) obtained from the measurements using the largest mask size (i.e. 8 or 5 mm depending on the sample). The values obtained with large aliquots are interpreted to be the reflection of the luminescence signal of the bulk deposit, hence, the bulk environmental dose rates. Furthermore, the analysis of smaller-sized aliquots (i.e. 3 and 1 mm mask sizes) has proven that the samples

dated in this study do not show incomplete zeroing, post-depositional disturbances or anomalous over-dispersion of D_E values, hence, in this case, usage of the large aliquots' D_E values to calculate the burial age of each sample is viable.

Furthermore, it might be possible to detect more than one distribution in any given sample with the use of histograms, provided that the amount of aliquots analyzed is large enough to detect a poly-modal behaviour. Bimodal distributions have been successfully identified using single-grains but seem to get lost or merged when using small single-aliquots (e.g. Jain et al., 2002). However, in a depositional environment such as the coastal one, where quartz grains have been transported and/or deposited either by water and/or wind, theoretically well-zeroed prior to burial, it might be possible to clearly identify multiple dose populations (i.e. poly-modal distributions), if existent. The former might potentially define different sediment sources, i.e. grains with a different “trap background”, hence luminescence sensitivity.

Another tool that might be useful to further understand the behaviour of the dose distribution of any given unheated geological sample is the Cumulative Frequency Curve (i.e. accumulated percentage of the frequency distribution). As in any sedimentological analysis, this curve is used to a) identify different populations within the sample; and b) better visualize the degree of normality of the distribution. The shape of the curve (i.e. “S”) is a useful visual tool to understand the different tails (if any) associated with the distribution, hence the different D_E populations present within any given sample, which in turn can be used to test the normality of the distribution. In a way, and to the sedimentologically trained eye, they are easier to visualize than frequency distributions. The closer to the verticality the S-shaped curve is, the more symmetrical the distribution, hence its associated standard deviation would be a low value. The more pronounced the S-shaped curve is, i.e. the tails of the “S” are gently sloping, the less symmetrical the distribution is, hence the higher the value of the standard deviation.

To further constrain the histogram analysis, a radial plot was constructed for each mask size of each sample dated. Besides displaying a standardised estimate of the Mean D_E (i.e. palaeodose), the radial plot also shows the relative error and precision of each aliquot value (i.e. each aliquot's D_E is plotted with its statistical uncertainty). Hence, over-dispersed aliquots (i.e. aliquots with high dose values and uncertainties > 20%) can be identified more clearly rather than with only a histogram (e.g. Lian and Roberts, 2006).

However, and because one of the rejection criteria for any given aliquot is an uncertainty > 20%, the dose distributions plotted herein exclude aliquots showing over-dispersed values. Hence, the typical one or two outliers seen in the

distributions showed for this research (generally pertaining to high dose values), may not be due to “bright grains” (i.e. aliquots containing “bright” grains with both higher than usual doses and uncertainties) but rather inhomogeneity in the dose rates within the sample, at a micro-scale.

APPENDIX VI

PARAMETERS FOR SKEWNESS

Even though specific mentioning of analytical procedures is almost non-existent in the luminescence literature, I have chosen to employ this analysis during the evaluation of the D_E values measured for each individual sample.

The following are the skewness ranges (dimensionless) utilized when establishing the normality of a D_E distribution. The values are based on the relationship between the skewness ranges used for typical sedimentological grain-size distributions, the skewness obtained for each sample using two different equations (see below), and the analysis of the cumulative frequency (%) of each D_E distributions.

Pearson's Coefficient of Skewness for a set of values:

$$\frac{3 * (\text{MEAN} - \text{MEDIAN})}{\text{STD DEV}}$$

Coefficient of Skewness set by default in Microsoft Excel for a set of values:

$$\frac{n}{(n-1)*(n-2)} \sum \left(\frac{X_i - \bar{X}}{\text{STD DEV}} \right)^3$$

Where: n = number of values

X_i = a value (i.e. D_E)

\bar{X} = the average of the set of values

The closer the skewness value is to zero, the more symmetrical (i.e. normal) the distribution is.

Excel	Degree of Normality	Pearson
<i>> 0.91</i>	<i>Highly skewed to high D_E values</i>	<i>>> 1</i>
<i>0.65 to 0.91</i>	<i>Skewed to high D_E values</i>	<i>> 0.81</i>
<i>0.31 to 0.64</i>	<i>Symmetrical</i>	<i>-0.80 to 0.80</i>
<i>-0.30 to 0.30</i>	<i>Unimodal – usually only one D_E value</i>	
<i>-0.64 to -0.31</i>	<i>Symmetrical</i>	
<i>-0.91 to -0.65</i>	<i>Skewed to low D_E values</i>	<i>< -0.81</i>
<i>< -0.91</i>	<i>Highly skewed to low D_E values</i>	<i><< - 1</i>

Fortunately, for the majority of the samples analyzed during this research, the D_E distribution showed skewness values in between + 0.64 and – 0.64, indicating the degree of symmetry of the distribution.

Nonetheless, when analyzing D_E distributions using frequency histograms, skewness coefficients should be used to quantify the degree of dispersion rather than only visualizing it. When establishing skewness ranges such as the ones presented in this research, they could help identify the type of D_E distribution such as when a sample has been submitted to incomplete zeroing or geo- bio-turbation (from both above and below the sample). If I had seen such kinds of high skewness values, the following could have been interpreted:

- Distribution highly skewed to low D_E values: diagnostic of turbation from above, and even zero signal grains.
- Distribution highly skewed to high D_E values: diagnostic of incomplete zeroing and/or turbation from underlying older layers. The problem here would be how to differentiate between the latter or the former, which would be impossible.

APPENDIX VII

PARAMETERS FOR OSL AGE CALCULATIONS

The following are the specifics regarding the parameters and errors input into *ANATOL* when calculating the OSL age of each fraction of quartz measured for each individual sample.

Overburden Density: 2 g/cm^3

Cosmic Dose Rate: obtained in *ANATOL* based on calculations by Prescott and Hutton (1988)

Cosmic-Ray Dose Rate Error: $\pm 5\%$ of its value

Water Saturation (W): measured water content (%) /100

Water Fraction (F): 0.8

Water Fraction Error: 0.2

Internal α : a-value = $0.04 \pm 10\%$

Internal β absorbed: depends on grain size and it is based on Mejdahl's Factor F (1979) given in *ANATOL*

Grain size fraction measured: 150-212 μm

Average fraction used for calculations: 180 μm

Given Factor F:

$U = 0.1370$ $Th = 0.1950$ $K = 0.0633$

External α : None (due to etching of quartz)

External β : given by NAA results on U, Th, and K contents

External γ : given by NAA results on U, Th, and K contents

Estimated Water Content

during measurement: 0 (i.e. dry sample)

Etching Error: $\pm 2\%$

Internal Doses for

grains of quartz: based on the average dose for granitic quartz by

Rink & Odom (1991)

$U = 0.06650 \pm 0.02194 \text{ ppm}$

$Th = 0.11350 \pm 0.04248 \text{ ppm}$

$K = 0 \pm 0 \%$ (removed by mineral separation)

Global Systematic Error: $\pm 10\%$

D_E : Final Mean D_E obtained excluding 2σ outliers

D_E Error: 1σ or 1 standard error depending on the symmetry of the distribution

NAA results specific concentrations obtained for U, Th, and K of each sample at the Nuclear Reactor, McMaster U.

ANATOL incorporates the energy release data of Adamiec and Aitken (1998).

APPENDIX VIII

AGE CALCULATION: TWO POSSIBLE MODELS – LINEAR OR INSTANT

ACCUMULATION

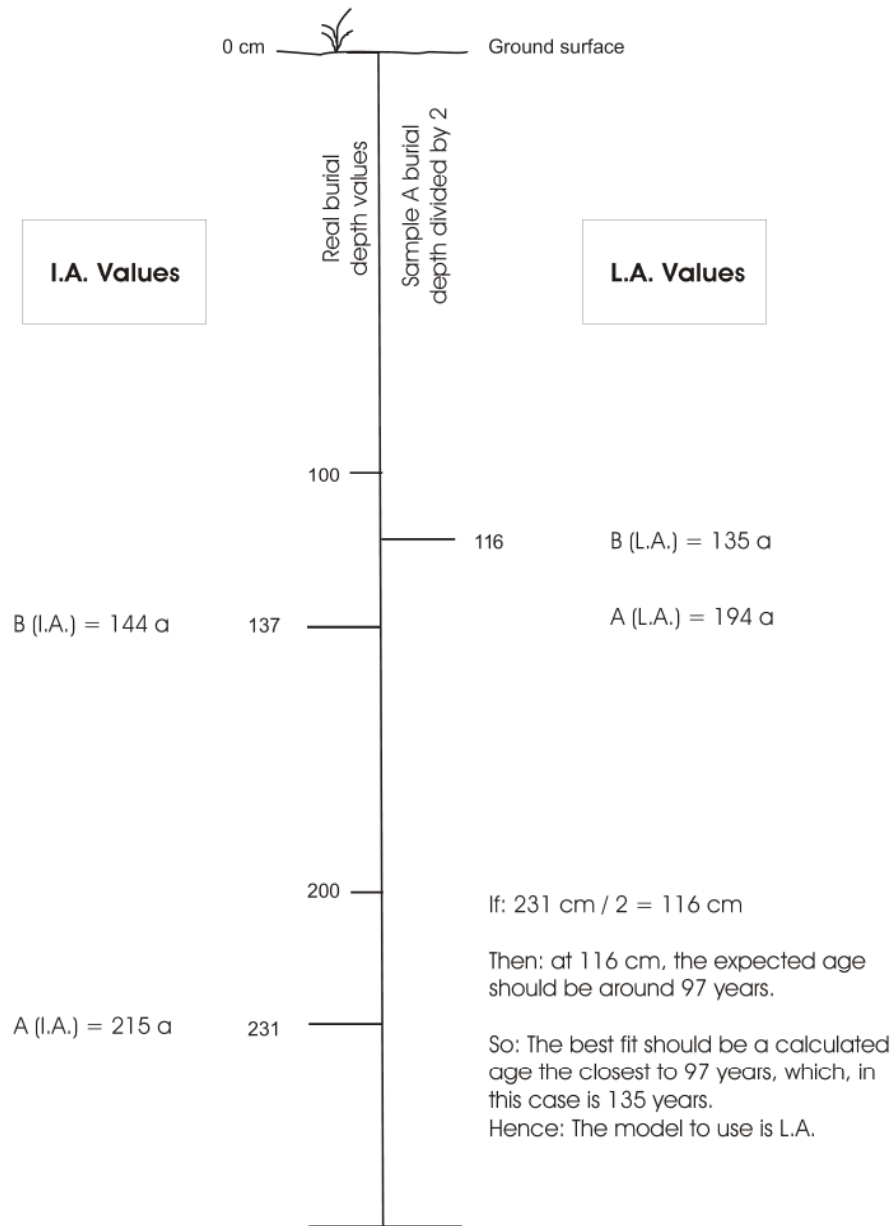
Both models are based on the burial depth of the sample, hence the value for cosmic dose rate to be applied in the calculation of the age of the sample. They try to account for the sedimentological history of the deposit, hence whether or not the deposition of sediment has been linear through time or instantaneous.

The instant accumulation model (I.A.) uses the cosmic dose rate calculated for the burial depth of any given sample. The linear accumulation model (L.A.) uses one half of that same cosmic dose rate. Whether one model or the other are used for any given sample depends on how truthful the ages obtained match the hypothesized geological evolution of the deposit. For example, ages obtained from archaeological layers (e.g. shell middens as seen in Chapters 4 and 5) with thin overburdens (i.e. < 1 m), should be calculated using I.A. than L.A. as their formation through geological time was rather instantaneous than the underlying geological layers that might have taken thousands of years to evolve. This is based on the fact that the history the burial depth of a sample changes through time, i.e. burial depth tends to increase as the sample does not stay at its original emplacement position infinitely; continuous sediment is deposited atop, building up the deposit both vertically and laterally.

The following example should help the reader understand the concept of I.A. vs L.A. for a given depositional environment where two OSL samples were dated by OSL: sample A taken at a burial depth of 231 cm and sample B from 137 cm, both below ground surface. The calculated ages (rounded off for practical purposes) for both samples are:

Sample	Age using I.A.	Age using L.A.
B	144	135
A	215	194

See following figure for explanation and model result.



APPENDIX IX

AGE CALCULATION: ACCOUNTING FOR GEOMETRY

It is important to appraise the geometry of the depositional environment where the sample (i.e. sediment core) was collected. A thick overburden can affect how soft cosmic rays attain the sample; the same might apply for the lateral geometry of the deposit itself. This in turn may affect the calculation of the age of the sample.

One of the key assumptions in OSL dating is that the targeted sedimentary deposit has constant, uniform and definable dose rates. Moreover, the dose rate is assumed constant over time due to the long $\frac{1}{2}$ lives of the radionuclides (^{238}U , ^{232}Th , and ^{40}K) involved and they are assumed not to migrate throughout the sedimentary deposit during its burial history (Aitken, 1998). The short-ranged α and β irradiations are part of the sample's internal dose rate component, and the long-ranged γ and cosmic radiations are part of the environment's external dose rate component.

The cosmic dose rate has been calculated to be 0.291 Gy/ka at sea level and at latitude 38°S (Prescott and Hutton, 1994). This value is valid for latitudes $> 40^\circ$, but should be corrected for a) altitudes generally surpassing 2,000 m above sea level and b) depth of the sample. The cosmic rays particle flux is assumed homogenous throughout the burial history of the sample, i.e. a sheet-like geometry to the horizon in all directions: a half hemisphere of at least 80 m in diameter (i.e. 2π geometry = 2 x a $\frac{1}{4}$ of a hemisphere).

Sedimentary bodies with different geometries such as, for example, ridges and swales of different heights and widths (i.e. undulated landscape), may react differently to the incoming cosmic flux, as the cosmic-ray dose rate gets attenuated with depth. Hence, it is important to investigate the geometry of the deposit to account for the distribution of the cosmic-ray dose rate, which may or may not affect the age calculation of any given sample collected from that deposit. This is indeed more important for those samples collected at depths < 50 cm (Prescott and Hutton, 1988; Prescott and Stephan, 1982), and more precise cosmic-ray dose rate calculations should be done for such cases. Nonetheless, if in any given sample / depositional environment, the β and γ dose rates have high values, the cosmic-ray dose rate effect may be minimal in comparison, so its consideration diminishes.

In the case of the ridges studied in this dissertation, the cosmic-ray dose rate was based on infinite planar 2π geometries, which were assumed for all the samples

dated, as all were situated at depths > 50 cm. All the optical ages calculated in this study used cosmic-ray dose rates calculated for infinite planar 2π geometries because of the angle of incidence of the muon shower, which is very close to the vertical (Prescott and Hutton, 1988). Hence, the only samples which would require more precise cosmic-ray dose rate calculations would be those located closer to the surface (i.e. < 50 cm-depth). In this study, the geometry of the ridges is not of much concern for the calculation of the cosmic input; however, this is an interesting point to take into account and further pursue if other were the environmental circumstances.

APPENDIX X

SAR-OSL DATED SAMPLES: SPECIFICS, AGES AND RESULTS

All the samples optically dated during this Ph.D. research are listed below. Specific Gy values for test and regenerative doses administered to each individual sample are given, as well as the selected pre-heat temperatures based on the PHP, DR and TT tests. Ages are provided with their respective *datum* and Final Mean D_E for each individual sample. Specific details such as each sample's real depth below surface, water content, and U, Th and K contents (obtained by NAA) are also given.

Two tables with all these results are given below.

Final results obtained for all the samples taken from beach/dune ridges along the different Barrier Islands near Apalachicola, NW Florida, USA, for this Ph.D. research.

Sample [a]	2σ/RR/A [b]	ED (Gy) [c]		U (ppm) [d]	Th (ppm) [d]	K (ppm) [d]	Water (%) [e] ^	Real Burial Depth (cm) [f]	Cosmic Dose Rate (μGy/a) [g] ^	Annual Dose (μGy/a) [h] ^	SAR-OSL Age (a) ^		Datum [i] *	A.D. or B.C.
		Mean	± 1σ								Value	± error		
St. Joseph Peninsula:														
Haven B	22/24/24	0.22	0.00	0.10 ± 0.1	0.39 ± 0.05	58 ± 9	5	108.93	197	262 ± 17	840	60	[06]	1,166
Haven A	24/24/24	0.24	0.01	0.14 ± 0.1	0.41 ± 0.06	44 ± 9	3	248.97	177	252 ± 17	950	80	[06]	1,056
Rish Park B	23/24/24	0.52	0.02	0.21 ± 0.1	0.72 ± 0.07	24 ± 12	3	63.26	216	327 ± 17	1,600	100	[05]	405
Rish Park A	22/24/24	0.57	0.04	0.15 ± 0.1	0.25 ± 0.05	20 ± 10	5	143.77	191	254 ± 17	2,200	200	[05]	-195
White Sands B	22/24/24	0.03	0.00	2.08 ± 0.1	7.88 ± 0.51	16 ± 10	3	62.38	218	1247 ± 31	24	1	[06]	1,982
White Sands A	17/18/18	0.07	0.00	0.60 ± 0.1	1.34 ± 0.11	49 ± 11	8	249.50	177	412 ± 17	170	10	[06]	1,836
Old Cedar 1	23/24/24	0.38	0.03	0.36 ± 0.1	2.81 ± 0.18	139 ± 40	3	25.00	215	407 ± 9	940	100	[05]*	1,065
Old Cedar Geo 1	21/24/24	0.47	0.03	0.16 ± 0.1	0.29 ± 0.05	112 ± 30	1	70.00	209	264 ± 5	1,800	130	[05]	205
Harvey B	16/18/18	0.39	0.04	0.22 ± 0.1	0.50 ± 0.06	60 ± 11	18	89.54	203	293 ± 15	1,300	200	[06]	706
Harvey A	18/18/18	0.51	0.01	0.29 ± 0.1	0.71 ± 0.07	46 ± 11	3	329.51	168	297 ± 17	1,700	100	[06]	306

Sample [a]	2σ/RR/A [b]	ED (Gy) [c]		U (ppm) [d]		Th (ppm) [d]	K (ppm) [d]	Water (%) [e] ^	Real Burial Depth (cm) [f]	Cosmic Dose Rate (μGy/a) [g] ^	Annual Dose (μGy/a) [h] ^	SAR-OSL Age (a) ^		Datum [i] *	A.D. or B.C.
		Mean	±1σ	Value	± error										
Deer Ridge SJ201	46/48/48	0.25	0.00	0.10 ± 0.1	0.20 ± 0.00	62 ± 6	19	135.14	192	239 ± 15	1,000	80	[04]	1,004	
Deer Ridge 1 B	22/24/24	0.38	0.02	0.16 ± 0.1	0.51 ± 0.06	71 ± 9	4	90.57	202	290 ± 17	1,300	100	[06]	706	
Deer Ridge 1 A	20/22/24	0.42	0.01	0.21 ± 0.1	0.38 ± 0.06	44 ± 9	3	169.82	187	276 ± 17	1,500	100	[06]	506	
Deer Ridge 2	22/24/24	0.39	0.01	0.10 ± 0.1	0.25 ± 0.05	60 ± 7	7	151.92	189	244 ± 16	1,600	100	[06]	406	
Wild B	22/24/24	0.20	0.01	0.21 ± 0.1	0.34 ± 0.06	51 ± 9	3	86.71	204	291 ± 17	690	60	[06]	1,316	
Wild A	23/24/24	0.25	0.00	0.25 ± 0.1	0.35 ± 0.06	49 ± 10	3	290.78	172	269 ± 17	930	70	[06]	1,076	
SJ002 1 B	22/23/23	0.04	0.01	0.26 ± 0.1	0.39 ± 0.04	58 ± 6	3	136.99	192	295 ± 17	140	20	[06]	1,866	
SJ002 1 A	22/24/24	0.05	0.01	0.17 ± 0.1	0.38 ± 0.04	30 ± 5	4	230.91	179	257 ± 17	190	30	[06]	1,816	
SJ002 2 B	22/23/23	0.03	0.00	0.15 ± 0.1	0.24 ± 0.03	47 ± 4	4	91.67	202	268 ± 17	100	8	[06]	1,906	
SJ002 2 A	23/23/23	0.03	0.00	0.17 ± 0.1	0.30 ± 0.03	43 ± 5	5	173.88	186	260 ± 17	120	8	[06]	1,886	
GPR 1 B	20/22/24	0.06	0.01	0.17 ± 0.1	0.29 ± 0.03	44 ± 5	5	99.05	200	272 ± 16	220	40	[06]	1,786	
GPR 1 A	22/24/24	0.06	0.00	0.15 ± 0.1	0.16 ± 0.03	52 ± 5	13	217.94	181	238 ± 15	250	20	[06]	1,756	

Sample [a]	2σ/RR/A [b]	ED (Gy) [c]		U (ppm) [d]	Th (ppm) [d]	K (ppm) [d]	Water (%) [e] ^	Real Burial Depth (cm) [f]	Cosmic Dose Rate (μGy/a) [σ] ^	Annual Dose (μGy/a) [h] ^	SAR-OSL Age (a) ^		Datum [i] *	A.D. or B.C.
		Mean	± 1σ								Value	± error		
Richardson Hammock:														
RH-TUE-1	23/24/24	0.47	0.02	0.22 ± 0.1	0.64 ± 0.08	49 ± 11	7	30.00	219	325 ± 17	1,400	100	[05]*	605
RH-TUE-2	23/24/24	0.84	0.04	0.12 ± 0.1	0.45 ± 0.05	46 ± 7	3	190.00	184	258 ± 17	3,300	300	[05]	-1,295
RH-GEO-1	23/24/24	1.41	0.12	0.59 ± 0.1	2.73 ± 0.18	53 ± 9	3	230.00	179	518 ± 19	2,700	400	[05]	-695
RH B	24/24/24	0.66	0.03	0.27 ± 0.1	0.37 ± 0.05	34 ± 10	6	170.08	187	286 ± 16	2,300	200	[05]	-295
RH A	24/24/24	0.85	0.05	0.29 ± 0.1	0.49 ± 0.05	38 ± 9	14	317.83	169	274 ± 15	3,100	300	[05]	-1,095
Mainland & Cape San Blas:														
Oak Ridge B	16/18/24	8.52	2.02	0.32 ± 0.1	1.04 ± 0.09	176 ± 13	14	118.43	195	352 ± 16	24,200	5,800	[06]	-22,194
Oak Ridge A	24/24/24	52.28	1.26	0.37 ± 0.1	1.11 ± 0.09	38 ± 8	16	213.18	181	339 ± 15	154,200	10,400	[06]	-152,194
Romanelli B	24/24/24	0.04	0.00	0.37 ± 0.1	0.90 ± 0.10	357 ± 16	3	84.96	205	396 ± 17	100	6	[06]	1,906
Romanelli A	23/24/24	0.49	0.02	1.53 ± 0.1	5.70 ± 0.40	148 ± 12	4	349.19	165	927 ± 26	530	40	[06]	1,476
Hogan B	23/24/24	0.08	0.01	0.18 ± 0.1	0.40 ± 0.10	328 ± 14	18	112.23	197	295 ± 15	270	30	[06]	1,736
Hogan A	23/24/24	0.10	0.00	0.25 ± 0.1	0.50 ± 0.10	380 ± 17	22	209.77	182	301 ± 15	330	20	[06]	1,676
Roy Eglin B	23/24/24	0.11	0.00	0.17 ± 0.1	0.20 ± 0.04	176 ± 17	14	90.14	203	277 ± 15	400	30	[04]	1,606
Roy Eglin A	22/24/24	0.21	0.00	0.41 ± 0.1	0.87 ± 0.07	78 ± 15	8	301.56	171	336 ± 16	630	40	[04]	1,376

Sample [a]	2σ/RR/A [b]	ED (Gy) [c]		U (ppm) [d]	Th (ppm) [d]	K (ppm) [d]	Water (%) [e] ^	Real Burial Depth (cm) [f]	Cosmic Dose Rate (μGy/a) [σ] ^	Annual Dose (μGy/a) [h] ^	SAR-OSL Age (a) ^		Datum [i] *	A.D. or B.C.
		Mean	± 1σ								Value	± error		
Little S. George Island:														
LSGI 1 B	17/18/18	0.47	0.03	0.16 ± 0.1	0.35 ± 0.05	988 ± 35	19	95.86	201	346 ± 14.8	1,400	100	[06]	606
LSGI 1 A	24/24/24	0.65	0.05	0.25 ± 0.1	0.93 ± 0.08	364 ± 18	3	214.38	181	347.7 ± 17.2	1,900	200	[06]	106
LSGI 2 B	22/24/24	0.12	0.01	0.16 ± 0.1	0.52 ± 0.06	222 ± 15	3	84.30	206	309.4 ± 16.9	390	40	[06]	1,616
LSGI 2 A	17/18/18	0.14	0.01	0.16 ± 0.1	0.56 ± 0.06	146 ± 13	8	192.69	184	278.8 ± 16.1	500	50	[06]	1,506
LSGI 3 B	10/12/12	0.01	0.00	0.36 ± 0.1	1.87 ± 0.14	284 ± 16	5	90.72	202	446 ± 17.8	22	4	[06]	1,984
LSGI 3 A	17/18/18	0.01	0.00	0.18 ± 0.1	0.68 ± 0.07	262 ± 16	7	158.76	188	307.4 ± 16.4	32	3	[06]	1,974
St. Vincent Island:														
SVI #0 OSL2	23/24/24	0.11	0.01	0.18 ± 0.1	0.42 ± 0.04	180 ± 20	19	102.40	199	286 ± 15	370	50	[04]	1,634
SVI #0 OSL1	23/24/24	0.12	0.01	0.15 ± 0.1	0.48 ± 0.04	220 ± 20	3	180.90	185	284 ± 17	410	60	[04]	1,594

Sample [a]	2σ/RR/A [b]	ED (Gy) [c]		U (ppm) [d]	Th (ppm) [d]	K (ppm) [d]	Water (%) [e] ^	Real Burial Depth (cm) [f]	Cosmic Dose Rate (μGy/a) [g] ^	Annual Dose (μGy/a) [h] ^	SAR-OSL Age (a) ^		Datum [i] *	A.D. or B.C.
		Mean	± 1σ								Value	± error		
SVI #1 OSL2	24/24/24	0.21	0.01	0.16 ± 0.1	0.43 ± 0.04	320 ± 20	23	100.80	199	297 ± 14	710	70	[04]	1,294
SVI #1 OSL1	24/24/24	0.28	0.02	0.35 ± 0.1	0.85 ± 0.06	240 ± 20	14	167.40	187	343 ± 15	810	100	[04]	1,194
SVI #2 OSL2	23/24/24	0.23	0.02	0.20 ± 0.1	0.52 ± 0.04	190 ± 10	14	99.90	199	300 ± 15	780	100	[04]	1,224
SVI #2 OSL1	23/24/24	0.45	0.04	0.13 ± 0.1	0.55 ± 0.04	130 ± 10	2	217.10	181	272 ± 17	1,640	210	[04]	364
SVI #2b OSL2	23/24/24	0.25	0.02	0.19 ± 0.1	0.57 ± 0.06	170 ± 10	16	98.50	200	299 ± 15	840	100	[04]	1,164
SVI #2b OSL1	23/24/24	0.30	0.02	0.15 ± 0.1	0.36 ± 0.04	150 ± 10	3	159.60	188	272 ± 17	1,100	130	[04]	904
SVI #3 OSL2	24/24/24	0.67	0.06	0.97 ± 0.1	4.18 ± 0.28	270 ± 20	7	103.80	198	725 ± 21	920	130	[04]	1,084
SVI #3 OSL1	24/24/24	0.76	0.10	0.53 ± 0.1	1.11 ± 0.08	190 ± 10	3	246.40	177	404 ± 17	1,890	290	[04]	114
SVI #5 OSL2	23/24/24	0.82	0.08	0.19 ± 0.1	0.31 ± 0.04	250 ± 50	19	103.60	198	286 ± 15	2,860	340	[04]	-856
SVI #5 OSL1	24/24/24	1.04	0.13	0.53 ± 0.1	0.84 ± 0.07	330 ± 50	14	222.60	180	382 ± 16	2,730	400	[04]	-726
SVI #6 OSL2	23/24/24	0.76	0.06	0.17 ± 0.1	0.35 ± 0.04	70 ± 30	24	88.90	204	273 ± 14	2,790	290	[04]	-786
SVI #6 OSL1	24/24/24	0.84	0.08	0.26 ± 0.1	0.55 ± 0.04	130 ± 20	9	156.10	189	303 ± 16	2,780	340	[04]	-776

Special Notes:

- [a] A and OSL1 correspond to samples taken towards the bottom of the core and B and OSL2 towards the top of the core, at least 1 m above A or OSL1.
 - [b] Aliquots measured to obtain the Final Mean ED and its error, accepted after complying to all criteria:
 $2\sigma = \#$ aliquots inside 2σ range ; RR = # aliquots inside recycling ratio ; A = total # aliquots measured
 - [c] Final Mean ED and error obtained from large aliquots (8 or 5 mm mask size depending on the sample).
 - [d] U, Th and K values determined by NAA at the Nuclear Reactor facility, McMaster University.
 - [e] Water content as a fraction of dry weight determined from laboratory measurements.
 - [f] Actual burial depth of the centre of the sample, considering compaction during coring.
 - [g] Cosmic-ray dose rate value calculated using an overburden density of 2 g/cm³. A 5% error was added for the age calculation.
 - [h] All β and γ dose rates were calculated based on U, Th and K concentrations of each sample accounting for moisture values of the sample.
 - [i] Datum for SAR-OSL ages is: [04] for A.D. 2004; [05] for A.D. 2005; [06] for A.D. 2006.
- ^ Values have been rounded to nearest sensible number of precision.
- * Only ages showing this symbol were calculated assuming instant sediment accumulation rates. Otherwise, all other ages were calculated assuming constant (i.e. linear) sediment accumulation rates.

Selected Temperatures and Single-Aliquot Regenerative-Dose Cycles used to determine the Final D_F for all samples measured for this Ph.D. research.

Sample #	IRSL/OSL	Ini ED Dose (Gy)	Initial ED & F Contam. [a]	Preheat T (°C)				Final ED Determination			SAR Cycles					
				PHP [b]	DRT [b]	TTT [b]	DRT Given Dose (Gy)	Preheat T (°C) [c]	Cutheat T (°C)	OSL T (°C)	Test Dose (Gy)	RD1 (Gy)	RD2 (Gy)	RD3 (Gy)	RD4 (Gy)	RD5 (Gy)

St. Joseph Peninsula:

Rish Park B	0.001	0.89	220	160	160	0	0.53	160	160	125	0.43	0.35	0.53	1.06	1.59	0	0.35
Rish Park A	0.001	0.89	220	160	160	0	0.53	160	160	125	0.43	0.35	0.53	1.06	1.59	0	0.35
White Sands B	0.004	0.26	220	240-280	280	0	0.26	280	160	125	0.35	0.26	0.35	0.52	0.69	0	0.26
White Sands A	0.002	0.35	220	240-280	280	0	0.26	280	160	125	0.35	0.26	0.35	0.52	0.69	0	0.26
Haven B	0.001	0.61	220	160	160	0	0.26	160	160	125	0.35	0.26	0.35	0.52	0.70	0	0.26
Haven A	0.001	0.61	220	160	160	0	0.26	160	160	125	0.35	0.26	0.35	0.52	0.70	0	0.26
Harvey B	0.002	0.61	220	160-200	200	0	0.69	200	160	125	0.43	0.43	0.87	1.73	2.60	0	0.43
Harvey A	0.003	0.61	220	160-200	200	0	0.69	200	160	125	0.43	0.43	0.87	1.73	2.60	0	0.43
Deer Ridge SJ201 A	0.001	1.01	220	160	160-240	0	0.35	160	160	125	0.45	0.36	0.54	0.73	0.91	0	0.36
Deer Ridge 1 B	0.002	0.61	220	160	160, 200	0	0.61	160	160	125	0.44	0.44	0.87	1.74	2.61	0	0.44
Deer Ridge 1 A	0.003	0.61	220	160	200, 280	0	0.87	160	160	125	0.44	0.44	0.87	1.74	2.61	0	0.44
Deer Ridge 2 A	0.002	0.61	220	160	160, 200	0	0.70	160	160	125	0.44	0.44	0.87	1.74	2.61	0	0.44
Wild B	0.003	0.52	220	160-200	200	0	0.35	200	160	125	0.35	0.26	0.35	0.52	0.69	0	0.26
Wild A	0.003	0.52	220	160-200	200	0	0.35	200	160	125	0.35	0.26	0.35	0.52	0.69	0	0.26
SJ002 1 B	0.004	0.35	220	160	200	0	0.26	200	160	125	0.35	0.26	0.35	0.53	0.70	0	0.26
SJ002 1 A	0.004	0.35	220	160, 280	200, 280	0	0.26	280	160	125	0.35	0.26	0.35	0.53	0.70	0	0.26
SJ002 2 B	0.002	0.53	220	160-280	280	0	0.26	280	160	125	0.35	0.26	0.35	0.53	0.70	0	0.26

SJ002 2 A	0.002	0.53	220	160-280	280	0	0.26	280	160	125	0.35	0.26	0.35	0.53	0.70	0	0.26
				Preheat T (°C)				Final ED Determination			SAR Cycles						
Sample #	IRSL/OSL	Ini ED Dose (Gy)	Initial ED & F Contam. [a]	PHP [b]	DRT [b]	TTT [b]	DRT Given Dose (Gy)	Preheat T (°C) [c]	Cutheat T (°C)	OSL T (°C)	Test Dose (Gy)	RD1 (Gy)	RD2 (Gy)	RD3 (Gy)	RD4 (Gy)	RD5 (Gy)	RD6 (Gy)
GPR 1 B	0.003	0.53	220	240, 280	160, 240	0	0.26	240	160	125	0.35	0.26	0.35	0.53	0.70	0	0.26
GPR 1 A	0.003	0.53	220	160, 280	200, 280	0	0.26	280	160	125	0.35	0.26	0.35	0.53	0.70	0	0.26

Richardson Hammock:

RH-TUE-1	0.001	0.97	220	160	160-280	0	0.62	280	160	125	0.88	0.53	1.06	2.12	3.18	0	0.53
RH-TUE-2	0.002	0.97	220	160	160-280	0	1.15	280	160	125	0.88	0.53	1.06	2.12	3.18	0	0.53
RH-GEO-1	0.001	0.97	220	240-280	160-280	0	2.12	280	160	125	0.88	0.53	1.06	2.12	3.18	0	0.53
RH B	0.001	3.96	220	160	200	0	0.35	200	160	125	0.95	0.52	0.95	1.91	2.86	0	0.52
RH A	0.001	3.96	220	160	200	0	0.44	200	160	125	0.95	0.52	0.95	1.91	2.86	0	0.52

Mainland & Cape San Blas:

Oak Ridge B	0.001	1.74	220	240-280	240	0	11.29	240	160	125	4.34	4.34	8.68	13.02	17.36	0	4.34
Oak Ridge A	0.001	1.74	220	240-280	280	0	86.98	280	160	125	43.41	43.41	86.81	130.22	173.62	0	43.41
Romanelli B	0.004	0.43	220	200-280	280	0	0.26	280	160	125	0.26	0.26	0.35	0.52	0.69	0	0.26
Romanelli A	0.002	0.43	220	160-200	160	0	2.60	160	160	125	0.87	1.30	2.60	3.90	5.20	0	1.30
Hogan B	0.001	0.43	220	160-200	160	0	0.26	160	160	125	0.26	0.26	0.35	0.52	0.69	0	0.26
Hogan A	0.003	0.43	220	200-280	280	0	0.26	280	160	125	0.26	0.26	0.35	0.52	0.69	0	0.26
Roy Eglin B	0.000	3.96	220	160	160-240	0	0.35	160	160	125	0.46	0.37	0.55	0.74	0.92	0	0.37
Roy Eglin A	0.001	3.96	220	160	160	0	0.35	160	160	125	0.46	0.37	0.55	0.74	0.92	0	0.37

Sample #	IRSL/OSL	Ini ED Dose (Gy)	Initial ED & F Contam. [a]	Preheat T (°C)			DRT Given Dose (Gy)	Final ED Determination			SAR Cycles					
				PHP [b]	DRT [b]	TTT [b]		Preheat T (°C) [c]	Cutheat T (°C)	OSL T (°C)	Test Dose (Gy)	RD1 (Gy)	RD2 (Gy)	RD3 (Gy)	RD4 (Gy)	RD5 (Gy)

Little S. George Island:

LSGI 1 B	0.002	0.61	220	160	160-240	0	0.61	160	160	125	0.61	0.44	0.88	1.75	2.63	0.00	0.44
LSGI 1 A	0.002	0.88	220	160-200	200	0	0.87	200	160	125	0.61	0.43	0.87	1.73	2.60	0.00	0.43
LSGI 2 B	0.004	0.35	220	160-240	200	0	0.26	200	160	125	0.26	0.26	0.35	0.52	0.69	0.00	0.26
LSGI 2 A	0.002	0.88	220	160-280	280	0	0.35	280	160	125	0.35	0.26	0.35	0.53	0.70	0.00	0.26
LSGI 3 B	0.002	0.35	220	160-240	240	0	0.26	240	160	125	0.26	0.26	0.35	0.52	0.69	0.00	0.26
LSGI 3 A	0.002	0.35	220	160-240	160-200	0	0.35	160	160	125	0.35	0.26	0.35	0.53	0.70	0.00	0.26

St. Vincent Island:

SVI #0 OSL2	0.005	0.81	220	160, 240, 280	160-200	0	0.36	160	160	125	0.45	0.36	0.54	0.72	0.90	0	0.36
SVI #0 OSL1	0.006	0.81	220	160, 240, 280	160-200	0	0.36	160	160	125	0.45	0.36	0.54	0.72	0.90	0	0.36
SVI #1 OSL2	0.005	0.81	220	160, 240, 280	160-200	0	0.50	160	160	125	0.45	0.36	0.54	0.72	0.90	0	0.36
SVI #1 OSL1	0.006	0.81	220	160, 240, 280	160-200	0	0.50	160	160	125	0.45	0.36	0.54	0.72	0.90	0	0.36
SVI #2 OSL2	0.005	0.81	220	160, 240, 280	160-200	0	0.50	160	160	125	0.45	0.36	0.54	0.72	0.90	0	0.36
SVI #2 OSL1	0.006	0.81	220	160, 240, 280	160-200	0	0.50	160	160	125	0.45	0.36	0.54	0.72	0.90	0	0.36
SVI #2b OSL2	0.005	0.81	220	160, 240, 280	160-200	0	0.50	160	160	125	0.45	0.36	0.54	0.72	0.90	0	0.36
SVI #2b OSL1	0.006	0.81	220	160, 240, 280	160-200	0	0.50	160	160	125	0.45	0.36	0.54	0.72	0.90	0	0.36
SVI #3 OSL2	0.005	2.26	220	160, 240, 280	160	0	0.62	160	160	125	0.90	0.45	0.90	1.81	2.71	0	0.45
SVI #3 OSL1	0.006	2.26	220	160, 240, 280	160	0	0.62	160	160	125	0.90	0.45	0.90	1.81	2.71	0	0.45
SVI #5 OSL2	0.005	2.34	220	160, 240, 280	160	0	0.80	160	160	125	1.98	0.54	1.08	2.16	4.33	0	0.54
SVI #5 OSL1	0.005	2.34	220	160, 240, 280	160	0	0.80	160	160	125	1.98	0.54	1.08	2.16	4.33	0	0.54
SVI #6 OSL2	0.005	2.34	220	160, 240, 280	160	0	0.80	160	160	125	1.98	0.54	1.08	2.16	4.33	0	0.54
SVI #6 OSL1	0.005	2.34	220	160, 240, 280	160	0	0.80	160	160	125	1.98	0.54	1.08	2.16	4.33	0	0.54

Special Notes:

- [a] Temperature (°C) at which the initial ED assessment and Feldspar Contamination test were made.
- [b] For Pre-heat Plateau test (PHP): Temperature(s) (°C) showing a plateau
For Dose Recovery Test (DRT): Best temperature(s) (°C) at which a given known dose was recovered.
For Thermal Transfer Test (TTT): 0 indicates no thermal transfer observed with temperature.
- [c] Best pre-heat value in accordance to PHP, DRT and TTT; used in the determination of the final ED.

.
THE END
.